



UNICAMP

UNIVERSIDADE ESTADUAL DE
CAMPINAS

Instituto de Matemática, Estatística e
Computação Científica

NELSON QUISPE CUBA

**A Besov spaces approach and numerical insights
to study: a conservation law with partially
nonlocal velocity and the inviscid surface
quasi-geostrophic equation**

**Uma abordagem de espaços de Besov e insights
numéricos para estudar: uma lei de conservação
com velocidade parcialmente não local e a
equação quase-geostrófica de superfície invíscida**

Campinas

2024

Nelson Quispe Cuba

**A Besov spaces approach and numerical insights to study:
a conservation law with partially nonlocal velocity and the
inviscid surface quasi-geostrophic equation**

**Uma abordagem de espaços de Besov e insights
numéricos para estudar: uma lei de conservação com
velocidade parcialmente não local e a equação
quase-geostrófica de superfície invíscida**

Tese apresentada ao Instituto de Matemática,
Estatística e Computação Científica da Uni-
versidade Estadual de Campinas como parte
dos requisitos exigidos para a obtenção do
título de Doutor em Matemática Aplicada.

Thesis presented to the Institute of Mathe-
matics, Statistics and Scientific Computing
of the University of Campinas in partial ful-
fillment of the requirements for the degree of
Doctor in Applied Mathematics.

Supervisor: Eduardo Cardoso de Abreu

Co-supervisor: Julio Cesar Valencia Guevara and John Alexander Pérez
Sepúlveda

Este trabalho corresponde à versão
final da Tese defendida pelo aluno
Nelson Quispe Cuba e orientado pelo
Prof. Dr. Eduardo Cardoso de Abreu.

Campinas

2024

Ficha catalográfica
Universidade Estadual de Campinas
Biblioteca do Instituto de Matemática, Estatística e Computação Científica
Ana Regina Machado - CRB 8/5467

Q48b Quispe Cuba, Nelson, 1991-
A Besov spaces approach and numerical insights to study : a conservation law with partially nonlocal velocity and the inviscid surface quasi-geostrophic equation / Nelson Quispe Cuba. – Campinas, SP : [s.n.], 2024.

Orientador: Eduardo Cardoso de Abreu.

Coorientadores: Julio Cesar Valencia Guevara e John Alexander Pérez Sepúlveda.

Tese (doutorado) – Universidade Estadual de Campinas, Instituto de Matemática, Estatística e Computação Científica.

1. Leis de conservação hiperbólicas. 2. Equação quase-geostrófica. 3. Espaços de Besov. 4. Método lagrangiano-euleriano. I. Abreu, Eduardo Cardoso de, 1974-. II. Valencia Guevara, Julio Cesar, 1985-. III. Pérez Sepúlveda, John Alexande, 1974-. IV. Universidade Estadual de Campinas. Instituto de Matemática, Estatística e Computação Científica. V. Título.

Informações Complementares

Título em outro idioma: Uma abordagem de espaços de Besov e insights numéricos para estudar : uma lei de conservação com velocidade parcialmente não local e a equação quase-geostrófica de superfície invíscida

Palavras-chave em inglês:

Hyperbolic conservation laws

Quasi-geostrophic equation

Besov spaces

Lagrangian-Eulerian method

Área de concentração: Matemática Aplicada

Titulação: Doutor em Matemática Aplicada

Banca examinadora:

Eduardo Cardoso de Abreu [Orientador]

Lucas Catão de Freitas Ferreira

Giuliano Angelo Zugliani

Wanderson José Lambert

Juan Carlos Juajibioy Otero

Data de defesa: 28-02-2024

Programa de Pós-Graduação: Matemática Aplicada

Identificação e informações acadêmicas do(a) aluno(a)

- ORCID do autor: <https://orcid.org/0009-0006-2905-7686>

- Currículo Lattes do autor: <http://lattes.cnpq.br/9335208849249086>

**Tese de Doutorado defendida em 28 de fevereiro de 2024 e aprovada
pela banca examinadora composta pelos Profs. Drs.**

Prof(a). Dr(a). EDUARDO CARDOSO DE ABREU

Prof(a). Dr(a). LUCAS CATÃO DE FREITAS FERREIRA

Prof(a). Dr(a). GIULIANO ANGELO ZUGLIANI

Prof(a). Dr(a). WANDERSON JOSÉ LAMBERT

Prof(a). Dr(a). JUAN CARLOS JUAJIBIOY OTERO

A Ata da Defesa, assinada pelos membros da Comissão Examinadora, consta no SIGA/Sistema de Fluxo de Dissertação/Tese e na Secretaria de Pós-Graduação do Instituto de Matemática, Estatística e Computação Científica.

Acknowledgements

First and foremost, I express my gratitude to God. I extend thanks to my advisor, Prof. Dr. Eduardo Cardoso de Abreu, and my co-advisors, Profs. Drs. Julio Cesar Valencia Guevara and John Alexander Pérez Sepúlveda, for their invaluable guidance, assistance, dedication, patience, and profound understanding throughout my doctoral journey. I am deeply grateful to the Institute of Mathematics, Statistics, and Scientific Computing (IMECC) - Graduate Program in Applied Mathematics - for providing me with the opportunity to pursue my studies at this esteemed institution. Additionally, I would like to acknowledge the Student Support Service (SAE) of UNICAMP for their unwavering assistance during the challenging initial phase of my doctoral studies amidst the COVID-19 pandemic. Their support was instrumental in helping me navigate through the first year of my doctorate.

A special thank you goes to my friends, whom I affectionately call my co-advisors, Gabriel de Santana and Edison Cuba. They were instrumental in helping me clarify doubts I had in pure mathematics throughout my work, and their encouragement was immensely motivating. During moments of exhaustion from the demanding day-to-day research, I am also grateful to my friend Pedro Godoi for his invaluable assistance with programming-related queries. Additionally, I extend my thanks to my friends at IMECC who contributed directly or indirectly to this thesis, including Roberto, Renata, Mariane, Danielzinho, Paulo, Dhuly, Erivaldo, Lohan, and others.

This study was financed in part by the Coordenação de Aperfeiçoamento de Pessoal de Nível Superior - Brasil (CAPES) - Finance Code 001.

Resumo

Esta tese centra-se na investigação analítica e numérica de um par de equações de transporte bidimensionais não-lineares e não-locais. Uma delas é bem conhecida, a equação quase-geostrófica de superfície. A outra é uma tentativa de generalizar uma lei de conservação unidimensional adicionando uma dimensão espacial, que chamamos uma lei de conservação com velocidade parcialmente não local. No estudo analítico, obtemos a boa colocação da equação quase-geostrófica de superfície inviscida e dessa lei de conservação com velocidade parcialmente não local dentro da estrutura dos espaços Besov-fracos-Morrey modificado e dos espaços de Besov clássico, respectivamente. Por outro lado, para a investigação numérica, empregamos aproximações para os operadores não-locais presentes em cada uma dessas equações de transporte e formulamos o método Lagrangiano-Euleriano 2D totalmente discreto para leis de conservação não local. Portanto, do ponto de vista computacional, fornecemos evidências numéricas para os aspectos teóricos e conduzimos uma investigação numérica sobre os critérios que regem a explosão do tipo de concentração em termos de concentração de massa, atenuação do tipo de regularização, a formação de singularidades e a emergência de gradientes abruptos em soluções para a equação quase-geostrófica de superfície e dessa lei de conservação com velocidade parcialmente não local.

Palavras-chave: Lei de conservação não local; Potencial de Riesz; Transformada de Hilbert; Transformada de Riesz; Superfície quase-geostrófica; Espaços de Besov; Espaços Besov-fracos-Morrey modificados; Estudo analítico-computacional; Superfícies não locais sem fluxo; Método Lagrangiano-Euleriano 2D não local totalmente discreto;

Abstract

This thesis focuses on the analytical and numerical investigation of a pair of nonlinear and nonlocal two-dimensional transport equations. One of them is well-known, the surface quasi-geostrophic equation. The other is an attempt to generalize a one-dimensional conservation law by adding a spatial dimension, which we call a conservation law with partially nonlocal velocity. In the analytical study, we obtain the well-posedness of the inviscid surface quasi-geostrophic equation and this conservation law with partially nonlocal velocity within the framework of modified Besov-weak-Morrey spaces and classical Besov spaces, respectively. On the other hand, for the numerical investigation, we employ approximations for the nonlocal operators present in each of these transport equations and formulate the 2D fully-discrete Lagrangian-Eulerian method. Therefore, from a computational standpoint, we provide numerical evidence for the theoretical aspects and conduct a numerical investigation into the criteria governing the attenuation of regularization type, the formation of singularities, and the emergence of abrupt gradients in solutions for the surface quasi-geostrophic equation and this conservation law with partially nonlocal velocity.

Keywords: Nonlocal conservation law; Riesz potential; Hilbert transform; Riesz transform; Surface quasi-geostrophic; Besov spaces; Modified Besov-weak-Morrey spaces; Analytical-computational study; Nonlocal no-flow surfaces; Nonlocal 2D fully-discrete Lagrangian-Eulerian method.

List of Figures

Figure 1 – Two-dimension cell, $R_{i,j}$ -cell.	59
Figure 2 – The construction of the control volume for the Lagrangian-Eulerian scheme $D_{i,j}^n$	70
Figure 3 – Location of $c_{i,j}$ coefficients.	71
Figure 4 – Motivation for the construction of $c_{i,j}$ coefficients.	72
Figure 5 – Numerical simulation for $\partial_t \theta + \nabla \cdot (\theta \Lambda_1^{\alpha-1} \mathcal{H}_1 \theta, \theta \Lambda_2^{\alpha-1} \mathcal{H}_2 \theta) = 0$ with a Gaussian initial data, $\alpha = 0.5$ and mesh $m = 512$ for a sequence of times $T = 0, 1, 3, 10$. On the top, you can observe a decrease in height and the initiation of diffusion in the numerical solution as time evolves, while on the bottom the numerical solution a shown diffusion-smooth and reduction in height as time evolves. Evidence of attenuation of regularization type.	82
Figure 6 – Numerical simulation for $\partial_t \theta + \nabla \cdot (\theta \Lambda_1^{\alpha-1} \mathcal{H}_1 \theta, \theta \Lambda_2^{\alpha-1} \mathcal{H}_2 \theta) = 0$ with a Gaussian initial data, $\alpha = 0.5$ and mesh $m = 1024$ for a sequence of times $T = 0.2, 1, 3, 5$. On the top, you can observe a decrease in height and the initiation of a diffusion in the numerical solution as time evolves, while on the bottom the numerical solution a shows a diffusion-smooth and minimal reduction in height as time evolves. Evidence of attenuation of regularization type.	83
Figure 7 – Numerical simulation for $\partial_t \theta - \nabla \cdot (\theta \Lambda_1^{\alpha-1} \mathcal{H}_1 \theta, \theta \Lambda_2^{\alpha-1} \mathcal{H}_2 \theta) = 0$ with a Gaussian initial data, $\alpha = 0.5$ and mesh $m = 512$ for a sequence of times $T = 0, 0.4, 1.5, 1.9, , 2, 2.1$. On the top, you can observe an increase in height and the initiation of concentration in the numerical solution as time progresses. In the middle, the numerical solution shows both concentration and an increasing height as time evolves. At the bottom, the approximate solution exhibits concentration and a rapid increase in height as time progresses. Evidence of blow-up of concentration type.	85
Figure 8 – Numerical simulation for $\partial_t \theta + \nabla \cdot (\theta \Lambda_1^{\alpha-1} \mathcal{H}_1 \theta, \theta \Lambda_2^{\alpha-1} \mathcal{H}_2 \theta) = 0$ with a weak Morrey initial data, $\alpha = 0.5$ and mesh $m = 100$ for a sequence of times $T = 0.0001, 0.1, 1, 4$. To better visualize the qualitative behavior, we keep the Z axis fixed. On the top, you can observe a decrease in height and the initiation of diffusion in the numerical solution as time evolves, while on the bottom the numerical solution shows a diffusion-smooth and minimal reduction in height as time evolves. Evidence of attenuation of regularization type.	87

Figure 9 – Numerical simulation for $\partial_t \theta + \nabla \cdot (\theta \Lambda_1^{\alpha-1} \mathcal{H}_1 \theta, \theta \Lambda_2^{\alpha-1} \mathcal{H}_2 \theta) = 0$ with a Gaussian initial data, $\alpha = 0.5$ and mesh $m = 250$ for a sequence of times $T = 0, 0.1, 2, 8$. On the top, you can observe a decrease in height and the initiation of diffusion in the numerical solution as time evolves, while on the bottom, the numerical solution shows a diffusion-smooth and minimal reduction in height as time evolves. Evidence of attenuation of regularization type.	88
Figure 10 – Numerical simulation for $\partial_t \theta + \nabla \cdot (\theta \Lambda_1^{\alpha-1} \mathcal{H}_1 \theta, \theta \Lambda_2^{\alpha-1} \mathcal{H}_2 \theta) = 0$ with a Gaussian initial data, $\alpha = 0.5$ and mesh $m = 512$ for a sequence of times $T = 0.0001, 0.001, 0.02, 0.024$. This simulation is divided into two columns, with simulations in the right column being a zoom of the simulations in the left column close to the origin, aiming to see the evolution in the singularity of the numerical solution. We have evidence of blow-up of concentration-type.	90
Figure 11 – Numerical simulation for $\partial_t \theta + \nabla \cdot (-\theta \Lambda_2^{\alpha-1} \mathcal{H}_2 \theta, \theta \Lambda_1^{\alpha-1} \mathcal{H}_1 \theta) = 0$ with a Gaussian initial data, $\alpha = 0.5$ and mesh $m = 128$ for a sequence of times $T = 0, 10, 50, 70$. In the left column, initially, the height of the numerical solution begins to grow, rotating counterclockwise and forming steeper gradients. In the following times, the height decreases and continues, forming steeper gradients as time evolves. Meanwhile, the pictures in the right column, represent the level sets of the surfaces found at the top. Evidence of attenuation with formation of abrupt gradients.	93
Figure 12 – Numerical simulation for $\partial_t \theta + \nabla \cdot (-\theta \Lambda_2^{\alpha-1} \mathcal{H}_2 \theta, \theta \Lambda_1^{\alpha-1} \mathcal{H}_1 \theta) = 0$ with a $g(x, y)$ initial data, $\alpha = 0.5$ and mesh $m = 128$ for a sequence of times $T = 0, 1, 4$. In the left column, the height of four peaks decreases forming two abrupt gradients in the opposite peaks as time evolves. Meanwhile, the pictures in right column, represent the level sets of the surfaces found at the top. Evidence of attenuation with formation of abrupt gradients.	94
Figure 13 – Numerical simulation for $\partial_t \theta + \nabla \cdot (-\theta \Lambda_2^{\alpha-1} \mathcal{H}_2 \theta, \theta \Lambda_1^{\alpha-1} \mathcal{H}_1 \theta) = 0$ with a $h(x, y)$ initial data, $\alpha = 0.5$ and mesh $m = 128$ for a sequence of times $T = 0, 10, 100$. In the left column, the height of the two peaks decreases, forming steeper gradients and coming together as time evolves. Meanwhile, the pictures in the right column, represent the level sets of the surfaces found at the top. Evidence of attenuation with formation of abrupt gradients.	95

Figure 14 – Numerical simulation for $\partial_t \theta + \nabla \cdot (-\theta \Lambda_2^{\alpha-1} \mathcal{H}_2 \theta, \theta \Lambda_1^{\alpha-1} \mathcal{H}_1 \theta) = 0$ with a $g(x, y)$ initial data, $\alpha = 0.5$ and mesh $m = 128$ for a sequence of times $T = 0, 1.2, 3$. In the left column, initially, the height of the two peaks decreases and forms steeper gradients. In the following times, the height increases and forms an abrupt gradient in each peak as time evolves. In this case, the peaks do not join. Meanwhile, the pictures in the right column represent the level sets of the surfaces found at the top. Evidence of the formation of an abrupt gradient without attenuation. 96

Figure 15 – Tracking some level sets of the numerical solution of $\partial_t \theta + \nabla \cdot (-\theta \Lambda_2^{\alpha-1} \mathcal{H}_2 \theta, \theta \Lambda_1^{\alpha-1} \mathcal{H}_1 \theta) = 0$ with Gaussian initial data, $\alpha = 0.5$ and mesh $m = 128$ for a sequence of times $T = 0, 10, 50, 70$. In the left column, we attempt to trace a level curve at half the initial data is height. As time progresses, this level curve loses convexity and separates into two different level curves. Meanwhile, in the pictures in the right column, the level curves are positioned at the top of the initial data. Here, the level curves also lose convexity and split into two distinct groups of level curves. 98

Figure 16 – The two figures at the top represent the last two simulations described in Figure 15. In [25] the authors study the geometric properties of SQG sharp fronts and α -patches; in this paper the SQG is given by $\partial_t \theta(x, y, t) + u(x, y, t) \cdot \nabla \theta(x, y, t) = 0$ with $u = (-\mathcal{R}_2 \theta, \mathcal{R}_1 \theta)$. The four figures at the bottom were taken from [25] and are simulations of the evolution of the ellipses with, the patch with initial data $z(x) = (\cos(x); 3\sin(x))$ displays a combination of a rotating motion with a smaller scale oscillation which leads to loss of convexity. As we can see, both simulations start with a regular and convex geometric figure; as time passes, these simulations lose convexity and form two types of deformed ellipses. 99

Figure 17 – The laplacian of Gaussian 2D Δu , where $u(x_1, x_2) = \frac{1}{\pi} e^{-\frac{x_1^2 + x_2^2}{8}}$ 125

Figure 18 – Numerical approximation of the Riesz transform \mathcal{R}_1 for Laplacian of Gaussian, considering a sequence of meshes $m = 16, 32, 64, 128, 256$. . . 126

Figure 19 – Numerical approximation of the Riesz transform \mathcal{R}_2 for Laplacian of Gaussian, considering a sequence of meshes $m = 16, 32, 64, 128, 256$. . . 127

Figure 20 – Numerical approximation simulation of the Riesz transform for a sequence of meshes $m = 16, 32, 64, 128, 256$. In the last picture we plot $-\frac{\partial^2 u}{\partial x_i \partial x_j}$. However, in the other pictures, we have a numerical approximation of the Riesz transform $\mathcal{R}_i \mathcal{R}_j(\Delta u)$, where $u(x_1, x_2) = \frac{1}{\pi} e^{-\frac{x_1^2 + x_2^2}{8}}$. 128

Figure 21 – Plot of the numerical error for the approximation of the Riesz transform to equation (4.46).	129
Figure 22 – Numerical simulations for $\partial_t \theta + \nabla \cdot (-\theta \mathcal{R}_2 \theta, \theta \mathcal{R}_1 \theta) = 0$ with a Gaussian initial data, $\alpha = 0.5$ and mesh $m = 64$ for a sequence of times $T = 0, 1, 10, 100$. On the top, you can observe a decrease in height of the approximate solution as time evolves, while on the bottom the approximate solution a shown diffusion and reduction in height as time evolves. Evidence of attenuation of regularization type.	132
Figure 23 – Numerical simulations for $\partial_t \theta + \nabla \cdot (-\theta \mathcal{R}_2 \theta, \theta \mathcal{R}_1 \theta) = 0$ with a Gaussian initial data, $\alpha = 0.5$ and mesh $m = 128$ for a sequence of times $T = 0, 0.1, 1, 10$. At the top, you can observe a decrease in height of the approximate solution as time evolves, while at the bottom, the approximate solution exhibits diffusion and a reduction in height over time. This provides evidence of an attenuation of a regularization type.	133
Figure 24 – Numerical simulations for $\partial_t \theta + \nabla \cdot (-\theta \mathcal{R}_2 \theta, \theta \mathcal{R}_1 \theta) = 0$ with the initial data $f(x, y) = \frac{3xy}{2\pi} \exp\{-(x^2 + y^2)/5\}$, $\alpha = 0.5$ and mesh $m = 128$ for a sequence of times $T = 0.0001, 0.1, 1, 10$. At the top, you can observe a decrease in height of the approximate solution as time evolves, while at the bottom, the approximate solution exhibits diffusion and a reduction in height over time. This provides evidence of an attenuation of a regularization type.	134

List of Tables

Table 1 – Error table for the numerical approximation of the Riesz transform to equation (4.46).	126
---	-----

Contents

1	Introduction	15
1.1	State of the Art	16
1.2	Motivation Examples	18
1.3	Aims and Objectives	19
1.3.1	Specific objectives for a conservation law with partially nonlocal velocity	19
1.3.2	Specific objectives for the SQG	19
1.4	Meaningful Contributions of the Thesis	20
1.5	Organization	21
2	Preliminaries and Basic Facts	22
2.1	Littewood-Paley Decomposition	22
2.2	Generalized Besov Spaces	23
2.2.1	Classical Besov spaces	24
2.2.2	The modified Besov-weak-Morrey space	25
3	A Conservation Law with Partially Nonlocal Velocity	28
3.1	Bernstein-type Inequality to Nonlocal Partial Operators in Besov spaces	29
3.2	Commutator Estimates in Besov Spaces	34
3.3	On the Well-Posedness of a Conservation Law with Partially Nonlocal Velocity in Besov Spaces	43
3.4	Numerical Study	56
3.4.1	The nonlocal No-Flow curve and the nonlocal Lagrangian-Eulerian approach for a conservation law with partially nonlocal velocity	58
3.4.2	Approximation of the partial Hilbert transform	59
3.4.3	Approximation of the partial Riesz potential	62
3.4.4	The No-Flow Curve in the Hyperbolic Conservation Law, the Simplest Case and Some Advantages	67
3.4.5	Numerical Experiments with the Lagrangian-Eulerian with Conservation Properties	75
3.4.6	A Lagrangian-Eulerian scheme for a conservation law with partially nonlocal velocity	75
3.5	Numerical Simulations for a Conservation Law with Partially Nonlocal Velocity	78
3.5.1	Simulations for measure initial data	81
3.5.2	Simulations for measured data of weak-Morrey type	86
3.6	The Model of a Conservation Law with Partially Nonlocal Velocity with Rotation	91

3.6.1	Numerical simulations for the model a conservation law with partially nonlocal velocity with rotation	91
3.7	Geometric Properties of Level Sets in the Model a conservation law with partially nonlocal velocity with Rotation	97
4	The Surface Quasi-Geostrophic Equation	100
4.1	Commutator Estimates in Modified Besov-weak-Morrey Spaces	101
4.2	On the Well-Posedness of the SQG in the Modified Besov-Morrey Spaces .	109
4.3	Numerical Study	117
4.3.1	A Lagrangian–Eulerian scheme for the SQG	118
4.3.2	Approximation of the Riesz transform	121
4.3.3	Numerical Simulations for the SQG	130
5	Conclusions and Perspectives	135
5.1	Concluding Remarks	136
5.2	Outlook for Future Work	138
	BIBLIOGRAPHY	140

1 Introduction

The present thesis aims to conduct an analytical-numerical study of two hyperbolic-type conservation laws; these are nonlinear nonlocal two-dimensional transport equations. One of them is the inviscid surface quasi-geostrophic equation, SQG (1.1). The other is an attempt to generalize a one-dimensional conservation law by adding a spatial dimension and addressing it dimension by dimension through spatial domain decomposition (in the spirit of an operator splitting methodology), which we call a conservation law with partially nonlocal velocity (1.3). These nonlocal transport equations are presented below.

The SQG in conservative form is given by

$$\begin{cases} \partial_t \theta + \nabla \cdot (\theta v) = 0 \\ \theta(x, 0) = \theta_0(x), \end{cases} \quad (1.1)$$

where $\theta = \theta(x, t)$ is a scalar function, $\theta : \mathbb{R}^2 \times [0, \infty) \longrightarrow \mathbb{R}$, which represents the temperature potential of the fluid, $v = (v_1, v_2)$ denote a velocity field such that $\nabla \cdot v = 0$ and the relationship between v and θ is through the Riesz transform \mathcal{R} ,

$$v = \mathcal{R}^\perp \theta = (-\mathcal{R}_2 \theta, \mathcal{R}_1 \theta) = (-\partial_2 (-\Delta)^{-\frac{1}{2}} \theta, \partial_1 (-\Delta)^{-\frac{1}{2}} \theta).$$

Here, the operator Δ is the Laplacian. We can also write the Riesz transform in classical form, that is, the integral singular operator [65],

$$\mathcal{R}_j(\theta)(x, t) = \frac{1}{2\pi} \text{p.v.} \int_{\mathbb{R}^2} \frac{(x_j - y_j)}{|x - y|^3} \theta(y, t) dy. \quad (1.2)$$

where $x = (x_1, x_2)$ and $y = (y_1, y_2)$ be elements in \mathbb{R}^2 , $t > 0$ and $j = 1, 2$.

On the other hand, a conservation law with partially nonlocal velocity is given by

$$\begin{cases} \partial_t \theta \pm \nabla \cdot (\theta v) = 0, \text{ with } v = (\Lambda_1^{\alpha-1} \mathcal{H}_1 \theta, \Lambda_2^{\alpha-1} \mathcal{H}_2 \theta) \\ \theta(x, 0) = \theta_0(x), \end{cases} \quad (1.3)$$

where $\theta : \mathbb{R}^2 \times [0, \infty) \longrightarrow \mathbb{R}$ is a scalar function, the initial data, $\theta_0(x)$, is not necessarily regular, moreover \mathcal{H}_i and $\Lambda_i^{\alpha-1}$ with $i = 1, 2$ are the nonlocal operators, the partial Hilbert transform and the partial Riesz potential respectively, which will be defined later.

In the analytical study, we obtain the well-posedness of the SQG and of a conservation law with partially nonlocal velocity model within the framework of modified Besov-weak-Morrey spaces and classical Besov spaces, respectively. For the numerical study, we have devised an enhanced, fully-discrete Lagrangian-Eulerian scheme to obtain

the numerical solution of these transport equations. Furthermore, we present potential theoretical insights based on numerical observations of the SQG and of a conservation law with partially nonlocal velocity.

1.1 State of the Art

This research introduces a novel approach to studying a two-dimensional nonlinear and nonlocal transport equation. To achieve this, we define partial nonlocal operators associated with the velocity field of this transport equation. This involves fixing one of the variable's coordinates and applying the nonlocal operator to the total variable, with one of them fixed. Consequently, we obtain an operator acting solely in one direction. It is important to note that this technique needs to be applied in both directions to cover the entire variable space. Subsequently, we apply this approach to the transport equation across the defined domain. We utilize this novel approach to analyze the SQG, giving rise to the emergence of a conservation law with partially nonlocal velocity. Additionally, we obtain the well-posedness of these nonlocal transport equations within the framework of Besov-type spaces.

The SQG comes from atmospheric science and describes the evolution of the potential temperature on the surface. Therefore, this equation describes the evolution of cold and warm air fronts in a thin layer in the atmosphere. For this reason, the SQG has applications in meteorology and oceanography, playing an important role in weather forecasting and improving the understanding of the temperature evolution of geophysical flows and, in particular, frontogenesis in the case of atmospheric flows [27, 31].

Constantin, Majda, and Tabak introduced the SQG to the mathematical community in [31], conducting numerical and analytical studies. Additionally, the SQG exhibits an analogy with the 3D Euler equations. So far, the mathematical study of the surface quasi-geostrophic equation has been divided into two significant cases: the inviscid case and the dissipative case.

The first inviscid case (1.1) is probably the most straightforward dynamical scalar equation. However, the global regularity problem remains open. In [31], it was established the local well-posedness and blow-up criterion of (4.1) in Sobolev spaces. The exciting fact about [31] is that the authors also make a numerical study of the problem besides being the first analytical study. Subsequently, there are various results available in different function spaces. For instance, on the Triebel-Lizorkin spaces in [26], on the Besov spaces in [67], on the Triebel-Lizorkin-Lorentz spaces in [71], on the Besov-Lorentz spaces in [73]. Recently, [72] demonstrated the well-posedness and blow-up criterion for the generalized surface quasi-geostrophic equation in Sobolev spaces.

The second case considers the dissipative term $\kappa(-\Delta)^\gamma \theta$ in the equation (1.1),

$$\partial_t \theta + \nabla \cdot (\theta v) = \kappa(-\Delta)^\gamma \theta.$$

In this case, it was studied the global well-posedness problem. More precisely, the study on the dissipative surface quasi-geostrophic equation unfolds in three directions: the sub-critical case $\gamma > 1/2$, the critical case $\gamma = 1/2$, and the super-critical case $\gamma < 1/2$. For more details of the sub-critical case, the reader should consult [33] and [62]. In [30], it addressed the global regularity issue for the critical case; in particular, it obtained a global existence result of the solution under a smallness condition on the initial data. Since then, global existence results for small initial data have been obtained in various functional settings, e.g., in Sobolev spaces in [34, 57], Besov spaces in [29, 1, 28, 70]. Two papers exist that resolve entirely the global regularity problem without a smallness condition. One is in [52] and the other in [24].

As noted earlier, the well-posedness theory of the surface quasi-geostrophic equation in the dissipative case has undergone thorough investigation in previous years. Numerous authors have successfully addressed global well-posedness, particularly for critical cases, as documented in the references [52, 24, 32, 1]. Nevertheless, limited attention has been given to the super-critical case, with only a handful of papers, such as [37, 51, 64], delving into the discussion of eventual regularity.

Recently, the dissipative case has been examined in various types of spaces, with intermittent regularities discussed in the following papers [53, 55, 68, 21, 66, 20, 15, 18].

In this research, we prove the well-posedness of the SQG in modified Besov-weak-Morrey spaces; this space was defined in [42] and in that work, the authors prove the well-posedness of the n -dimensional Euler Equation.

On the other hand, considering that a conservation law with partially nonlocal velocity is our proposed model that has a new structure, as a first study, we show the well-posedness this model in classical Besov spaces.

Furthermore, this research presents new advances in numerical schemes designed to solve two-dimensional nonlocal transport equations numerically. The proposed method is based on the concept of Lagrangian-Eulerian No-Flow curves. This approach has been previously employed in fully-discrete Lagrangian-Eulerian schemes, as evidenced by existing literature [9, 6]. The schemes presented in this thesis are suitable for numerically studying nonlocal transport equations with initial data that are not necessarily regular. In this context, the frontal advance and novelty in terms of the Lagrangian-Eulerian approach is the generalization of the underlying concept of *local no-flow curves* to *nonlocal no-flow curves* linked to both a conservation law with partially nonlocal velocity (hereafter, 1D+1/2) and the inviscid surface quasi-geostrophic equation.

1.2 Motivation Examples

The motivation for this thesis initially arises from the study of [38] and [2]. In these works, the authors study the global well-posedness and finite-time blowing-up of solutions for a nonlinear one-dimensional transport equation with nonlocal velocity

$$u_t - (u\mathcal{H}(u))_x = \nu u_{xx},$$

with $\nu > 0$ and measure initial data. Such a model arises in fluid mechanics and vortex-sheet problems, among other situations. Its nonlocal feature comes from the presence of a singular integral operator Hilbert transform \mathcal{H} in the velocity field. For the viscous case $\nu > 0$, the authors obtain an explicit condition on the size of the initial data, which implies the global well-posedness in the framework of pseudo-measure spaces. Furthermore, they numerically study the blow-up of concentration type and global diffusion-smooth behavior of solutions. In the inviscid case ($\nu = 0$), simulations of the model $u_t - (u\mathcal{H}(u))_x = 0$ provide evidence that the solution exhibits a blow-up of concentration type with mass preservation. Conversely, an attenuation effect is observed for the model with the opposite sign in the flux $u_t + (u\mathcal{H}(u))_x = 0$, initialized with any non-trivial positive measure as initial data. The solution manifests the behavior already described in both cases; this numerical solutions were obtained by the Lagrangian-Eulerian method.

In the same line, in the work [47], the study of the numerical solution of the same one-dimensional nonlinear and nonlocal transport equation was continued, but with the addition of the operator Riesz potential in the velocity field. In fact, the author considers the model

$$u_t \pm (u\Lambda^{\alpha-1}\mathcal{H}u)_x = 0,$$

with $0 < \alpha < 1$, getting similar results to the previous one.

The two presented one-dimensional nonlinear and nonlocal equations can be interpreted as the 1D quasi-geostrophic equation. In concrete, [38] and [47] study one-dimensional versions of the SQG that involve the Hilbert transform and Riesz potential operators from both numerical and analytical perspectives, initially motivated by the numerical part and giving interesting and novel results in the analytical part. From a computational point of view, a natural way to transit to the two-dimensional case is to consider an intermediate model, which we call the a conservation law with partially nonlocal velocity. This model is defined by a conservation law that contains a vector velocity field with components defined by partial nonlocal operators, i.e., one-dimensional operators acting on each axis separately.

1.3 Aims and Objectives

The general objectives are to study two nonlocal transport equations analytically and numerically, namely the SQG and a conservation law with partially nonlocal velocity. Additionally, leveraging numerical observations, we aim to propose new theoretical insights that enhance our understanding of these two transport equations.

1.3.1 Specific objectives for a conservation law with partially nonlocal velocity

Analytical:

- Study the well-posedness of the solution of a conservation law with partially nonlocal velocity and a conservation law with partially nonlocal velocity with rotation in classical Besov spaces.
- Study the Bernstein's inequality for the nonlocal partial operators.
- Study the estimates of commutator operator in classical Besov spaces for a conservation law with partially nonlocal velocity.

Numerical:

- Study the implementation of fully-discrete Lagrangian–Eulerian method for a conservation law with partially nonlocal velocity.
- Study the numerical approximations from the partial Riesz potential and the partial transform of Hilbert.
- Study the numerical solution of a conservation law with partially nonlocal velocity and positive flux: $\partial_t \theta + \nabla \cdot (\theta \Lambda_1^{\alpha-1} \mathcal{H}_1 \theta, \theta \Lambda_2^{\alpha-1} \mathcal{H}_2 \theta) = 0$.
- Study the numerical solution of a conservation law with partially nonlocal velocity and negative flux: $\partial_t \theta - \nabla \cdot (\theta \Lambda_1^{\alpha-1} \mathcal{H}_1 \theta, \theta \Lambda_2^{\alpha-1} \mathcal{H}_2 \theta) = 0$.

Numerical for a conservation law with partially nonlocal velocity with rotation:

- Study the numerical solution of a conservation law with partially nonlocal velocity with rotation

$$\partial_t \theta + \nabla \cdot (-\theta \Lambda_2^{\alpha-1} \mathcal{H}_2 \theta, \theta \Lambda_1^{\alpha-1} \mathcal{H}_1 \theta) = 0.$$

1.3.2 Specific objectives for the SQG

Analytical:

- Study the well-posedness of the SQG in the modified Besov-weak-Morrey spaces.

Numerical:

- Study the implementation of fully-discrete Lagrangian–Eulerian method for the SQG.
- Study the numerical approximations and validation of the Riesz transform.
- Study the numerical solution of the SQG: $\partial_t \theta + \nabla \cdot (-\theta \mathcal{R}_2 \theta, \theta \mathcal{R}_1 \theta) = 0$.

1.4 Meaningful Contributions of the Thesis

We summarize the main contributions of this work in the following bullet points:

- One of the principal contributions of this thesis is a novel approach to studying a two-dimensional nonlocal transport equation. This involves defining nonlocal operators connected to the velocity field in the form of partial nonlocal operators. Consequently, this leads to a new conservation law with partially nonlocal velocity and a novel structure and introduces new mathematical properties. Furthermore, the computational cost in numerical simulations is significantly lower compared to the original equation.
- This new approach was employed to conduct numerical and analytical investigations of the SQG, resulting in the formulation of a new equation referred to as a conservation law with partially nonlocal velocity. In the analytical part, as an initial exploration of this model, we successfully established its well-posedness in the classical Besov spaces. A noteworthy contribution in this context was the demonstration of the Bernstein inequality, considering nonlocal partial operators (the partial Hilbert transform and the partial Riesz potential), and the estimates of two commutator operators were also made considering these nonlocal partial operators. The contribution in the numerical part, in turn, was that we successfully implemented the fully-discrete Lagrangian–Eulerian method for this model and the numerical approximation of the partial nonlocal operators involved in the model. Furthermore, the numerical simulations of a conservation law with partially nonlocal velocity show similar qualitative behaviors to the 1D case of SQG that were studied in [2] and [47]. The other outstanding contribution is that by rotating the coordinates of the velocity field, a conservation law with partially nonlocal velocity with rotation is obtained; we observed that the numerical simulations for this model closely resemble those obtained for the SQG in [31, 46, 25]. We might be dealing with a prototype for SQG.

- Another significant contribution in the analytical part is the demonstration of the well-posedness of the SQG in a novel space requiring less regularity, namely, the modified Besov weak-Morrey space. This broadens the set of initial data for which SQG possesses a unique solution. In the numerical aspect, our contribution involves successfully implementing the 2D fully-discrete Lagrangian-Eulerian method for the SQG. Additionally, we approximated and validated the Riesz Transform numerically. Furthermore, we conducted the first numerical simulations for the SQG, considering three different types of initial data.

1.5 Organization

The remaining content of this work is structured as follows: Chapter 2, is intended for the preliminaries and basic results; here we will introduce the classical Besov spaces and the modified Besov-weak-Morrey spaces along with the elemental properties that will be used in the following chapters. In Chapter 3, is intended for the numerical and analytical study of a conservation law with partially nonlocal velocity and a conservation law with partially nonlocal velocity with rotation. For the analytical study, we furnish the proof of the well-posedness of the solution for this model within the framework of classical Besov spaces. On the numerical study, we develop the fully-discrete Lagrangian-Eulerian numerical scheme for a conservation law with partially nonlocal velocity, as well as the numerical approximations arising from nonlinear and nonlocal operators, the partial Riesz potential and the partial Riesz transform and we present the numerical simulations considering both measured initial data and measured initial data of weak Morrey type. In Chapter 4, we embark on a study analogous to the preceding chapter, by focusing on the SQG equation. Here, we aim to prove the well-posedness of the solution for this equation within the modified Besov weak-Morrey spaces framework. Furthermore, we present a numerical approximation with validation of the Riesz transform, and the numerical simulations measured initial data. Finally, in Chapter 5, we present conclusions and future perspectives.

2 Preliminaries and Basic Facts

In this chapter, we define the Besov and the modified Besov-weak-Morrey spaces and present some of their fundamental properties. These properties serve as the foundation for the proofs of a conservation law with partially nonlocal velocity and the SQG, which will be discussed in the following chapters.

2.1 Littlewood-Paley Decomposition

The Littlewood-Paley decomposition is a fundamental concept in Harmonic analysis, especially in exploring Fourier analysis and its diverse applications. This decomposition involves expressing a single function as a sum of functions with distinct frequencies. It is an indispensable tool for deciphering the local behavior of functions based on their frequency content. For more details, see [19], [45], [42], [70]. Widely applied across various mathematical domains, including partial differential equations, probability theory, and number theory, the Littlewood-Paley decomposition allows a comprehensive analysis of the functions.

In order to introduce the Littlewood-Paley decomposition, we write for each $j \in \mathbb{Z}$

$$D_j = \{\xi \in \mathbb{R}^n : \frac{3}{4}2^j \leq |\xi| \leq \frac{8}{3}2^j\} \quad \text{and} \quad B_j = \{\xi \in \mathbb{R}^n : |\xi| \leq \frac{4}{3}2^j\}.$$

Moreover, we consider a non-negative radial function $\varphi \in C_c^\infty(\mathbb{R}^n)$ satisfying $\text{supp}(\varphi) \subset D_0$ and

$$\sum_{j \in \mathbb{Z}} \varphi_j(\xi) = 1, \forall \xi \in \mathbb{R}^n \setminus \{0\} \quad \text{where} \quad \varphi_j(\xi) := \varphi(2^{-j}\xi) \quad \text{or} \quad \hat{\varphi}_j(\xi) = 2^{2j}\hat{\varphi}(2^j\xi),$$

note that, $\text{supp}\varphi_j \subset D_j$ for all $j \in \mathbb{Z}$.

Furthermore, define ψ as $\psi(\xi) := \sum_{j \leq -1} \varphi_j(\xi)$, if $\xi \neq 0$, and $\psi(0) := 1$. So, $\psi \in C_c^\infty(\mathbb{R}^n \setminus \{0\})$, $\text{supp}(\psi) \subset B_0$ and

$$\psi(\xi) + \sum_{j \geq 0} \varphi_j(\xi) = 1, \quad \forall \xi \in \mathbb{R}^n.$$

For simplicity in the calculations, we also define the functions $\tilde{\varphi}_j := \sum_{|k-j| \leq 1} \varphi_k$, $\tilde{\psi} = \psi + \varphi$ and the set $\tilde{D}_j = D_{j-1} \cup D_j \cup D_{j+1}$. Then, in D_j , we have that $\tilde{\varphi}_j \equiv 1$, $\varphi_j = \tilde{\varphi}_j \varphi_j$, for all $j \in \mathbb{Z}$, and $\psi = \tilde{\psi} \psi$. The localization operators Δ_j , $\bar{\Delta}_j$ and S_j are

defined as

$$\begin{aligned}
\Delta_j f &= \varphi_j(D)f = \mathcal{F}^{-1} \left(\varphi_j \hat{f} \right) = 2^{jn} \left(\mathcal{F}^{-1} \varphi(2^j \cdot) \right) * f, \quad \forall j \in \mathbb{Z}, \\
\bar{\Delta}_j f &= \Delta_j f, \quad \text{if } j \geq 0, \\
\bar{\Delta}_{-1} f &= \psi(D)f = \mathcal{F}^{-1} \left(\psi \hat{f} \right) = \mathcal{F}^{-1}(\psi) * f, \\
\bar{\Delta}_j f &= 0, \quad \text{if } j \leq -2, \\
S_j f &= \psi_j(D)f = \mathcal{F}^{-1} \left(\psi_j \hat{f} \right) = 2^{jn} \left(\mathcal{F}^{-1} \psi(2^j \cdot) \right) * f, \quad \forall j \in \mathbb{Z},
\end{aligned}$$

where $\psi_j(\xi) = \psi(2^{-j}\xi)$. From the relations of supports φ_j and ψ_j we will get the orthogonality of localization operators

$$\Delta_j \Delta_k f = 0, \quad \text{if } |j - k| \geq 2, \quad (2.1)$$

$$\Delta_j (S_{k-2} g \Delta_k f) = 0, \quad \text{if } |j - k| \geq 3. \quad (2.2)$$

The Littlewood-Paley decomposition of f is obtained through the operators S_k and Δ_j , this is, $f = S_k f + \sum_{j \geq k} \Delta_j f$, for all $f \in \mathcal{S}'(\mathbb{R}^n)$ and $k \in \mathbb{Z}$. Moreover, if $\lim_{k \rightarrow -\infty} S_k f = 0$ in \mathcal{S}' (as in the case for $f \in L^\infty \setminus \{\text{constants}\}$), then the equality $f = \sum_{j \in \mathbb{Z}} \Delta_j f$ is called the homogeneous Littlewood-Paley decomposition of f [54]. On the other hand, using Bony's paraproduct [22], it follows that for $f, g \in \mathcal{S}'$ we can define the product $f \cdot g$ as

$$fg = T_f g + T_g f + R(f, g), \quad (2.3)$$

$$\text{where } T_f g = \sum_{j \geq 2} S_{j-2} f \bar{\Delta}_j g \quad \text{and} \quad R(f, g) = \sum_{j \geq -1} \bar{\Delta}_j f \sum_{|j-j'| \leq 2} \bar{\Delta}_{j'} g.$$

2.2 Generalized Besov Spaces

This section is dedicated to collecting basic notations, definitions, tools, and properties about some operators and functional spaces that will be useful for our ends.

The following definitions and results were obtained from [42].

Definition 1. Let $E \subset \mathcal{S}'(\mathbb{R}^n)$ be a Banach space, $1 \leq r \leq \infty$ and $s \in \mathbb{R}$. The inhomogeneous Besov- E space BE_r^s is defined as

$$BE_r^s = \left\{ f \in \mathcal{S}'(\mathbb{R}^n); \|f\|_{BE_r^s} < \infty \right\},$$

where

$$\|f\|_{BE_r^s} := \begin{cases} \left(\sum_{j \geq -1} 2^{jsr} \|\bar{\Delta}_j f\|_E^r \right)^{1/r} & \text{if } r < \infty \\ \sup_{j \geq -1} 2^{js} \|\bar{\Delta}_j f\|_E, & \text{if } r = \infty. \end{cases}$$

Similarly, the homogeneous Besov- E space $\dot{B}E_r^s$ is defined as

$$\dot{B}E_r^s = \left\{ f \in \mathcal{S}'(\mathbb{R}^n)/\mathcal{P}(\mathbb{R}^n); \|f\|_{\dot{B}E_r^s} < \infty \right\},$$

where $\mathcal{P}(\mathbb{R}^n)$ denotes the space of polynomials in \mathbb{R}^n , and

$$\|f\|_{\dot{B}E_r^s} := \begin{cases} \left(\sum_{j \in \mathbb{Z}} 2^{jsr} \|\Delta_j f\|_E^r \right)^{1/r} & \text{if } r < \infty \\ \sup_{j \in \mathbb{Z}} 2^{js} \|\Delta_j f\|_E, & \text{if } r = \infty. \end{cases}$$

2.2.1 Classical Besov spaces

The classical Besov space is a particular case when $E = L^p$ with $1 \leq p \leq \infty$, we will define it as $BE_r^s := B_{p,r}^s$ and $\dot{B}E_r^s := \dot{B}_{p,r}^s$, this is

Definition 2. Let $1 \leq r \leq \infty$ and $s \in \mathbb{R}$. The classical inhomogeneous Besov space $B_{p,r}^s$ is defined as

$$B_{p,r}^s = \left\{ f \in \mathcal{S}'(\mathbb{R}^n); \|f\|_{B_{p,r}^s} < \infty \right\},$$

where

$$\|f\|_{B_{p,r}^s} := \begin{cases} \left(\sum_{j \geq -1} 2^{jsr} \|\bar{\Delta}_j f\|_{L^p}^r \right)^{1/r} & \text{if } r < \infty \\ \sup_{j \geq -1} 2^{js} \|\bar{\Delta}_j f\|_{L^p}, & \text{if } r = \infty. \end{cases}$$

Similarly, the classical homogeneous Besov space $\dot{B}_{p,r}^s$ is defined as

$$\dot{B}_{p,r}^s = \left\{ f \in \mathcal{S}'(\mathbb{R}^n)/\mathcal{P}(\mathbb{R}^n); \|f\|_{\dot{B}_{p,r}^s} < \infty \right\},$$

where

$$\|f\|_{\dot{B}_{p,r}^s} := \begin{cases} \left(\sum_{j \in \mathbb{Z}} 2^{jsr} \|\Delta_j f\|_{L^p}^r \right)^{1/r}, & \text{if } r < \infty \\ \sup_{j \in \mathbb{Z}} 2^{js} \|\Delta_j f\|_{L^p} & \text{if } r = \infty. \end{cases}$$

The fundamental properties of classical Besov spaces are outlined in [74].

Basics proprieties of classical Besov spaces

Proposition 1. Let $s \in \mathbb{R}$, $1 \leq p \leq \infty$ and $1 \leq q \leq \infty$.

- (I) If $s > 0$, then $B_{p,r}^s = \dot{B}_{p,r}^s \cap L^p$, and $\|f\|_{B_{p,r}^s} = \|f\|_{\dot{B}_{p,r}^s} + \|f\|_{L^p}$;
- (II) If $s_1 \leq s_2$, then $B_{p,r}^{s_2} \subset B_{p,r}^{s_1}$. If $1 \leq r_1 \leq r_2 \leq \infty$, then $\dot{B}_{p,r_1}^s \subset \dot{B}_{p,r_2}^s$ and $B_{p,r_1}^s \subset B_{p,r_2}^s$;
- (III) If $s > \frac{n}{p}$, then $B_{p,r}^s \hookrightarrow L^\infty$. If $p_1 \leq p_2$, $s_1 - \frac{n}{p_1} > s_2 - \frac{n}{p_2}$, then $B_{p_1,r_1}^{s_1} \hookrightarrow B_{p_2,r_2}^{s_2}$;
- (IV) If $s > 0, p \geq 1$, then $\|uv\|_{B_{p,\infty}^s} \leq C\|u\|_{L^\infty}\|v\|_{B_{p,\infty}^s} + C\|u\|_{B_{p,\infty}^s}\|v\|_{L^\infty}$.

2.2.2 The modified Besov-weak-Morrey space

The following definitions and results were obtained from [42]. In what follows, we will define the modified weak-Morrey space and the modified Besov-weak-Morrey space. We denote by $|A|$ the measure of a Lebesgue set $A \subset \mathbb{R}^n$ for notational convenience.

Definition 3. For f a Lebesgue measurable functions in \mathbb{R}^n , the distribution function of f is the function d_f defined on $[0, \infty[$ as follows:

$$\begin{aligned} d_f : [0, \infty[&\longrightarrow \mathbb{R}^+ \\ \alpha &\longrightarrow d_f(\alpha) = |\{x \in \mathbb{R}^n : |f(x)| > \alpha\}|. \end{aligned}$$

Definition 4. For $0 < p < \infty$ the space $\text{weak-}L^p(\mathbb{R}^n) = L^{p,\infty}$, is defined as the set of all measurable functions f such that the quantity

$$\begin{aligned} \|f\|_{L^{p,\infty}} &= \inf \left\{ c > 0 : d_f(\alpha) \geq \frac{c^p}{\alpha^p}, \forall \alpha > 0 \right\} \\ &= \sup \left\{ \gamma d_f(\gamma)^{1/p} : \gamma > 0 \right\}, \end{aligned}$$

is finite.

Definition 5. For $1 < p \leq l \leq \infty$ the weak Morrey space, $WM_p^l(\mathbb{R}^n) = WM_p^l$, is defined as the set of all tempered distribution functions $f \in S'(\mathbb{R}^n)$ such that

$$\|f\|_{WM_p^l} = \sup_{x_0 \in \mathbb{R}^n, R > 0} \left\{ R^{\frac{n}{l} - \frac{n}{p}} \|f \cdot 1_{B(x_0, R)}\|_{L^{p,\infty}} \right\},$$

is finite, where $1_{B(x_0, R)}$ denotes the indicator function of the open ball $B(x_0, R)$. Note that, $\frac{n}{l} - \frac{n}{p} \leq 0$.

Definition 6. Let $1 < p \leq l \leq \infty$. The modified weak-Morrey space $W\tilde{\mathcal{M}}_p^l = W\tilde{\mathcal{M}}_p^l(\mathbb{R}^n)$ is defined as the set of all measurable functions such that

$$\|f\|_{W\tilde{\mathcal{M}}_p^l} := \sup_{x_0 \in \mathbb{R}^n} \sup_{R \geq 1} R^{\frac{n}{l} - \frac{n}{p}} \|f \cdot 1_{B(x_0, R)}\|_{L^{p,\infty}(D(x_0, R))} < \infty. \quad (2.4)$$

Definition 7. Let $1 < p \leq l \leq \infty, 1 < r \leq \infty$ and $s \in \mathbb{R}$. The inhomogeneous modified Besov-Weak-Morrey space $BW\tilde{\mathcal{M}}_{p,r}^{l,s}(\mathbb{R}^n) = BW\tilde{\mathcal{M}}_{p,r}^{l,s}$ is defined as

$$BW\tilde{\mathcal{M}}_{p,r}^{l,s} = \left\{ f \in S'(\mathbb{R}^n) : \|f\|_{BW\tilde{\mathcal{M}}_{p,r}^{l,s}} < \infty \right\},$$

where

$$\|f\|_{BW\tilde{\mathcal{M}}_{p,r}^{l,s}} := \begin{cases} \left(\sum_{j \geq -1} 2^{jsr} \|\bar{\Delta}_j f\|_{W\tilde{\mathcal{M}}_p^l}^r \right)^{1/r} & ; r < \infty, \\ \sup_{j \geq -1} 2^{js} \|\bar{\Delta}_j f\|_{W\tilde{\mathcal{M}}_p^l} & ; r = \infty. \end{cases}$$

Basics proprieties of Besov-weak-Morrey spaces

Below, we present some lemmas taken from [42] that we will use in the proof of the well-posedness; see Theorem 3.

Lemma 1. (Convolution in modified Morrey spaces) Let $1 < p \leq l \leq \infty$ and $\eta \in L^1(\mathbb{R}^n)$. Then, there exists $C > 0$ (independent of η) such that

$$\|\eta * f\|_{W\tilde{\mathcal{M}}_p^l} \leq C \|\eta\|_{L^1} \|f\|_{W\tilde{\mathcal{M}}_p^l}, \quad \text{for all } f \in W\tilde{\mathcal{M}}_p^l. \quad (2.5)$$

Lemma 2. Let $1 < p < \infty$. The Riesz transform is bounded in $W\tilde{\mathcal{M}}_p^l$.

Lemma 3 (Bernstein-type inequalities in modified Morrey spaces). Let $1 < p \leq l \leq \infty$.

1. Given $C_1 > 0$, there exists $C > 0$ such that

$$\|D^\gamma f\|_{W\tilde{\mathcal{M}}_p^l} \leq C 2^{j|\gamma|} \|f\|_{W\tilde{\mathcal{M}}_p^l}, \quad (2.6)$$

for all $j \in \mathbb{Z}$ and $f \in W\tilde{\mathcal{M}}_p^l$ such that $\text{supp}(\hat{f}) \subset D(0, C_1 2^j)$.

2. For $j \geq -1$, we have that

$$\|f\|_{L^\infty} \leq C 2^{j\frac{n}{p}} \|f\|_{W\tilde{\mathcal{M}}_p^l}, \quad (2.7)$$

for all $f \in W\tilde{\mathcal{M}}_p^l$ such that $\text{supp}(\hat{f}) \subset D(0, C_1 2^j)$. Moreover, if $j \leq -2$, we have

$$\|f\|_{L^\infty} \leq C 2^{j\frac{n}{l}} \|f\|_{W\tilde{\mathcal{M}}_p^l}, \quad (2.8)$$

for all $f \in W\tilde{\mathcal{M}}_p^l$ such that $\text{supp}(\hat{f}) \subset D(0, C_1 2^j)$.

3. Let $C_2 > C_1 > 0$, $j \in \mathbb{Z}$ and $f \in W\tilde{\mathcal{M}}_p^l$ be such that $\text{supp}(\hat{f}) \subset \{\xi \in \mathbb{R}^n; C_1 2^j \leq |\xi| < C_2 2^j\}$. Then, there exists a constant $C > 0$ depending on γ, n, C_1, C_2 such that

$$\|f\|_{W\tilde{\mathcal{M}}_p^l} \leq C 2^{-j|\gamma|} \|D^\gamma f\|_{W\tilde{\mathcal{M}}_p^l}. \quad (2.9)$$

Lemma 4. *Let $1 < p, l \leq \infty$ and assume that $X : \mathbb{R}^n \rightarrow \mathbb{R}^n$ is a volume-preserving diffeomorphism such that*

$$|X(x_0) - X(y_0)| \leq \gamma |x_0 - y_0|, \quad \forall x_0, y_0 \in \mathbb{R}^n, \quad (2.10)$$

for some fixed $\gamma \geq 1$, where $|\cdot|$ stands for the Euclidean norm in \mathbb{R}^n . Then, there exists a positive constant $C = C(n, p, l, \gamma)$ such that

$$C^{-1} \|f\|_{W\tilde{\mathcal{M}}_p^l} \leq \|f \circ X\|_{W\tilde{\mathcal{M}}_p^l} \leq C \|f\|_{W\tilde{\mathcal{M}}_p^l}. \quad (2.11)$$

For further reference, we recall that if $u : \mathbb{R}^n \times [0, T] \rightarrow \mathbb{R}^n$ is a continuous vector field that is Lipschitzian in the first variable for each fixed $t \in [0, T]$, and $X : \mathbb{R}^n \times [0, T] \rightarrow \mathbb{R}^n$ is the flow defined by

$$\begin{cases} \frac{\partial X(x_0, t)}{\partial t} = u(X(x_0, t), t) \\ X(x_0, 0) = x_0, \end{cases} \quad (2.12)$$

then

$$|X(x_0, t) - X(y_0, t)| \leq e^{\int_0^t b(t') dt'} |x_0 - y_0|, \quad (2.13)$$

where $b(t')$ is the Lipschitz constant.

3 A Conservation Law with Partially Nonlocal Velocity

This chapter aims to show the existence, uniqueness and continued dependence of the solution of a conservation law with partially nonlocal velocity (1.3) in the Besov spaces. This conservation law is,

$$\begin{cases} \partial_t \theta \pm \nabla \cdot (\theta v) = 0, \text{ with } v = (\Lambda_1^{\alpha-1} \mathcal{H}_1 \theta, \Lambda_2^{\alpha-1} \mathcal{H}_2 \theta) \\ \theta(x, y, 0) = \theta_0(x, y), \end{cases}$$

where $\theta : \mathbb{R}^2 \times [0, \infty) \longrightarrow \mathbb{R}$ is a scalar function, the initial data $\theta_0(x, y)$ is not necessarily regular; moreover \mathcal{H}_i and $\Lambda_i^{\alpha-1}$, with $i = 1, 2$, are the nonlinear and nonlocal operators, the partial Hilbert transform and the partial Riesz potential, respectively, which are defined as follows.

Definition 8 (*The partial Hilbert transform*). Given a function $f : \mathbb{R}^2 \longrightarrow \mathbb{R}$, we can define the partial Hilbert transform on the X -axis and on the Y -axis as

$$\mathcal{H}_1[f(x, y)] = \frac{1}{\pi} \text{ p.v. } \int_{-\infty}^{\infty} \frac{f(u, y)}{x - u} du, \quad (3.1)$$

$$\mathcal{H}_2[f(x, y)] = \frac{1}{\pi} \text{ p.v. } \int_{-\infty}^{\infty} \frac{f(x, v)}{y - v} dv. \quad (3.2)$$

Definition 9 (*The partial Riesz potential*). Given a function $f : \mathbb{R}^2 \longrightarrow \mathbb{R}$ such that $f \in L^p(\mathbb{R}^2)$, for $\alpha \in (0, 1)$ we can define the partial Riesz potential on the X -axis and on the Y -axis as

$$\Lambda_1^{\alpha-1}[f(x, y)] = c_\alpha \int_{\mathbb{R}} \frac{f(u, y)}{|x - u|^\alpha} du, \quad (3.3)$$

$$\Lambda_2^{\alpha-1}[f(x, y)] = c_\alpha \int_{\mathbb{R}} \frac{f(x, v)}{|y - v|^\alpha} dv. \quad (3.4)$$

where, $c_\alpha = \frac{\Gamma(\frac{\alpha}{2})}{2^{1-\alpha} \sqrt{\pi} \Gamma(\frac{1-\alpha}{2})}$.

In order to tackle the SQG transport equation differently, we use a new dimension-by-dimension approach via spatial domain decomposition. Specifically, about the two-dimensional nonlocal operator of the velocity field in the SQG, namely the Riesz transform, this operator will now be given by the composition of the partials nonlocal operators: the partial Hilbert transform and the partial Riesz potential; hence, we obtain a new transport equation doubly nonlocal where the velocity field is obtained by the composition of the partial Hilbert transform and the partial Riesz potential, this new

equation transport we call as a conservation law with partially nonlocal velocity. This can permit the interpretation of a conservation law with partially nonlocal velocity as an intermediary framework between the 1D quasi-geostrophic equation and the SQG.

In [45], we find an equivalent form of the Hilbert transform defined through a distribution function on $\mathcal{S}'(\mathbb{R})$. The significance of defining the Hilbert transform in an equivalent manner lies in its application to regularize the velocity field in the proof of Theorem 2.

We begin by defining a distribution W_0 in $\mathcal{S}'(\mathbb{R})$ as follows:

$$\langle W_0, \zeta \rangle = \frac{1}{\pi} \lim_{\epsilon \rightarrow 0} \int_{\epsilon \leq |x| < 1} \frac{\zeta(x)}{x} dx + \frac{1}{\pi} \int_{|x| \geq 1} \frac{\zeta(x)}{x} dx, \quad (3.5)$$

for $\zeta \in \mathcal{S}(\mathbb{R})$.

Thence, the truncated Hilbert transform of $f \in \mathcal{S}(\mathbb{R})$ (at height ϵ) is defined by

$$H^{(\epsilon)}(f)(x) = \frac{1}{\pi} \int_{|y| \geq \epsilon} \frac{f(x-y)}{y} dy = \frac{1}{\pi} \int_{|x-y| \geq \epsilon} \frac{f(y)}{x-y} dy. \quad (3.6)$$

Then, the Hilbert transform of $f \in \mathcal{S}(\mathbb{R})$ is defined by

$$\mathcal{H}(f)(x) = (W_0 * f)(x) = \lim_{\epsilon \rightarrow 0} H^{(\epsilon)}(f)(x). \quad (3.7)$$

The following theorem will prove the Bernstein inequality in Besov spaces subject to partial nonlocal operators: the partial Riesz potential and the partial Hilbert transform. Unlike the article [69] or similar works, in our demonstration, we will use the partial Fourier transform several times, defined for instance in [43].

3.1 Bernstein-type Inequality to Nonlocal Partial Operators in Besov spaces

Theorem 1 (Bernstein inequality). *Let $\alpha \in \mathbb{R}$, $f \in \mathcal{S}(\mathbb{R}^2)$ and $1 \leq p \leq q \leq \infty$.*

(I) *If f satisfies*

$$\text{supp } \hat{f} \subset \{\xi \in \mathbb{R}^2 : |\xi| \leq 2^j\},$$

for some integer j , then

$$\|\Lambda_1^\alpha f\|_{L^q(\mathbb{R}^2)} \leq C 2^{j\alpha + 2j(\frac{1}{p} - \frac{1}{q})} \|f\|_{L^p(\mathbb{R}^2)}. \quad (3.8)$$

$$\|\Lambda_1^\alpha \mathcal{H}_1 f\|_{L^q(\mathbb{R}^2)} \leq C 2^{j\alpha + 2j(\frac{1}{p} - \frac{1}{q})} \|f\|_{L^p(\mathbb{R}^2)}. \quad (3.9)$$

(II) *If f satisfies*

$$\text{supp } \hat{f} \subset \{\xi \in \mathbb{R}^2 : K_1 2^j \leq |\xi| \leq K_2 2^j\}, \quad (3.10)$$

for some integer j and constants $0 < K_1 \leq K_2$, then

$$C_1 2^{j\alpha} \|f\|_{L^q(\mathbb{R}^2)} \leq \|\Lambda_1^\alpha f\|_{L^q(\mathbb{R}^2)} \leq C_2 2^{j\alpha+2j(\frac{1}{p}-\frac{1}{q})} \|f\|_{L^p(\mathbb{R}^2)}. \quad (3.11)$$

$$\tilde{C}_1 2^{j(\alpha-1)} \|f\|_{L^q(\mathbb{R}^2)} \leq \|\Lambda_1^{\alpha-1} \mathcal{H}_1 f\|_{L^q(\mathbb{R}^2)} \leq \tilde{C}_2 2^{j(\alpha-1)+2j(\frac{1}{p}-\frac{1}{q})} \|f\|_{L^p(\mathbb{R}^2)}. \quad (3.12)$$

where C_1, \tilde{C}_1, C_2 and \tilde{C}_2 are constants depending on α, p and q only.

Proof. We will start by proving (I); it is enough to prove that

$$\|f\|_{L^q} \leq C 2^{2j(\frac{1}{p}-\frac{1}{q})} \|f\|_{L^p}, \quad (3.13)$$

and

$$\|\Lambda_1^\alpha f\|_{L^p} \leq C 2^{\alpha j} \|f\|_{L^p}. \quad (3.14)$$

As \hat{f} is supported in B_j and $\psi_j \equiv 1$ on B_j , since if $\xi \in \text{supp} \hat{f}$ so $|\xi| < 2^j$ then for all $j \geq 0$ we will have $|2^{-j}\xi| < 2^j$, follow that $\varphi_j(2^{-j}\xi) = 0$, hence $\psi_j(\xi) = \psi_j(\xi) + \sum_{j \geq 0} \varphi_j(2^{-j}\xi) = 1$. It follows that $\hat{f} = \psi_j \hat{f}$ or, in an equivalent form, $f = \check{\psi}_j * f$. Thus, Young's inequality implies that

$$\|f\|_{L^q} \leq \|\check{\psi}_j\|_{L^{p_1}} \|f\|_{L^p}, \quad (3.15)$$

where $\frac{1}{p_1} = 1 + \frac{1}{q} - \frac{1}{p}$. Direct computations by using a change of variables implies that

$$\|\check{\psi}_j\|_{L^{p_1}} = 2^{2j(\frac{1}{p}-\frac{1}{q})} \|\check{\psi}\|_{L^{p_1}}.$$

By replacing this last fact into (3.15), we get (3.13).

Throughout the work, we will use the notations $\xi = (\xi_1, \xi_2)$ and $x = (x_1, x_2)$, with $x \neq 0$. Fourier transform of the *partial Riesz potential*,

$$\begin{aligned} (\Lambda_1^\alpha f)^\wedge(\xi) &= \int_{\mathbb{R}^2} e^{-2\pi i x \cdot \xi} \Lambda_1^\alpha f(x) dx \\ &= \iint e^{-2\pi i x_1 \xi_1} e^{-2\pi i x_2 \xi_2} \Lambda_1^\alpha f(x_1, x_2) dx_1 dx_2 \\ &= \int e^{-2\pi i x_2 \xi_2} \left\{ \int e^{-2\pi i x_1 \xi_1} \Lambda_1^\alpha f(\cdot, x_2) dx_1 \right\} dx_2 \\ &= \int e^{-2\pi i x_2 \xi_2} \mathcal{F}_1 \{ \Lambda_1^\alpha f(\cdot, x_2) \} dx_2. \end{aligned}$$

The previous calculations are correct as long as $f \in \mathcal{S}(\mathbb{R}^2)$; for the general case, consider $f \in \mathcal{S}'(\mathbb{R}^2)$. Since, $\mathcal{F}_1 \{ \Lambda_1^\alpha f(\cdot, x_2) \} = |\xi_1|^\alpha \mathcal{F}_1 \{ f(\cdot, x_2) \}$, so

$$\begin{aligned} (\Lambda_1^\alpha f)^\wedge(\xi) &= \int e^{-2\pi i x_2 \xi_2} |\xi_1|^\alpha \mathcal{F}_1 \{ f(\cdot, x_2) \} dx_2 \\ &= |\xi_1|^\alpha \int e^{-2\pi i x_2 \xi_2} \mathcal{F}_1 \{ f(\cdot, x_2) \} dx_2 \\ &= |\xi_1|^\alpha \hat{f}(\xi) \\ &= \psi_j(\xi) |\xi_1|^\alpha \hat{f}(\xi). \end{aligned} \quad (3.16)$$

Therefore,

$$\Lambda_1^\alpha f = M_j * f, \quad (3.17)$$

where, $M_j = \mathcal{F}^{-1} \{ \psi_j(\xi) |\xi_1|^\alpha \}$, from the fact that $\psi_j(\xi) = \psi(2^{-j}\xi)$ and by changing variables, we get

$$\begin{aligned} M_j &= 2^{j\alpha} 2^{2j} \int_{\mathbb{R}^2} e^{2\pi i x \cdot 2^j \xi} \psi(\xi) |\xi_1|^\alpha d\xi \\ &:= 2^{j\alpha} 2^{2j} N. \end{aligned}$$

Notice that, $N(2^j x) = \mathcal{F}^{-1} \{ \psi(\cdot) |\cdot|^\alpha \} (2^j x)$, as $\psi \in \mathcal{S}$ and $|\cdot|^\alpha$ is a polynomial, so $\psi(\cdot) |\cdot|^\alpha \in \mathcal{S}$. Thus $N(2^j x) \in \mathcal{S}$, then there is $C > 0$, in particular $C = C(m)$ with $m > 0$, such that $|N(2^j x)| \leq C |2^j x|^{-m}$. So we have

$$\begin{aligned} |M_j(x)| &= 2^{j\alpha} 2^{2j} |N(2^j x)| \\ &\leq C 2^{j\alpha} 2^{2j} |2^j x|^{-m}, \end{aligned}$$

i.e., M_j is bounded. Moreover, thinking B as a ball with center at the origin and $m > 2$, we have

$$\begin{aligned} \|M_j\|_{L^1} &= \int_{\mathbb{R}^2} |M_j(x)| dx \\ &= \int_B |M_j(x)| dx + \int_{\mathbb{R}^2 \setminus B} |M_j(x)| dx \\ &\leq \int_B C 2^{j\alpha} 2^{2j} |2^j x|^{-1} dx + \int_{\mathbb{R}^2 \setminus B} C 2^{j\alpha} 2^{2j} |2^j x|^{-m} dx \\ &\leq C 2^{j\alpha} 2^j \int_B |x|^{-1} dx + C 2^{j\alpha} 2^{j(1-m)} \int_{\mathbb{R}^2 \setminus B} |x|^{-m} dx \\ &\leq C 2^{j\alpha} 2^j + C 2^{j\alpha} 2^{j(1-m)} \\ &\leq C 2^{j\alpha}. \end{aligned}$$

Then, applying Young's inequality to (3.17), we get

$$\begin{aligned} \|\Lambda_1^\alpha f\|_{L^p} &\leq \|M_j\|_{L^1} \|f\|_{L^p} \\ &\leq C 2^{j\alpha} \|f\|_{L^p}, \end{aligned}$$

with this, we are proving (3.14), consequently we demonstrated (3.8). To prove (3.9) it will suffice to consider $g = \mathcal{H}_1 f$, continue the accounts with g and, at the end apply Young's inequality in g .

Now will prove (II), for this case also is it suffices to show

$$\|f\|_{L^q} \leq C 2^{2j(\frac{1}{p} - \frac{1}{q})} \|f\|_{L^p}, \quad (3.18)$$

and

$$C2^{\alpha j}\|f\|_{L^p} \leq \|\Lambda_1^\alpha f\|_{L^p} \leq C2^{\alpha j}\|f\|_{L^p}. \quad (3.19)$$

As the $\text{supp } \hat{f}$ is in an annulus, then from the Littlewood–Paley decomposition, there is a φ_j that is supported in D_j such that $\text{supp } \hat{f} \subset \text{supp } \varphi_j$, so

$$\hat{f} = \varphi_j \hat{f}, \quad (3.20)$$

that is $f = \check{\varphi} * f$. Thus, Young's inequality implies that

$$\|f\|_{L^q} = \|\check{\varphi}\|_{L^{p_1}} \|f\|_{L^p}, \quad (3.21)$$

where $\frac{1}{p_1} = 1 + \frac{1}{q} - \frac{1}{p}$. Direct computations by using a change of variables implies that

$$\|\check{\varphi}_j\|_{L^{p_1}} = 2^{2j(\frac{1}{p} - \frac{1}{q})} \|\check{\varphi}\|_{L^{p_1}}.$$

By replacing this last fact into (3.21), we get (3.18).

On other hand, proceeding as in (3.16), we get

$$(\Lambda_1^\alpha f)^\wedge(\xi) = \psi_j(\xi) |\xi_1|^\alpha \hat{f}(\xi), \quad (3.22)$$

even more,

$$\Lambda_1^\alpha f = K_j * f, \quad (3.23)$$

where, $K_j = \mathcal{F}^{-1} \{ \psi_j(\xi) |\xi_1|^\alpha \}$ and a direct computations by using a change of variables implies that

$$\begin{aligned} K_j &= 2^{j\alpha} 2^{2j} \int_{\mathbb{R}^2} e^{2\pi i x \cdot 2^j \xi} \psi_0(\xi) |\xi_1|^\alpha d\xi \\ &:= 2^{j\alpha} 2^{2j} I. \end{aligned}$$

Notice that, by integration by parts, we have

$$\begin{aligned} I &= \int_{\mathbb{R}^2} e^{2\pi i x \cdot 2^j \xi} \psi(\xi) |\xi_1|^\alpha d\xi \\ &= \frac{1}{2\pi i 2^j x_1} \int_{\mathbb{R}^2} \left(\frac{\partial}{\partial \xi_1} e^{2\pi i x \cdot 2^j \xi} \right) (\psi(\xi) |\xi_1|^\alpha) d\xi \\ &= \frac{-1}{2\pi i 2^j x_1} \int_{\mathbb{R}^2} e^{2\pi i x \cdot 2^j \xi} \frac{\partial}{\partial \xi_1} (\psi(\xi) |\xi_1|^\alpha) d\xi \\ &= \frac{-1}{(2\pi i 2^j x_1)^2} \int_{\mathbb{R}^2} \frac{\partial}{\partial \xi_1} e^{2\pi i x \cdot 2^j \xi} \frac{\partial}{\partial \xi_1} (\psi(\xi) |\xi_1|^\alpha) d\xi \\ &= \frac{1}{(2\pi i 2^j x_1)^2} \int_{\mathbb{R}^2} e^{2\pi i x \cdot 2^j \xi} \frac{\partial^2}{\partial \xi_1^2} (\psi(\xi) |\xi_1|^\alpha) d\xi, \end{aligned}$$

the previous integrals are well-defined since the support of ψ does not have any neighborhood of the origin. Even more,

$$(2^j x_1)^2 I = -\frac{1}{(2\pi)^2} \int_{\mathbb{R}^2} e^{2\pi i x \cdot 2^j \xi} \frac{\partial^2}{\partial \xi_1^2} (\psi(\xi) |\xi_1|^\alpha) d\xi,$$

similarly, we get

$$(2^j x_2)^2 I = -\frac{1}{(2\pi)^2} \int_{\mathbb{R}^2} e^{2\pi i x \cdot 2^j \xi} \frac{\partial^2}{\partial \xi_2^2} (\psi(\xi) |\xi_1|^\alpha) d\xi,$$

adding the previous results, we get

$$\begin{aligned} ((2^j x_1)^2 + (2^j x_2)^2) I &= -\frac{1}{(2\pi)^2} \int_{\mathbb{R}^2} e^{2\pi i x \cdot 2^j \xi} \left\{ \frac{\partial^2}{\partial \xi_1^2} (\psi(\xi) |\xi_1|^\alpha) + \frac{\partial^2}{\partial \xi_2^2} (\psi(\xi) |\xi_1|^\alpha) \right\} d\xi \\ |2^j x|^2 I &= -\frac{1}{(2\pi)^2} \int_{\mathbb{R}^2} e^{2\pi i x \cdot 2^j \xi} \Delta (\psi(\xi) |\xi_1|^\alpha) d\xi. \end{aligned}$$

So,

$$\begin{aligned} \left| |2^j x|^2 I \right| &\leq \frac{1}{(2\pi)^2} \int_{\mathbb{R}^2} |e^{2\pi i x \cdot 2^j \xi}| |\Delta (\psi(\xi) |\xi_1|^\alpha)| d\xi \\ &= \frac{C}{(2\pi)^2} \int_{\mathbb{R}^2} |\Delta (\psi(\xi) |\xi_1|^\alpha)| d\xi \\ &= \frac{C}{(2\pi)^2} \|\Delta (\psi(\xi) |\xi_1|^\alpha)\|_{L^1} \\ &\leq C, \end{aligned}$$

that is,

$$|I| \leq C |2^j x|^{-2},$$

in general using the maximum norm in \mathbb{R}^2 we can obtain an $m \in \mathbb{N}$ such that

$$|I| \leq C |2^j x|^{-m},$$

then, applying absolute value to K_j , we have

$$\begin{aligned} |K_j| &= 2^{j\alpha} 2^{2j} |I| \\ &\leq C 2^{j\alpha} 2^{2j} |2^j x|^{-m}, \end{aligned}$$

i.e. K_j is bounded, and note that thinking B as a ball with center at the origin and $m > 2$,

we have

$$\begin{aligned}
\|K_j\|_{L^1} &= \int_{\mathbb{R}^2} |K_j(x)| dx \\
&= \int_B |K_j(x)| dx + \int_{\mathbb{R}^2 \setminus B} |K_j(x)| dx \\
&\leq \int_B C 2^{j\alpha} 2^{2j} |2^j x|^{-1} dx + \int_{\mathbb{R}^2 \setminus B} C 2^{j\alpha} 2^{2j} |2^j x|^{-m} dx \\
&\leq C 2^{j\alpha} 2^j \int_B |x|^{-1} dx + C 2^{j\alpha} 2^{j(1-m)} \int_{\mathbb{R}^2 \setminus B} |x|^{-m} dx \\
&\leq C 2^{j\alpha} 2^j + C 2^{j\alpha} 2^{j(1-m)} \\
&\leq C 2^{j\alpha}.
\end{aligned}$$

Then, applying Young's inequality to (3.23), we get

$$\begin{aligned}
\|\Lambda_1^\alpha f\|_{L^p} &\leq \|K_j\|_{L^1} \|f\|_{L^p} \\
&\leq C 2^{j\alpha} \|f\|_{L^p},
\end{aligned}$$

this proves the right half of (3.19). To prove the left half of (3.19), we have that $\text{supp}\{(\Lambda_1^\alpha f)^\wedge(\xi)\} = \text{supp}\{|\xi_1|^\alpha \hat{f}(\xi)\}$ is in an annulus since $\text{supp}\hat{f}$ is in an annulus, then the right half of (3.19), we have

$$\begin{aligned}
\|f\|_{L^p} &= \|\Lambda_1^{-\alpha} \Lambda_1^\alpha f\|_{L^p} \\
&\leq C 2^{-\alpha j} \|\Lambda_1^\alpha f\|_{L^p},
\end{aligned}$$

that is,

$$C 2^{\alpha j} \|f\|_{L^p} \leq \|\Lambda_1^\alpha f\|_{L^p}.$$

To prove (3.12), it will suffice to consider $g = \mathcal{H}_1 f$ continue with computations with g and, at the end apply Young's inequality in g . This completes the proof of this theorem. \square

3.2 Commutator Estimates in Besov Spaces

This section contains estimates for the commutator estimates in the context of Besov spaces. Such estimates are essential to prove the well-posedness of a conservation law with partially nonlocal velocity (1.3).

Proposition 2. *Let $\lambda > 0, \alpha \in (0, 1), p \in [1, \infty]$ be given. Assume $r > 2/p$. Then there exist constant $C > 0$ such that*

$$2^{j\lambda} \|[\Delta_j, v] \Lambda_1^\alpha u\|_{L^p} \leq C \left(\|v\|_{B_{p,\infty}^{r+1}} \|u\|_{B_{p,\infty}^{\lambda+\alpha-1}} + \|u\|_{B_{p,\infty}^{r+\alpha}} \|v\|_{B_{p,\infty}^\lambda} \right), \quad (3.24)$$

where the brackets represent the commutator operator given by

$$[\Delta_j, f]g := \Delta_j(fg) - f\Delta_j g, \quad (3.25)$$

for suitable functions f and g .

Proof. By using Bony's decomposition (2.41) and the orthogonality relations of the localization operator from [19], the commutator can be written as

$$\begin{aligned} [\Delta_j, v]\Lambda_1^\alpha u &= \sum_{|j-k|\leq 4} \Delta_j(S_{k-1}v\Delta_k(\Lambda_1^\alpha u)) + \sum_{|j-k|\leq 4} \Delta_j(S_{k-1}(\Lambda_1^\alpha u)\Delta_k v) \\ &\quad + \sum_{|k-\tilde{k}|\leq 1} \Delta_j(\Delta_k v\Delta_{\tilde{k}}(\Lambda_1^\alpha u)) - \sum_{|j-k|\leq 1} S_{k-1}v\Delta_k(\Delta_j\Lambda_1^\alpha u) \\ &\quad - \sum_{k\geq j+1} S_{k-1}(\Delta_j\Lambda_1^\alpha u)\Delta_k v - \sum_{|k-\tilde{k}|\leq 1} \Delta_k v\Delta_{\tilde{k}}(\Delta_j\Lambda_1^\alpha u) \\ &= \sum_{|j-k|\leq 4} \Delta_j(S_{k-1}v\Delta_k(\Lambda_1^\alpha u)) - \sum_{|j-k|\leq 4} S_{k-1}v\Delta_k(\Delta_j\Lambda_1^\alpha u) \\ &\quad + \sum_{|j-k|\leq 4} \Delta_j(S_{k-1}(\Lambda_1^\alpha u)\Delta_k v) + \sum_{|k-\tilde{k}|\leq 1} \Delta_j(\Delta_k v\Delta_{\tilde{k}}(\Lambda_1^\alpha u)) \\ &\quad - \sum_{k\geq j+1} S_{k-1}(\Delta_j\Lambda_1^\alpha u)\Delta_k v - \sum_{|k-\tilde{k}|\leq 1} \Delta_k v\Delta_{\tilde{k}}(\Delta_j\Lambda_1^\alpha u) \\ &= \sum_{|j-k|\leq 4} \{\Delta_j(S_{k-1}v\Delta_k(\Lambda_1^\alpha u)) - S_{k-1}v\Delta_k(\Delta_j\Lambda_1^\alpha u)\} + \sum_{|j-k|\leq 4} \Delta_j(S_{k-2}(\Lambda_1^\alpha u)\Delta_k v) \\ &\quad + \sum_{|k-j|\leq 3} \sum_{|k-\tilde{k}|\leq 1} \Delta_j(\Delta_k v\Delta_{\tilde{k}}(\Lambda_1^\alpha u)) - \sum_{k\geq j+1} S_{k-1}(\Delta_j\Lambda_1^\alpha u)\Delta_k v \\ &\quad - \sum_{|k-\tilde{k}|\leq 1} \sum_{|\tilde{k}-j|\leq 1} \Delta_k v\Delta_{\tilde{k}}(\Delta_j\Lambda_1^\alpha u) \\ &:= I_1 + I_2 + I_3 + I_4 + I_5. \end{aligned}$$

We commence by independently estimating the terms above. To initiate, let us observe

$$\begin{aligned} I_1 &= \sum_{|k-j|\leq 4} 2^{2j} \int_{\mathbb{R}^2} h(2^j(x-y)) \{S_{k-1}v(y) - S_{k-1}v(x)\} \Delta_k \Lambda_1^\alpha u(y) dy \\ &= \sum_{|k-j|\leq 4} 2^{2j} \int_{\mathbb{R}^2} h(2^j(x-y)) \left\{ - \int_0^1 \nabla \{S_{k-1}v(x + \tau(y-x))\} \cdot (x-y) d\tau \right\} \Delta_k \Lambda_1^\alpha u(y) dy \\ &= - \sum_{|k-j|\leq 4} 2^{2j} \int_{\mathbb{R}^2} h(z) \left\{ \int_0^1 \nabla \{S_{k-1}v(x - 2^{-j}z\tau)\} \cdot 2^{-j}z d\tau \right\} \Delta_k \Lambda_1^\alpha u(x - 2^{-j}z) (2^{-2j}) dz \\ &= \sum_{|k-j|\leq 4} -2^{-j} \int_{\mathbb{R}^2} h(z) \left\{ \int_0^1 \nabla \{S_{k-1}v(x - 2^{-j}z\tau)\} \cdot z d\tau \right\} \Delta_k \Lambda_1^\alpha u(x - 2^{-j}z) dz, \end{aligned}$$

applying absolute value, we get

$$\begin{aligned}
|I_1| &\leq \sum_{|k-j|\leq 4} 2^{-j} \int_{\mathbb{R}^2} |h(z)| \left\{ \int_0^1 \left| \nabla \{S_{k-1}v(x - 2^{-j}z\tau)\} \cdot z \right| d\tau \right\} \left| \Delta_k \Lambda_1^\alpha u(x - 2^{-j}z) \right| dz \\
&\leq \sum_{|k-j|\leq 4} 2^{-j} \int_{\mathbb{R}^2} |h(z)| \left\{ \int_0^1 \|\nabla S_{k-1}v\|_{L^\infty} \|z\| d\tau \right\} \left| \Delta_k \Lambda_1^\alpha u(x - 2^{-j}z) \right| dz \\
&= \sum_{|k-j|\leq 4} 2^{-j} \|\nabla S_{k-1}v\|_{L^\infty} \int_{\mathbb{R}^2} |h(z)| \|z\| \left| \Delta_k \Lambda_1^\alpha u(x - 2^{-j}z) \right| dz.
\end{aligned}$$

So after applying the norm $\|\cdot\|_{L^p}$, Young's inequality, from (3.11) of Theorem 1 and the third item of Proposition 1, we have

$$\begin{aligned}
\|I_1\|_{L^p} &\leq \sum_{|k-j|\leq 4} 2^{-j} \|\nabla S_{k-1}v\|_{L^\infty} \int_{\mathbb{R}^2} |h(z)| \|z\| \|\Lambda_1^\alpha \Delta_k u\|_{L^p} dz \\
&\leq \sum_{|k-j|\leq 4} 2^{-j} \|\nabla S_{k-1}v\|_{L^\infty} \|\Lambda_1^\alpha \Delta_k u\|_{L^p} \int_{\mathbb{R}^2} |h(z)| \|z\| dz \\
&= \sum_{|k-j|\leq 4} 2^{-j} \|S_{k-1} \nabla v\|_{L^\infty} \|\Lambda_1^\alpha \Delta_k u\|_{L^p} C \\
&\leq \sum_{k=j-4}^{j+4} C 2^{-j} \|\nabla v\|_{L^\infty} C 2^{\alpha k} \|\Delta_k u\|_{L^p} \\
&\leq C 2^{-j} \|\nabla v\|_{B_{p,\infty}^{r,\infty}} \sum_{k=j-4}^{j+4} 2^{\alpha k} \|\Delta_k u\|_{L^p} \\
&\leq C 2^{-j} \|v\|_{B_{p,\infty}^{r+1}} \sum_{k=j-4}^{j+4} 2^{\alpha k} \|\Delta_k u\|_{L^p},
\end{aligned}$$

the last inequality is due to immersion is due to immersion; for more details, see the first item of Theorem 2.2 of [63]. In addition, we must have that $r > 2/p$.

Then,

$$\begin{aligned}
2^{j\lambda} \|I_1\|_{L^p} &\leq C 2^{(\lambda-1)j} \|v\|_{B_{p,\infty}^{r+1}} \sum_{k=j-4}^{j+4} 2^{\alpha k} \|\Delta_k u\|_{L^p} \\
&= C \|v\|_{B_{p,\infty}^{r+1}} \sum_{k=j-4}^{j+4} 2^{(\lambda-1)(j-k)} 2^{(\lambda-1+\alpha)k} \|\Delta_k u\|_{L^p} \\
&\leq C \|v\|_{B_{p,\infty}^{r+1}} \|u\|_{B_{p,\infty}^{\lambda+\alpha-1}} \sum_{k=-4}^4 2^{(\lambda-1)k} \\
&\leq C \|v\|_{B_{p,\infty}^{r+1}} \|u\|_{B_{p,\infty}^{\lambda+\alpha-1}}.
\end{aligned}$$

We also have the following estimate through the Hölder and Young inequalities, in addition to the third item of Proposition 1

$$\begin{aligned}
\|I_2\|_{L^p} &\leq \sum_{|k-j|\leq 4} \|\Delta_j(S_{k-1}\Lambda_1^\alpha u \Delta_k v)\|_{L^p} \\
&\leq \sum_{|k-j|\leq 4} C \|S_{k-1}\Lambda_1^\alpha u \Delta_k v\|_{L^p} \\
&\leq \sum_{|k-j|\leq 4} C \|S_{k-1}\Lambda_1^\alpha u\|_{L^\infty} \|\Delta_k v\|_{L^p} \\
&\leq \sum_{k=j-4}^{j+4} C \|\Lambda_1^\alpha u\|_{L^\infty} \|\Delta_k v\|_{L^p} \\
&\leq C \sum_{k=j-4}^{j+4} \|\Lambda_1^\alpha u\|_{B_{p,\infty}^r} \|\Delta_k v\|_{L^p} \\
&\leq C \sum_{k=j-4}^{j+4} \|u\|_{B_{p,\infty}^{r+\alpha}} \|\Delta_k v\|_{L^p}.
\end{aligned}$$

The last inequality was derived from the following auxiliary argument, wherein the inequalities (3.11) and (3.8) of Bernstein's Theorem are employed

$$\begin{aligned}
\|\Lambda_1^\alpha u\|_{B_{p,\infty}^r} &= \sup_{j\geq 0} 2^{jr} \|\Delta_j \Lambda_1^\alpha u\|_{L^p} + \|S_0 \Lambda_1^\alpha u\|_{L^p} \\
&= \sup_{j\geq 0} 2^{jr} \|\Lambda_1^\alpha \Delta_j u\|_{L^p} + \|\Lambda_1^\alpha S_0 u\|_{L^p} \\
&\leq \sup_{j\geq 0} 2^{jr} C_2 2^{j\alpha} \|\Delta_j u\|_{L^p} + C_1 \|S_0 u\|_{L^p} \\
&\leq C \left(\sup_{j\geq 0} 2^{j(r+\alpha)} \|\Delta_j u\|_{L^p} + \|S_0 u\|_{L^p} \right) \\
&= \|u\|_{B_{p,\infty}^{r+\alpha}},
\end{aligned}$$

then

$$\begin{aligned}
2^{j\lambda} \|I_2\|_{L^p} &\leq C 2^{j\lambda} \|u\|_{B_{p,\infty}^{r+\alpha}} \sum_{k=j-4}^{j+4} \|\Delta_k v\|_{L^p} \\
&= C \|u\|_{B_{p,\infty}^{r+\alpha}} \sum_{k=j-4}^{j+4} 2^{(j-k)\lambda} 2^{k\lambda} \|\Delta_k v\|_{L^p} \\
&\leq C \|u\|_{B_{p,\infty}^{r+\alpha}} \|v\|_{B_{p,\infty}^\lambda} \sum_{k=-4}^4 2^{k\lambda} \\
&\leq C \|u\|_{B_{p,\infty}^{r+\alpha}} \|v\|_{B_{p,\infty}^\lambda}.
\end{aligned}$$

Analogously, we estimate I_3 using the Young and Hölder inequalities, in addition

to (3.11) of Theorem 1 and from first item of Proposition 1

$$\begin{aligned}
\|I_3\|_{L^p} &\leq \sum_{|k-j|\leq 3} \sum_{|k-\tilde{k}|\leq 1} \|\Delta_j(\Delta_k v \Delta_{\tilde{k}} \Lambda_1^\alpha u)\|_{L^p} \\
&\leq \sum_{|k-j|\leq 3} \sum_{|k-\tilde{k}|\leq 1} C \|\Delta_k v\|_{L^p} \|\Lambda_1^\alpha \Delta_{\tilde{k}} u\|_{L^\infty} \\
&\leq \sum_{|k-j|\leq 3} \sum_{|k-\tilde{k}|\leq 1} C \|\Delta_k v\|_{L^p} C_2 2^{\alpha \tilde{k}} \|\Delta_{\tilde{k}} u\|_{L^\infty} \\
&\leq C 2^{-j\lambda} \sum_{|k-j|\leq 3} \sum_{|k-\tilde{k}|\leq 1} 2^{(j-k)\lambda} \left\{ \sup_{k\geq 0} 2^{k\lambda} \|\Delta_k v\|_{L^p} \right\} \left\{ \sup_{\tilde{k}\geq 0} 2^{\tilde{k}\alpha} \|\Delta_{\tilde{k}} u\|_{L^\infty} \right\} \\
&= C 2^{-j\lambda} \sum_{|k-j|\leq 3} \sum_{|k-\tilde{k}|\leq 1} 2^{(j-k)\lambda} \|v\|_{B_{p,\infty}^\lambda} \|u\|_{B_{\infty,\infty}^\alpha} \\
&= C 2^{-j\lambda} C \|v\|_{B_{p,\infty}^\lambda} \|u\|_{B_{\infty,\infty}^\alpha} \\
&= C 2^{-j\lambda} \|v\|_{B_{p,\infty}^\lambda} \|u\|_{B_{p,\infty}^{r+\alpha}},
\end{aligned}$$

then

$$2^{j\lambda} \|I_3\|_{L^p} \leq C \|v\|_{B_{p,\infty}^\lambda} \|u\|_{B_{p,\infty}^{r+\alpha}}.$$

Similarly, we estimate I_4

$$\begin{aligned}
\|I_4\|_{L^p} &\leq \sum_{k\geq j+1} \|S_{k-1} \Delta_j \Lambda_1^\alpha u \Delta_k v\|_{L^p} \\
&\leq \sum_{k\geq j+1} \|S_{k-1} \Delta_j \Lambda_1^\alpha u\|_{L^\infty} \|\Delta_k v\|_{L^p} \\
&\leq 2^{-j\lambda} \sum_{k\geq j+1} 2^{(j-k)\lambda} C \|\Lambda_1^\alpha u\|_{L^\infty} 2^{k\lambda} \|\Delta_k v\|_{L^p} \\
&= 2^{-j\lambda} C \|\Lambda_1^\alpha u\|_{L^\infty} 2^{k\lambda} \|\Delta_k v\|_{L^p} \\
&\leq C 2^{-j\lambda} \|\Lambda_1^\alpha u\|_{B_{p,\infty}^r} \left\{ \sup_{k\geq 0} 2^{k\lambda} \|\Delta_k v\|_{L^p} + \|S_0(v)\|_{L^p} \right\} \\
&\leq C 2^{-j\lambda} \|u\|_{B_{p,\infty}^{r+\alpha}} \|v\|_{B_{p,\infty}^\lambda},
\end{aligned}$$

then

$$2^{j\lambda} \|I_4\|_{L^p} \leq C \|u\|_{B_{p,\infty}^{r+\alpha}} \|v\|_{B_{p,\infty}^\lambda}.$$

Finally,

$$\begin{aligned}
\|I_5\|_{L^p} &\leq \sum_{|j''-j'|\leq 1} \sum_{|j'-j|\leq 1} \|\Delta_{j''}v\Delta_{j'}\Delta_j\Lambda_1^\alpha u\|_{L^p} \\
&\leq \sum_{|j''-j'|\leq 1} \sum_{|j'-j|\leq 1} \|\Delta_{j''}v\|_{L^p} \|\Delta_{j'}\Delta_j\Lambda_1^\alpha u\|_{L^\infty} \\
&\leq \sum_{|j''-j'|\leq 1} \sum_{|j'-j|\leq 1} C \|\Delta_{j''}v\|_{L^p} \|\Lambda_1^\alpha u\|_{L^\infty} \\
&= C \|\Lambda_1^\alpha u\|_{L^\infty} \sum_{|j''-j'|\leq 1} \sum_{|j'-j|\leq 1} \|\Delta_{j''}v\|_{L^p} \\
&\leq C \|u\|_{B_{p,\infty}^{r+\alpha}} \sum_{|j''-j'|\leq 1} \sum_{|j'-j|\leq 1} \|\Delta_{j'}v\|_{L^p},
\end{aligned}$$

proceeding analogously to the previous estimates, we have

$$2^{j\lambda} \|I_5\|_{L^p} \leq C \|u\|_{B_{p,\infty}^{r+\alpha}} \|v\|_{B_{p,\infty}^\lambda},$$

and collecting the estimates above, we obtain

$$2^{j\lambda} \|[\Delta_j, v]\Lambda_1^\alpha u\|_{L^p} \leq C (\|u\|_{B_{p,\infty}^{\lambda+\alpha-1}} \|v\|_{B_{p,\infty}^{r+1}} + \|v\|_{B_{p,\infty}^\lambda} \|u\|_{B_{p,\infty}^{r+\alpha}}).$$

□

Proposition 3. *Let $\lambda > 0, \alpha \in (0, 1), p \in [1, \infty]$ be given. Assume $r > 2/p$. Then there exist constant $C > 0$ such that*

$$2^{j\lambda} \|[\Delta_j, \Lambda_1^{\alpha-1} \mathcal{H}_1 u] \partial_1 v\|_{L^p} \leq C (\|u\|_{B_{p,\infty}^{r+\alpha}} \|v\|_{B_{p,\infty}^\lambda} + \|v\|_{B_{p,\infty}^{r+1}} \|u\|_{B_{p,\infty}^{\lambda+\alpha-1}}), \quad (3.26)$$

where the brackets $[\cdot, \cdot]$ denote the commutator operator.

Proof. By using Bony's decomposition (2.41) and the orthogonality relations of the localization operator from [19], the commutator can be written as

$$\begin{aligned}
[\Delta_j, \Lambda_1^{\alpha-1} \mathcal{H}_1 u] \partial_1 v &= \sum_{|j-k|\leq 4} \Delta_j (S_{k-1} \Lambda_1^{\alpha-1} \mathcal{H}_1 u \Delta_k \partial_1 v) + \sum_{|j-k|\leq 4} \Delta_j (S_{k-1} \partial_1 v \Delta_k \Lambda_1^{\alpha-1} \mathcal{H}_1 u) \\
&+ \sum_{|k-\tilde{k}|\leq 1} \Delta_j (\Delta_k \Lambda_1^{\alpha-1} \mathcal{H}_1 u \Delta_{\tilde{k}} \partial_1 v) - \sum_{|j-k|\leq 4} S_{k-1} \Lambda_1^{\alpha-1} \mathcal{H}_1 u \Delta_k \Delta_j \partial_1 v \\
&- \sum_{k \geq j} S_{k-1} \Delta_j \partial_1 v \Delta_k \Lambda_1^{\alpha-1} \mathcal{H}_1 u - \sum_{|j'-j''|\leq 1, |j-j''|\leq 2} \Delta_{j'} \Delta_j \partial_1 v \Delta_{j''} \Lambda_1^{\alpha-1} \mathcal{H}_1 u \\
&= \sum_{|j-k|\leq 4} \{ \Delta_j (S_{k-1} \Lambda_1^{\alpha-1} \mathcal{H}_1 u \Delta_k \partial_1 v) - S_{k-1} \Lambda_1^{\alpha-1} \mathcal{H}_1 u \Delta_j \Delta_k \partial_1 v \} \\
&+ \sum_{|j-k|\leq 4} \Delta_j (S_{k-1} \partial_1 v \Delta_k \Lambda_1^{\alpha-1} \mathcal{H}_1 u) + \sum_{|k-j|\leq 3} \sum_{|k-\tilde{k}|\leq 1} \Delta_j (\Delta_k \Lambda_1^{\alpha-1} \mathcal{H}_1 u \Delta_{\tilde{k}} \partial_1 v) \\
&- \sum_{k \geq j} S_{k-1} \Delta_j \partial_1 v \Delta_k \Lambda_1^{\alpha-1} \mathcal{H}_1 u - \sum_{|j''-j'|\leq 1} \sum_{|j'-j|\leq 1} \Delta_{j''} \Delta_j \partial_1 v \Delta_{j'} \Lambda_1^{\alpha-1} \mathcal{H}_1 u \\
&:= L_1 + L_2 + L_3 + L_4 + L_5.
\end{aligned}$$

The estimates for each term will be obtained similarly to those in the previous proposition.

$$\begin{aligned}
L_1 &= \sum_{|j-k| \leq 4} 2^{2j} \int_{\mathbb{R}^2} h(2^j(x-y)) \{S_{k-1} \Lambda_1^{\alpha-1} \mathcal{H}_1 u(y) - S_{k-1} \Lambda_1^{\alpha-1} \mathcal{H}_1 u(x)\} \Delta_k \partial_1 v(y) dy \\
&= \sum_{|j-k| \leq 4} 2^{2j} \int_{\mathbb{R}^2} h(2^j(x-y)) \left\{ \int_0^1 \nabla [S_{k-1} \Lambda_1^{\alpha-1} \mathcal{H}_1 u(x + \tau(y-x))] \cdot (x-y) d\tau \right\} \Delta_k \partial_1 v(y) dy \\
&= \sum_{|j-k| \leq 4} 2^{2j} \int_{\mathbb{R}^2} h(z) \left\{ \int_0^1 \nabla [S_{k-1} \Lambda_1^{\alpha-1} \mathcal{H}_1 u(x - 2^{-j}z)] \cdot 2^{-j}z d\tau \right\} \Delta_k \partial_1 v(x - 2^{-j}z) (2^{-j})^2 dz \\
&= \sum_{|j-k| \leq 4} 2^{-j} \int_{\mathbb{R}^2} h(z) \left\{ \int_0^1 \nabla [S_{k-1} \Lambda_1^{\alpha-1} \mathcal{H}_1 u(x - 2^{-j}z)] \cdot z d\tau \right\} \Delta_k \partial_1 v(x - 2^{-j}z) dz,
\end{aligned}$$

applying absolute value, we get

$$\begin{aligned}
|L_1| &\leq \sum_{|j-k| \leq 4} 2^{-j} \int_{\mathbb{R}^2} |h(z)| \left\{ \int_0^1 \left| \nabla [S_{k-1} \Lambda_1^{\alpha-1} \mathcal{H}_1 u(x - 2^{-j}z)] \cdot z \right| d\tau \right\} \left| \Delta_k \partial_1 v(x - 2^{-j}z) \right| dz \\
&\leq \sum_{|j-k| \leq 4} 2^{-j} \int_{\mathbb{R}^2} |h(z)| \left\{ \int_0^1 \left\| \nabla S_{k-1} \Lambda_1^{\alpha-1} \mathcal{H}_1 u \right\|_{L^\infty} |z| d\tau \right\} \left| \Delta_k \partial_1 v(x - 2^{-j}z) \right| dz \\
&\leq \sum_{|j-k| \leq 4} 2^{-j} \left\| \nabla S_{k-1} \Lambda_1^{\alpha-1} \mathcal{H}_1 u \right\|_{L^\infty} \int_{\mathbb{R}^2} |h(z)| |z| \left| \Delta_k \partial_1 v(x - 2^{-j}z) \right| dz,
\end{aligned}$$

then, after applying the norm $\|\cdot\|_{L^p}$, Young's inequality, the classic Bernstein's inequality, see item (b) of Proposition 2.3 from [54], we have

$$\begin{aligned}
\|L_1\|_{L^p} &\leq \sum_{|j-k| \leq 4} 2^{-j} \left\| S_{k-1} \nabla \Lambda_1^{\alpha-1} \mathcal{H}_1 u \right\|_{L^\infty} \int_{\mathbb{R}^2} |h(z)| |z| \left\| \Delta_k \partial_1 v \right\|_{L^p} dz \\
&\leq \sum_{|j-k| \leq 4} 2^{-j} C \left\| \nabla \Lambda_1^{\alpha-1} \mathcal{H}_1 u \right\|_{L^\infty} \left\| \Delta_k \partial_1 v \right\|_{L^p} \int_{\mathbb{R}^2} |h(z)| |z| dz \\
&= \sum_{|j-k| \leq 4} 2^{-j} C \left\| \nabla \Lambda_1^{\alpha-1} \mathcal{H}_1 u \right\|_{L^\infty} \left\| \partial_1 \Delta_k v \right\|_{L^p} C \\
&\leq \sum_{|j-k| \leq 4} C 2^{-j} \left\| \nabla \Lambda_1^{\alpha-1} \mathcal{H}_1 u \right\|_{B_{p,\infty}^r} 2^k \left\| \Delta_k v \right\|_{L^p} \\
&\leq C 2^{-j} \left\| \Lambda_1^{\alpha-1} \mathcal{H}_1 u \right\|_{B_{p,\infty}^{r+1}} \sum_{|j-k| \leq 4} 2^k \left\| \Delta_k v \right\|_{L^p} \\
&\leq C 2^{-j} \|u\|_{B_{p,\infty}^{r+\alpha}} \sum_{|j-k| \leq 4} 2^k \left\| \Delta_k v \right\|_{L^p}.
\end{aligned}$$

Notice that $r > 2/p$ and the last inequality was derived from the following auxiliary

argument, wherein the inequalities (3.12) and (3.9) of Bernstein's Theorem are employed.

$$\begin{aligned}
\|\Lambda_1^{\alpha-1}\mathcal{H}_1u\|_{B_{p,\infty}^{r+1}} &= \sup_{j \geq 0} 2^{j(r+1)} \|\Delta_j \Lambda_1^{\alpha-1} \mathcal{H}_1 u\|_{L^p} + \|S_0 \Lambda_1^{\alpha-1} \mathcal{H}_1 u\|_{L^p} \\
&= \sup_{j \geq 0} 2^{j(r+1)} \|\Lambda_1^{\alpha-1} \mathcal{H}_1 \Delta_j u\|_{L^p} + \|\Lambda_1^{\alpha-1} \mathcal{H}_1 S_0 u\|_{L^p} \\
&\leq \sup_{j \geq 0} 2^{j(r+1)} C_2 2^{j(\alpha-1)} \|\Delta_j u\|_{L^p} + C_1 \|S_0 u\|_{L^p} \\
&\leq C \left(\sup_{j \geq 0} 2^{j(r+\alpha)} \|\Delta_j u\|_{L^p} + \|S_0 u\|_{L^p} \right) \\
&= \|u\|_{B_{p,\infty}^{r+\alpha}},
\end{aligned}$$

then

$$\begin{aligned}
2^{j\lambda} \|L_1\|_{L^p} &\leq C 2^{(\lambda-1)j} \|u\|_{B_{p,\infty}^{r+\alpha}} \sum_{|j-k| \leq 4} 2^k \|\Delta_k v\|_{L^p} \\
&= C \|u\|_{B_{p,\infty}^{r+\alpha}} \sum_{|j-k| \leq 4} 2^{(\lambda-1)(j-k)} 2^{\lambda k} \|\Delta_k v\|_{L^p} \\
&\leq C \|u\|_{B_{p,\infty}^{r+\alpha}} \|v\|_{B_{p,\infty}^\lambda} \sum_{|k| \leq 4} 2^{(\lambda-1)k} \\
&\leq C \|u\|_{B_{p,\infty}^{r+\alpha}} \|v\|_{B_{p,\infty}^\lambda}.
\end{aligned}$$

We also have the following estimate through the Hölder and Young inequalities, in addition to the third item of Proposition 1 and from (3.12) of Theorem 1,

$$\begin{aligned}
\|L_2\|_{L^p} &\leq \sum_{|j-k| \leq 4} \|S_{k-1} \partial_1 v\|_{L^\infty} \|\Delta_k \Lambda_1^{\alpha-1} \mathcal{H}_1 u\|_{L^p} \\
&\leq \sum_{|j-k| \leq 4} C \|\partial_1 v\|_{L^\infty} \|\Delta_k \Lambda_1^{\alpha-1} \mathcal{H}_1 u\|_{L^p} \\
&\leq C \sum_{|j-k| \leq 4} \|\nabla v\|_{B_{p,\infty}^r} \|\Lambda_1^{\alpha-1} \mathcal{H}_1 \Delta_k u\|_{L^p} \\
&\leq C \sum_{|j-k| \leq 4} \|v\|_{B_{p,\infty}^{r+1}} \tilde{C} 2^{k(\alpha-1)} \|\Delta_k u\|_{L^p},
\end{aligned}$$

so,

$$\begin{aligned}
2^{j\lambda} \|L_2\|_{L^p} &\leq C 2^{j\lambda} \|v\|_{B_{p,\infty}^{r+1}} \sum_{|j-k| \leq 4} 2^{k(\alpha-1)} \|\Delta_k u\|_{L^p} \\
&= C \|v\|_{B_{p,\infty}^{r+1}} \sum_{|j-k| \leq 4} 2^{(j-k)\lambda} 2^{(\lambda+\alpha-1)k} \|\Delta_k u\|_{L^p} \\
&\leq C \|v\|_{B_{p,\infty}^{r+1}} \|u\|_{B_{p,\infty}^{\lambda+\alpha-1}} \sum_{|k| \leq 4} 2^{k\lambda} \\
&\leq C \|v\|_{B_{p,\infty}^{r+1}} \|u\|_{B_{p,\infty}^{\lambda+\alpha-1}}.
\end{aligned}$$

We have also,

$$\begin{aligned}
\|L_3\|_{L^p} &\leq \sum_{|k-j|\leq 3} \sum_{|k-\bar{k}|\leq 1} C \|\Delta_k \Lambda_1^{\alpha-1} \mathcal{H}_1 u\|_{L^p} \|\Delta_{\bar{k}} \partial_1 v\|_{L^\infty} \\
&\leq C \sum_{|k-j|\leq 3} \sum_{|k-\bar{k}|\leq 1} \|\Lambda_1^{\alpha-1} \mathcal{H}_1 \Delta_k u\|_{L^p} \|\partial_1 v\|_{L^\infty} \\
&\leq C \sum_{|k-j|\leq 3} \sum_{|k-\bar{k}|\leq 1} \|\Lambda_1^{\alpha-1} \mathcal{H}_1 \Delta_k u\|_{L^p} \|\nabla v\|_{L^\infty} \\
&\leq C \sum_{|k-j|\leq 3} \sum_{|k-\bar{k}|\leq 1} 2^{k(\alpha-1)} \|\Delta_k u\|_{L^p} \|v\|_{B_{p,\infty}^{r+1}} \\
&\leq C 2^{-j\lambda} \sum_{|k-j|\leq 3} \sum_{|k-\bar{k}|\leq 1} 2^{(j-k)\lambda} \{2^{(\lambda+\alpha-1)k} \|\Delta_k u\|_{L^p}\} \|v\|_{B_{p,\infty}^{r+1}} \\
&\leq C 2^{-j\lambda} \|u\|_{B_{p,\infty}^{\lambda+\alpha-1}} \|v\|_{B_{p,\infty}^{r+1}},
\end{aligned}$$

so,

$$2^{j\lambda} \|L_3\|_{L^p} \leq C \|u\|_{B_{p,\infty}^{\lambda+\alpha-1}} \|v\|_{B_{p,\infty}^{r+1}}.$$

By proceeding similarly, we will obtain the estimates for L_4 and L_5 :

$$\begin{aligned}
\|L_4\|_{L^p} &\leq \sum_{k \geq j} C \|\partial_1 v\|_{L^\infty} \|\Lambda_1^{\alpha-1} \mathcal{H}_1 \Delta_k u\|_{L^p} \\
&\leq \sum_{k \geq j} \|\nabla v\|_{L^\infty} \tilde{C} 2^{k(\alpha-1)} \|\Delta_k u\|_{L^p} \\
&\leq C 2^{-j\lambda} \sum_{k \geq j} 2^{(j-k)\lambda} \|\nabla v\|_{B_{p,\infty}^r} 2^{k(\lambda+\alpha-1)} \|\Delta_k u\|_{L^p} \\
&\leq C 2^{-j\lambda} \|v\|_{B_{p,\infty}^{r+1}} \|u\|_{B_{p,\infty}^{\lambda+\alpha-1}},
\end{aligned}$$

so

$$2^{j\lambda} \|L_4\|_{L^p} \leq C \|v\|_{B_{p,\infty}^{r+1}} \|u\|_{B_{p,\infty}^{\lambda+\alpha-1}}.$$

Finally,

$$\begin{aligned}
\|L_5\|_{L^p} &\leq \sum_{|j''-j'|\leq 1} \sum_{|j'-j|\leq 1} \|\partial_1 v\|_{L^\infty} \|\Lambda_1^{\alpha-1} \mathcal{H}_1 \Delta_{j'} u\|_{L^p} \\
&\leq \sum_{|j''-j'|\leq 1} \sum_{|j'-j|\leq 1} \|\nabla v\|_{L^\infty} \|\Lambda_1^{\alpha-1} \mathcal{H}_1 \Delta_{j'} u\|_{L^p} \\
&\leq \sum_{|j''-j'|\leq 1} \sum_{|j'-j|\leq 1} \|\nabla v\|_{B_{p,\infty}^r} C 2^{j'(\alpha-1)} \|\Delta_{j'} u\|_{L^p} \\
&\leq C \sum_{|j''-j'|\leq 1} \sum_{|j'-j|\leq 1} \|v\|_{B_{p,\infty}^{r+1}} 2^{(\alpha-1)j'} \|\Delta_{j'} u\|_{L^p},
\end{aligned}$$

so,

$$\begin{aligned} 2^{j\lambda} \|L_5\|_{L^p} &\leq C \|v\|_{B_{p,\infty}^{r+1}} \sum_{|j''-j'|\leq 1} \sum_{|j'-j|\leq 1} 2^{(j-j')\lambda} 2^{(\lambda+\alpha-1)j'} \|\Delta_{j'} u\|_{L^p} \\ &\leq C \|v\|_{B_{p,\infty}^{r+1}} \|u\|_{B_{p,\infty}^{\lambda+\alpha-1}}. \end{aligned}$$

By collecting the estimates above, we obtain

$$2^{j\lambda} \left\| [\Delta_j, \Lambda_1^{\alpha-1} \mathcal{H}_1 u] \partial_1 v \right\|_{L^p} \leq C (\|u\|_{B_{p,\infty}^r} \|v\|_{B_{p,\infty}^{\gamma+\alpha}} + \|u\|_{B_{p,\infty}^{\lambda+\alpha-1}} \|v\|_{B_{p,\infty}^{r+1}}).$$

□

Without loss of generality, Proposition 2 and Proposition 3 remain valid for nonlinear and nonlocal operators in the other direction, i.e., in $\Lambda_2^{\alpha-1}$ and \mathcal{H}_2 .

3.3 On the Well-Posedness of a Conservation Law with Partially Nonlocal Velocity in Besov Spaces

The Theorem 2 is one of the main theoretical results of our research. This theorem guarantees the existence, uniqueness, and continuous dependence of the solution of a conservation law with partially nonlocal velocity in classical Besov spaces. Before commencing the proof of Theorem 2, we present some results that will be used throughout the proof of this theorem.

In order to regularize the velocity field, let us consider a symmetric and nonnegative smooth function $\rho \in C_c^\infty(\mathbb{R})$ such that $\int_{\mathbb{R}} \rho(s) \, ds = 1$. Now, for a small $\epsilon > 0$ define, $\rho_\epsilon(s) = \epsilon^{-1} \rho(\frac{s}{\epsilon})$. Also, given a function $\theta(x, y)$ defined in \mathbb{R}^2 , we denote by $*_1$ and $*_2$ the partial convolutions:

$$(\rho *_1 \theta)(x, y) = \int_{\mathbb{R}} \rho(x-s) \theta(s, y) \, ds, \quad (3.27)$$

$$(\rho *_2 \theta)(x, y) = \int_{\mathbb{R}} \rho(y-s) \theta(x, s) \, ds, \quad (3.28)$$

respectively.

We defined,

$$\begin{aligned} P_{1,\epsilon} \theta &:= c_\alpha (|x|^{-\alpha} * \rho_\epsilon) * (\mathcal{H}_1 \theta) \\ &= c_\alpha (|x|^{-\alpha} * \rho_\epsilon) * (W_0 * \theta_y) \\ &= c_\alpha |x|^{-\alpha} * (W_0 * (\rho_\epsilon * \theta_y)) \\ &= c_\alpha |x|^{-\alpha} * (W_0 * (\rho_\epsilon *_1 \theta)) \\ &= c_\alpha |x|^{-\alpha} * \mathcal{H}_1 (\rho_\epsilon *_1 \theta) \\ &= \Lambda_1^{\alpha-1} \mathcal{H}_1 \theta_{1,\epsilon}, \end{aligned}$$

where

$$\theta_{1,\epsilon} = \rho_\epsilon *_1 \theta. \quad (3.29)$$

Notice that $\theta_y \in \mathcal{S}(\mathbb{R})$ and $\rho_\epsilon *_1 \theta \in \mathcal{S}(\mathbb{R})$. Similarly we can get $P_{2,\epsilon}\theta = \Lambda_2^{\alpha-1}\mathcal{H}_2\theta_{2,\epsilon}$, where

$$\theta_{2,\epsilon} = \rho *_2 \theta. \quad (3.30)$$

Thus, the regularized velocity field is given by $(\Lambda_1^{\alpha-1}\mathcal{H}_1\theta_{1,\epsilon}, \Lambda_2^{\alpha-1}\mathcal{H}_2\theta_{2,\epsilon})$.

Furthermore, for fixed j , the functions $\theta_{i,\epsilon}$ and $\Delta_j\theta_{i,\epsilon}$ with $i = 1, 2$ are bounded by θ and $\Delta_j\theta$ respectively in $L^1(\mathbb{R}^2)$.

In fact, from Young's inequality, it follows that

$$\begin{aligned} \|\theta_{1,\epsilon}\|_{L^1(\mathbb{R}^2)} &= \int_{\mathbb{R}^2} |\theta_{1,\epsilon}(x, y)| \, dx \, dy \\ &= \int_{\mathbb{R}} \left(\int_{\mathbb{R}} |\rho_\epsilon *_1 \theta| \, dx \right) dy \\ &= \int_{\mathbb{R}} \|\rho_\epsilon *_1 \theta\|_{L^1} dy \\ &\leq \int_{\mathbb{R}} C \|\theta_y\|_{L^1} dy \\ &= C \int_{\mathbb{R}} \int_{\mathbb{R}} |\theta_y(x)| \, dx \, dy \\ &= C \|\theta\|_{L^1(\mathbb{R}^2)}. \end{aligned}$$

Analogously, we can obtain $\|\theta_{2,\epsilon}\|_{L^1(\mathbb{R}^2)} \leq C \|\theta\|_{L^1(\mathbb{R}^2)}$.

On the other hand, the definition of the partial convolution $*_1$, see (3.27), we have

$$\begin{aligned} \Delta_j\theta_{1,\epsilon}(x, y) &= 2^{2j}[(\mathcal{F}^{-1}\varphi(2^j\cdot)) *_1 \theta_{1,\epsilon}](x, y) \\ &= 2^{2j} \int_{\mathbb{R}} \int_{\mathbb{R}} \mathcal{F}^{-1}\varphi(2^j(x-u, y-v))\theta_{1,\epsilon}(u, v) \, du \, dv \\ &= 2^{2j} \int_{\mathbb{R}} [\mathcal{F}^{-1}\varphi(2^j(\cdot, y-v)) *_1 (\rho_\epsilon *_1 \theta)](x) \, dv \\ &= 2^{2j} \int_{\mathbb{R}} [\rho_\epsilon *_1 (\mathcal{F}^{-1}\varphi(2^j(\cdot, y-v)) *_1 \theta)](x) \, dv \\ &= (\rho_\epsilon *_1 \Delta_j\theta)(x, y), \end{aligned}$$

then, by Young's inequality, we have

$$\|\Delta_j\theta_{1,\epsilon}\|_{L^1(\mathbb{R}^2)} \leq C \|\Delta_j\theta\|_{L^1(\mathbb{R}^2)}.$$

Analogous, it can be demonstrated that $\Delta_j\theta_{2,\epsilon}(x, y) = (\rho *_2 \Delta_j\theta)(x, y)$ and $\|\Delta_j\theta_{2,\epsilon}\|_{L^1(\mathbb{R}^2)} \leq C \|\Delta_j\theta\|_{L^1(\mathbb{R}^2)}$.

Notice that, for $\lambda > 0$

$$\begin{aligned} \|\theta_{1,\epsilon}\|_{B_{1,\infty}^\lambda(\mathbb{R}^2)} &= \sup_{j \geq 0} 2^{\lambda j} \|\Delta_j \theta_{1,\epsilon}\|_{L^1(\mathbb{R}^2)} + \|S_0 \theta_{1,\epsilon}\|_{L^1(\mathbb{R}^2)} \\ &\leq \sup_{j \geq 0} 2^{\lambda j} C \|\Delta_j \theta\|_{L^1(\mathbb{R}^2)} + C \|\theta\|_{L^1(\mathbb{R}^2)} \\ &\leq C \|\theta\|_{B_{1,\infty}^\lambda(\mathbb{R}^2)}. \end{aligned} \quad (3.31)$$

Analogous, we get $\|\theta_{2,\epsilon}\|_{B_{1,\infty}^\lambda(\mathbb{R}^2)} \leq C \|\theta\|_{B_{1,\infty}^\lambda(\mathbb{R}^2)}$.

Moreover, in the following result nonlocal operators depend only on one variable. This particular result is cited multiple times in the proof of Theorem 2.

Claim 3.3.1. *For $\alpha \in \mathbb{R}$, we have*

$$\frac{d}{dx}(\Lambda^{\alpha-1} \mathcal{H}\theta) = \Lambda^\alpha \theta. \quad (3.32)$$

In fact, from the definitions, $(\Lambda^{\alpha-1} \theta)^\wedge(\xi) = |\xi|^{\alpha-1} \hat{\theta}(\xi)$ and $(\mathcal{H}\theta)^\wedge(\xi) = -\frac{i\xi}{|\xi|} \hat{\theta}(\xi)$ follow that

$$\begin{aligned} \left\{ \frac{d}{dx} \Lambda^{\alpha-1}(\mathcal{H}\theta) \right\}^\wedge(\xi) &= i\xi \{ \Lambda^{\alpha-1}(\mathcal{H}\theta) \}^\wedge(\xi) \\ &= i\xi \{ |\xi|^{\alpha-1} (\mathcal{H}\theta)^\wedge(\xi) \} \\ &= i\xi \left\{ |\xi|^{\alpha-1} \left(-\frac{i\xi}{|\xi|} \hat{\theta}(\xi) \right) \right\} \\ &= |\xi|^\alpha \hat{\theta}(\xi) \\ &= (\Lambda^\alpha \theta)^\wedge(\xi) \end{aligned}$$

by taking the inverse Fourier Transform, we obtain the desired.

Lemma 5. *Let $\alpha \in [0, 1]$ and $\gamma > 3$. Assume that $w, u_1, u_2 \in B_{1,\infty}^\lambda$ and*

$$\partial_t w - \nabla \cdot \{w(\Lambda_1^{\alpha-1} \mathcal{H}_1 u_1, \Lambda_2^{\alpha-1} \mathcal{H}_2 u_2)\} = g, \quad (3.33)$$

then,

$$\int_{\mathbb{R}^2} \text{sgn}(\Delta_j w) \partial_t \Delta_j w dx dy \leq \sum_{i=1}^2 C 2^{-j\gamma} \|u_i\|_{B_{1,\infty}^{\gamma+\alpha-1}} \|w\|_{B_{1,\infty}^\gamma} + \int_{\mathbb{R}^2} \text{sgn}(\Delta_j w) \Delta_j g dx dy, \quad (3.34)$$

where, Δ_j is the localization operator and $g = g(w, u_1, u_2)$.

Proof. Equation (3.33) can be expressed as

$$\partial_t w = \sum_{i=1}^2 \partial_i w \Lambda_i^{\alpha-1} \mathcal{H}_i u_i + \sum_{i=1}^2 w \Lambda_i^\alpha u_i + g,$$

multiplying by the Δ_j localization operator, we have from the definition of commutators (3.25) that

$$\Delta_j \partial_t w = \sum_{i=1}^2 \left\{ [\Delta_j, \Lambda_i^{\alpha-1} \mathcal{H}_i u_i] \partial_i w + \Lambda_i^{\alpha-1} \mathcal{H}_i u_i \Delta_j \partial_i w + [\Delta_j, w] \Lambda_i^\alpha u_i + w \Delta_j \Lambda_i^\alpha u_i \right\} + \Delta_j g.$$

Now, by multiplying both sides by $\text{sgn}(\Delta_j w) = \frac{\Delta_j w}{|\Delta_j w|}$ and integrating over \mathbb{R}^2 we obtain:

$$\int_{\mathbb{R}^2} \text{sgn}(\Delta_j w) \partial_t \Delta_j w \, dx \, dy := J_1 + J_2 + J_3 + J_4 + \int_{\mathbb{R}^2} \text{sgn}(\Delta_j w) g \, dx \, dy. \quad (3.35)$$

Then, to estimate J_1 , Proposition 3 is employed; in this case we take $r = \gamma - 1 > 2$

$$\begin{aligned} J_1 &\leq \sum_{i=1}^2 \int_{\mathbb{R}^2} \left| \text{sgn}(\Delta_j w) [\Delta_j, \Lambda_i^{\alpha-1} \mathcal{H}_i u_i] \partial_i w \right| dx \, dy \\ &= \sum_{i=1}^2 \left\| [\Delta_j, \Lambda_i^{\alpha-1} \mathcal{H}_i u_i] \partial_i w \right\|_{L^1(\mathbb{R}^2)} \\ &\leq \sum_{i=1}^2 2^{-j\gamma} \left\{ C \|u_i\|_{B_{1,\infty}^{r+\alpha}} \|w\|_{B_{1,\infty}^\gamma} + C \|w\|_{B_{1,\infty}^{r+1}} \|u_i\|_{B_{1,\infty}^{\gamma+\alpha-1}} \right\} \\ &\leq \sum_{i=1}^2 2^{-j\gamma} \left\{ C \|u_i\|_{B_{1,\infty}^{\gamma+\alpha-1}} \|w\|_{B_{1,\infty}^\gamma} + C \|w\|_{B_{1,\infty}^\gamma} \|u_i\|_{B_{1,\infty}^{\gamma+\alpha-1}} \right\} \\ &\leq \sum_{i=1}^2 C 2^{-j\gamma} \|u_i\|_{B_{1,\infty}^{\gamma+\alpha-1}} \|w\|_{B_{1,\infty}^\gamma}. \end{aligned}$$

To estimate J_2 , we use integration by parts, and from the third item of Proposition 1 for $r = \gamma - 1 > 2$, we have

$$\begin{aligned} J_2 &= \int_{\mathbb{R}^2} \sum_{i=1}^2 \Lambda_i^{\alpha-1} \mathcal{H}_i u_i \text{sgn}(\Delta_j w) \partial_i \Delta_j w \, dx \, dy \\ &= \sum_{i=1}^2 \int_{\mathbb{R}^2} \Lambda_i^{\alpha-1} \mathcal{H}_i u_i \partial_i |\Delta_j w| \, dx \, dy \\ &= - \sum_{i=1}^2 \int_{\mathbb{R}^2} \Lambda_i^\alpha u_i |\Delta_j w| \, dx \, dy \\ &\leq \sum_{i=1}^2 \|\Lambda_i^\alpha u_i\|_{L^\infty} \int_{\mathbb{R}^2} |\Delta_j w| \, dx \, dy \\ &\leq \sum_{i=1}^2 C \|\Lambda_i^\alpha u_i\|_{B_{1,\infty}^r} \|\Delta_j w\|_{L^1} \\ &\leq \sum_{i=1}^2 C 2^{-j\gamma} \|u_i\|_{B_{1,\infty}^{r+\alpha}} \{2^{j\gamma} \|\Delta_j w\|_{L^1}\} \\ &\leq \sum_{i=1}^2 C 2^{-j\gamma} \|u_i\|_{B_{1,\infty}^{\gamma+\alpha-1}} \|w\|_{B_{1,\infty}^\gamma}. \end{aligned}$$

To estimate J_3 , we use Proposition 2, and we take $r = \gamma - 1 > 2$

$$\begin{aligned}
J_3 &\leq \sum_{i=1}^2 \int_{\mathbb{R}^2} |\operatorname{sgn}(\Delta_j w) [\Delta_j, w] \Lambda_i^\alpha u_i| dx dy \\
&\leq \sum_{i=1}^2 \|[\Delta_j, w] \Lambda_i^\alpha u_i\|_{L^1} \\
&\leq \sum_{i=1}^2 2^{-j\gamma} \left\{ C \|w\|_{B_{1,\infty}^{r+1}} \|u_i\|_{B_{1,\infty}^{\lambda+\alpha-1}} + C \|\theta_{i,\epsilon}^{(n)}\|_{B_{1,\infty}^{r+\alpha}} + \|\theta^{(n+1)}\|_{B_{1,\infty}^\lambda} \right\} \\
&= \sum_{i=1}^2 2^{-j\gamma} \left\{ C \|w\|_{B_{1,\infty}^\gamma} \|u_i\|_{B_{1,\infty}^{\gamma+\alpha-1}} + C \|u_i\|_{B_{1,\infty}^{\gamma+\alpha-1}} + \|w\|_{B_{1,\infty}^\lambda} \right\} \\
&= C 2^{-j\gamma} \|u_i\|_{B_{1,\infty}^{\gamma+\alpha-1}} \|w\|_{B_{1,\infty}^\gamma}.
\end{aligned}$$

On the other hand, defining $\operatorname{sgn}_\delta(\Delta_j w) = \frac{\Delta_j w}{\sqrt{(\Delta_j w)^2 + \delta}}$ we have to $\operatorname{sgn}_\delta(\Delta_j w) \longrightarrow \operatorname{sgn}(\Delta_j w)$ when $\delta \rightarrow 0$. Furthermore

$$\begin{aligned}
\partial_i \{\operatorname{sgn}_\delta(\Delta_j w) w\} &= \partial_i \{\operatorname{sgn}_\delta(\Delta_j w)\} w + \operatorname{sgn}_\delta(\Delta_j w) \partial_i w \\
&= \frac{\partial_i(\Delta_j w)}{(\Delta_j w)^2 + \delta} \left\{ \sqrt{(\Delta_j w)^2 + \delta} - \frac{(\Delta_j w)^2}{\sqrt{(\Delta_j w)^2 + \delta}} \right\} w + \operatorname{sgn}_\delta(\Delta_j w) \partial_i w \\
&= \frac{\partial_i(\Delta_j w)}{\sqrt{(\Delta_j w)^2 + \delta}^3} (\delta w) + \operatorname{sgn}_\delta(\Delta_j w) \partial_i w \longrightarrow \operatorname{sgn}(\Delta_j w) \partial_i w,
\end{aligned}$$

so, $\partial_i \{\operatorname{sgn}_\delta(\Delta_j w) w\} \longrightarrow \operatorname{sgn}(\Delta_j w) \partial_i w$ when $\delta \rightarrow 0$.

Finally, we estimate J_4 using integration by parts, from (3.12) of Theorem 1, from the third item of Proposition 1, the first item of Theorem 2.2 from [63], for $r = \gamma - 1$, we have

$$\begin{aligned}
J_4 &\approx \sum_{i=1}^2 \int_{\mathbb{R}^2} \operatorname{sgn}_\delta(\Delta_j w) w \partial_i (\Lambda_i^{\alpha-1} \mathcal{H}_i \Delta_j u_i) dx dy \\
&= - \sum_{i=1}^2 \int_{\mathbb{R}^2} \operatorname{sgn}(\Delta_j w) \partial_i \{w\} (\Lambda_i^{\alpha-1} \mathcal{H}_i \Delta_j u_i) dx dy \\
&\leq \sum_{i=1}^2 \|\partial_i w\|_{L^\infty} \|\Lambda_i^{\alpha-1} \mathcal{H}_i \Delta_j u_i\|_{L^1} \\
&= \sum_{i=1}^2 C 2^{-j\lambda} \|\nabla w\|_{L^\infty} 2^{j(\lambda+\alpha-1)} \|\Delta_j u_i\|_{L^1} \\
&\leq \sum_{i=1}^2 C 2^{-j\gamma} \|w\|_{B_{1,\infty}^{r+1}} \|u_i\|_{B_{1,\infty}^{\gamma+\alpha-1}} \\
&\leq \sum_{i=1}^2 C 2^{-j\gamma} \|u_i\|_{B_{1,\infty}^{\gamma+\alpha-1}} \|w\|_{B_{1,\infty}^\gamma}.
\end{aligned}$$

Notice that, $[\Delta_j, w]\Lambda_i^\alpha u_i + w\Delta_j\Lambda_i^\alpha u_i = \Delta_j\{w\Lambda_i^\alpha u_i\}$, so

$$J := \int_{\mathbb{R}^2} \operatorname{sgn}(\Delta_j w) \sum_{i=1}^2 \Delta_j \{w\Lambda_i^\alpha u_i\} dx dy = J_3 + J_4 \leq \sum_{i=1}^2 C2^{-j\gamma} \|u_i\|_{B_{1,\infty}^{\gamma+\alpha-1}} \|w\|_{B_{1,\infty}^\gamma}.$$

Thus, by using the previous estimates in (3.35), we obtain

$$\int_{\mathbb{R}^2} \operatorname{sgn}(\Delta_j w) \partial_t \Delta_j w dx dy \leq \sum_{i=1}^2 C2^{-j\gamma} \|u_i\|_{B_{1,\infty}^{\gamma+\alpha-1}} \|w\|_{B_{1,\infty}^\gamma} + \int_{\mathbb{R}^2} \operatorname{sgn}(\Delta_j w) g dx dy.$$

□

Theorem 2. Let $\alpha \in [0, 1]$ and $\lambda > 5$. Assume that the initial data $\theta_0 \in B_{1,\infty}^\lambda$. Then we can find $T = T(\|\theta_0\|_{B_{1,\infty}^\lambda})$, such that a unique solution θ to (1.3) on $[0, T] \times \mathbb{R}^2$ exists. Moreover, this solution belongs to $C^1([0, T]; B_{1,\infty}^{\lambda+\alpha-2}) \cap L^\infty([0, T]; B_{1,\infty}^\beta)$, and $\beta \in [\lambda + \alpha - 2, \lambda]$.

Proof. We begin the proof of Theorem 2 by constructing a sequence $\{\theta^{(n)}\}$, defined recursively by solving the following equations

$$\begin{cases} \theta^{(1)} = S_2(\theta_0) \\ \partial_t \theta^{(n+1)} = \nabla \cdot \left\{ \theta^{(n+1)} (\Lambda_1^{\alpha-1} \mathcal{H}_1 \theta_{1,\epsilon}^{(n)}, \Lambda_2^{\alpha-1} \mathcal{H}_2 \theta_{2,\epsilon}^{(n)}) \right\} \\ \theta^{(n+1)}((x, y), 0) = \theta_0^{(n+1)} = S_{n+2} \theta_0. \end{cases} \quad (3.36)$$

Since $\theta^{(n+1)}$ solves the linear system, we can always find the sequence. Notice that the second equation from (3.36) is a particular case of Lemma 5 with $w = \theta^{(n+1)}$, $u_1 = \theta_{1,\epsilon}^{(n)}$, $u_2 = \theta_{2,\epsilon}^{(n)}$ and $g = 0$, where $\theta_{1,\epsilon}$ and $\theta_{2,\epsilon}$ are defined in (3.29) and (3.30) respectively, for $\gamma = \lambda$, we have

$$\begin{aligned} \int_{\mathbb{R}^2} \operatorname{sgn}(\Delta_j \theta^{(n+1)}) \partial_t \Delta_j \theta^{(n+1)} dx dy &\leq \sum_{i=1}^2 C2^{-j\lambda} \|\theta_{i,\epsilon}^{(n)}\|_{B_{1,\infty}^{\lambda+\alpha-1}} \|\theta^{(n+1)}\|_{B_{1,\infty}^\lambda} \\ &\leq C2^{-j\lambda} \|\theta^{(n)}\|_{B_{1,\infty}^{\lambda+\alpha-1}} \|\theta^{(n+1)}\|_{B_{1,\infty}^\lambda}. \end{aligned}$$

Furthermore, observe that

$$\int_{\mathbb{R}^2} \operatorname{sgn}(\Delta_j \theta^{(n+1)}) \partial_t \Delta_j \theta^{(n+1)} dx dy = \int_{\mathbb{R}^2} \partial_t |\Delta_j \theta^{(n+1)}| dx dy = \frac{d}{dt} \|\Delta_j \theta^{(n+1)}\|_{L^1}, \quad (3.37)$$

then integrating from 0 to t in (3.35), the fact that $\theta_0^{(n+1)} = S_{n+2} \theta_0$, Young's inequality, and applying $\sup_{j \geq -1} 2^{j\lambda}$, we have

$$\begin{aligned} \sup_{j \geq -1} 2^{j\lambda} \|\Delta_j \theta^{(n+1)}\|_{L^1} &\leq \sup_{j \geq -1} 2^{j\lambda} C \|\Delta_j \theta_0\|_{L^1} + \sup_{j \geq -1} 2^{j\lambda} C2^{-j\lambda} \int_0^t \|\theta^{(n+1)}\|_{B_{1,\infty}^\lambda} \|\theta^{(n)}\|_{B_{1,\infty}^\lambda} d\tau \\ \|\theta^{(n+1)}\|_{B_{1,\infty}^\lambda} &\leq C \|\theta_0\|_{B_{1,\infty}^\lambda} + C \int_0^t \|\theta^{(n+1)}\|_{B_{1,\infty}^\lambda} \|\theta^{(n)}\|_{B_{1,\infty}^\lambda} d\tau, \end{aligned}$$

by the Grönwall inequality integral form, it follows that

$$\|\theta^{(n+1)}\|_{B_{1,\infty}^\lambda} \leq C\|\theta_0\|_{B_{1,\infty}^\lambda} \exp\left\{C \int_0^t \|\theta^{(n)}\|_{B_{1,\infty}^\lambda} d\tau\right\}, \quad (3.38)$$

with C independent of n .

Claim 3.3.2. *Defining $X_T := C([0, T]; B_{1,\infty}^\lambda)$, we get*

$$\|\theta^{(n+1)}\|_{X_T} \leq C\|\theta_0\|_{B_{1,\infty}^\lambda} \exp\left\{CT\|\theta^{(n)}\|_{X_T}\right\}, \quad (3.39)$$

where $\|\theta^{(n+1)}\|_{X_T} = \sup_{0 \leq t \leq T} \|\theta^{(n+1)}\|_{B_{1,\infty}^\lambda}$.

In fact, by taking $t \leq T$, we have (3.38)

$$\begin{aligned} \|\theta^{(n+1)}\|_{B_{1,\infty}^\lambda} &\leq C\|\theta_0\|_{B_{1,\infty}^\lambda} \exp\left\{C \int_0^t \sup_{0 \leq \tau \leq T} \|\theta^{(n)}\|_{B_{1,\infty}^\lambda} d\tau\right\} \\ &= C\|\theta_0\|_{B_{1,\infty}^\lambda} \exp\left\{C \int_0^t \|\theta^{(n)}\|_{X_T} d\tau\right\} \\ &= C\|\theta_0\|_{B_{1,\infty}^\lambda} \exp\left\{C\|\theta^{(n)}\|_{X_T} t\right\} \\ &\leq C\|\theta_0\|_{B_{1,\infty}^\lambda} \exp\left\{CT\|\theta^{(n)}\|_{X_T}\right\}, \end{aligned} \quad (3.40)$$

and take the supremum for $t \in [0, T]$, we obtain (3.39).

The following statement asserts that the sequence $\{\theta^{(n)}\}$ is bounded by the initial data θ_0 in the space $B_{1,\infty}^\lambda$.

Claim 3.3.3. *If $\exp\left\{2C^2T_0\|\theta_0\|_{B_{1,\infty}^\lambda}\right\} \leq 2$, then $\sup_{0 \leq t \leq T_0} \|\theta^{(n)}\|_{B_{1,\infty}^\lambda} \leq 2C\|\theta_0\|_{B_{1,\infty}^\lambda}$ for all $n \geq 1$.*

In fact, the proof is by induction. Let $T_0 \leq T$, for $n = 1$, from Young's inequality, we have

$$\begin{aligned} \sup_{0 \leq t \leq T_0} \|\theta^{(1)}\|_{B_{1,\infty}^\lambda} &= \sup_{0 \leq t \leq T_0} \|S_2\theta_0\|_{B_{1,\infty}^\lambda} \\ &\leq C \sup_{0 \leq t \leq T_0} \|\theta_0\|_{B_{1,\infty}^\lambda} \\ &\leq 2C\|\theta_0\|_{B_{1,\infty}^\lambda}. \end{aligned}$$

Assume it holds for n ; we show it also holds for $n + 1$. From (3.38) and proceeding as in (3.40), we can obtain

$$\begin{aligned} \sup_{0 \leq t \leq T_0} \|\theta^{(n+1)}\|_{B_{1,\infty}^\lambda} &\leq C\|\theta_0\|_{B_{1,\infty}^\lambda} \exp\left\{CT_0 \sup_{0 \leq \tau \leq T_0} \|\theta^{(n)}\|_{B_{1,\infty}^\lambda}\right\} \\ &\leq C\|\theta_0\|_{B_{1,\infty}^\lambda} \exp\left\{CT_0 2C\|\theta_0\|_{B_{1,\infty}^\lambda}\right\} \\ &\leq 2C\|\theta_0\|_{B_{1,\infty}^\lambda}. \end{aligned}$$

Let $Y_T := C([0, T]; B_{1,\infty}^{\lambda+\alpha-2})$. We will prove that the sequence $(\theta^{(n)})$ is Cauchy in Y_{T_1} for some $T_1 \in (0, T_0)$. Considering the difference $\theta^{(n+1)} - \theta^{(n)}$, and to the linearity of $\Lambda_i^{\alpha-1}$ and \mathcal{H}_i for $i = 1, 2$, we get

$$\begin{aligned} \partial_t(\theta^{(n+1)} - \theta^{(n)}) &= \nabla \cdot \left\{ \theta^{(n+1)} (\Lambda_1^{\alpha-1} \mathcal{H}_1 \theta_{1,\epsilon}^{(n)}, \Lambda_2^{\alpha-1} \mathcal{H}_2 \theta_{2,\epsilon}^{(n)}) \right\} \\ &\quad - \nabla \cdot \left\{ \theta^{(n)} (\Lambda_1^{\alpha-1} \mathcal{H}_1 \theta_{1,\epsilon}^{(n-1)}, \Lambda_2^{\alpha-1} \mathcal{H}_2 \theta_{2,\epsilon}^{(n-1)}) \right\} \\ &= \nabla \cdot \left\{ (\theta^{(n+1)} - \theta^{(n)}) (\Lambda_1^{\alpha-1} \mathcal{H}_1 \theta_{1,\epsilon}^{(n)}, \Lambda_2^{\alpha-1} \mathcal{H}_2 \theta_{2,\epsilon}^{(n)}) \right\} + \\ &\quad + \nabla \cdot \left\{ \theta^{(n)} (\Lambda_1^{\alpha-1} \mathcal{H}_1 (\theta_{1,\epsilon}^{(n)} - \theta_{1,\epsilon}^{(n-1)}), \Lambda_2^{\alpha-1} \mathcal{H}_2 (\theta_{2,\epsilon}^{(n)} - \theta_{2,\epsilon}^{(n-1)})) \right\} \\ &:= D_1 + D_2, \end{aligned}$$

with initial datum $(\theta^{(n+1)} - \theta^{(n)})(x, y, 0) = \Delta_{n+1} \theta_0$.

Also, note that this is a particular case of Lemma 5 with $w = \theta^{(n+1)} - \theta^{(n)}$, $u_1 = \theta_{1,\epsilon}^{(n)}$, $u_2 = \theta_{2,\epsilon}^{(n)}$ and $g = D_2$, where $\theta_{1,\epsilon}$ and $\theta_{2,\epsilon}$ are defined in (3.29) and (3.30) respectively; for $\gamma = \lambda + \alpha - 2$, we have

$$\begin{aligned} &\int_{\mathbb{R}^2} \text{sgn}\{\Delta_j(\theta^{(n+1)} - \theta^{(n)})\} \partial_t \Delta_j(\theta^{(n+1)} - \theta^{(n)}) dx dy \leq \\ &\sum_{i=1}^2 C 2^{-j(\lambda+\alpha-2)} \|u_i\|_{B_{1,\infty}^{\lambda+2\alpha-3}} \|\theta^{(n+1)} - \theta^{(n)}\|_{B_{1,\infty}^{\lambda+\alpha-2}} + \int_{\mathbb{R}^2} \text{sgn}\{\Delta_j(\theta^{(n+1)} - \theta^{(n)})\} \Delta_j D_2 dx dy \leq \\ &\sum_{i=1}^2 C 2^{-j(\lambda+\alpha-2)} \|\theta^{(n)}\|_{B_{1,\infty}^{\lambda}} \|\theta^{(n+1)} - \theta^{(n)}\|_{B_{1,\infty}^{\lambda+\alpha-2}} + \int_{\mathbb{R}^2} \text{sgn}\{\Delta_j(\theta^{(n+1)} - \theta^{(n)})\} \Delta_j D_2 dx dy, \end{aligned} \quad (3.41)$$

from the definition of commutators (3.25), we find that

$$\begin{aligned} \Delta_j D_2 &= \sum_{i=1}^2 [\Delta_j, \Lambda_i^{\alpha-1} \mathcal{H}_i (\theta_{i,\epsilon}^{(n)} - \theta_{i,\epsilon}^{(n-1)})] \partial_i \theta^{(n)} + \sum_{i=1}^2 \Lambda_i^{\alpha-1} \mathcal{H}_i (\theta_{i,\epsilon}^{(n)} - \theta_{i,\epsilon}^{(n-1)}) \Delta_j \partial_i \theta^{(n)} \\ &\quad + \sum_{i=1}^2 [\Delta_j, \theta^{(n)}] \Lambda_i^{\alpha} (\theta_{i,\epsilon}^{(n)} - \theta_{i,\epsilon}^{(n-1)}) + \sum_{i=1}^2 \theta^{(n)} \Delta_j \Lambda_i^{\alpha} (\theta_{i,\epsilon}^{(n)} - \theta_{i,\epsilon}^{(n-1)}). \end{aligned}$$

so,

$$\int_{\mathbb{R}^2} \text{sgn}\{\Delta_j(\theta^{(n+1)} - \theta^{(n)})\} \Delta_j D_2 dx dy := J'_1 + J'_2 + J'_3 + J'_4. \quad (3.42)$$

We estimate J'_1, J'_2, J'_3 and J'_4 analogously to J_1, J_2, J_3 , and J_4 , respectively. For

J'_1 of Proposition 3, in this case, we take $r = \lambda - 2 > 2$

$$\begin{aligned}
J'_1 &\leq \sum_{i=1}^2 \left\| [\Delta_j, \Lambda_i^{\alpha-1} \mathcal{H}_i(\theta_{i,\epsilon}^{(n)} - \theta_{i,\epsilon}^{(n-1)})] \partial_i \theta^{(n)} \right\|_{L^1} \\
&\leq \sum_{i=1}^2 2^{-j(\lambda+\alpha-2)} \left\{ C \left\| \theta_{i,\epsilon}^{(n)} - \theta_{i,\epsilon}^{(n-1)} \right\|_{B_{1,\infty}^{\lambda+\alpha-2}} \left\| \theta^{(n)} \right\|_{B_{1,\infty}^{\lambda+\alpha-2}} \right. \\
&\quad \left. + C \left\| \theta^{(n)} \right\|_{B_{1,\infty}^{\lambda+\alpha-1}} \left\| \theta_{i,\epsilon}^{(n)} - \theta_{i,\epsilon}^{(n-1)} \right\|_{B_{1,\infty}^{\lambda+\alpha-2+(\alpha-1)}} \right\} \\
&\leq \sum_{i=1}^2 2^{-j(\lambda+\alpha-2)} \left\{ C \left\| \theta_{i,\epsilon}^{(n)} - \theta_{i,\epsilon}^{(n-1)} \right\|_{B_{1,\infty}^{\lambda+\alpha-2}} \left\| \theta^{(n)} \right\|_{B_{1,\infty}^{\lambda}} + C \left\| \theta^{(n)} \right\|_{B_{1,\infty}^{\lambda}} \left\| \theta_{i,\epsilon}^{(n)} - \theta_{i,\epsilon}^{(n-1)} \right\|_{B_{1,\infty}^{\lambda+\alpha-2}} \right\} \\
&\leq C 2^{-j(\lambda+\alpha-2)} \left\| \theta^{(n)} \right\|_{B_{1,\infty}^{\lambda}} \left\| \theta^{(n)} - \theta^{(n-1)} \right\|_{B_{1,\infty}^{\lambda+\alpha-2}}.
\end{aligned}$$

For J'_2 of the integration by parts and from the third item of Proposition 1, we also take $r = \lambda - 2 > 2$ here

$$\begin{aligned}
J'_2 &= - \sum_{i=1}^2 \int_{\mathbb{R}^2} \operatorname{sgn}\{\Delta_j(\theta^{(n+1)} - \theta^{(n)})\} \partial_i \{\Lambda_i^{\alpha-1} \mathcal{H}_i(\theta_{i,\epsilon}^{(n)} - \theta_{i,\epsilon}^{(n-1)})\} \Delta_j \theta^{(n)} dx dy \\
&\leq \sum_{i=1}^2 \left\| \Lambda_i^{\alpha}(\theta_{i,\epsilon}^{(n)} - \theta_{i,\epsilon}^{(n-1)}) \right\|_{L^\infty} \int_{\mathbb{R}^2} |\Delta_j \theta^{(n)}| dx dy \\
&\leq \sum_{i=1}^2 C \left\| \Lambda_i^{\alpha}(\theta_{i,\epsilon}^{(n)} - \theta_{i,\epsilon}^{(n-1)}) \right\|_{B_{1,\infty}^r} \left\| \Delta_j \theta^{(n)} \right\|_{L^1} \\
&\leq \sum_{i=1}^2 C 2^{-j(\lambda+\alpha-2)} \left\| \theta_{i,\epsilon}^{(n)} - \theta_{i,\epsilon}^{(n-1)} \right\|_{B_{1,\infty}^{r+\alpha}} \left\| \theta^{(n)} \right\|_{B_{1,\infty}^{\lambda+\alpha-2}} \\
&\leq \sum_{i=1}^2 C 2^{-j(\lambda+\alpha-2)} \left\| \theta_{i,\epsilon}^{(n)} - \theta_{i,\epsilon}^{(n-1)} \right\|_{B_{1,\infty}^{\lambda+\alpha-2}} \left\| \theta^{(n)} \right\|_{B_{1,\infty}^{\lambda+\alpha-2}} \\
&\leq C 2^{-j(\lambda+\alpha-2)} \left\| \theta^{(n)} \right\|_{B_{1,\infty}^{\lambda}} \left\| \theta_{i,\epsilon}^{(n)} - \theta_{i,\epsilon}^{(n-1)} \right\|_{B_{1,\infty}^{\lambda+\alpha-2}}.
\end{aligned}$$

For J'_3 of Proposition 2, with $r = \lambda - 2 > 2$ and from the third item of Proposition 1

$$\begin{aligned}
J'_3 &\leq \sum_{i=1}^2 \left\| [\Delta_j, \theta^{(n)}] \Lambda_i^{\alpha}(\theta_{i,\epsilon}^{(n)} - \theta_{i,\epsilon}^{(n-1)}) \right\|_{L^1} \\
&\leq \sum_{i=1}^2 2^{-j(\lambda+\alpha-2)} \left\{ C \left\| \theta^{(n)} \right\|_{B_{1,\infty}^{\lambda-1}} \left\| \theta_{i,\epsilon}^{(n)} - \theta_{i,\epsilon}^{(n-1)} \right\|_{B_{1,\infty}^{\lambda+\alpha-2+(\alpha-1)}} \right. \\
&\quad \left. + C \left\| \theta_{i,\epsilon}^{(n)} - \theta_{i,\epsilon}^{(n-1)} \right\|_{B_{1,\infty}^{\lambda+\alpha-2}} \left\| \theta^{(n)} \right\|_{B_{1,\infty}^{\lambda+\alpha-2}} \right\} \\
&\leq \sum_{i=1}^2 2^{-j(\lambda+\alpha-2)} \left\{ C \left\| \theta^{(n)} \right\|_{B_{1,\infty}^{\lambda}} \left\| \theta_{i,\epsilon}^{(n)} - \theta_{i,\epsilon}^{(n-1)} \right\|_{B_{1,\infty}^{\lambda+\alpha-2}} + C \left\| \theta_{i,\epsilon}^{(n)} - \theta_{i,\epsilon}^{(n-1)} \right\|_{B_{1,\infty}^{\lambda+\alpha-2}} \left\| \theta^{(n)} \right\|_{B_{1,\infty}^{\lambda}} \right\} \\
&\leq C 2^{-j(\lambda+\alpha-2)} \left\| \theta^{(n)} \right\|_{B_{1,\infty}^{\lambda}} \left\| \theta^{(n)} - \theta^{(n-1)} \right\|_{B_{1,\infty}^{\lambda+\alpha-2}}.
\end{aligned}$$

Finally, for J'_4 of the integration by parts, from inequality (3.12) of Theorem 1 and from the third item of Proposition 1, in this case $r = \lambda - 1$

$$\begin{aligned}
J'_4 &= - \sum_{i=1}^2 \int_{\mathbb{R}^2} \operatorname{sgn}\{\Delta_j(\theta^{(n+1)} - \theta^{(n)})\} \partial_i \theta^{(n)} \{\Lambda_i^{\alpha-1} \mathcal{H}_i \Delta_j(\theta_{i,\epsilon}^{(n)} - \theta_{i,\epsilon}^{(n-1)})\} dx dy \\
&\leq \sum_{i=1}^2 \|\nabla \theta^{(n)}\|_{L^\infty} \|\Lambda_i^{\alpha-1} \mathcal{H}_i \Delta_j(\theta_{i,\epsilon}^{(n)} - \theta_{i,\epsilon}^{(n-1)})\|_{L^1} \\
&\leq \sum_{i=1}^2 \|\nabla \theta^{(n)}\|_{B_{1,\infty}^r} C 2^{j(\alpha-1)} \|\Delta_j(\theta_{i,\epsilon}^{(n)} - \theta_{i,\epsilon}^{(n-1)})\|_{L^1} \\
&\leq \sum_{i=1}^2 C 2^{-j(\lambda+\alpha-2)} \|\theta^{(n)}\|_{B_{1,\infty}^{r+1}} \|\theta_{i,\epsilon}^{(n)} - \theta_{i,\epsilon}^{(n-1)}\|_{B_{1,\infty}^{\lambda+\alpha-2+(\alpha-1)}} \\
&\leq C 2^{-j(\lambda+\alpha-2)} \|\theta^{(n)}\|_{B_{1,\infty}^\lambda} \|\theta^{(n)} - \theta^{(n-1)}\|_{B_{1,\infty}^{\lambda+\alpha-2}},
\end{aligned}$$

then in (3.42), we get

$$\int_{\mathbb{R}^2} \operatorname{sgn}\{\Delta_j(\theta^{(n+1)} - \theta^{(n)})\} \Delta_j D_2 dx dy \leq C 2^{-j(\lambda+\alpha-2)} \|\theta^{(n)}\|_{B_{1,\infty}^\lambda} \|\theta^{(n)} - \theta^{(n-1)}\|_{B_{1,\infty}^{\lambda+\alpha-2}}. \quad (3.43)$$

On the other hand, from the orthogonality of the localization operator Δ_j and Young's inequality, we have

$$\begin{aligned}
\|\theta_0^{(n+1)} - \theta_0^{(n)}\|_{B_{1,\infty}^{\lambda+\alpha-2}} &= \|\Delta_{n+1} \theta_0\|_{B_{1,\infty}^{\lambda+\alpha-2}} \\
&= \sup_{j \geq -1} 2^{j(\lambda+\alpha-2)} \|\Delta_j \Delta_{n+1} \theta_0\|_{L^1} \\
&= \sup_{n \leq j \leq n+2} 2^{j\lambda} 2^{j(\alpha-2)} \|\Delta_{n+1} \Delta_j \theta_0\|_{L^1} \\
&\leq 2^{n(\alpha-2)} \sup_{n \leq j \leq n+2} 2^{j\lambda} C \|\Delta_j \theta_0\|_{L^1} \\
&\leq C 2^{n(\alpha-2)} \|\theta_0\|_{B_{1,\infty}^{\lambda+\alpha-2}}.
\end{aligned}$$

Hence, from (3.37), (3.41) and (3.43), we obtain

$$\begin{aligned}
\frac{d}{dt} \|\Delta_j(\theta^{(n+1)} - \theta^{(n)})\|_{L^1} &= \int_{\mathbb{R}^2} \partial_t |\Delta_j(\theta^{(n+1)} - \theta^{(n)})| dx dy \leq \\
&C 2^{-j(\lambda+\alpha-2)} \|\theta^{(n)}\|_{B_{1,\infty}^\lambda} \left\{ \|\theta^{(n+1)} - \theta^{(n)}\|_{B_{1,\infty}^{\lambda+\alpha-2}} + \|\theta^{(n)} - \theta^{(n-1)}\|_{B_{1,\infty}^{\lambda+\alpha-2}} \right\},
\end{aligned}$$

integrating the extremes from 0 to t and using $\sup_{j \geq -1} 2^{j(\lambda+\alpha-2)}$

$$\begin{aligned}
\sup_{j \geq -1} 2^{j(\lambda+\alpha-2)} \|\Delta_j(\theta^{(n+1)} - \theta^{(n)})\|_{L^1} &\leq \sup_{j \geq -1} 2^{j(\lambda+\alpha-2)} \|\Delta_j(\theta_0^{(n+1)} - \theta_0^{(n)})\|_{L^1} + \\
&\sup_{j \geq -1} C \int_0^t \|\theta^{(n)}\|_{B_{1,\infty}^\lambda} \left\{ \|\theta^{(n+1)} - \theta^{(n)}\|_{B_{1,\infty}^{\lambda+\alpha-2}} + \|\theta^{(n)} - \theta^{(n-1)}\|_{B_{1,\infty}^{\lambda+\alpha-2}} \right\} d\tau,
\end{aligned}$$

so,

$$\begin{aligned}
\|\theta^{(n+1)} - \theta^{(n)}\|_{B_{1,\infty}^{\lambda+\alpha-2}} &\leq \|\theta_0^{(n+1)} - \theta_0^{(n)}\|_{B_{1,\infty}^{\lambda+\alpha-2}} \\
&\quad + C \int_0^t \sup_{0 \leq t \leq T_1} \|\theta^{(n)}\|_{B_{1,\infty}^\lambda} \sup_{0 \leq t \leq T_1} \|\theta^{(n)} - \theta^{(n-1)}\|_{B_{1,\infty}^{\lambda+\alpha-2}} d\tau \\
&\quad + C \int_0^t \sup_{0 \leq t \leq T_1} \|\theta^{(n)}\|_{B_{1,\infty}^\lambda} \|\theta^{(n+1)} - \theta^{(n)}\|_{B_{1,\infty}^{\lambda+\alpha-2}} d\tau \\
&\leq C 2^{n(\alpha-2)} \|\theta_0\|_{B_{1,\infty}^\lambda} + C \int_0^t 2C \|\theta_0\|_{B_{1,\infty}^\lambda} \|\theta^{(n)} - \theta^{(n-1)}\|_{Y_{T_1}} d\tau \\
&\quad + C \int_0^t 2C \|\theta_0\|_{B_{1,\infty}^\lambda} \|\theta^{(n+1)} - \theta^{(n)}\|_{B_{1,\infty}^{\lambda+\alpha-2}} d\tau \\
&\leq C 2^{n(\alpha-2)} \|\theta_0\|_{B_{1,\infty}^\lambda} + 2C \|\theta_0\|_{B_{1,\infty}^\lambda} \|\theta^{(n)} - \theta^{(n-1)}\|_{Y_{T_1}} \int_0^t d\tau \\
&\quad + 2C \|\theta_0\|_{B_{1,\infty}^\lambda} \int_0^t \|\theta^{(n+1)} - \theta^{(n)}\|_{B_{1,\infty}^{\lambda+\alpha-2}} d\tau \\
&\leq C 2^{n(\alpha-2)} \|\theta_0\|_{B_{1,\infty}^\lambda} + 2CT_1 \|\theta_0\|_{B_{1,\infty}^\lambda} \|\theta^{(n)} - \theta^{(n-1)}\|_{Y_{T_1}} \\
&\quad + 2C \|\theta_0\|_{B_{1,\infty}^\lambda} \int_0^t \|\theta^{(n+1)} - \theta^{(n)}\|_{B_{1,\infty}^{\lambda+\alpha-2}} d\tau,
\end{aligned}$$

by the integral version of Grönwall inequality, we get

$$\begin{aligned}
\|\theta^{(n+1)} - \theta^{(n)}\|_{B_{1,\infty}^{\lambda+\alpha-2}} &\leq \left(C 2^{n(\alpha-2)} \|\theta_0\|_{B_{1,\infty}^\lambda} + 2CT_1 \|\theta_0\|_{B_{1,\infty}^\lambda} \|\theta^{(n)} - \theta^{(n-1)}\|_{Y_{T_1}} \right) \\
&\quad \exp \left\{ 2C \|\theta_0\|_{B_{1,\infty}^\lambda} \int_0^t d\tau \right\} \\
&\leq \left(C 2^{n(\alpha-2)} \|\theta_0\|_{B_{1,\infty}^\lambda} + 2CT_1 \|\theta_0\|_{B_{1,\infty}^\lambda} \|\theta^{(n)} - \theta^{(n-1)}\|_{Y_{T_1}} \right) \\
&\quad \exp \left\{ 2CT_1 \|\theta_0\|_{B_{1,\infty}^\lambda} \right\} \\
&\leq C' 2^{n(\alpha-2)} + C' T_1 \exp \{ C' T_1 \} \|\theta^{(n)} - \theta^{(n-1)}\|_{Y_{T_1}},
\end{aligned}$$

where, $T_1 \in [0; T_0]$, and the constant $C' = C'(\|\theta_0\|_{B_{1,\infty}^\lambda})$. Thus, if $C' T_1 \exp \{ C' T_1 \} < 1/2$, we can deduce that $\theta^{(n)}$ converges to $\theta \in L^\infty([0; T_1]; B_{1,\infty}^{\lambda+\alpha-2})$ in Y_{T_1} .

Taking $\beta = (1-s)(\lambda + \alpha - 2) + s\lambda$ where $0 \leq s \leq 1$, we have

$$\|\theta^{(n)} - \theta\|_{B_{1,\infty}^\beta} = \|\theta^{(n)} - \theta\|_{B_{1,\infty}^{\lambda+\alpha-2}}^{1-s} \|\theta^{(n)} - \theta\|_{B_{1,\infty}^\lambda}^s,$$

as we have for all $n \in \mathbb{N}$ and $0 \leq t \leq T_1$ that $\theta^{(n)}$ is bounded by the initial condition $\theta_0 \in B_{1,\infty}^\lambda$, then $(\theta^{(n)} - \theta)$ is limited in $B_{1,\infty}^\lambda$. Hence, by the well-known interpolation inequality in the Besov spaces, we have $\theta^{(n)} \rightarrow \theta$ in $L^\infty([0; T_1]; B_{1,\infty}^\beta)$ for all $\beta \in [\lambda + \alpha - 2, \lambda]$. Let $n \rightarrow \infty$, we have $\theta^{(n)} \rightarrow \theta$. Thus, we find that θ is a solution to (1.3) in $B_{1,\infty}^\beta$.

Uniqueness and continuous dependence: Suppose θ and σ are both elements of $L^\infty([0; T_1]; B_{1,\infty}^\beta)$, representing two solutions of a conservation law with partially nonlocal

velocity (1.3) associated with the initial conditions θ_0 and σ_0 . Considering the difference $\partial_t \theta - \partial_t \sigma$, we have

$$\begin{aligned} \partial_t(\theta - \sigma) &= \nabla \cdot \{\theta(\Lambda_1^{\alpha-1} \mathcal{H}_1 \theta, \Lambda_2^{\alpha-1} \mathcal{H}_2 \theta)\} + \nabla \cdot \{\sigma(\Lambda_1^{\alpha-1} \mathcal{H}_1 \sigma, \Lambda_2^{\alpha-1} \mathcal{H}_2 \sigma)\} \\ &\quad + \nabla \cdot \{\sigma(\Lambda_1^{\alpha-1} \mathcal{H}_1 \theta, \Lambda_2^{\alpha-1} \mathcal{H}_2 \theta)\} - \nabla \cdot \{\theta(\Lambda_1^{\alpha-1} \mathcal{H}_1 \sigma, \Lambda_2^{\alpha-1} \mathcal{H}_2 \sigma)\} \\ &= \nabla \cdot \{(\theta - \sigma)(\Lambda_1^{\alpha-1} \mathcal{H}_1 \theta, \Lambda_2^{\alpha-1} \mathcal{H}_2 \theta)\} + \nabla \cdot \{\sigma(\Lambda_1^{\alpha-1} \mathcal{H}_1(\theta - \sigma), \Lambda_2^{\alpha-1} \mathcal{H}_2(\theta - \sigma))\} \\ &:= D_3 + D_4. \end{aligned}$$

This also is a particular case of Lemma 5 with $w = \theta - \sigma$, $u_1 = u_2 = \theta$ and $g = D_4$, for $\gamma = \beta$, we have

$$\begin{aligned} &\int_{\mathbb{R}^2} \operatorname{sgn}\{\Delta_j(\theta - \sigma)\} \partial_t \Delta_j(\theta - \sigma) dx dy \leq \\ &C 2^{-j\beta} \|\theta\|_{B_{1,\infty}^{\beta+\alpha-1}} \|\theta - \sigma\|_{B_{1,\infty}^\beta} + \int_{\mathbb{R}^2} \operatorname{sgn}\{\Delta_j(\theta - \sigma)\} \Delta_j D_4 dx dy \leq \\ &C 2^{-j\beta} \|\theta\|_{B_{1,\infty}^\beta} \|\theta - \sigma\|_{B_{1,\infty}^\beta} + \int_{\mathbb{R}^2} \operatorname{sgn}\{\Delta_j(\theta - \sigma)\} \Delta_j D_4 dx dy, \end{aligned} \quad (3.44)$$

from the definition of commutators (3.25), we find that

$$\begin{aligned} \Delta_j D_4 &= \sum_{i=1}^2 [\Delta_j, \Lambda_i^{\alpha-1} \mathcal{H}_i(\theta - \sigma)] \partial_i \sigma + \sum_{i=1}^2 \Lambda_i^{\alpha-1} \mathcal{H}_i(\theta - \sigma) \Delta_j \partial_i \sigma + \sum_{i=1}^2 [\Delta_j, \sigma] \Lambda_i^\alpha(\theta - \sigma) \\ &\quad + \sum_{i=1}^2 \sigma \Delta_j \Lambda_i^\alpha(\theta - \sigma), \end{aligned}$$

so,

$$\int_{\mathbb{R}^2} \operatorname{sgn}\{\Delta_j(\theta - \sigma)\} \Delta_j D_4 dx dy := K'_1 + K'_2 + K'_3 + K'_4. \quad (3.45)$$

Then, we have the following estimates:

For K'_1 of the Proposition 3 with $r = \beta - 1$ and Proposition 1

$$\begin{aligned} K'_1 &= \sum_{i=1}^2 \left\| [\Delta_j, \Lambda_i^{\alpha-1} \mathcal{H}_i(\theta - \sigma)] \partial_i \sigma \right\|_{L^1} \\ &\leq \sum_{i=1}^2 2^{-j\beta} \left\{ C \|\theta - \sigma\|_{B_{1,\infty}^{r+\alpha}} \|\sigma\|_{B_{1,\infty}^\beta} + C \|\sigma\|_{B_{1,\infty}^{r+1}} \|\theta - \sigma\|_{B_{1,\infty}^{\beta+\alpha-1}} \right\} \\ &\leq \sum_{i=1}^2 2^{-j\beta} \left\{ C \|\theta - \sigma\|_{B_{1,\infty}^{\beta+\alpha-1}} \|\sigma\|_{B_{1,\infty}^\beta} + C \|\sigma\|_{B_{1,\infty}^\beta} \|\theta - \sigma\|_{B_{1,\infty}^{\beta+\alpha-1}} \right\} \\ &\leq C 2^{-j\beta} \|\sigma\|_{B_{1,\infty}^\beta} \|\theta - \sigma\|_{B_{1,\infty}^\beta}. \end{aligned}$$

For K'_2 of the integration by parts and from the third item of Proposition 1, we also take $r = \beta - \alpha > 2$ here

$$\begin{aligned} K'_2 &\leq \sum_{i=1}^2 2^{-j\beta} C \|\theta - \sigma\|_{B_{1,\infty}^{r+\alpha}} \|\sigma\|_{B_{1,\infty}^\beta} \\ &\leq C 2^{-j\beta} \|\theta - \sigma\|_{B_{1,\infty}^\beta} \|\sigma\|_{B_{1,\infty}^\beta}. \end{aligned}$$

For K'_3 of Proposition 2, with $r = \beta - 1 > 2$ and from the third item of Proposition 1

$$\begin{aligned} K'_3 &\leq \sum_{i=1}^2 2^{-j\beta} \left\{ C \|\sigma\|_{B_{1,\infty}^{r+1}} \|\theta - \sigma\|_{B_{1,\infty}^{\beta+\alpha-1}} + C \|\theta - \sigma\|_{B_{1,\infty}^{r+\alpha}} + \|\sigma\|_{B_{1,\infty}^\beta} \right\} \\ &= \sum_{i=1}^2 2^{-j\beta} \left\{ C \|\sigma\|_{B_{1,\infty}^\beta} \|\theta - \sigma\|_{B_{1,\infty}^{\beta+\alpha-1}} + C \|\theta - \sigma\|_{B_{1,\infty}^{\beta+\alpha-1}} \|\sigma\|_{B_{1,\infty}^\beta} \right\} \\ &= C 2^{-j\beta} \|\sigma\|_{B_{1,\infty}^\beta} \|\theta - \sigma\|_{B_{1,\infty}^\beta}. \end{aligned}$$

Finally, for K'_4 of the integration by parts, from inequality (3.12) of Theorem 1 and from the third item of Proposition 1. For this case $r = \beta - 1$

$$\begin{aligned} K'_4 &\leq \sum_{i=1}^2 \|\nabla \sigma\|_{L^\infty} C 2^{j(\alpha-1)} \|\Delta_j(\theta - \sigma)\|_{L^1} \\ &\leq \sum_{i=1}^2 C 2^{-j\beta} \|\sigma\|_{B_{1,\infty}^{r+1}} \|\theta - \sigma\|_{B_{1,\infty}^{\beta+\alpha-1}} \\ &\leq C 2^{-j\beta} \|\sigma\|_{B_{1,\infty}^\beta} \|\theta - \sigma\|_{B_{1,\infty}^{\beta+\alpha-1}} \\ &\leq C 2^{-j\beta} \|\sigma\|_{B_{1,\infty}^\beta} \|\theta - \sigma\|_{B_{1,\infty}^\beta} \end{aligned}$$

then in (3.45), we get

$$\begin{aligned} \int_{\mathbb{R}^2} \frac{d}{dt} |\Delta_j(\theta - \sigma)| dx dy &\leq C 2^{-j\beta} \|\theta\|_{B_{1,\infty}^\beta} \|\theta - \sigma\|_{B_{1,\infty}^\beta} + C 2^{-j\beta} \|\sigma\|_{B_{1,\infty}^\beta} \|\theta - \sigma\|_{B_{1,\infty}^\beta} \\ \int_0^t \frac{d}{dt} \|\Delta_j(\theta - \sigma)\|_{L^1} d\tau &\leq \int_0^t C 2^{-j\beta} \left\{ \|\theta\|_{B_{1,\infty}^\beta} + \|\sigma\|_{B_{1,\infty}^\beta} \right\} \|\theta - \sigma\|_{B_{1,\infty}^\beta} d\tau \\ \|\Delta_j(\theta - \sigma)\|_{L^1} - \|\Delta_j(\theta_0 - \sigma_0)\|_{L^1} &\leq C 2^{-j\beta} \int_0^t \left\{ \|\theta\|_{B_{1,\infty}^\beta} + \|\sigma\|_{B_{1,\infty}^\beta} \right\} \|\theta - \sigma\|_{B_{1,\infty}^\beta} d\tau, \end{aligned}$$

through $\sup_{j \geq -1} 2^{j\beta}$, we obtain

$$\begin{aligned} \|\theta - \sigma\|_{B_{1,\infty}^\beta} &\leq \|\theta_0 - \sigma_0\|_{B_{1,\infty}^\beta} + C \int_0^t \left\{ \|\theta\|_{B_{1,\infty}^\beta} + \|\sigma\|_{B_{1,\infty}^\beta} \right\} \|\theta - \sigma\|_{B_{1,\infty}^\beta} d\tau \\ &\leq \|\theta_0 - \sigma_0\|_{B_{1,\infty}^\beta} + C \int_0^t \left\{ \sup_{0 \leq t \leq T_1} \|\theta\|_{B_{1,\infty}^\beta} + \sup_{0 \leq t \leq T_1} \|\sigma\|_{B_{1,\infty}^\beta} \right\} \|\theta - \sigma\|_{B_{1,\infty}^\beta} d\tau \\ &\leq \|\theta_0 - \sigma_0\|_{B_{1,\infty}^\beta} + C \int_0^t \left\{ 2C \|\theta_0\|_{B_{1,\infty}^\beta} + 2C \|\sigma_0\|_{B_{1,\infty}^\beta} \right\} \|\theta - \sigma\|_{B_{1,\infty}^\beta} d\tau \\ &\leq \|\theta_0 - \sigma_0\|_{B_{1,\infty}^\beta} + C' \int_0^t \|\theta - \sigma\|_{B_{1,\infty}^\beta} d\tau, \end{aligned}$$

where $C' = C'(\|\theta_0\|_{B_{1,\infty}^\beta})$ and by the Grönwall inequality integral form, we have

$$\begin{aligned} \|\theta - \sigma\|_{B_{1,\infty}^\beta} &\leq \|\theta_0 - \sigma_0\|_{B_{1,\infty}^\beta} \exp \left\{ C' \int_0^t d\tau \right\} \\ &\leq \|\theta_0 - \sigma_0\|_{B_{1,\infty}^\beta} \exp \{ C' T_1 \}, \end{aligned}$$

if $\theta_0 = \sigma_0$ we get the uniqueness of solutions in $C([0; T_1]; B_{1,\infty}^\beta)$. The proof is complete. \square

3.4 Numerical Study

In this section, we aim to devise an enhanced, fully-discrete nonlocal Lagrangian-Eulerian method based on the improved concept of space-time No-Flow curve. This scheme is specifically crafted to adeptly address the complexities arising from the application of the partial doubly nonlocal operator $\Lambda_i^{\alpha-1}\mathcal{H}_i$ with $i = 1, 2$ to hyperbolic conservation laws. Here, $\Lambda_i^{\alpha-1}$ represents the partial Riesz potential transform, and \mathcal{H}_i represents the partial Hilbert transform.

The construction of the Lagrangian-Eulerian scheme is rooted in the novel concept of the No-Flow curve, which was initially introduced in [12] and rigorously analyzed for fully discrete schemes with a solid mathematical foundation. A significant feature of this method is the dynamic tracking of the No-Flow curve forward in time, on a per-time-step basis. This represents a substantial improvement compared to the classical backward tracking of characteristic curves over each time step interval, which is based on the strong form of the problem. Furthermore, one notable advantage of this method is that it does not require the eigenvalues to determine the CFL condition; instead, it can be obtained from the No-Flow curve.

As described in [11], the one-dimensional dynamic forward tracking Lagrangian-Eulerian numerical scheme can be integrated into monotone and "Total Variation Diminishing" (TVD) schemes. Similar to the one-dimensional approach presented in [49], it can be verified that this new no-flow finite volume Lagrangian-Eulerian scheme converges to the unique entropy solution for conservation laws that feature a discontinuous spacetime-dependent flux. The proposed scheme is noteworthy for being free of local Riemann problem solutions and not requiring adaptive space-time discretizations. This feature is relevant for real-world, non-trivial applications found in recent literature. These applications include scenarios with conservation laws featuring a discontinuous flux function [16, 23, 39, 49, 50, 59], point sources [36, 39, 48, 58], and resonant models [9, 44, 61].

We introduce a Lagrangian-Eulerian approach based on the principles outlined in [12]. For the sake of presentation, let us consider a generic 1D (local) scalar hyperbolic conservation law, denoted as $u = u(x, t)$, with the governing equation $\partial_t u + \partial_x H(u) = 0$. The formulation of the fully-discrete nonlocal Lagrangian-Eulerian scheme represents an improved and, actually, a substantial novel interpretation of the *integral tube concept* as firstly introduced [41, 40] for *local* parabolic problems and linear transport problems [17] for flow in porous media. Therefore, in the new context, this integral tube is now subject to the condition $\mathcal{O}\left(\frac{H(u)}{u}\right) \propto \left[\frac{\Delta x}{\Delta t}\right]$, which is referred to as the No-Flow curve (as described in [12, 11]). These quantities, u and $H(u)$, are obtained from the local scalar hyperbolic conservation law, and with the aid of suitable stability estimates, this approach proves to be highly effective in practical computations. Additionally, it results in a weak CFL

condition that is not contingent on the derivative of the flux function $H(u)$, but instead relies solely on the local behavior of the No-Flow curve.

For a more in-depth understanding of these concepts, see [7] and [8]. These two recent works have been examined through weak asymptotic analysis, as detailed in [10], [4], and [5]. They have provided further insights into the concept of the No-Flow curve within semi-discrete Lagrangian-Eulerian formulations. It is also noteworthy that the initial numerical analysis for the fully-discrete Lagrangian-Eulerian scheme for scalar local hyperbolic problems was presented in [61].

The concept of the No-Flow curve has been extended in various directions to tackle multidimensional initial value problems for both local scalar models and local systems of conservation laws. Recently in [2], the authors formally apply, for the first time, a fully-discrete Lagrangian-Eulerian scheme for study global well-posedness and finite time blow-up of solutions for a nonlinear 1D transport equation with nonlocal velocity given as $u_t \pm (u\mathcal{H}(u))_x = \nu u_{xx}$ where $\nu > 0$, along with measure initial data in the inviscid case when $\nu = 0$. Such models arise in fluid mechanics in vortex-sheet problems and its nonlocal feature comes from the presence of a singular integral operator (Hilbert transform $\mathcal{H}(u)$) in the velocity field; see, e.g., [2] for more details on how and why the nonlocal Hilbert transform arises in the context of fluid dynamics. Additionally, in [47], a fully-discrete Lagrangian-Eulerian scheme was formally applied for a numerical investigation to demonstrate evidence of blow-up and explore other qualitative properties of solutions for a nonlinear 1D transport equation with doubly nonlocal velocity, involving the interaction between the Riesz potential denoted as $\Lambda^{\alpha-1}$ and the Hilbert transform denoted as \mathcal{H} . The equation of interest is given as $u_t \pm (u\Lambda^{\alpha-1}\mathcal{H}(u))_x = 0$. Therefore, [2] and [47] were the first to implement the fully-discrete nonlocal Lagrangian-Eulerian scheme for the 1D case.

Continuing in the same direction, we aim to implement the fully-discrete nonlocal Lagrangian-Eulerian method to numerically investigate the global well-posedness, evidence of blow-up, attenuation, and other proprieties geometrics of the solutions of a conservation law with partially nonlocal velocity (3.46). In this equation, the velocity field is obtained through the composition of two nonlocal partial operators.

$$\begin{cases} \partial_t \theta \pm \nabla \cdot (\theta v) = 0, \text{ with } v = (\Lambda_1^{\alpha-1} \mathcal{H}_1 \theta, \Lambda_2^{\alpha-1} \mathcal{H}_2 \theta) \\ \theta(x, y, 0) = \theta_0(x, y), \end{cases} \quad (3.46)$$

where $(x, y, t) \in \Omega \times (t_0, T] \subset \mathbb{R}^2 \times \mathbb{R}^+$ and $\theta_0 \in L^p(\mathbb{R}^2) \cup \{\eta\}$ with $\eta \in W\tilde{\mathcal{M}}_p^l$ (modified weak-Morrey space) which is defined as $\eta(x, y) = \frac{1}{x^2 + y^2}$, that is, $\theta_0 : \Omega \times \{0\} \longrightarrow \mathbb{R}$ is a not necessarily regular function, and $T = t_f > 0$.

3.4.1 The nonlocal No-Flow curve and the nonlocal Lagrangian-Eulerian approach for a conservation law with partially nonlocal velocity

In this subsection, we are going to present the numerical approximations we will use to solve numerically the underlying conservation law with partially nonlocal velocity.

First, we define the space-time domain, or the no-flow tube, in one spatial variable, this is

$$D_j^n = \{(t, x) / t^n \leq t \leq t^{n+1}, \sigma_j^n(t) \leq x \leq \sigma_{j+1}^n(t)\}. \quad (3.47)$$

To $u = u(x, t)$, a conserved variable in 1D case, we define the approximations

$$U_j^n = \frac{1}{h} \int_{x_{j-\frac{1}{2}}^n}^{x_{j+\frac{1}{2}}^n} u(x, t^n) dx, \quad \text{and} \quad \bar{U}_j^{n+1} = \frac{1}{h_j^{n+1}} \int_{\bar{x}_{j-\frac{1}{2}}^{n+1}}^{\bar{x}_{j+\frac{1}{2}}^{n+1}} u(x, t^{n+1}) dx \quad j \in \mathbb{Z}, \quad (3.48)$$

$j, n = 1, 2, 3, 4, \dots$. The first is in the original grid (homogeneous grid in t^n time) and the second one (non-homogeneous grid in t^{n+1} time).

To $u = u(x, y, t)$, a conserved variable, in 2D case, we use an approximation of the form

$$U_{i,j}^n \approx \frac{1}{\Delta y} \frac{1}{\Delta x} \int_{y_{j-\frac{1}{2}}^n}^{y_{j+\frac{1}{2}}^n} \int_{x_{i-\frac{1}{2}}^n}^{x_{i+\frac{1}{2}}^n} u(x, y, t^n) dx dy, \quad (3.49)$$

$$\bar{U}_{i,j}^{n+1} \approx \frac{1}{\bar{\Delta y}^{n+1}} \frac{1}{\bar{\Delta x}^{n+1}} \int_{\bar{y}_{j-\frac{1}{2}}^{n+1}}^{\bar{y}_{j+\frac{1}{2}}^{n+1}} \int_{\bar{x}_{i-\frac{1}{2}}^{n+1}}^{\bar{x}_{i+\frac{1}{2}}^{n+1}} u(x, y, t^{n+1}) dx dy. \quad (3.50)$$

Again, the first is in the original grid (homogeneous grid in t^n time) and the second one (non-homogeneous grid in t^{n+1} time). The approximations defined before having a sense when they join with the following definitions for $i, j = 1, 2, \dots$

In the time level t^n , we have

$$(x_i^n, y_j^n) = (i\Delta x, j\Delta y) \quad \text{and} \quad (x_{i\pm\frac{1}{2}}^n, y_{j\pm\frac{1}{2}}^n) = \left(i\Delta x \pm \frac{\Delta x}{2}, j\Delta y \pm \frac{\Delta y}{2}\right),$$

on the uniform local grid (or primal grid). Here

$$\Delta x^n = x_{i+\frac{1}{2},j}^n - x_{i-\frac{1}{2},j}^n \quad \text{and} \quad \Delta y^n = y_{i,j+\frac{1}{2}}^n - y_{i,j-\frac{1}{2}}^n \quad \text{for} \quad i, j = 1, 2, \dots,$$

where $(x_{i\pm\frac{1}{2}}^n, y_{j\pm\frac{1}{2}}^n)$ are the corners of the (i, j) -cell. For the nonuniform grid in the time level t^{n+1} , we have

$$\bar{\Delta x}^{n+1} = \bar{x}_{i+\frac{1}{2},j}^{n+1} - \bar{x}_{i-\frac{1}{2},j}^{n+1} \quad \text{and} \quad \bar{\Delta y}^{n+1} = \bar{y}_{i,j+\frac{1}{2}}^{n+1} - \bar{y}_{i,j-\frac{1}{2}}^{n+1} \quad \text{for} \quad i, j = 1, 2, \dots$$

The pair (x_i^n, y_j^n) are the centers of the region $R_{i,j}^n = [x_{i-\frac{1}{2}}^n, x_{i+\frac{1}{2}}^n] \times [y_{j-\frac{1}{2}}^n, y_{j+\frac{1}{2}}^n]$ with $i, j = 1, 2, \dots$, which we call (i, j) -cell in time t^n . Furthermore, on each (i, j) -cell in time t^n . The approximate solution of u is $U_{i,j}^n$ in each cell $[x_{i-\frac{1}{2}}^n, x_{i+\frac{1}{2}}^n] \times [y_{j-\frac{1}{2}}^n, y_{j+\frac{1}{2}}^n]$ (see Figure 1) and the approximation of u in the non-uniform grid is $\bar{U}_{i,j}^{n+1}$ in the non regular cell $[\bar{x}_{i-\frac{1}{2}}^{n+1}, \bar{x}_{i+\frac{1}{2}}^{n+1}] \times [\bar{y}_{j-\frac{1}{2}}^{n+1}, \bar{y}_{j+\frac{1}{2}}^{n+1}]$. All these approximations, along with the initial condition

$$U(x_j^0, y_j^0, t^0) = U_{i,j}^0.$$

The control volume of the Lagrangian-Eulerian scheme in 2D will denoted by $D_{i,j}^n$ see [12] and [9]. This control volume is a solid in \mathbb{R}^3 and is composed of triples (x, y, t) situated between the regions $R_{i,j}^n$ and $\bar{R}_{i,j}^{n+1}$, where $\bar{R}_{i,j}^{n+1}$ is determined by the No-Flow curves $\sigma_{i,j}^n(t)$ with $i, j = 1, 2, \dots$ and $t^n \leq t \leq t^{n+1}$. Thus, the border of the control volume $D_{i,j}^n$ is given by $\partial D_{i,j}^n = R_{i,j}^n \cup S_{i,j}^n \cup \bar{R}_{i,j}^{n+1}$, where

- $R_{i,j}^n = [x_{i-\frac{1}{2}}^n, x_{i+\frac{1}{2}}^n] \times [y_{j-\frac{1}{2}}^n, y_{j+\frac{1}{2}}^n] \subset \mathbb{R}^2$ is the entry of the no-flow surface region,
- $\bar{R}_{i,j}^{n+1} = [\bar{x}_{i-\frac{1}{2}}^{n+1}, \bar{x}_{i+\frac{1}{2}}^{n+1}] \times [\bar{y}_{j-\frac{1}{2}}^{n+1}, \bar{y}_{j+\frac{1}{2}}^{n+1}] \subset \mathbb{R}^2$ is the exit of the no-flow surface region, and
- $S_{i,j}^n \subset \mathbb{R}^3$, is the lateral surface of the no-flow region.

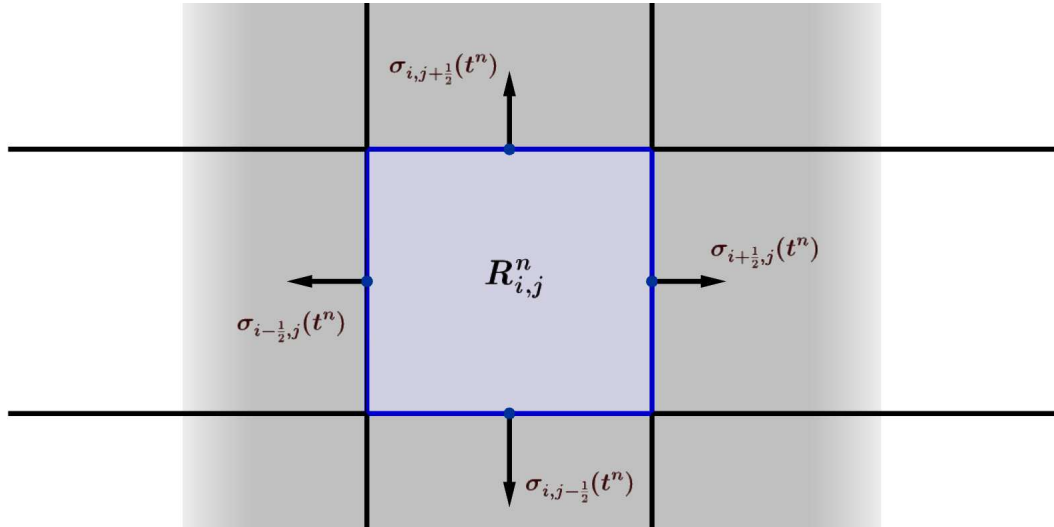


Figure 1 – Two-dimension cell, $R_{i,j}$ -cell.

3.4.2 Approximation of the partial Hilbert transform

For a function $f : \mathbb{R}^2 \rightarrow \mathbb{R}$ the definition of the partial Hilbert transform on the X axis and on the Y are given by

$$\begin{aligned} \mathcal{H}_1[f(x, y)] &= \frac{1}{\pi} \text{p.v.} \int_{-\infty}^{\infty} \frac{f(u, y)}{x - u} du = \frac{1}{\pi} \lim_{\epsilon \rightarrow 0^+} \int_{|u-x|>\epsilon} \frac{f(u, y)}{x - u} du, \\ \mathcal{H}_2[f(x, y)] &= \frac{1}{\pi} \text{p.v.} \int_{-\infty}^{\infty} \frac{f(x, v)}{y - v} dv = \frac{1}{\pi} \lim_{\epsilon \rightarrow 0^+} \int_{|v-y|>\epsilon} \frac{f(x, v)}{y - v} dv. \end{aligned}$$

For $\Delta x > 0$, let $\tau_x = \{x_n = x_0 + n\Delta x\}_{n=0}^N$ be a uniform grid on the X axis of $N + 1$ points that determine the closed interval $I_{\tau_x} = [x_0, x_N]$. Given a fixed $y \in \mathbb{R}$ and assuming that the grid must be such that the function $f(x, y)$ can be approximated by zero outside $I_{\tau_x} \times \{y\} = [x_0, x_N] \times [y]$. Then, for each interior point $(x_k, y) \in I_{\tau_x} \times \{y\}$ with $k = 1, \dots, N - 1$, we can approximate the partial Hilbert transform on the X axis as

$$\begin{aligned} \mathcal{H}_1[f(x_k, y)] &\approx \frac{1}{\pi} \lim_{\epsilon \rightarrow 0^+} \sum_{n=0}^{N-1} \int_{|u-x_k|>\epsilon, x_n \leq u \leq x_{n+1}} \frac{f(u, y)}{x_k - u} du \\ &= \frac{1}{\pi} \lim_{\epsilon \rightarrow 0^+} \left[\int_{x_{k-1}}^{x_k - \epsilon} \frac{f(u, y)}{x_k - u} du + \int_{x_k + \epsilon}^{x_{k+1}} \frac{f(u, y)}{x_k - u} du \right] \\ &\quad + \frac{1}{\pi} \sum_{n=0}^{k-2} \int_{x_n}^{x_{n+1}} \frac{f(u, y)}{x_k - u} du + \frac{1}{\pi} \sum_{n=k+1}^{N-1} \int_{x_n}^{x_{n+1}} \frac{f(u, y)}{x_k - u} du. \end{aligned} \quad (3.51)$$

Note that, in the previous approximation, the y is fixed, and if the values of nodes $f(x_k, y)$ are known in each interval $[x_n, x_{n+1}]$ the function $f(u, y)$ is approximated by linear polynomial interpolation,

$$f(u, y) \approx f(x_n, y) + \frac{f(x_{n+1}, y) - f(x_n, y)}{\Delta x} (u - x_n), \quad (3.52)$$

using the approximation (3.52) in the approximation of the partial Hilbert transform on the X axis (3.51) we will get

$$\begin{aligned} \mathcal{H}_1[f(x_k, y)] &\approx -\frac{1}{\pi} \{f(x_{k+1}, y) - f(x_{k-1}, y) \\ &\quad + \sum_{n=1}^{N-1-k} [-(1 - (n+1)b_n)f(x_{k+n}, y) + (1 - nb_n)f(x_{k+n+1}, y)] \\ &\quad + \sum_{n=1}^{k-1} [(1 - (n+1)b_n)f(x_{k-n}, y) - (1 - nb_n)f(x_{k-n-1}, y)]\}, \end{aligned} \quad (3.53)$$

where

$$b_n = \log\left(\frac{n+1}{n}\right).$$

The expression on the right-hand side of equation (3.53) defines a linear operator that approximates the partial Hilbert transform on the X axis for the vector $F = (f(x_0, y), f(x_1, y), \dots, f(x_N, y))$ at the interior points within the grid I_{τ_x} . This operator is de as the discrete partial Hilbert transform on the X axis, represented as \mathcal{H}_{τ_x} , and it can be expressed in matrix form as

$$\mathcal{H}_{\tau_x} F = AF_{\text{int}} + CF_{\text{bnd}}, \quad (3.54)$$

where the vector F has been split into its projection on internal nodes $F_{\text{int}} = (f(x_1, y), \dots, f(x_{N-1}, y))$ and boundary points $F_{\text{bnd}} = (f(x_0, y), f(x_N, y))$, whereas A is a $(N-1) \times (N-1)$ antisymmetric Toeplitz matrix,

$$A = \begin{pmatrix} a_0 & a_1 & \cdots & a_{N-3} & a_{N-2} \\ -a_1 & a_0 & \cdots & a_{N-4} & a_{N-3} \\ \vdots & \vdots & \vdots & \vdots & \vdots \\ -a_{N-2} & -a_{N-3} & \cdots & -a_1 & a_0 \end{pmatrix}, \quad (3.55)$$

where the matrix entries are given by

$$a_k = -\frac{1}{\pi} \begin{cases} 0, & \text{for } k = 0, \\ 2b_1, & \text{for } k = 1, \\ (k+1)b_k - (k-1)b_{k-1}, & \text{for } k > 1, \end{cases} \quad (3.56)$$

and C is a rectangular $(N-1) \times 2$ matrix

$$C = \begin{pmatrix} 0 & C_{N-1} \\ -c_1 & C_{N-2} \\ \vdots & \vdots \\ -C_{N-1} & 0 \end{pmatrix}, \quad (3.57)$$

where

$$c_k = -\frac{1}{\pi}(1 - kb_k).$$

Remark: An antisymmetric Toeplitz matrix is completely defined by its first row. Thus the evaluation of the $N-1$ elements (a_0, \dots, a_{N-2}) is enough to completely determine A .

Analogously, for the discrete partial Hilbert transform on the Y axis, we take $\Delta y > 0$, let $\tau_y = \{y_n = y_0 + n\Delta y\}_{n=0}^N$ be a uniform grid on the Y axis of $N+1$ points that determine the closed interval $I_{\tau_y} = [y_0, y_N]$. Given a fixed $x \in \mathbb{R}$ and assuming that the grid must be such that the function $f(x, y)$ can be approximated by zero outside $\{x\} \times I_{\tau_y} = [x] \times [y_0, y_N]$. Then, for each interior point $(x, y_k) \in \{x\} \times I_{\tau_y}$ with $k = 1, \dots, N-1$, we have

$$\begin{aligned} \mathcal{H}_2[f(x, y_k)] &\approx \frac{1}{\pi} \lim_{\epsilon \rightarrow 0^+} \sum_{n=0}^{N-1} \int_{|v-y_k|>\epsilon, y_n \leq u \leq y_{n+1}} \frac{f(x, v)}{y_k - v} dv \\ &= \frac{1}{\pi} \lim_{\epsilon \rightarrow 0^+} \left[\int_{y_{k-1}}^{y_k - \epsilon} \frac{f(x, v)}{y_k - v} dv + \int_{y_k + \epsilon}^{y_{k+1}} \frac{f(x, v)}{y_k - v} dv \right] \\ &\quad + \frac{1}{\pi} \sum_{n=0}^{k-2} \int_{y_n}^{y_{n+1}} \frac{f(x, v)}{y_k - v} dv + \frac{1}{\pi} \sum_{n=k+1}^{N-1} \int_{y_n}^{y_{n+1}} \frac{f(x, v)}{y_k - v} dv. \end{aligned} \quad (3.58)$$

Notice that, in the previous approximation the x is fixed and if the values of nodes $f(x, y_k)$ are known in each interval $[y_n, y_{n+1}]$ the function $f(x, v)$ is approximated by linear polynomial interpolation,

$$f(x, v) \approx f(x, y_n) + \frac{f(x, y_{n+1}) - f(x, y_n)}{\Delta y}(v - y_n), \quad (3.59)$$

using the approximation (3.59) in the approximation of the partial Hilbert transform on the Y axis (3.58), we will get

$$\begin{aligned} \mathcal{H}_2[f(x, y_k)] &\approx -\frac{1}{\pi} \{f(x, y_{k+1}) - f(x, y_{k-1}) \\ &\quad + \sum_{n=1}^{N-1-k} [-(1 - (n+1)b_n)f(x, y_{k+n}) + (1 - nb_n)f(x, y_{k+n+1})] \\ &\quad + \sum_{n=1}^{k-1} [(1 - (n+1)b_n)f(x, y_{k-n}) - (1 - nb_n)f(x, y_{k-n-1})]\}, \end{aligned} \quad (3.60)$$

where

$$b_n = \log\left(\frac{n+1}{n}\right).$$

The expression on the right-hand side of equation (3.60) establishes a linear operator that provides an approximation of the partial Hilbert transform on the Y axis for the vector $\tilde{F} = (f(x, y_0), f(x, y_1), \dots, f(x, y_N))$ at the interior points within the grid $\{x\} \times I_{\tau_y}$. This operator is defined as the discrete partial Hilbert transform on the Y axis, denoted as \mathcal{H}_{τ_y} , and it can be expressed in matrix form as

$$\mathcal{H}_{\tau_y} \tilde{F} = A \tilde{F}_{\text{int}} + C \tilde{F}_{\text{bnd}}, \quad (3.61)$$

where the vector \tilde{F} has been split into its projection on internal nodes $\tilde{F}_{\text{int}} = (f(x, y_1), \dots, f(x, y_{N-1}))$ and boundary points $\tilde{F}_{\text{bnd}} = (f(x, y_0), f(x, y_N))$, additionally, the matrices A and C have already been defined.

3.4.3 Approximation of the partial Riesz potential

For a function $f : \mathbb{R}^2 \longrightarrow \mathbb{R}$ and a parameter $\alpha \in (0, 1)$, the definition of the partial Riesz potential on the X axis and the Y axis is as follows:

$$\begin{aligned} \Lambda_1^{\alpha-1}[f(x, y)] &= c_\alpha \int_{\mathbb{R}} \frac{f(u, y)}{|x - u|^\alpha} du, \\ \Lambda_2^{\alpha-1}[f(x, y)] &= c_\alpha \int_{\mathbb{R}} \frac{f(x, v)}{|y - v|^\alpha} dv, \end{aligned}$$

where,

$$c_\alpha = \frac{\Gamma(\frac{\alpha}{2})}{2^{1-\alpha} \sqrt{\pi} \Gamma(\frac{1-\alpha}{2})}. \quad (3.62)$$

For $\Delta x > 0$, let $\tau_x = \{x_n = x_0 + n\Delta x\}_{n=0}^N$ be a uniform grid on the X axis of $N + 1$ points that determine the closed interval $I_{\tau_x} = [x_0, x_N]$. Given a fixed $y \in \mathbb{R}$ and assuming that the grid must be such that the function $f(x, y)$ can be approximated by zero outside $I_{\tau_x} \times \{y\} = [x_0, x_N] \times [y]$. Then, for each interior point $(x_k, y) \in I_{\tau_x} \times \{y\}$ with $k = 1, \dots, N - 1$, then we can approximate the partial Riesz potential on the X axis as

$$\begin{aligned} \Lambda_1^{\alpha-1}[f(x_k, y)] &\approx c_\alpha \sum_{n=0}^{N-1} \int_{x_n}^{x_{n+1}} \frac{f(u, y)}{|x_k - u|^\alpha} du \\ &= c_\alpha \left(\sum_{n=0}^{N-1} \int_{x_n}^{x_{n+1}} \frac{f(u, y)}{(x_k - u)^\alpha} du + \sum_{n=0}^{N-1} \int_{x_n}^{x_{n+1}} \frac{f(u, y)}{(u - x_k)^\alpha} du \right). \end{aligned} \quad (3.63)$$

Notice that, in the previous approximation, the variable y remains fixed, and if the values of nodes $f(x_k, y)$ are known in each interval $[x_n, x_{n+1}]$, we can approximate the function $f(u, y)$ using linear polynomial interpolation

$$f(u, y) \approx f(x_n, y) + \frac{f(x_{n+1}, y) - f(x_n, y)}{\Delta x} (u - x_n). \quad (3.64)$$

For calculation purposes, we omit the constant c_α , and using the approximation (3.64) in the partial Riesz potential approximation (3.63), we get

$$\begin{aligned}
\Lambda_1^{\alpha-1}[f(x_k, y)] &\approx \sum_{n=0}^{k-1} \int_{x_n}^{x_{n+1}} \left(\frac{f(x_n, y)}{(x_k - u)^\alpha} + \frac{f(x_{n+1}, y) - f(x_n, y)}{\Delta x} \cdot \frac{(u - x_n)}{(x_k - u)^\alpha} \right) du \\
&+ \sum_{n=k}^{N-1} \int_{x_n}^{x_{n+1}} \left(\frac{f(x_n, y)}{(x_k - u)^\alpha} + \frac{f(x_{n+1}, y) - f(x_n, y)}{\Delta x} \cdot \frac{(u - x_n)}{(x_k - u)^\alpha} \right) du \\
&= \sum_{n=0}^{k-1} -f(x_n, y) \left[\frac{(x_k - u)^{1-\alpha}}{1-\alpha} \right]_{u=x_n}^{u=x_{n+1}} + \sum_{n=0}^{k-1} \frac{f(x_{n+1}, y) - f(x_n, y)}{\Delta x} \int_{x_n}^{x_{n+1}} \frac{(u - x_n)}{(x_k - u)^\alpha} du \\
&+ \sum_{n=k}^{N-1} f(x_n, y) \left[\frac{(u - x_k)^{1-\alpha}}{1-\alpha} \right]_{u=x_n}^{u=x_{n+1}} + \sum_{n=k}^{N-1} \frac{f(x_{n+1}, y) - f(x_n, y)}{\Delta x} \int_{x_n}^{x_{n+1}} \frac{(u - x_n)}{(x_k - u)^\alpha} du \\
&= \sum_{n=0}^{k-1} -f(x_n, y) \left[\frac{(x_k - u)^{1-\alpha}}{1-\alpha} \right]_{u=x_n}^{u=x_{n+1}} + \sum_{n=0}^{k-1} \frac{f(x_{n+1}, y) - f(x_n, y)}{\Delta x} \times \\
&\int_{x_n}^{x_{n+1}} \left(\frac{x_k - x_n}{(x_k - u)^\alpha} - \frac{1}{(x_k - u)^{\alpha-1}} \right) du + \sum_{n=k}^{N-1} f(x_n, y) \left[\frac{(u - x_k)^{1-\alpha}}{1-\alpha} \right]_{u=x_n}^{u=x_{n+1}} \\
&+ \sum_{n=k}^{N-1} \frac{f(x_{n+1}, y) - f(x_n, y)}{\Delta x} \int_{x_n}^{x_{n+1}} \left(\frac{x_k - x_n}{(x_k - u)^\alpha} + \frac{1}{(x_k - u)^{\alpha-1}} \right) du \\
&= \sum_{n=0}^{k-1} -\frac{f(x_n, y)}{1-\alpha} \{ (x_k - x_{n+1})^{1-\alpha} - (x_k - x_n)^{1-\alpha} \} \\
&+ \sum_{n=0}^{k-1} \frac{f(x_{n+1}, y) - f(x_n, y)}{\Delta x} \left\{ \frac{-(x_k - x_n)}{1-\alpha} [(x_k - x_{n+1})^{1-\alpha} - (x_k - x_n)^{1-\alpha}] \right. \\
&+ \left. \frac{(x_k - x_{n+1})^{2-\alpha} - (x_k - x_n)^{2-\alpha}}{2-\alpha} \right\} + \sum_{n=k}^{N-1} \frac{f(x_n, y)}{1-\alpha} \{ (x_{n+1} - x_k)^{1-\alpha} - (x_n - x_k)^{1-\alpha} \} \\
&+ \sum_{n=k}^{N-1} \frac{f(x_{n+1}, y) - f(x_n, y)}{\Delta x} \left\{ \frac{(x_k - x_n)}{1-\alpha} [(x_{n+1} - x_k)^{1-\alpha} - (x_n - x_k)^{1-\alpha}] \right. \\
&+ \left. \frac{(x_{n+1} - x_k)^{2-\alpha} - (x_n - x_k)^{2-\alpha}}{2-\alpha} \right\},
\end{aligned}$$

given that $x_k = k\Delta x$ for $k = 0, \dots, N$, so

$$\begin{aligned}
\Lambda_1^{\alpha-1}[(f(x_k, y))] &= \sum_{n=0}^{k-1} -\frac{f(x_n, y)\Delta x^{1-\alpha}}{1-\alpha} \{ (k-n-1)^{1-\alpha} - (k-n)^{1-\alpha} \} \\
&+ \sum_{n=0}^{k-1} \left\{ \frac{-(k-n)}{1-\alpha} [(k-n-1)^{1-\alpha} - (k-n)^{1-\alpha}] + \frac{(k-n-1)^{2-\alpha} - (k-n)^{2-\alpha}}{2-\alpha} \right\} \times \\
&\frac{f(x_{n+1}, y) - f(x_n, y)}{\Delta x^{1-\alpha}} + \sum_{n=k}^{N-1} \frac{f(x_n, y)\Delta x^{1-\alpha}}{1-\alpha} [(n+1-k)^{1-\alpha} - (n-k)^{1-\alpha}] \\
&+ \sum_{n=k}^{N-1} \left\{ \frac{(k-n)}{1-\alpha} [(n+1-k)^{1-\alpha} - (n-k)^{1-\alpha}] + \frac{(n+1-k)^{2-\alpha} - (n-k)^{2-\alpha}}{2-\alpha} \right\} \times \\
&\frac{f(x_{n+1}, y) - f(x_n, y)}{\Delta x^{1-\alpha}},
\end{aligned}$$

to simplify the notation, we introduce a change of indices as follows: $m = n - k$, which implies $n = k - m$

$$\begin{aligned}
\Lambda_1^{\alpha-1}[f(x_k, y)] = & \\
& \Delta x^{1-\alpha} \sum_{n=0}^{k-1} - \left\{ (1-m) \frac{(m-1)^{1-\alpha} - m^{1-\alpha}}{1-\alpha} + \frac{(m-1)^{2-\alpha} - m^{2-\alpha}}{2-\alpha} \right\} f(x_{k-m}, y) + \\
& \Delta x^{1-\alpha} \sum_{n=0}^{k-1} f(x_{k-m+1}, y) \left\{ \frac{-m}{1-\alpha} ((m-1)^{1-\alpha} - m^{1-\alpha}) + \frac{(m-1)^{2-\alpha} - m^{2-\alpha}}{2-\alpha} \right\} + \\
& \Delta x^{1-\alpha} \sum_{n=k}^{N-1} \left((1-(k-n)) \frac{(n+1-k)^{1-\alpha} - (n-k)^{1-\alpha}}{1-\alpha} - \frac{(n+1-k)^{2-\alpha} - (n-k)^{2-\alpha}}{2-\alpha} \right) \times \\
& f(x_n, y) + \Delta x^{1-\alpha} \sum_{n=k}^{N-1} f(x_{n+1}, y) \times \\
& \left(\frac{k-n}{1-\alpha} \{ (n+1-k)^{1-\alpha} - (n-k)^{1-\alpha} \} + \frac{(n+1-k)^{2-\alpha} - (n-k)^{2-\alpha}}{2-\alpha} \right),
\end{aligned}$$

again, changing the indices $m = n - k + 1 \rightarrow n = m + k - 1$, we have that the approximation is

$$\begin{aligned}
\Lambda_1^{\alpha-1}[f(x_k, y)] = & \\
& + \Delta x^{1-\alpha} \sum_{m=1}^k \left[-f(x_{k-m}, y) \left\{ (1-m) \left(\frac{m^{1-\alpha} - (m-1)^{1-\alpha}}{1-\alpha} \right) + \frac{m^{2-\alpha} - (m-1)^{2-\alpha}}{2-\alpha} \right\} \right] \\
& + \Delta x^{1-\alpha} \sum_{n=0}^{k-1} f(x_{k-m+1}, y) \left(\frac{m}{1-\alpha} [m^{1-\alpha} - (m-1)^{1-\alpha}] - \frac{m^{2-\alpha} - (m-1)^{2-\alpha}}{2-\alpha} \right) \\
& + \Delta x^{1-\alpha} \sum_{m=1}^{N-k} \left[f(x_{m+k-1}, y) \left\{ m \left(\frac{m^{1-\alpha} - (m-1)^{1-\alpha}}{1-\alpha} \right) - \frac{m^{2-\alpha} - (m-1)^{2-\alpha}}{2-\alpha} \right\} \right] \\
& + \Delta x^{1-\alpha} \sum_{m=1}^{N-k} f(x_{m+k}, y) \left(\frac{(1-m)}{1-\alpha} [m^{1-\alpha} - (m-1)^{1-\alpha}] + \frac{m^{2-\alpha} - (m-1)^{2-\alpha}}{2-\alpha} \right).
\end{aligned}$$

Finally, we have that the numerical approximation of the partial Riesz potential on the X axis that was obtained is:

$$\begin{aligned}
\Lambda_1^{\alpha-1}[f(x_k, y)] \approx & \Delta x^{1-\alpha} \sum_{m=1}^k \{ f(x_{k-m}, y) [(1-m)a_m + b_m] + f(x_{k-m+1}, y)(ma_m - b_m) \} \\
& + \Delta x^{1-\alpha} \sum_{m=1}^{N-k} \{ f(x_{m+k-1}, y)(ma_m - b_m) + f(x_{m+k}, y)[(1-m)a_m + b_m] \},
\end{aligned} \tag{3.65}$$

where

$$a_m = \frac{m^{1-\alpha} - (m-1)^{1-\alpha}}{1-\alpha}; \quad b_m = \frac{m^{2-\alpha} - (m-1)^{2-\alpha}}{2-\alpha}.$$

The right-hand side of (3.65) defines a linear operator that computes the partial Riesz potential of $F = (f(x_0, y), f(x_1, y), \dots, f(x_{N-1}, y), f(x_N, y))$ on the X axis at the interior points of $I_{\tau_x} \times \{y\}$. If we denote by

$$F_{int} = (f(x_1, y), f(x_2, y), \dots, f(x_{N-1}, y)) \quad \text{and} \quad F_{bnd} = (f(x_0), f(x_N)), \quad (3.66)$$

then

$$\Lambda^{\alpha-1} F \approx (A + B)F_{int} + DF_{bnd}, \quad (3.67)$$

where

$$A = \begin{pmatrix} \tilde{a}_1 & \tilde{a}_2 & \tilde{a}_3 & \tilde{a}_4 & & \tilde{a}_{N-2} & \tilde{a}_{N-1} \\ \tilde{a}_2 & \tilde{a}_1 & \tilde{a}_2 & \tilde{a}_3 & & & \tilde{a}_{N-2} \\ \tilde{a}_3 & \tilde{a}_2 & \tilde{a}_1 & \tilde{a}_2 & & & \tilde{a}_{N-3} \\ \tilde{a}_4 & \tilde{a}_3 & \tilde{a}_2 & \tilde{a}_1 & & & \tilde{a}_{N-3} \\ & & & & & & \\ & & & & & & \\ \tilde{a}_{N-2} & & & & & \tilde{a}_2 & \tilde{a}_1 & \tilde{a}_2 \\ \tilde{a}_{N-1} & \tilde{a}_{N-2} & & & & \tilde{a}_3 & \tilde{a}_2 & \tilde{a}_1 \end{pmatrix}, \quad (3.68)$$

with

$$\tilde{a}_k = \begin{cases} -2a_1, & k = 1, \\ ka_k - (k-2)a_{k-1}, & k = 2, \dots, N-1, \end{cases}$$

$$B = \begin{pmatrix} \tilde{b}_1 & \tilde{b}_2 & \tilde{b}_3 & \tilde{b}_4 & & \tilde{b}_{N-1} \\ \tilde{b}_2 & \tilde{b}_1 & \tilde{b}_2 & \tilde{b}_3 & & \tilde{b}_{N-2} \\ \tilde{b}_3 & \tilde{b}_2 & \tilde{b}_1 & \tilde{b}_2 & & \tilde{b}_{N-3} \\ \tilde{b}_4 & \tilde{b}_3 & \tilde{b}_2 & \tilde{b}_1 & & \tilde{b}_{N-3} \\ & & & & & \\ & & & & & \\ \tilde{b}_{N-2} & & & & & \tilde{b}_2 & \tilde{b}_1 & \tilde{b}_2 \\ \tilde{b}_{N-1} & & & & & \tilde{b}_3 & \tilde{b}_2 & \tilde{b}_1 \end{pmatrix}, \quad (3.69)$$

with

$$\tilde{b}_k = \begin{cases} -2b_1, & k = 1, \\ b_{k-1} - b_k, & k = 2, \dots, N-1, \end{cases}$$

$$C = \begin{pmatrix} c_1 & c_{N-1} \\ c_2 & c_{N-2} \\ c_3 & c_{N-3} \\ c_4 & c_{N-4} \\ & \\ & \\ & \\ & \\ c_{N-2} & c_2 \\ c_{N-1} & c_1 \end{pmatrix}, \quad (3.70)$$

where

$$c_k = (1 - k)a_k + b_k, \quad k = 1, \dots, N - 1.$$

Fixing an $x \in \mathbb{R}$ and proceeding analogously with the calculations made, we can approximate the partial Riesz potential operator on the Y axis,

$$\begin{aligned} \Lambda_2^{\alpha-1}[f(x, y_k)] &\approx \Delta y^{1-\alpha} \sum_{m=1}^k [f(x, y_{k-m})\{(1-m)a_m + b_m\} + f(x, y_{k-m+1}, y)(ma_m - b_m)] \\ &\quad + \Delta y^{1-\alpha} \sum_{m=1}^{N-k} [f(x, y_{m+k-1})\{ma_m - b_m\} + f(x, y_{m+k})[(1-m)a_m + b_m]]. \end{aligned} \quad (3.71)$$

The right-hand side of (3.71) defines a linear operator that computes the partial Riesz potential of $\tilde{F} = (f(x, y_0), f(x, y_1), \dots, f(x, y_{N-1}, y), f(x, y_N))$ on the Y axis at the interior points of $\{x\} \times I_{\tau_y}$. If we denote by

$$\tilde{F}_{int} = (f(x, y_1), f(x, y_2), \dots, f(x, y_{N-1})) \quad \text{and} \quad \tilde{F}_{bnd} = (f(x, y_0), f(x, y_N)), \quad (3.72)$$

then

$$\Lambda^{\alpha-1}\tilde{F} \approx (A + B)\tilde{F}_{int} + D\tilde{F}_{bnd}, \quad (3.73)$$

where the matrices A, B , and D have already been defined.

3.4.4 The No-Flow Curve in the Hyperbolic Conservation Law, the Simplest Case and Some Advantages

The first problem we will consider is the simple conservation law

$$\frac{\partial u}{\partial t} + \frac{\partial H(u)}{\partial x} = 0, \quad u(x, 0) = \eta(x), \quad (3.74)$$

which is equivalent to, see [12],

$$\begin{cases} \frac{\partial \gamma_i^n}{\partial t} = \frac{H(u)}{u}, & \gamma_i^n(t^n) = x_i^n, \\ \int_{\bar{x}_{j-\frac{1}{2}}^{n+1}}^{\bar{x}_{j+\frac{1}{2}}^{n+1}} u(x, t^{n+1}) dx = \int_{x_j^n}^{x_{j+1}^n} u(x, t^n) dx. \end{cases} \quad (3.75)$$

Here, x_i is the center of the cell $[x_{i-\frac{1}{2}}, x_{i+\frac{1}{2}}]$, $i = 1, 2, 3, \dots$. In the representation (3.75), $\frac{H(u)}{u}$ is the non-flow curve in the theory sense. And

$$f_i = \frac{H(U_i^n)}{U_i^n}, \quad (3.76)$$

is the non-flow curve in the numeric sense, hereinafter the No-Flow curve. The Lagrangian-Eulerian method is defined as (see details in [12])

$$U_i^{n+1} = U_i^n - \frac{k^n}{h} [F(U_i, U_{i+1}^n) - F(U_{i-1}^n, U_i^n)], \quad (3.77)$$

where the associated *Lagrangian-Eulerian numerical flux function* that depends explicitly on the mesh parameters h, k and the No-Flow curve f_i , is defined by

$$F(U_i^n, U_{i+1}^n, h, k) = \frac{1}{4} \left[\frac{h}{k^n} (U_j^n - U_{i+1}^n) + \frac{h}{h_i^{n+1}} (f_{i+1}^n + f_i^n) (U_{i+1}^n + U_i^n) \right]. \quad (3.78)$$

This numerical method has a CFL condition, called weak-CFL because it does not depend on the derivative, which depends only on the No-Flow curve. The CFL condition is

$$\max_i \{|f_i|\} \frac{\Delta t}{\Delta x} \leq \frac{1}{2}.$$

The No-Flow curve adds some advantages to the numerical method, for example, the fact of not depending on the derivative. This fact can be noted in the CFL condition, making the method more versatile and robust.

For example, when we consider the Cauchy problem for the inviscid 1D transport model with nonlocal flux, like in [2], we rewrite model (3.74) in the computational domain $[a, b]$ (with $\nu = 0$),

$$u_t(x, t) - (F(t, x, u))_x = 0, \quad (x, t) \in \bar{\Omega} \times (0, T], \quad (3.79)$$

$$u(a, t) = 0, \quad u(b, t) = 0, \quad t \in [0, T], \quad (3.80)$$

$$u(x, 0) = f(x), \quad x \in \Omega, \quad (3.81)$$

where $F(t, x, u) := (\mathcal{H}(u)u)$; recall that \mathcal{H} is the Hilbert transform, which is given by the principal value (1.6) from [2]. Then, if we consider U^n as an approximation of u in all domains, we can use the numerical method (3.77) and (3.78) only replacing f_i by

$\frac{F(t^n, x_i, U^n)}{U^n} = \mathcal{H}(U^n)$ but now, f_i represents a nonlocal operator, not a function. The Hilbert transform approximation can be done as explained before.

The Lagrangian-Eulerian method for the 2D initial value problem for hyperbolic of conservation laws is:

$$\begin{cases} \frac{\partial u}{\partial t} + \frac{\partial f(u)}{\partial x} + \frac{\partial g(u)}{\partial y} = 0, & (x, y, t) \in \Omega \times (t^0, T], \\ u(x, y, t^0) = \eta(x, y), & (x, y) \in \Omega. \end{cases} \quad (3.82)$$

Assuming that the integration volume is impermeable through its lateral surface $S_{i,j}^n$, and that there is only flow through this volume at the inlet $R_{i,j}^n$ and outlet $\bar{R}_{i,j}^{n+1}$, the divergence theorem allows us to write the conservation law (3.82) as (see details in [6])

$$\begin{cases} \iint_{\bar{R}_{i,j}^{n+1}} u(x, y, t^{n+1}) d\bar{R}_{i,j}^{n+1} = \iint_{R_{i,j}^n} u(x, y, t^n) dR_{i,j}^n \\ \begin{cases} \sigma'_{i\pm\frac{1}{2},j}(t) = \frac{f(u)}{u}, & \begin{cases} \sigma'_{i,j\pm\frac{1}{2}}(t) = \frac{g(u)}{u}, \\ \sigma_{i\pm\frac{1}{2},j}(t^n) = x_{i\pm\frac{1}{2}}, & \begin{cases} \sigma_{i,j\pm\frac{1}{2}}(t^n) = y_{j\pm\frac{1}{2}}, \end{cases} \end{cases} \end{cases} \end{cases} \quad (3.83)$$

In the previous problem, we can identify the non-flow curves in the theoretical sense; these are $\frac{f(u)}{u}$ and $\frac{g(u)}{u}$; they start from the midpoints of the sides of the cell $R_{i,j}^n$, see figure 3.4.4. Using the approximations $U_{i\pm\frac{1}{2},j}^n$, $U_{i,j\pm\frac{1}{2}}^n$ to u in the midpoints of the cell $R_{i,j}^n$ we have the approximate problem to (3.83)

$$\begin{cases} \iint_{\bar{R}_{i,j}^{n+1}} u(x, y, t^{n+1}) d\bar{R}_{i,j}^{n+1} = \iint_{R_{i,j}^n} u(x, y, t^n) dR_{i,j}^n \\ \begin{cases} \sigma'_{i\pm\frac{1}{2},j}(t) = \frac{f(U_{i\pm\frac{1}{2},j}^n)}{U_{i\pm\frac{1}{2},j}^n}, & \begin{cases} \sigma'_{i,j\pm\frac{1}{2}}(t) = \frac{g(U_{i,j\pm\frac{1}{2}}^n)}{U_{i,j\pm\frac{1}{2}}^n}, \\ \sigma_{i\pm\frac{1}{2},j}(t^n) = x_{i\pm\frac{1}{2}}, & \begin{cases} \sigma_{i,j\pm\frac{1}{2}}(t^n) = y_{j\pm\frac{1}{2}}. \end{cases} \end{cases} \end{cases} \end{cases} \quad (3.84)$$

This last problem is the basis for constructing the Lagrangian-Eulerian method in two spatial dimensions. Let us look at this; take the first equation called the *conservation identity* in this context

$$\iint_{\bar{R}_{i,j}^{n+1}} u(x, y, t^{n+1}) d\bar{R}_{i,j}^{n+1} = \iint_{R_{i,j}^n} u(x, y, t^n) dR_{i,j}^n. \quad (3.85)$$

The numerical approximations $U_{i,j}^n$ and $\bar{U}_{i,j}^{n+1}$ appearing in (3.49) and (3.50) join with the *conservation identity* (3.85) can be used to calculate naturally the following identity,

$$\bar{U}_{i,j}^{n+1} = \frac{1}{\bar{R}_{i,j}} \int_{\bar{R}_{i,j}^{n+1}} u(x, y, t^{n+1}) dA = \frac{R_{i,j}}{\bar{R}_{i,j}} \frac{1}{R_{i,j}} \int_{R_{i,j}^n} u(x, y, t^n) dA = \frac{R_{i,j}}{\bar{R}_{i,j}} U_{i,j}^n, \quad (3.86)$$

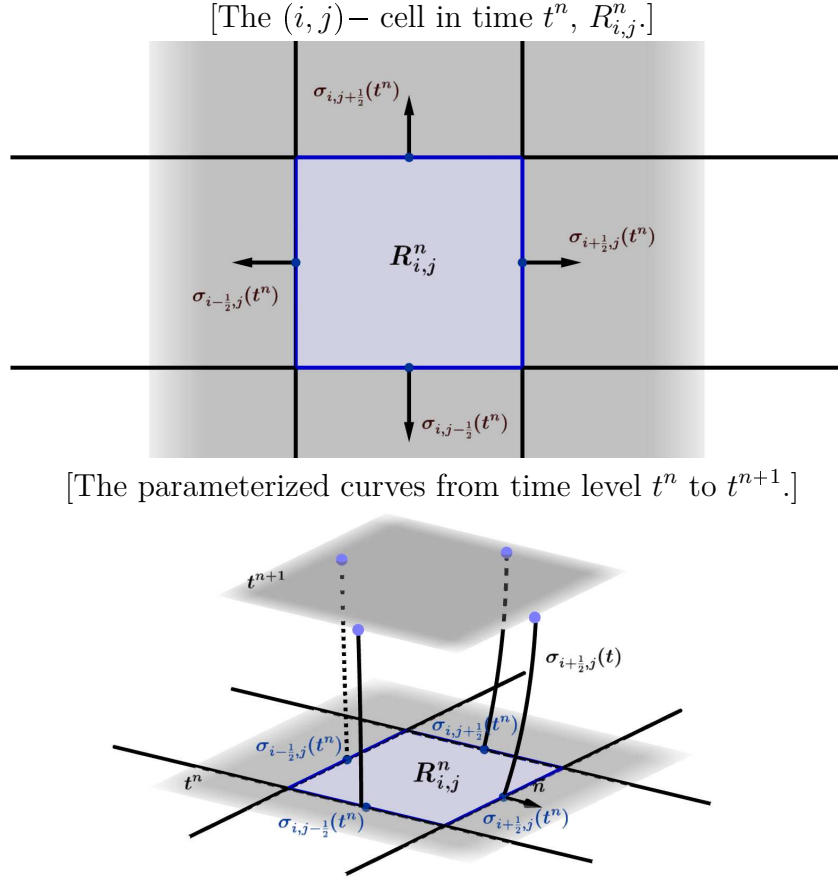


Figure 2 – The construction of the control volume for the Lagrangian-Eulerian scheme $D_{i,j}^n$.

We recall that, here the No-Flow curve are defined in the same way as before in the case of one dimension as $\frac{f(U_{i+\frac{1}{2},j}^n)}{U_{i+\frac{1}{2},j}^n} \equiv f_{i+\frac{1}{2},j}$, $\frac{f(U_{i-\frac{1}{2},j}^n)}{U_{i-\frac{1}{2},j}^n} \equiv f_{i-\frac{1}{2},j}$, $\frac{g(U_{i,j-\frac{1}{2}}^n)}{U_{i,j-\frac{1}{2}}^n} \equiv g_{i,j-\frac{1}{2}}$, $\frac{g(U_{i,j+\frac{1}{2}}^n)}{U_{i,j+\frac{1}{2}}^n} \equiv g_{i,j+\frac{1}{2}}$. Thus, we may approximate curves at $t^n < t < t^{n+1}$ as: $\sigma_{i-\frac{1}{2},j}(t) \approx (x_{i-\frac{1}{2}}, y_j) + (t - t^n)f_{i-\frac{1}{2},j}$, $\sigma_{i+\frac{1}{2},j}(t) \approx x_{i+\frac{1}{2}} + (t - t^n)f_{i+\frac{1}{2},j}$, $\sigma_{i,j-\frac{1}{2}}(t) \approx y_{j-\frac{1}{2}} + (t - t^n)g_{i,j-\frac{1}{2}}$, and $\sigma_{i,j+\frac{1}{2}}(t) \approx y_{j+\frac{1}{2}} + (t - t^n)g_{i,j+\frac{1}{2}}$. The approximation of the volume $D_{i,j}^n$ gives (see Figure 2):

$$D_{i,j} = \{(t, x, y) / t^n \leq t < t^{n+1}, \sigma_{i-\frac{1}{2},j}(t) \leq x < \sigma_{i+\frac{1}{2},j}(t), \sigma_{i,j-\frac{1}{2}}(t) \leq y < \sigma_{i,j+\frac{1}{2}}(t)\}.$$

Finally, the Lagrangian-Eulerian scheme with conservation property is given by:

STEP I (Lagrangian Forward Evolution, see Figure 3.4.4)

$$\bar{U}_{i,j}^{n+1} = \frac{A(R_{i,j})}{A(\bar{R}_{i,j})} U_{i,j}^n, \quad \text{with } A(R_{i,j}) = h^2 \text{ and } A(\bar{R}_{i,j}) = h_i^n \times h_j^n \quad (3.87)$$

where $h_i^n \times h_j^n = (h - (f_{i-1/2,j} + f_{i+1/2,j})\Delta t) \times (h - (g_{i,j-1/2} + g_{i,j+1/2})\Delta t)$.

STEP II (Eulerian Remap, see Figure 3)

$$U_{i,j}^n = \frac{1}{A(\bar{R}_{i,j})} (K_1 + K_2 + K_3), \quad (3.88)$$

where $K_1 \equiv c_{11}\bar{U}_{i-1,j-1}^{n+1} + c_{12}\bar{U}_{i,j-1}^{n+1} + c_{13}\bar{U}_{i+1,j-1}^{n+1}$, $K_2 \equiv c_{21}\bar{U}_{i-1,j}^{n+1} + c_{22}\bar{U}_{i,j}^{n+1} + c_{23}\bar{U}_{i+1,j}^{n+1}$ and $K_3 \equiv c_{31}\bar{U}_{i-1,j+1}^{n+1} + c_{32}\bar{U}_{i,j+1}^{n+1} + c_{33}\bar{U}_{i+1,j+1}^{n+1}$.

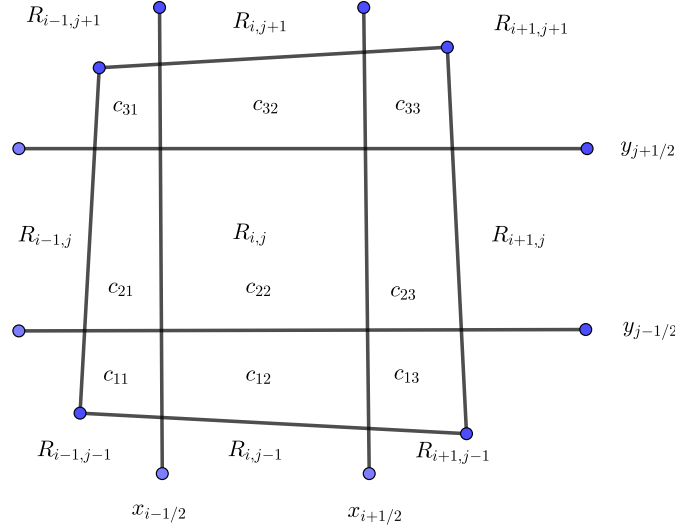
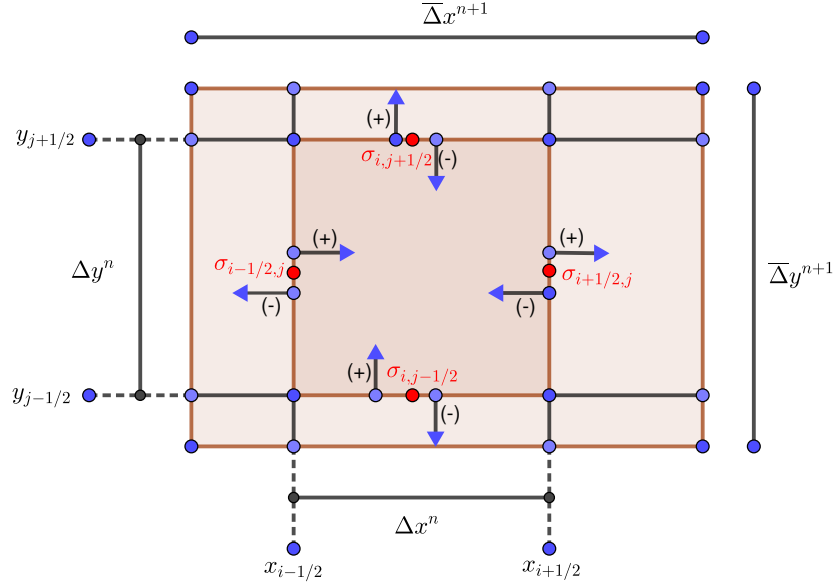


Figure 3 – Location of $c_{i,j}$ coefficients.

The construction of the coefficients of the Eulerian remap, $c_{i,j}$, can be obtained from the definition of $f_{i\pm 1/2,j}^n$ and $g_{i,j\pm 1/2}^n$ (see Figure 4). For this construction the motivation is given by

$$\begin{aligned}
c_{11} &= (-f_{i-1/2,j}^n \Delta t)(-g_{i,j-1/2}^n \Delta t) \\
c_{12} &= (\Delta x)(-g_{i,j-1/2}^n \Delta t) \\
c_{13} &= (f_{i+1/2,j}^n \Delta t)(-g_{i,j-1/2}^n \Delta t) \\
c_{21} &= (-f_{i-1/2,j}^n \Delta t)(\Delta y) \\
c_{22} &= (\Delta x)(\Delta y) \\
c_{23} &= (f_{i+1/2,j}^n \Delta t)(\Delta y) \\
c_{31} &= (-f_{i-1/2,j}^n \Delta t)(g_{i,j+1/2}^n \Delta t) \\
c_{32} &= (\Delta x)(g_{i,j+1/2}^n \Delta t) \\
c_{33} &= (-f_{i+1/2,j}^n \Delta t)(g_{i,j+1/2}^n \Delta t)
\end{aligned}$$

Figure 4 – Motivation for the construction of $c_{i,j}$ coefficients.

Next, we define the vector

$$C_x = [C_{xl}, C_{x0}, C_{xr}] \quad (3.89)$$

where,

$$\begin{aligned}
C_{xl} &= 0.5(1 + \text{sign}(f_{i-1/2,j}^n))f_{i-1/2,j}^n \Delta t \\
C_{xr} &= 0.5(1 - \text{sign}(f_{i+1/2,j}^n))f_{i+1/2,j}^n \Delta t \\
C_{x0} &= \Delta x - C_{xl} - C_{xr}.
\end{aligned}$$

Similarly, let us define the vector

$$C_y = [C_{yl}, C_{y0}, C_{yr}] \quad (3.90)$$

where

$$\begin{aligned} C_{yl} &= 0.5(1 + \text{sign}(g_{i,j-1/2}^n)g_{i,j-1/2}^n\Delta t) \\ C_{yr} &= 0.5(1 - \text{sign}(g_{i,j+1/2}^n)g_{i,j+1/2}^n\Delta t) \\ C_{y0} &= \Delta y - C_{yl} - C_{yr}. \end{aligned}$$

Then, the coefficients of the Eulerian remap $c_{i,j}$ from (3.87)-(3.88) are defined as the matrix entries

$$C = (c_{i,j}) = C_x^T C_y = \begin{bmatrix} C_{xl}C_{yl} & C_{xl}C_{y0} & C_{xl}C_{yr} \\ C_{x0}C_{yl} & C_{x0}C_{y0} & C_{x0}C_{yr} \\ C_{xr}C_{yl} & C_{xr}C_{y0} & C_{xr}C_{yr} \end{bmatrix}. \quad (3.91)$$

By definition of matrix, step II

$$A_{i,j} = \begin{bmatrix} \overline{U}_{i-1,j-1}^{n+1} & \overline{U}_{i,j-1}^{n+1} & \overline{U}_{i+1,j-1}^{n+1} \\ \overline{U}_{i-1,j}^{n+1} & \overline{U}_{i,j}^{n+1} & \overline{U}_{i+1,j}^{n+1} \\ \overline{U}_{i-1,j+1}^{n+1} & \overline{U}_{i,j+1}^{n+1} & \overline{U}_{i+1,j+1}^{n+1} \end{bmatrix} \quad (3.92)$$

the Lagrangian forward evolution (Step I) and the Eulerian remap (Step II) over the original grid may be recast as:

$$U_{i,j}^{n+1} = C_x A_{i,j}^T C_y^T, \quad (3.93)$$

or in the form of a conservative monotone scheme, as,

$$U_{i,j}^{n+1} = U_{i,j}^n - \lambda^x \Delta_+^x F(U_{i-p,i-r}^n, \dots, U_{i+q+1,j+s+1}^n) - \lambda^y \Delta_+^y G(U_{i-p,j-r}^n, \dots, U_{i+q+1,j+s+1}^n) \quad (3.94)$$

where $\lambda^x = \Delta t / \Delta x$, $\lambda^y = \Delta t / \Delta y$, $(\Delta_+^x)_{j,k} = U_{j+1,k} - U_{j,k}$ and $(\Delta_+^y)_{j,k} = U_{j,k+1} - U_{j,k}$, and taking $h = \Delta x = \Delta y$, we have,

$$\begin{aligned} F(U_{i-1,j-1}^n, \dots, U_{i+1,j+1}^n) = \\ F_R(U_{i,j-1}^n, U_{i-1,j-1}^n, U_{i-1,j}^n, U_{i,j}^n, U_{i,j-1}^n) - F_L(U_{i-1,j+1}^n, U_{i-1,j}^n, U_{i,j-1}^n, U_{i,j}^n, U_{i,j+1}^n), \end{aligned}$$

where

$$\begin{aligned} F_R &= h C_{xl} \left(\overline{U}_{i+1,j}^{n+1} - \overline{U}_{i,j}^{n+1} \right) - \\ &C_{xl} C_{yr} \left(\overline{U}_{i-1,j+1}^{n+1} - \overline{U}_{i-1,j}^{n+1} - (\overline{U}_{i,j+1}^{n+1} - \overline{U}_{i,j}^{n+1}) \right) + \frac{1}{2} (f(U_{i-1,j}^n) + 2f(U_{i,j}^n) + f(U_{i+1,j}^n)), \\ F_L &= h C_{xl} C_{yl} \left(\overline{U}_{i-1,j}^{n+1} - \overline{U}_{i,j}^{n+1} \right) - \\ &C_{xl} C_{yl} \left(\overline{U}_{i-1,j-1}^{n+1} - \overline{U}_{i,j-1}^{n+1} - (\overline{U}_{i-1,j}^{n+1} - \overline{U}_{i,j}^{n+1}) \right) + \frac{1}{2} (f(U_{i-1,j}^n) + 2f(U_{i,j}^n) + f(U_{i+1,j}^n)). \end{aligned}$$

and

$$\begin{aligned}
& G(U_{i-1,j-1}^n, \dots, U_{i+1,j+1}^n) = \\
& G_R(U_{i-1,j}^n, U_{i,j}^n, U_{i+1,j+1}^n, U_{i,j+1}^n, U_{i+1,j}^n) - G_L(U_{i+1,j}^n, U_{i,j}^n, U_{i,j-1}^n, U_{i+1,j}^n, U_{i,j+1}^n), \\
& G_R = hC_{yl} \left(\bar{U}_{i,j+1}^{n+1} - \bar{U}_{i,j}^{n+1} \right) - \\
& C_{xr} * C_{yl} \left(\bar{U}_{i+1,j-1}^{n+1} - \bar{U}_{i+1,j}^{n+1} - (\bar{U}_{i,j-1}^{n+1} - \bar{U}_{i,j}^{n+1}) \right) + \frac{1}{2}(g(U_{i,j-1}^n) + 2g(U_{i,j}^n) + g(U_{i,j+1}^n)), \\
& G_L = hC_{yl} \left(\bar{U}_{i,j-1}^{n+1} - \bar{U}_{i,j}^{n+1} \right) - \\
& C_{xr} * C_{yr} \left(\bar{U}_{i+1,j+1}^{n+1} - \bar{U}_{i+1,j}^{n+1} - (\bar{U}_{i,j+1}^{n+1} - \bar{U}_{i,j}^{n+1}) \right) + \frac{1}{2}(g(U_{i,j-1}^n) + 2g(U_{i,j}^n)g(U_{i,j+1}^n)).
\end{aligned}$$

We can note that F and G satisfy condition (3.26) from [6]; this implies that the equation is consistent with (3.82), and thus, the numerical method to 2D-hyperbolic equations is monotone.

The CFL condition based on the No-Flow curves, which is called weak-CFL condition in this context, is given by

$$\max_{i,j} \{|f_{i-1/2,j}^n|, |f_{i+1/2,j}^n|, |g_{i,j-1/2}^n|, |g_{i,j+1/2}^n|\} \frac{\Delta t}{\Delta x} \leq \frac{1}{2}. \quad (3.95)$$

To Improve numerically the solution of the generalized ODE system

$$\begin{cases} \sigma'_{i\pm\frac{1}{2},j}(t) = \frac{f(U_{i\pm\frac{1}{2},j})}{U_{i\pm\frac{1}{2},j}}, & \sigma'_{i,j\pm\frac{1}{2}}(t) = \frac{g(U_{i,j\pm\frac{1}{2}})}{U_{i,j\pm\frac{1}{2}}}, \\ \sigma_{i\pm\frac{1}{2},j}(t^n) = x_{i\pm\frac{1}{2}}, & \sigma_{i,j\pm\frac{1}{2}}(t^n) = y_{j\pm\frac{1}{2}}, \end{cases} \quad (3.96)$$

with conservation and robustness solutions, for example, to $\sigma_{i-1/2,j}^n(t)$ of the differential system

$$\begin{cases} \sigma'_{i-\frac{1}{2},j}(t) = \frac{f(U_{i-\frac{1}{2},j})}{U_{i-\frac{1}{2},j}}, \\ \sigma_{i\pm\frac{1}{2},j}(t^n) = x_{i-\frac{1}{2}}, \end{cases} \quad (3.97)$$

we may use the approximations

$$\begin{aligned}
U_{i-\frac{1}{2},j} &= \frac{1}{h} \int_{x_{i-1,j}^n}^{x_{i,j}^n} L(x,t) dx = \frac{1}{h} \left(\int_{x_{i-1,j}^n}^{x_{i-\frac{1}{2},j}^n} L_{i-1,j}(x,t) dx + \int_{x_{i-\frac{1}{2},j}^n}^{x_{i,j}^n} L_{i,j}(x,t) dx \right) \\
&= \frac{1}{2}(U_{i-1,j} + U_{i,j}) + \frac{1}{8}(U'_{i,j} - U'_{i,j-1}).
\end{aligned} \quad (3.98)$$

Distinct and high-order approximations are also acceptable for $\frac{d\sigma_{j-1/2}^n(t)}{dt} = \frac{f(u)}{u}$ as in (3.83). As in [6], the piecewise constant numerical data is reconstructed into a piecewise linear approximation through the use of MUSCL-type interpolants:

$$L_{i,j}(x, t) = u_{i,j}(t) + (x - x_j) \frac{1}{\Delta x} u'_{i,j}. \quad (3.99)$$

For the numerical derivative $\frac{1}{\Delta x} u'_{i,j}$, there are several choices of slope limiters for scalar case [6, 8].

Finally, to show the reconstruction's flexibility, we use the nonlinear Lagrange polynomial in $U_{i-1,j}^n$, $U_{i,j-1}^n$, $U_{i,j}^n$, $U_{i,j+1}^n$ and $U_{i+1,j}^n$. So, equation (3.87) reads

$$\bar{U}_{i,j}^{n+1} = \frac{1}{h_j^{n+1}} \int_{s_{j-\frac{1}{2}}^n}^{s_{j+\frac{1}{2}}^n} P_2(x, y) ds, \quad (3.100)$$

where $s = x, y$ and

$$\begin{aligned} P_2(x, y) = & U_{i-1,j}^n L_{-1}(x - x_i) + U_{i,j-1}^n L_{-1}(y - y_j) + U_{i,j}^n L_0(x - x_i) + U_{i,j}^n L_0(y - y_j) \\ & + U_{i+1,j}^n L_1(x - x_j) + U_{i,j+1}^n L_1(y - y_j) \end{aligned}$$

and

$$L_{\pm 1}(x) = \frac{1}{2} \left[\left(\frac{x}{h} \pm \frac{1}{2} \right)^2 - \frac{1}{4} \right], \quad L_0(x) = 1 - \left(\frac{x}{h} \right)^2.$$

3.4.5 Numerical Experiments with the Lagrangian-Eulerian with Conservation Properties

We present a benchmark comprehensive set of numerical tests that explore the role of the accuracy of our new 2D Lagrangian-Eulerian scheme with conservation properties.

3.4.6 A Lagrangian–Eulerian scheme for a conservation law with partially nonlocal velocity

In this subsection, our objective is to develop a fully-discrete nonlocal Lagrangian-Eulerian scheme, utilizing the concept of the space-time No-Flow curve. This scheme is crafted to tackle a conservation law featuring partially nonlocal velocity, specifically of a conservation law with partially nonlocal velocity. In this model, the velocity field is obtained by composing nonlocal partial operators: the partial Riesz potential $\Lambda_i^{\alpha-1}$ and the partial Hilbert transform \mathcal{H}_i for $i = 1, 2$. Notice that, in equation (3.49), the variable $u(x, y, t)$ represents $\theta(x, y, t)$ and is the solution to a conservation law with partially

nonlocal velocity:

$$\begin{cases} \partial_t \theta \pm \nabla \cdot (\theta \Lambda_1^{\alpha-1} \mathcal{H}_1 \theta, \theta \Lambda_2^{\alpha-1} \mathcal{H}_2 \theta) = 0, \quad \forall (x, y, t) \in \Omega \times \mathbb{R}^+ \\ \theta(x, y, 0) = \theta_0. \end{cases}$$

Furthermore, we know from Subsection 3.4.1 that the border of the volume control $D_{i,j}^n$ is given by $\partial D_{i,j}^n = R_{i,j}^n \cup S_{i,j}^n \cup \overline{R}_{i,j}^{n+1}$. At first, we do not know exactly what the non-flow surface $S_{i,j}^n$ looks like, we only know that the edge of the ingress coincides with $\partial R_{i,j}^n$ in the t^n plane, and the outlet end of surface $S_{i,j}^n$ which intersects the t^{n+1} plane. Assuming that the surface $S_{i,j}^n$ is defined by a family of No-Flow curves represented as $\gamma(t)$ for the time interval $t^n \leq t \leq t^{n+1}$, we will proceed to establish a representative parametrized curve $\gamma_{i\pm 1/2,j}^n(t)$ and $\gamma_{i,j\pm 1/2}^n(t)$ at the midpoint of each side on the boundary $\partial R_{i,j}^n$. These parametrized curves will be determined using scalar functions, denoted as $\sigma_{i\pm 1/2,j}^n(t)$ and $\sigma_{i,j\pm 1/2}^n(t)$, over the time interval $t^n \leq t \leq t^{n+1}$. These scalar functions are designed in such a way that, at the initial time $t = t^n$, they satisfy the conditions $\sigma_{i\pm 1/2,j}^n(t^n) = x_{i\pm 1/2}$ and $\sigma_{i,j\pm 1/2}^n(t^n) = y_{j\pm 1/2}$. Furthermore, it should be noted that these four functions will intersect the t^{n+1} plane at the time instant t^{n+1} , as depicted in Figure 2. Then to build $\overline{R}_{i,j}^{n+1}$, we define the four parametric curves as follows

$$\gamma_{i\pm 1/2,j}^n(t) = [\sigma_{i\pm 1/2,j}^n(t), y_j, t]^T, \quad \gamma_{i,j\pm 1/2}^n(t) = [x_i, \sigma_{i,j\pm 1/2}^n(t), t]^T \quad \text{with } t^n \leq t \leq t^{n+1}. \quad (3.101)$$

So, we have to $\gamma_{i\pm 1/2,j}^n(t), \gamma_{i,j\pm 1/2}^n(t) \in S_{i,j}^n$ for $t^n < t < t^{n+1}$.

According to [6] the construction of No-Flow side curves is not unique. Notice that, for $t^n < t < t^{n+1}$ we have that $\gamma_{i\pm 1/2,j}^n(t)$ is in plane- y_j , $\gamma_{i,j\pm 1/2}^n(t)$ is in plane- x_i , furthermore

$$\frac{d}{dt} \gamma_{i\pm 1/2,j}^n(t) = \left[\frac{d}{dt} \sigma_{i\pm 1/2,j}^n(t), 0, 1 \right]^T \quad \text{and} \quad \frac{d}{dt} \gamma_{i,j\pm 1/2}^n(t) = \left[0, \frac{d}{dt} \sigma_{i,j\pm 1/2}^n(t), 1 \right]^T$$

In this manner, we obtain the following initial value problems for a conservation law with partially nonlocal velocity

$$\begin{cases} \frac{d}{dt} \sigma_{i\pm 1/2,j}^n(t) &= \pm \Lambda_1^{\alpha-1} \mathcal{H}_1 \theta(\sigma_{i\pm 1/2,j}^n(t), y_j, t) \\ \sigma_{i\pm 1/2,j}^n(t^n) &= x_{i\pm 1/2} \end{cases} \quad (3.102)$$

and

$$\begin{cases} \frac{d}{dt} \sigma_{i,j\pm 1/2}^n(t) &= \pm \Lambda_2^{\alpha-1} \mathcal{H}_2 \theta(x_i, \sigma_{i,j\pm 1/2}^n(t), t) \\ \sigma_{i,j\pm 1/2}^n(t^n) &= y_{j\pm 1/2} \end{cases} \quad (3.103)$$

where approximating of $\Lambda_1^{\alpha-1} \mathcal{H}_1$ and $\Lambda_2^{\alpha-1} \mathcal{H}_2$ are made using an approximation of the partial Riesz potential and the partial Hilbert transform, respectively, as defined in the

previous sections. Approximating the $\sigma_{i\pm 1/2,j}^n(t)$ and $\sigma_{i,j\pm 1/2}^n(t)$ curves by Taylor's series, we obtain

$$\begin{aligned}\sigma_{i\pm 1/2,j}^n(t) &= \sigma_{i\pm 1/2,j}^n(t^n) + \frac{d}{dt}\sigma_{i\pm 1/2,j}^n(t^n)(t - t^n) \\ \sigma_{i,j\pm 1/2}^n(t) &= \sigma_{i,j\pm 1/2}^n(t^n) + \frac{d}{dt}\sigma_{i,j\pm 1/2}^n(t^n)(t - t^n).\end{aligned}$$

Thus, from (3.102) we obtain, an approximation for $\sigma_{i\pm 1/2,j}^n(t)$

$$\sigma_{i\pm 1/2,j}^n(t) = x_{i\pm 1/2}^n + (t - t^n)f_{i\pm 1/2,j}^n \quad \text{for } t^n \leq t \leq t^{n+1} \quad (3.104)$$

where, $f_{i\pm 1/2,j}^n = \pm \Lambda_1^{\alpha-1} \mathcal{H}_1 \theta(\sigma_{i\pm 1/2,j}^n(t), y_j^n, t)$.

Similarly, from (3.103), we obtain an approximation for $\sigma_{i,j\pm 1/2}^n(t)$

$$\sigma_{i,j\pm 1/2}^n(t) = y_{j\pm 1/2}^n + (t - t^n)g_{i,j\pm 1/2}^n \quad \text{for } t^n \leq t \leq t^{n+1} \quad (3.105)$$

where, $g_{i,j\pm 1/2}^n = \pm \Lambda_2^{\alpha-1} \mathcal{H}_2 \theta(x_i^n, \sigma_{i,j\pm 1/2}^n(t), t)$.

So, a significant finding emerges: the No-Flow curves $f_{i\pm 1/2,j}^n$ and $g_{i,j\pm 1/2}^n$ approximate the velocity nonlocal $\Lambda_1^{\alpha-1} \mathcal{H}_1 \theta(\sigma_{i\pm 1/2,j}^n(t), y_j^n, t)$ and $\Lambda_2^{\alpha-1} \mathcal{H}_2 \theta(x_i^n, \sigma_{i,j\pm 1/2}^n(t), t)$, respectively, for this type of conservation law.

Moreover, the approximation to the control volume $D_{i,j}^n$ is given by

$$D_{i,j}^n = \{(x, y, t) \mid \sigma_{i-1/2,j}^n(t) < x < \sigma_{i+1/2,j}^n(t), \sigma_{i,j-1/2}^n(t) < y < \sigma_{i,j+1/2}^n(t), t^n < t < t^{n+1}\}. \quad (3.106)$$

The conservative fully-discrete nonlocal Lagrangian-Eulerian scheme for a conservation law with partially nonlocal velocity, is presented in the following steps.

1. *The Lagrangian forward evolution* is given by

$$\bar{\Theta}_{i,j}^{n+1} = \frac{A(R_{i,j}^n)}{A(\bar{R}_{i,j}^{n+1})} \Theta_{i,j}^n \quad \text{with } A(R_{i,j}^n) = \Delta x \times \Delta y \quad \text{and } A(\bar{R}_{i,j}^{n+1}) = \bar{\Delta x}^{n+1} \times \bar{\Delta y}^{n+1} \quad (3.107)$$

where, $\Delta x = \Delta y$, $\bar{\Delta x}^{n+1} = \Delta x + (f_{i+1/2,j}^n - f_{i-1/2,j}^n) \Delta t$, and $\bar{\Delta y}^{n+1} = \Delta y + (g_{i,j+1/2}^n - g_{i,j-1/2}^n) \Delta t$

2. *The Eulerian remap* is given by

$$\Theta_{i,j}^{n+1} = \frac{1}{A(\bar{R}_{i,j}^{n+1})} (K_1 + K_2 + K_3) \quad (3.108)$$

where

$$\begin{aligned}K_1 &\equiv c_{11} \bar{\Theta}_{i-1,j-1}^{n+1} + c_{12} \bar{\Theta}_{i,j-1}^{n+1} + c_{13} \bar{\Theta}_{i+1,j-1}^{n+1} \\ K_2 &\equiv c_{21} \bar{\Theta}_{i-1,j}^{n+1} + c_{22} \bar{\Theta}_{i,j}^{n+1} + c_{23} \bar{\Theta}_{i+1,j}^{n+1} \\ K_3 &\equiv c_{31} \bar{\Theta}_{i-1,j+1}^{n+1} + c_{32} \bar{\Theta}_{i,j+1}^{n+1} + c_{33} \bar{\Theta}_{i+1,j+1}^{n+1}\end{aligned}$$

3. The construction of the coefficients of the Eulerian remap, $c_{i,j}$, can be obtained from the definition of $f_{i\pm 1/2,j}^n$ and $g_{i,j\pm 1/2}^n$, analogous to the 2D Lagrangian-Eulerian method presented in subsection 3.4.4

Next, we proceed to define the vector

$$C_x = [C_{xm}, C_{x0}, C_{xp}] \quad (3.109)$$

where

$$\begin{aligned} C_{xp} &= 0.5(1 + \text{sign}(f_{i+1/2,j}^n))f_{i+1/2,j}^n\Delta t \\ C_{xm} &= 0.5(1 - \text{sign}(f_{i-1/2,j}^n))|f_{i+1/2,j}^n|\Delta t \\ C_{x0} &= \Delta x + \text{sign}(f_{i+1/2,j}^n)C_{xp} - \text{sign}(f_{i-1/2,j}^n)C_{xm}. \end{aligned}$$

Similarly, let us define the vector

$$C_y = [C_{ym}, C_{y0}, C_{yp}] \quad (3.110)$$

where

$$\begin{aligned} C_{yp} &= 0.5(1 + \text{sign}(g_{i,j+1/2}^n))g_{i,j+1/2}^n\Delta t \\ C_{ym} &= 0.5(1 - \text{sign}(g_{i,j-1/2}^n))|g_{i,j-1/2}^n|\Delta t \\ C_{y0} &= \Delta y + \text{sign}(g_{i,j+1/2}^n)C_{yp} - \text{sign}(g_{i,j-1/2}^n)C_{ym}. \end{aligned}$$

Then, the coefficients of the Eulerian remap $c_{i,j}$ from (3.107)-(3.108) are defined as the matrix entries

$$C = (c_{i,j}) = C_x^T C_y = \begin{bmatrix} C_{xm}C_{ym} & C_{xm}C_{y0} & C_{xm}C_{yp} \\ C_{x0}C_{ym} & C_{x0}C_{y0} & C_{x0}C_{yp} \\ C_{xp}C_{ym} & C_{xp}C_{y0} & C_{xp}C_{yp} \end{bmatrix}. \quad (3.111)$$

The CFL condition based on the No-Flow curves, is also called weak is given by

$$\max_{i,j} \{|f_{i-1/2,j}^n|, |f_{i+1/2,j}^n|, |g_{i,j-1/2}^n|, |g_{i,j+1/2}^n|\} \frac{\Delta t}{\Delta x} \leq \frac{1}{2}. \quad (3.112)$$

3.5 Numerical Simulations for a Conservation Law with Partially Nonlocal Velocity

Similar to the findings in the paper by [2], we will understand in our results that the term *blow-up* means solutions assuming singular measures concerning the Lebesgue measure in \mathbb{R}^2 but preserving the initial total mass, e.g., giving mass to lines (singular

lines with mass concentration but preserving the initial total mass, for this, we take the initial non-negative data and check that the solution remains non-negative). For simplicity in writing, we name it as *blow-up of concentration type with mass preserving* or simply *blow-up of concentration type*, when there is no chance of misunderstanding.

This section presents the numerical solutions to a conservation law with partially nonlocal velocity (1.3). In this model, the velocity field is obtained through the composition of the partial Riesz potential and the partial Hilbert transform. For the numerical solution, we employ the novel full-discrete nonlocal Lagrangian-Eulerian numerical scheme developed in Subsection 3.4.6, see [12] and [6], together with the numerical approximation of nonlocal operators of the partial Riesz potential (3.65) and (3.71), as well as of the partial Hilbert transform (3.53) and (3.60). We performed numerical simulations considering initial data that belong to the Schwartz spaces $\mathcal{S}(\mathbb{R}^2)$ as well as the weak-Morrey spaces $W\mathcal{M}_p^l(\mathbb{R}^2)$ and we provide new insights into the conservation law at hand such as blow-up and attenuation behaviors.

The idea is to investigate numerically how the initial data influences the existence of the global smooth diffusion, the formation of abrupt gradients, and the formation of blow-up in finite time of solution for a conservation law with partially nonlocal velocity. Thus, possible natural questions are: solution's blow-up or attenuation behaviors depend on the measure data, the sign of flux from a conservation law with partially nonlocal velocity, or other factors. Do solutions evolve as a singular measure? Or do they regularize (a diffusion mechanism along with mass-preserving) for $t > 0$? As we had already anticipated, we chose two initial datas we choose two types of initial data $f(x, y)$. The first is to measure initial data belonging to the Schwartz spaces $\mathcal{S}(\mathbb{R}^2)$ and the other is to measure initial data which was obtained through an adaptation of an element from the weak-Morrey space $W\mathcal{M}_p^l(\mathbb{R}^2)$ and will be detailed later. Suppose we gather qualitative information about the solutions, such as attenuation of regularization type or blow-up of concentration type. In that case, it enables us to gain insights into the required characteristics of the initial mass for a global-in-time flow for the conservation law under consideration.

To perform a numerical study of a conservation law with partially nonlocal velocity (1.3) and deepen our comprehension of the nonlinear and nonlocal interactions within Besov spaces type, we have developed a robust and coherent methodology for addressing model (1.3) within a finite computational domain $\Omega = [a, b] \times [c, d]$ based on our previously rigorous findings, we can discern the most straightforward and mathematically accurate approach for addressing boundary conditions: expanding the domain to a sufficient extent to prevent any disruptive spurious reflections from affecting the numerical simulations. We describe our numerical experiments concerning two possibilities depending on the sign of flux from a conservation law with partially nonlocal velocity; the first is

when the flux has a positive signal, this is, $\partial_t \theta + \nabla \cdot (\theta \Lambda_1^{\alpha-1} \mathcal{H}_1 \theta, \theta \Lambda_2^{\alpha-1} \mathcal{H}_2 \theta) = 0$, which we will *a conservation law with partially nonlocal velocity and positive flux*; the other possibility is when the flux has negative signal, i. e., $\partial_t \theta - \nabla \cdot (\theta \Lambda_1^{\alpha-1} \mathcal{H}_1 \theta, \theta \Lambda_2^{\alpha-1} \mathcal{H}_2 \theta) = 0$, which we will *a conservation law with partially nonlocal velocity and negative flux*.

So, we proceed to reformulation the (1.3) model within the computational domain $\Omega = [a, b] \times [c, d]$

$$\begin{cases} \partial_t \theta \pm \nabla \cdot (\theta \Lambda_1^{\alpha-1} \mathcal{H}_1 \theta, \theta \Lambda_2^{\alpha-1} \mathcal{H}_2 \theta) = 0, & (x, y, t) \in \Omega \times (0, T], \\ \theta(x, y, 0) = \theta_0(x, y), & (x, y) \in \Omega, \end{cases} \quad (3.113)$$

where $\Lambda_1^{\alpha-1}$ and $\Lambda_2^{\alpha-1}$ are the partial Riesz potential, which are given by (3.3) and (3.4), respectively, \mathcal{H}_1 and \mathcal{H}_2 are the partial Hilbert transform, which are given by (3.1) and (3.2) respectively. Furthermore $\theta_0(x, y)$ will be a

(I) the 2D Gaussian pulse with compact support initial condition, $\theta_0(x, y) = \frac{e^{-\frac{(x^2+y^2)}{8}}}{\pi}$

(II) the 2D weak-Morrey type initial condition, $\theta_0(x, y) = (\|x\|^2 + \|y\|^2)^{-1} 1_{A_{\delta,R}}$, where $1_{A_{\delta,R}}$ is the characteristic function from $A_{\delta,R}$, this is,

$$A_{\delta,R} = \{(x, y) \in \mathbb{R}^2; \delta < (x^2 + y^2)^{1/2} < R\},$$

here $\delta = \delta(m)$ and $R = R(m)$, where m is the mesh size.

Notice that we have a uniform estimate for the $W\tilde{\mathcal{M}}_p^l$ space norm:

$$\|(x^2 + y^2)^{-1} 1_{A_{\delta,R}}\|_{W\tilde{\mathcal{M}}_p^l} \leq \|(x^2 + y^2)^{-1}\|_{W\tilde{\mathcal{M}}_p^l} \quad \forall \delta, R > 0.$$

To simplify notation, we will henceforth refer to the initial data mentioned above as “Gaussian” and “weak-Morrey”, respectively.

We describe our numerical experiments related on to two approaches for formulating from a conservation law with partially nonlocal velocity for different data types f . Furthermore, for simulations throughout the thesis we use computers with the following characteristics: Intel(R) Xeon(R) CPU E5-2643 v2 @ 3.50GHz, 128GB Ram, and Intel(R) Xeon(R) Silver 4216 CPU @ 2.10GHz, 32GB Ram. Our simulations for *a conservation law with partially nonlocal velocity and negative flux* provide evidence that the blow-up state is a two-dimensional Dirac measure with the same mass of f and supported at $(x_0, y_0) \in \mathbb{R}^2$; the position of (x_0, y_0) depends on f . However, for *a conservation law with partially nonlocal velocity and negative positive*, we were able to compute qualitatively correct approximations by showing strong evidence of attenuation of regularization type with mass-preserving. Furthermore, the gradient in the positive flux exhibits a decreasing trend, as depicted in Figure 5, Figure 6, Figure 8, and Figure 9. However, the gradient in

the negative flux exhibits an increasing trend, as depicted in the images in Figure 7, and Figure 10.

In summary, the numerical studies conducted from Figure 5 to Figure 7 (Section 3.5.1) and from Figure 8 to Figure 10 (Section 3.5.2), computational results reveal that even with a relatively coarse mesh grid, the full-discrete nonlocal Lagrangian-Eulerian scheme is effective in solving numerically the underlying a conservation law with partially nonlocal velocity (1.1). For concreteness, if we consider *the negative flux* with measure initial data or measure initial data weak-Morrey type, we found numerical evidence of blow-up of concentration type for the solution. On the other hand, if we consider *the positive flux* with measure initial data or measure initial data weak-Morrey type, we found a kind of attenuation type regularization for the solution.

We will present simulations in two distinct sections for a more comprehensive numerical exploration of a conservation law with partially nonlocal velocity qualitative behavior. Section 3.5.1 will examine simulations with measure initial data, while Section 3.5.2 will focus on simulations with initial data of the weak Morrey type. Within each subsection, there will be further division into two sub-subsections, one dedicated to *a conservation law with partially nonlocal velocity with positive flux* and the other to *a conservation law with partially nonlocal velocity model with negative flux*.

3.5.1 Simulations for measure initial data

In this subsection, we will numerically present evidence of regularization of attenuation type and evidence of blow-up of concentration type for the solution θ from a conservation law with partially nonlocal velocity (1.3). Our analysis will specifically consider measure initial data focusing on the Gaussian.

Positive flux

We determined a numerical solution using mesh grid cells $m = 512$ and refined mesh grid cells $m = 1024$ for *a conservation law with partially nonlocal velocity and positive flux* (3.113). These results are shown in Figure 5 and Figure 6, with Gaussian initial data. The machine simulation time was 32 days and 50 days, respectively. At the top of Figure 5 (from left to right), it is evident that as time progresses, the numerical solution height diminishes noticeably along the gradient and the first signs of the diffusive process are seen. At the bottom, a similar pattern is observed, albeit with a less pronounced decrease in height; nevertheless, the gradient continues decreasing, and now the diffusive process is more. Consequently, we have observed compelling evidence of attenuation of regularization type for the solution θ of *a conservation law with partially nonlocal velocity and positive flux*. It is worth noting that the numerical solution is identical for a mesh grid refinement, this is shown in Figure 6.

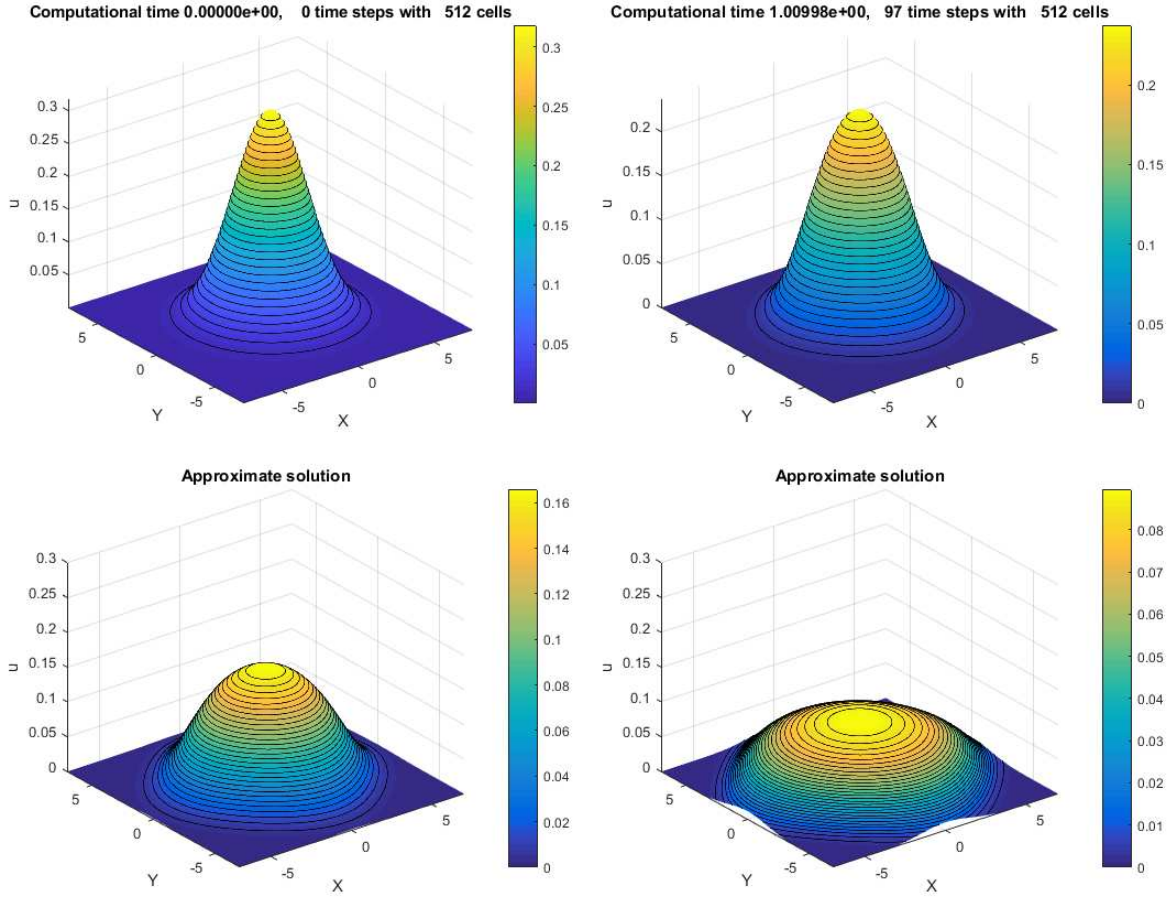


Figure 5 – Numerical simulation for $\partial_t \theta + \nabla \cdot (\theta \Lambda_1^{\alpha-1} \mathcal{H}_1 \theta, \theta \Lambda_2^{\alpha-1} \mathcal{H}_2 \theta) = 0$ with a Gaussian initial data, $\alpha = 0.5$ and mesh $m = 512$ for a sequence of times $T = 0, 1, 3, 10$. On the top, you can observe a decrease in height and the initiation of diffusion in the numerical solution as time evolves, while on the bottom the numerical solution is shown diffusion-smooth and reduction in height as time evolves. Evidence of attenuation of regularization type.

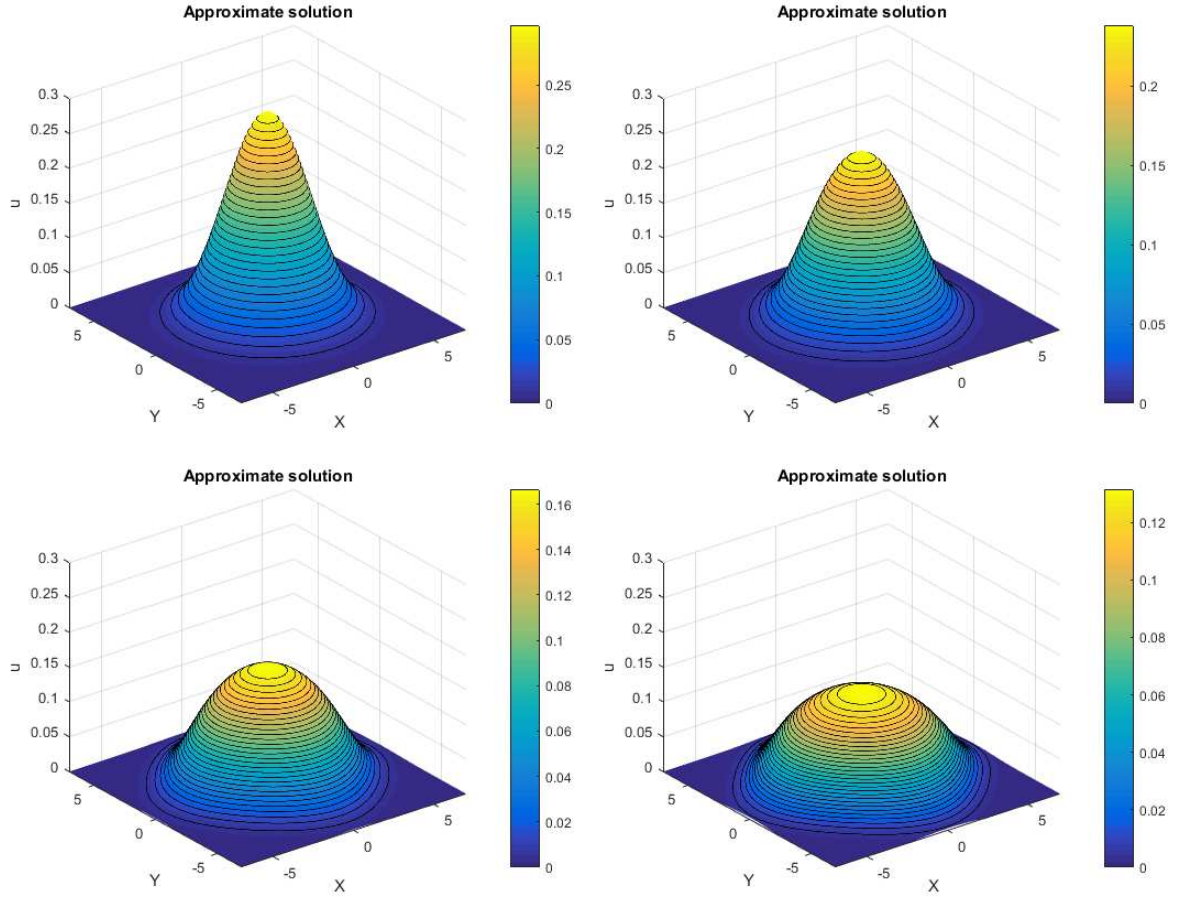


Figure 6 – Numerical simulation for $\partial_t \theta + \nabla \cdot (\theta \Lambda_1^{\alpha-1} \mathcal{H}_1 \theta, \theta \Lambda_2^{\alpha-1} \mathcal{H}_2 \theta) = 0$ with a Gaussian initial data, $\alpha = 0.5$ and mesh $m = 1024$ for a sequence of times $T = 0.2, 1, 3, 5$. On the top, you can observe a decrease in height and the initiation of a diffusion in the numerical solution as time evolves, while on the bottom the numerical solution shows a diffusion-smooth and minimal reduction in height as time evolves. Evidence of attenuation of regularization type.

Negative flux

We determined a numerical solution with mesh grid cells $m = 512$ for a conservation law with partially nonlocal velocity and negative flux (3.113) with Gaussian initial data. These results are illustrated in Figure 7, and the machine simulation time was 9 days.

At the top of Figure 7 (from left to right), it is evident that the height of the solution increases along the gradient as time progresses and the first signs of the concentration process are seen. In the middle, we observe both an increase in height and gradient, and the concentration process continues. Moving to the bottom, a similar pattern is observed, but the height increases even more dramatically, the gradient continues to increase significantly. Furthermore, the concentration is given at the origin of the coordinates. Consequently, we find compelling evidence of blow-up of concentration type for the solution θ of a conservation law with partially nonlocal velocity with negative flux. Notice that in this simulation, the concentration near the origin exhibits a square shape. This arises from the definition of the nonlocal operators, namely the partial Hilbert transform and the partial Riesz potential. These operators generate attraction nuclei, one along the X-axis and the other along the Y-axis. When they act simultaneously, a concentration is obtained near the origin of the coordinates, forming a square around it.

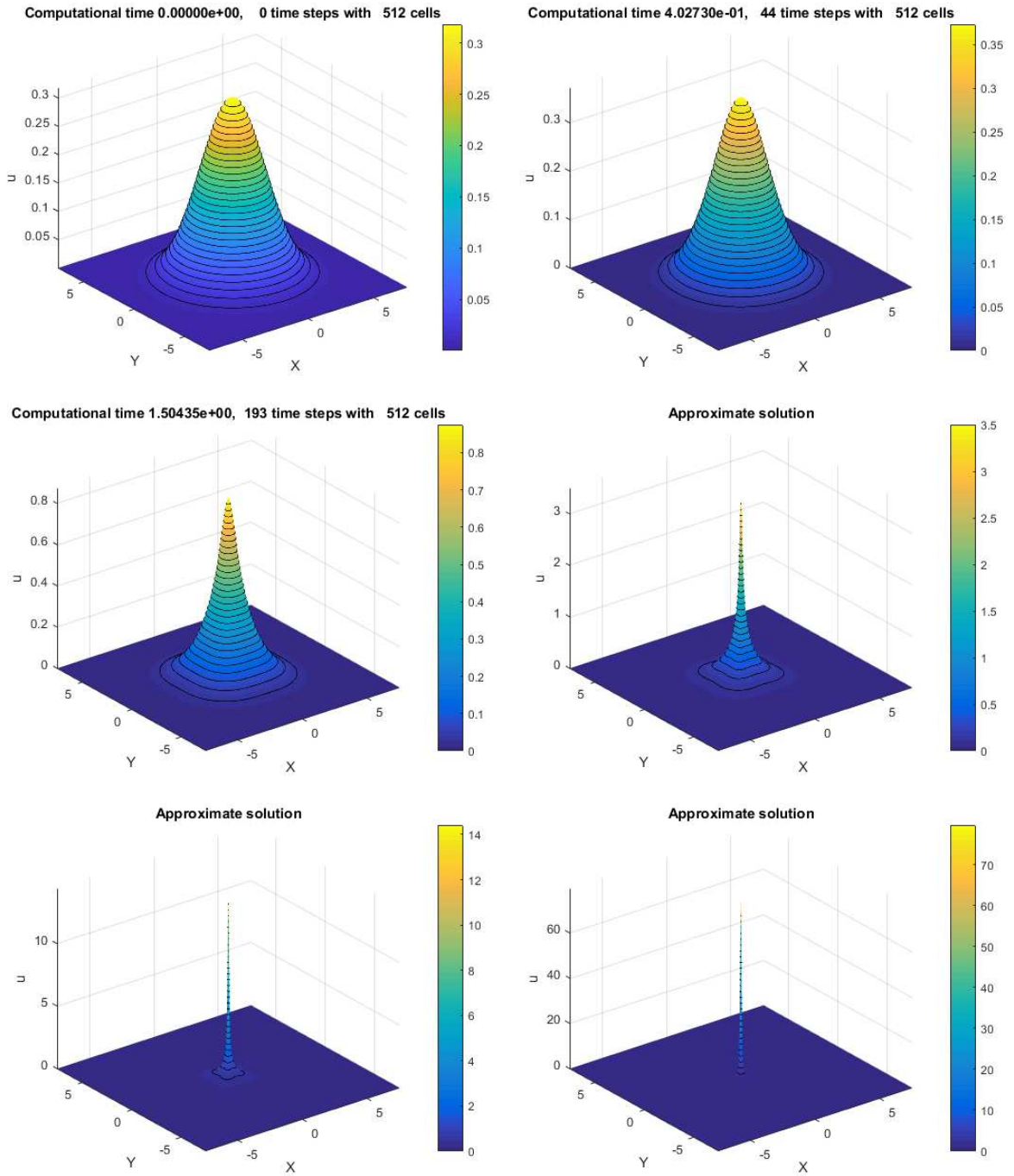


Figure 7 – Numerical simulation for $\partial_t \theta - \nabla \cdot (\theta \Lambda_1^{\alpha-1} \mathcal{H}_1 \theta, \theta \Lambda_2^{\alpha-1} \mathcal{H}_2 \theta) = 0$ with a Gaussian initial data, $\alpha = 0.5$ and mesh $m = 512$ for a sequence of times $T = 0, 0.4, 1.5, 1.9, 2, 2.1$. On the top, you can observe an increase in height and the initiation of concentration in the numerical solution as time progresses. In the middle, the numerical solution shows both concentration and an increasing height as time evolves. At the bottom, the approximate solution exhibits concentration and a rapid increase in height as time progresses. Evidence of blow-up of concentration type.

3.5.2 Simulations for measured data of weak-Morrey type

In this subsection, we will present evidence of regularization of attenuation type and evidence of blow-up of concentration type for the solution θ of a conservation law with partially nonlocal velocity. Our analysis will consider both measure initial data and measure initial data of weak-Morrey type.

Positive flux

We determined a numerical solution with a mesh grid cells $m = 100$ and a mesh grid refinement $m = 250$ for *a conservation law with partially nonlocal velocity and positive flux*. These results are shown in Figure 8 and Figure 9, respectively, with weak-Morrey initial data. The machine simulation time was approximately 2 days and 15 days, respectively.

To better visualize the qualitative behavior in Figure 8, we have kept the Z axis fixed. In the top row of Figure 8 (from left to right), it can be observed that as time progresses, the height of the weak-Morrey profile decreases along the gradient and the first signs of the diffusive process are seen. At the bottom, a similar pattern is observed. While the Z axis remains fixed, we cannot precisely discern the height of the profile of the solution. However, referencing the color bar in each image makes it apparent that the height of the weak-Morrey profile diminishes, displaying diffusive behavior. As a result, we have obtained evidence of regularization of attenuation type for the solution θ of *a conservation law with partially nonlocal velocity and positive flux*. In Figure 6, we have an identical numerical solution for the same model with a mesh grid refinement.

On the other hand, in the upper part of Figure 9 (from left to right), it is clear that as time progresses, the height of the solution profile decreases along the gradient and the first signs of the diffusive process are seen. In the lower part, we observe a similar pattern; although the height decreases to a lesser extent, the gradient continues to decrease and now the diffusive process is more. Consequently, we have obtained evidence of regularization of attenuation-type for the solution θ of *a conservation law with partially nonlocal velocity and positive flux*.

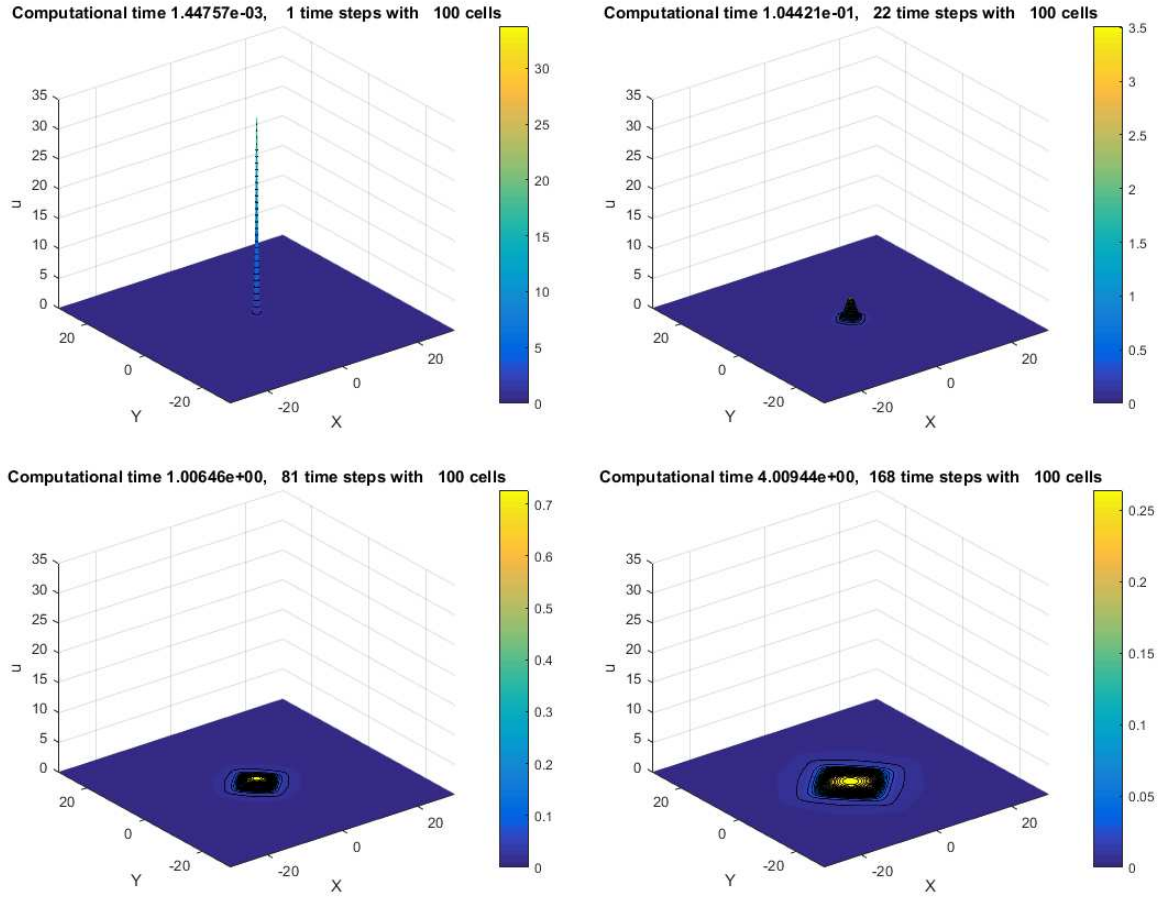


Figure 8 – Numerical simulation for $\partial_t \theta + \nabla \cdot (\theta \Lambda_1^{\alpha-1} \mathcal{H}_1 \theta, \theta \Lambda_2^{\alpha-1} \mathcal{H}_2 \theta) = 0$ with a weak Morrey initial data, $\alpha = 0.5$ and mesh $m = 100$ for a sequence of times $T = 0.0001, 0.1, 1, 4$. To better visualize the qualitative behavior, we keep the Z axis fixed. On the top, you can observe a decrease in height and the initiation of diffusion in the numerical solution as time evolves, while on the bottom the numerical solution shows a diffusion-smooth and minimal reduction in height as time evolves. Evidence of attenuation of regularization type.

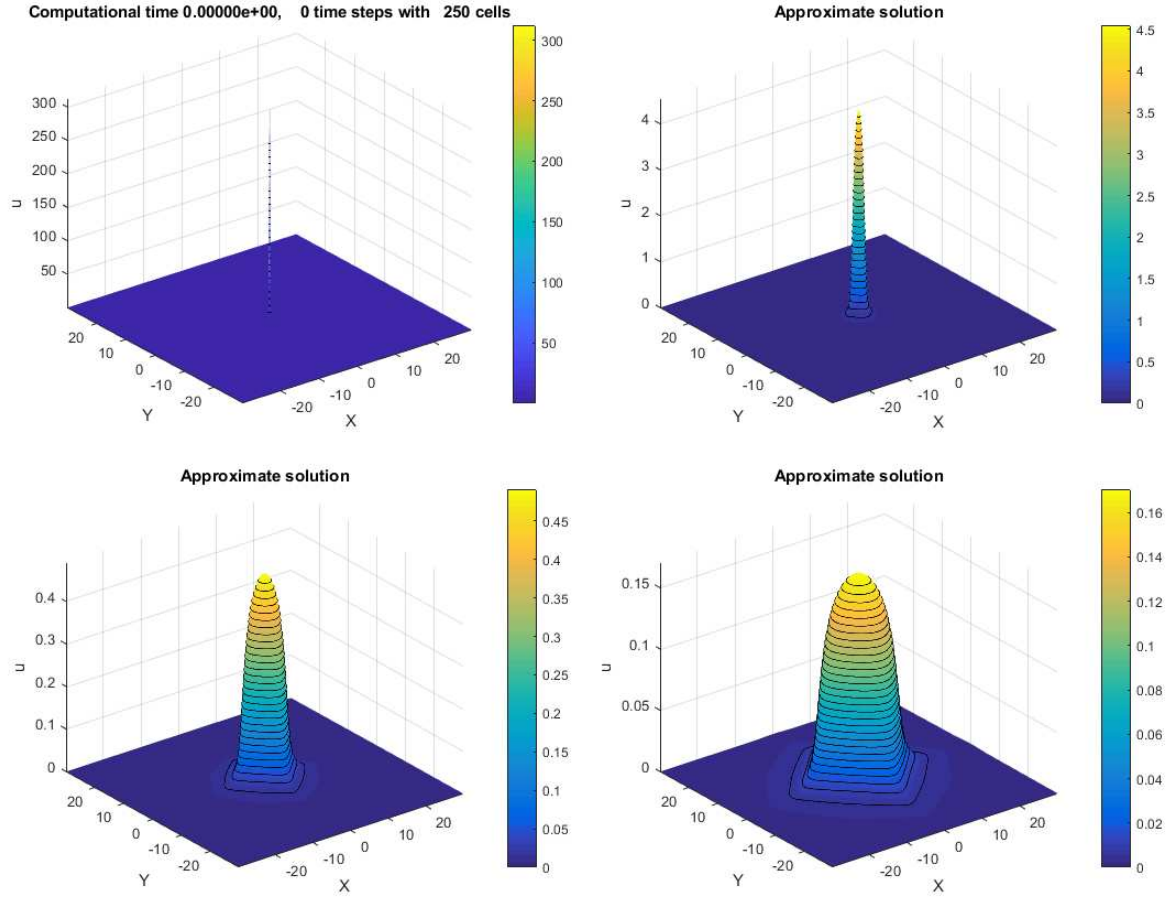


Figure 9 – Numerical simulation for $\partial_t \theta + \nabla \cdot (\theta \Lambda_1^{\alpha-1} \mathcal{H}_1 \theta, \theta \Lambda_2^{\alpha-1} \mathcal{H}_2 \theta) = 0$ with a Gaussian initial data, $\alpha = 0.5$ and mesh $m = 250$ for a sequence of times $T = 0, 0.1, 2, 8$. On the top, you can observe a decrease in height and the initiation of diffusion in the numerical solution as time evolves, while on the bottom, the numerical solution shows a diffusion-smooth and minimal reduction in height as time evolves. Evidence of attenuation of regularization type.

Negative flux

We determined a numerical solution with mesh grid cells $m = 512$ for a *conservation law with partially nonlocal velocity and negative flux* (3.113) with weak-Morrey initial data. This result is illustrated in Figure 10 and the machine simulation time was 32 days. Examining the early times, we can observe a subtle numerical diffusion. At the bottom, we can see that the height of the numerical solution increases along the gradient and the concentration process as time passes. As a result, we have evidence of blow-up type concentration for the solution θ of a *conservation law with partially nonlocal velocity and negative flux*.

An important observation is that for all simulations in this chapter, we used $CFL = 0.5$. However, in the simulation shown in Figure 10, we used $CFL = 0.125$. This adjustment was necessary because, for a value close to $CFL = 0.5$, there was instability in the numerical solution.

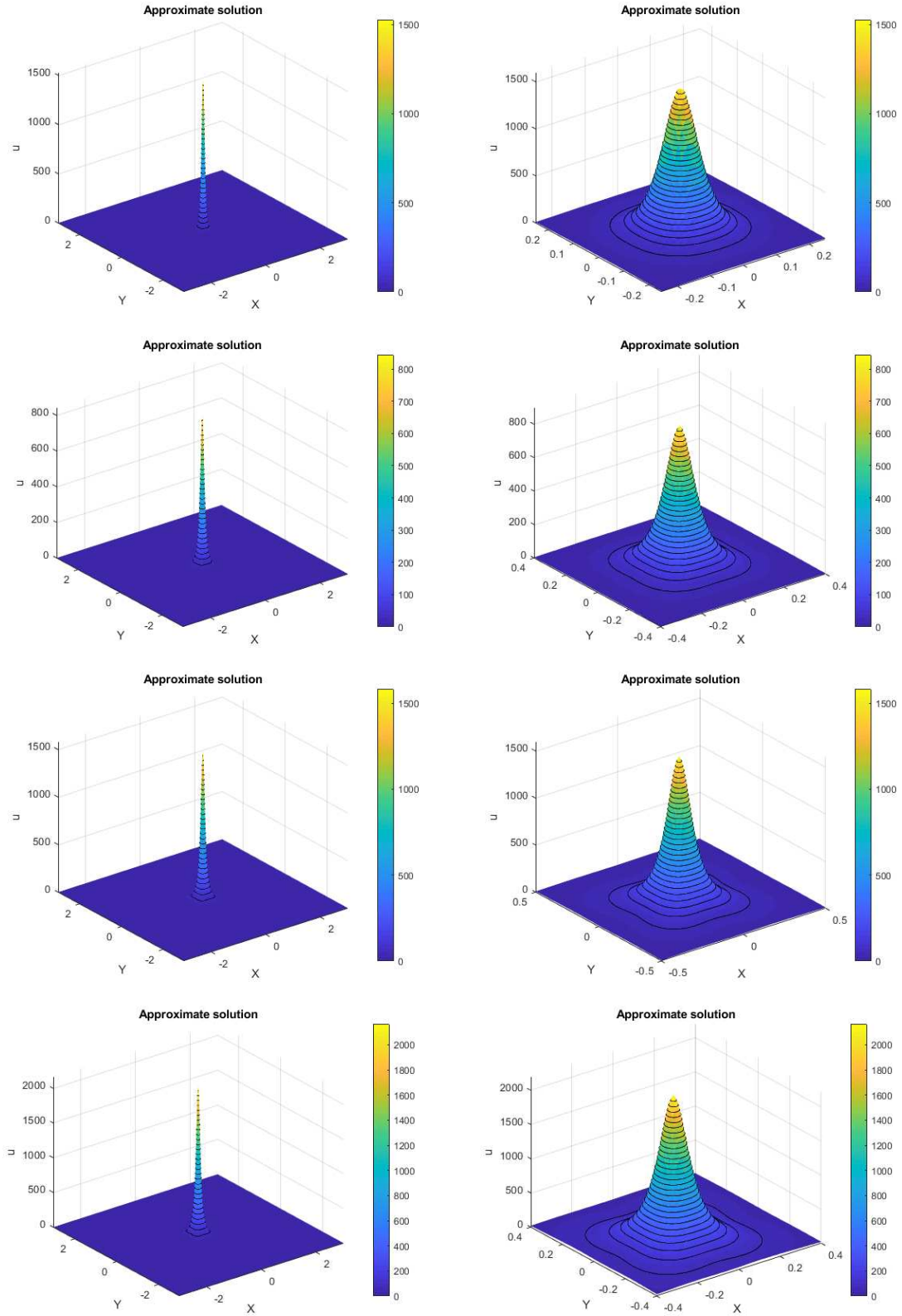


Figure 10 – Numerical simulation for $\partial_t \theta + \nabla \cdot (\theta \Lambda_1^{\alpha-1} \mathcal{H}_1 \theta, \theta \Lambda_2^{\alpha-1} \mathcal{H}_2 \theta) = 0$ with a Gaussian initial data, $\alpha = 0.5$ and mesh $m = 512$ for a sequence of times $T = 0.0001, 0.001, 0.02, 0.024$. This simulation is divided into two columns, with simulations in the right column being a zoom of the simulations in the left column close to the origin, aiming to see the evolution in the singularity of the numerical solution. We have evidence of blow-up of concentration-type.

3.6 The Model of a Conservation Law with Partially Nonlocal Velocity with Rotation

The work by [38] and [47] can be interpreted as addressing the one-dimensional SQG. Our primary question is whether we can derive the SQG or gather meaningful information by extending these prior works to two dimensions. This extension involves working with nonlocal partial operators in the velocity field, precisely the partial Hilbert transform and the partial Riesz potential. This gives rise to the inception of a conservation law with partially nonlocal velocity, and, as observed in the previous section, the numerical and theoretical outcomes of the 1D case are maintained. As observed, for the velocity field of a conservation law with partially nonlocal velocity to exhibit some similarity with the velocity field of the SQG equation, a rotation is absent in the coordinates of our model's velocity field; doing this rotation, we obtain a new model which we will call the model of a conservation law with partially nonlocal velocity 3.114. Our current inquiry is whether this model can provide theoretical and numerical insights into the well-known SQG equation. The answers to these questions will be elucidated in this section.

$$\begin{cases} \partial_t \theta + \nabla \cdot (-\theta \Lambda_2^{\alpha-1} \mathcal{H}_2 \theta, \theta \Lambda_1^{\alpha-1} \mathcal{H}_1 \theta) = 0, & (x, y, t) \in \mathbb{R}^2 \times \mathbb{R}, \\ \theta(x, y, 0) = \theta_0, \end{cases} \quad (3.114)$$

where $\Lambda_1^{\alpha-1}$ and $\Lambda_2^{\alpha-1}$ are the partial Riesz potential, which are given by (3.3) and (3.4) respectively, \mathcal{H}_1 and \mathcal{H}_2 are the partial Hilbert transform, which are given by (3.1) and (3.2) respectively. Furthermore, the initial data θ_0 is in L^p .

The well-posedness of the model of a conservation law with partially nonlocal velocity with rotation is assured by the well-posedness of a conservation law with partially nonlocal velocity, as established in Theorem 2. This guarantee arises from the fact that we are merely altering the order of the coordinates in the velocity field. Consequently, the calculations in the proof of the theorem will remain equivalent to a constant factor.

3.6.1 Numerical simulations for the model a conservation law with partially nonlocal velocity with rotation

To perform a numerical study of the model of a conservation law with partially nonlocal velocity with rotation (3.115) and deepen our comprehension of the nonlinear and nonlocal interactions within the Besov spaces type, we have developed a robust and coherent methodology for addressing model (3.115) within a finite computational domain $\Omega = [a, b] \times [c, d]$ analogous to a conservation law with partially nonlocal velocity. We describe our numerical experiments concerning *the model of a conservation law with partially nonlocal velocity with rotation* : $\partial_t \theta + \nabla \cdot (-\theta \Lambda_2^{\alpha-1} \mathcal{H}_2 \theta, \theta \Lambda_1^{\alpha-1} \mathcal{H}_1 \theta) = 0$.

So, we proceed to rephrase model (1.3) within the computational domain $\Omega = [a, b] \times [c, d]$

$$\begin{cases} \partial_t \theta + \nabla \cdot (-\theta \Lambda_2^{\alpha-1} \mathcal{H}_2 \theta, \theta \Lambda_1^{\alpha-1} \mathcal{H}_1 \theta) = 0, & (x, y, t) \in \Omega \times (0, T], \\ \theta(x, y, 0) = f(x, y), & (x, y) \in \Omega, \end{cases} \quad (3.115)$$

where $f(x, y)$ will be a

(I) the 2D Gaussian pulse with compact support initial condition

$$f(x, y) = \frac{1}{\pi} \exp\left\{-\frac{(x^2 + y^2)}{8}\right\}$$

(II) the 2D positive negative initial condition,

$$g(x, y) = 3xy \exp\left\{-\frac{(x^2 + y^2)}{5}\right\},$$

(III) $h(x, y) = \omega(x - 3, y) + \omega(x + 3, y)$, where

$$\omega(x, y) = \begin{cases} 2 \exp\left\{-\frac{1}{1 - x^2 - y^2}\right\} & ; x^2 + y^2 < 1 \\ 0 & ; x^2 + y^2 \geq 1 \end{cases},$$

(IV) $k(x, y) = \zeta(x - 3, y) - \zeta(x + 3, y)$, where

$$\zeta(x, y) = \begin{cases} \exp\left\{-\frac{(x^2 + y^2)}{5}\right\} & ; x^2 + y^2 < (2.8)^2 \\ 0 & ; x^2 + y^2 \geq (2.8)^2 \end{cases}.$$

Simulations

In this subsection, we present numerical simulations for *the model a conservation law with partially nonlocal velocity with rotation* considering various types of initial data. The simulations conducted here were performed with mesh grid cells of $m = 128$ and $m = 256$, and the simulation time on the machine ranged from approximately 1 to 2 days. We expect that for a mesh grid refinement to obtain the same qualitative behavior.

The novelty of the simulations in this subsection is that, along with illustrating the qualitative behavior of the numerical solution as time progresses, we also provide the level curves at each stage. This facilitates a deeper understanding of the numerical solution's behavior. In Figure 11, Figure 12 and Figure 13, we observe that the height of the numerical solution decreases, rotating counterclockwise and forming steeper gradients as time progresses. However, in Figure 14, the height of the numerical solution increases slightly, still rotating counterclockwise and forming steeper gradients over time.

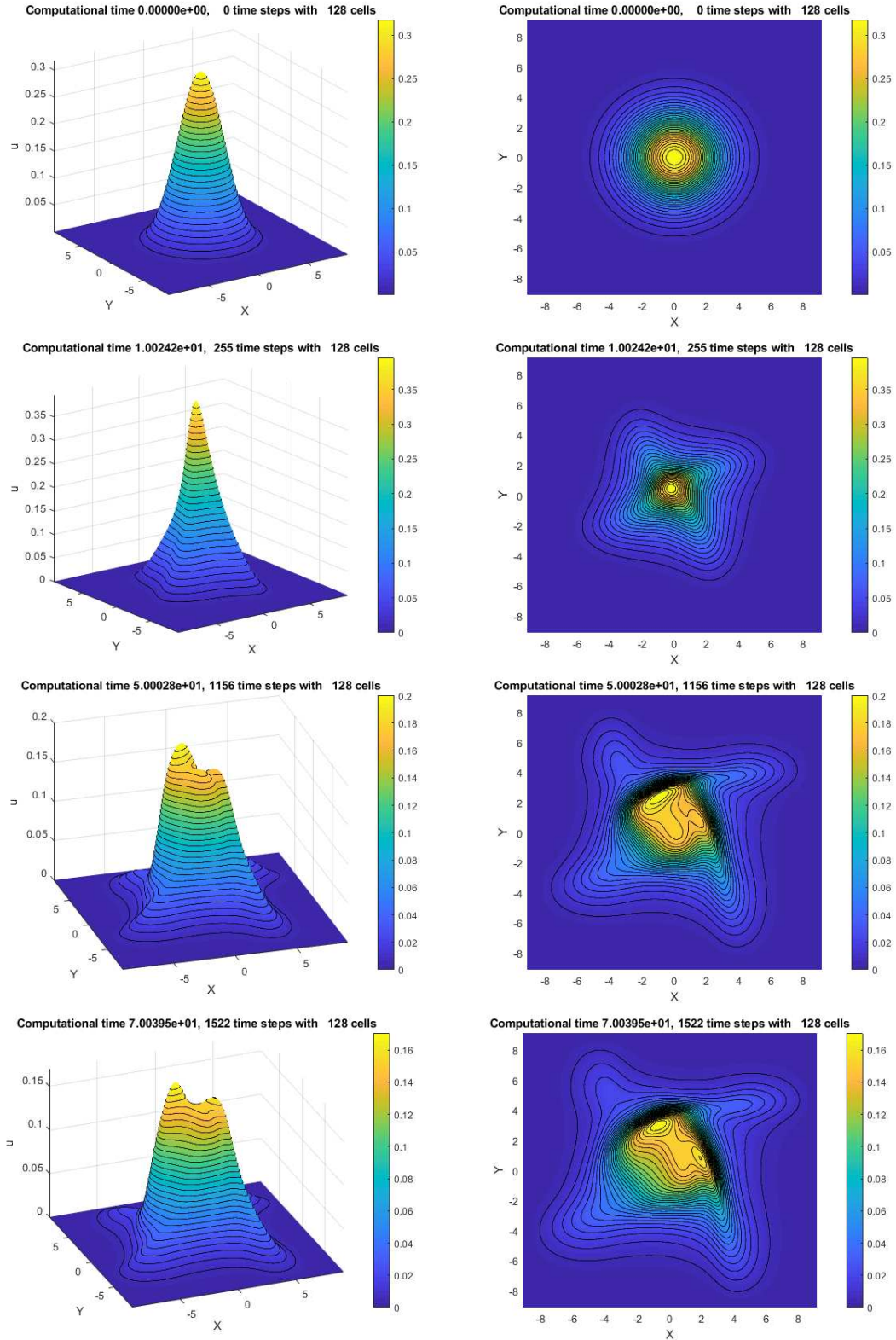


Figure 11 – Numerical simulation for $\partial_t \theta + \nabla \cdot (-\theta \Lambda_2^{\alpha-1} \mathcal{H}_2 \theta, \theta \Lambda_1^{\alpha-1} \mathcal{H}_1 \theta) = 0$ with a Gaussian initial data, $\alpha = 0.5$ and mesh $m = 128$ for a sequence of times $T = 0, 10, 50, 70$. In the left column, initially, the height of the numerical solution begins to grow, rotating counterclockwise and forming steeper gradients. In the following times, the height decreases and continues, forming steeper gradients as time evolves. Meanwhile, the pictures in the right column, represent the level sets of the surfaces found at the top. Evidence of attenuation with formation of abrupt gradients.

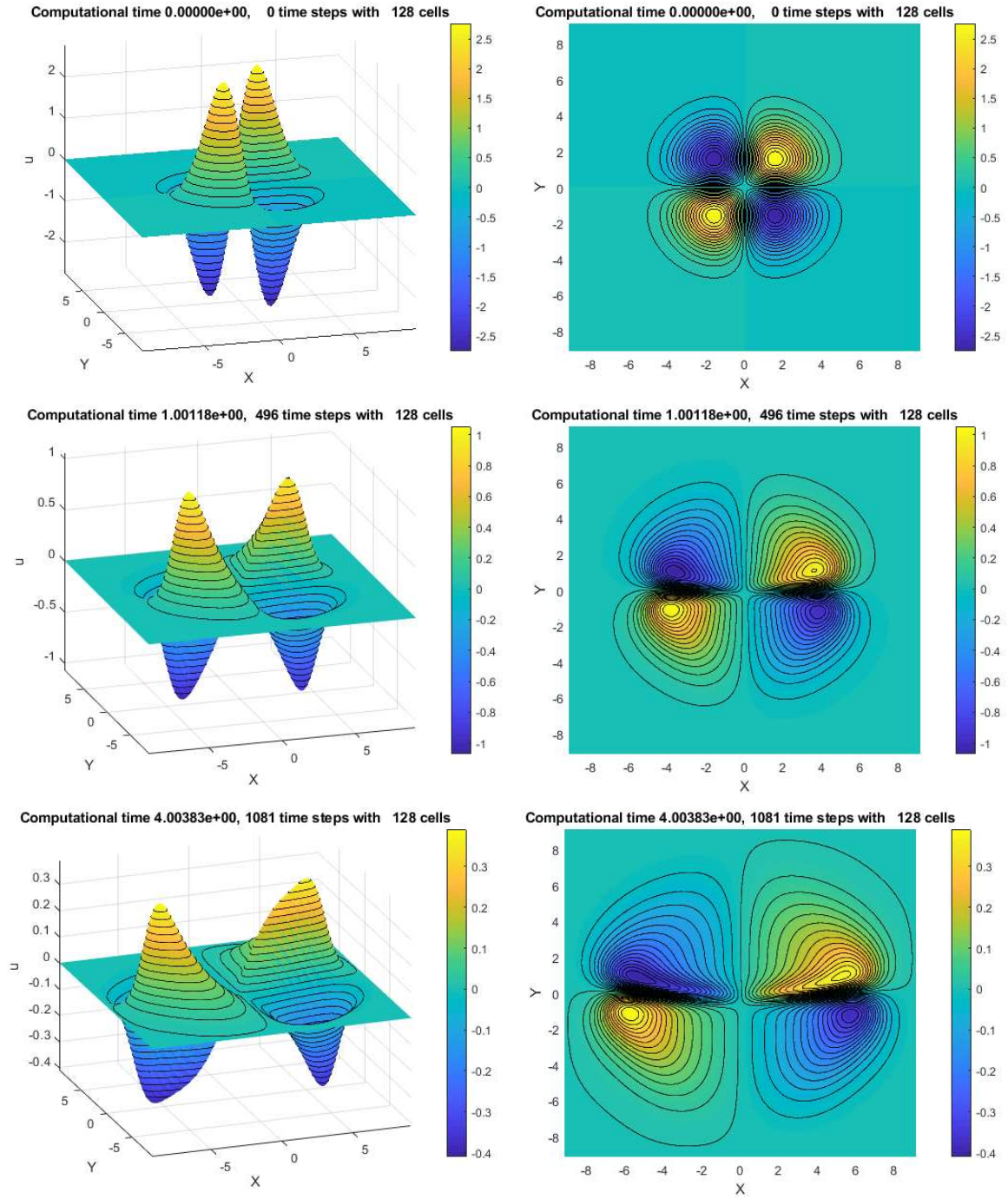


Figure 12 – Numerical simulation for $\partial_t \theta + \nabla \cdot (-\theta \Lambda_2^{\alpha-1} \mathcal{H}_2 \theta, \theta \Lambda_1^{\alpha-1} \mathcal{H}_1 \theta) = 0$ with a $g(x, y)$ initial data, $\alpha = 0.5$ and mesh $m = 128$ for a sequence of times $T = 0, 1, 4$. In the left column, the height of four peaks decreases forming two abrupt gradients in the opposite peaks as time evolves. Meanwhile, the pictures in right column, represent the level sets of the surfaces found at the top. Evidence of attenuation with formation of abrupt gradients.

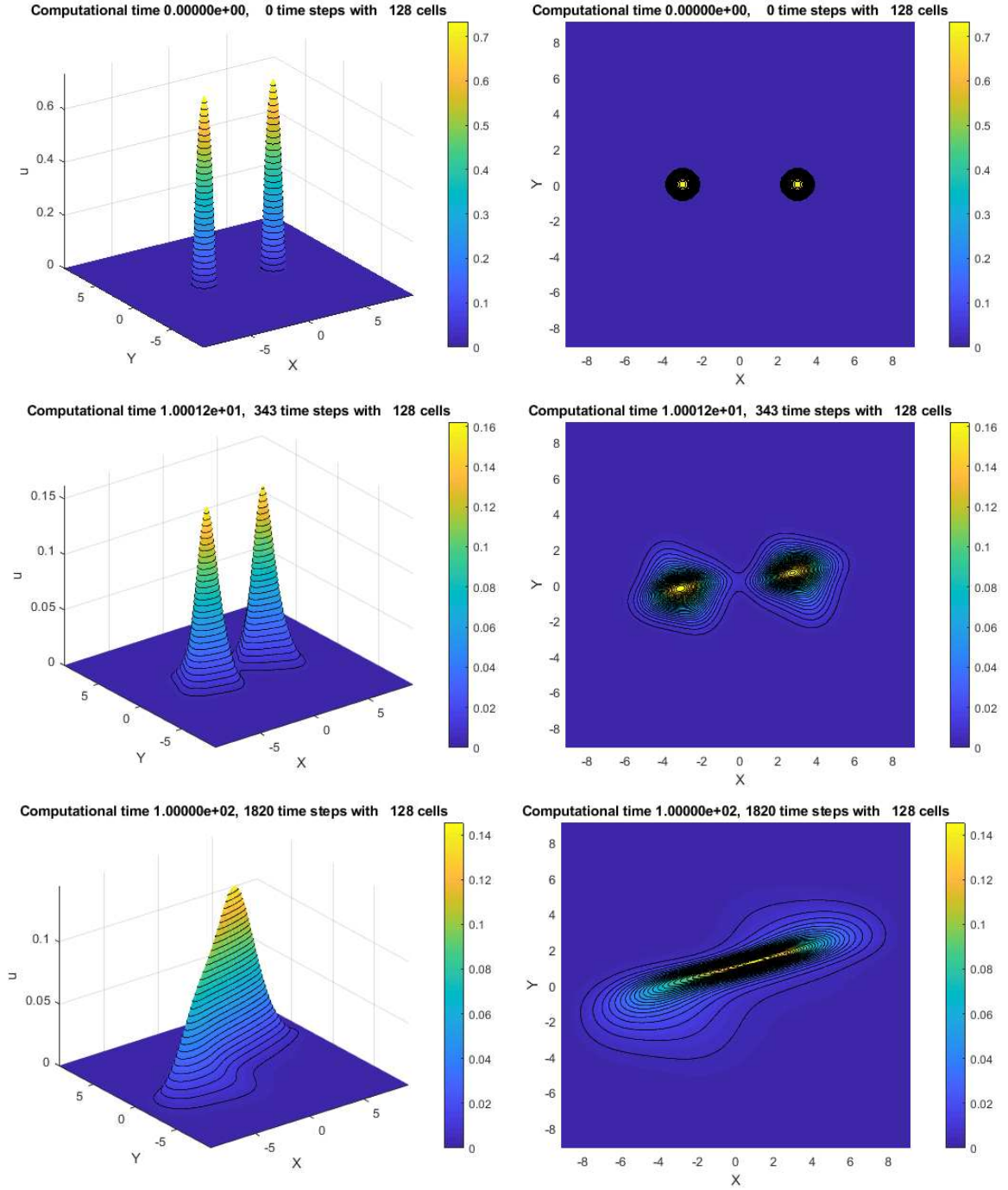


Figure 13 – Numerical simulation for $\partial_t \theta + \nabla \cdot (-\theta \Lambda_2^{\alpha-1} \mathcal{H}_2 \theta, \theta \Lambda_1^{\alpha-1} \mathcal{H}_1 \theta) = 0$ with a $h(x, y)$ initial data, $\alpha = 0.5$ and mesh $m = 128$ for a sequence of times $T = 0, 10, 100$. In the left column, the height of the two peaks decreases, forming steeper gradients and coming together as time evolves. Meanwhile, the pictures in the right column, represent the level sets of the surfaces found at the top. Evidence of attenuation with formation of abrupt gradients.

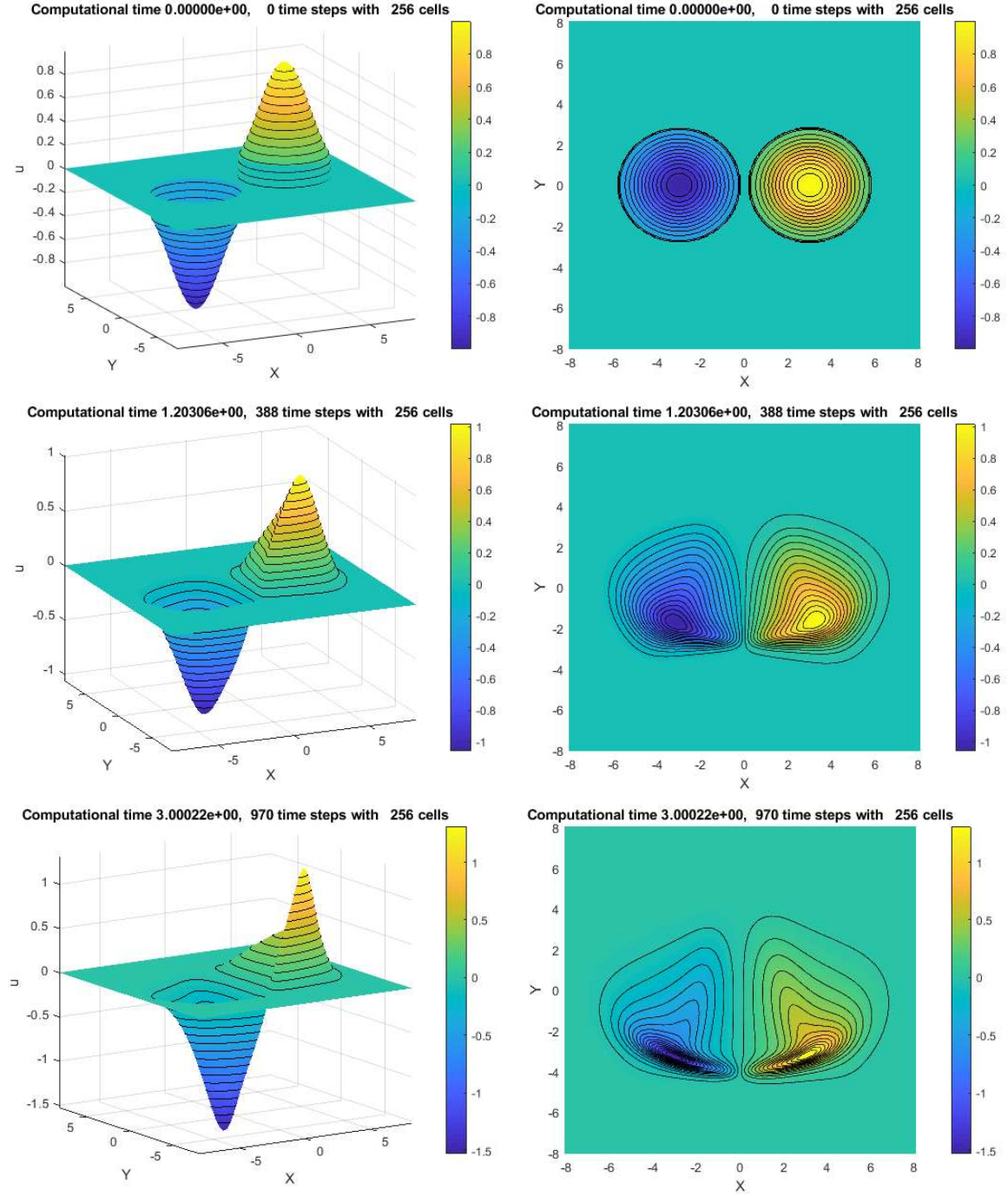


Figure 14 – Numerical simulation for $\partial_t \theta + \nabla \cdot (-\theta \Lambda_2^{\alpha-1} \mathcal{H}_2 \theta, \theta \Lambda_1^{\alpha-1} \mathcal{H}_1 \theta) = 0$ with a $g(x, y)$ initial data, $\alpha = 0.5$ and mesh $m = 128$ for a sequence of times $T = 0, 1.2, 3$. In the left column, initially, the height of the two peaks decreases and forms steeper gradients. In the following times, the height increases and forms an abrupt gradient in each peak as time evolves. In this case, the peaks do not join. Meanwhile, the pictures in the right column represent the level sets of the surfaces found at the top. Evidence of the formation of an abrupt gradient without attenuation.

3.7 Geometric Properties of Level Sets in the Model a conservation law with partially nonlocal velocity with Rotation

In [25], the authors investigate various geometric properties of the SQG sharp fronts and α -patches. To achieve this, they characterize the interface region (i.e., the area where discontinuity arises due to rapid transitions between different air masses) using a closed curve with a period of 2π . The objective is to study the evolution at the border of this interface and, in turn, determine the qualitative behavior of the problem. In this study, guided by numerical simulations, the authors provide proof for two results regarding the behavior of SQG sharp fronts and α -patches. Furthermore, they establish that ellipses are not rotational solutions and demonstrate that initially, convex interfaces may lose this property in finite time.

Inspired by this work, we attempted to track some level sets for the numerical solution, and obtain geometric information from these level sets, for this case considering the Gaussian as the initial data, see Figure 15. As we can see in our simulations, we also obtained a similar result to [25], see Figure 16.

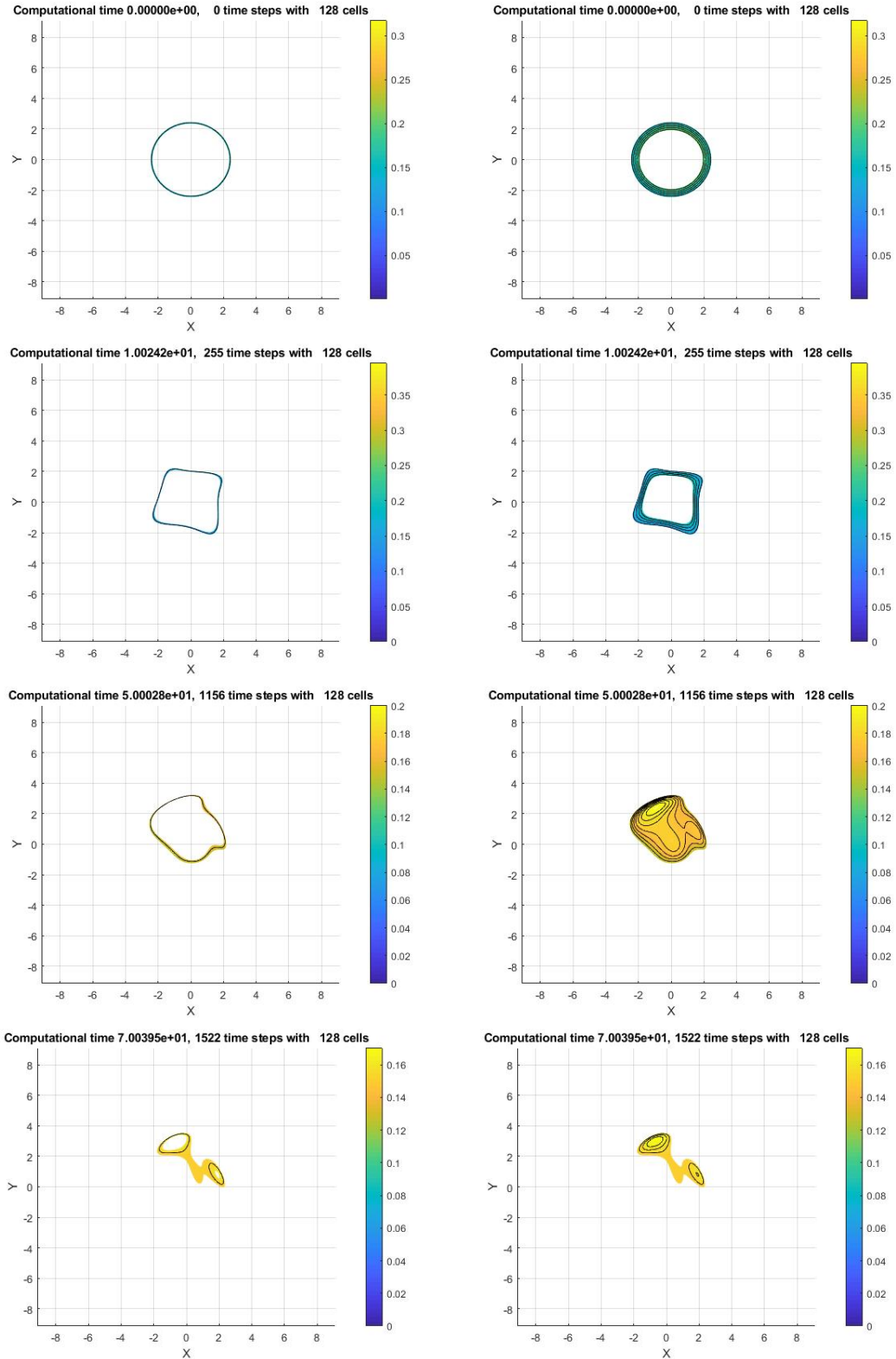


Figure 15 – Tracking some level sets of the numerical solution of $\partial_t \theta + \nabla \cdot (-\theta \Lambda_2^{\alpha-1} \mathcal{H}_2 \theta, \theta \Lambda_1^{\alpha-1} \mathcal{H}_1 \theta) = 0$ with Gaussian initial data, $\alpha = 0.5$ and mesh $m = 128$ for a sequence of times $T = 0, 10, 50, 70$. In the left column, we attempt to trace a level curve at half the initial data is height. As time progresses, this level curve loses convexity and separates into two different level curves. Meanwhile, in the pictures in the right column, the level curves are positioned at the top of the initial data. Here, the level curves also lose convexity and split into two distinct groups of level curves.

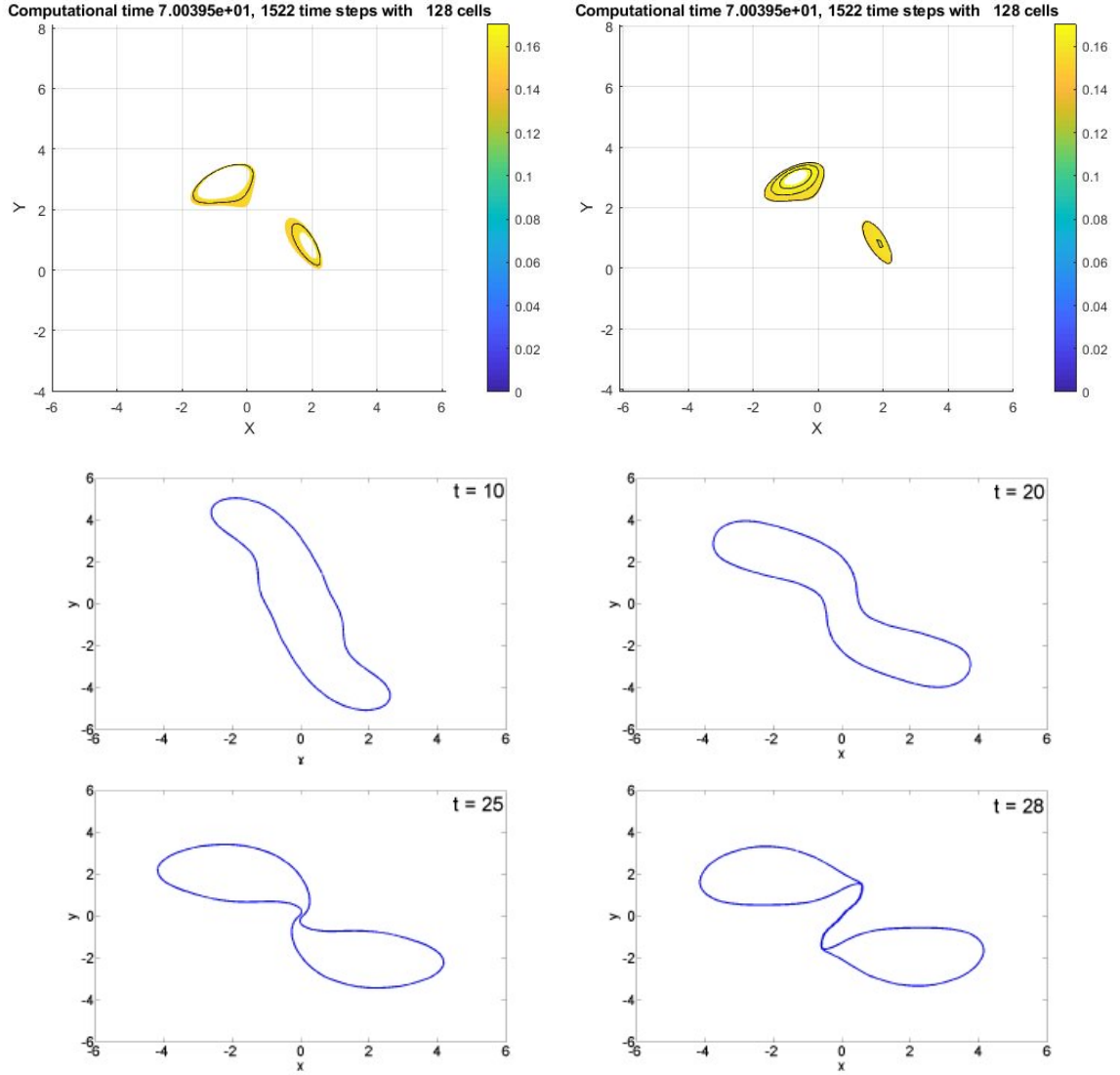


Figure 16 – The two figures at the top represent the last two simulations described in Figure 15. In [25] the authors study the geometric properties of SQG sharp fronts and α -patches; in this paper the SQG is given by $\partial_t \theta(x, y, t) + u(x, y, t) \cdot \nabla \theta(x, y, t) = 0$ with $u = (-\mathcal{R}_2 \theta, \mathcal{R}_1 \theta)$. The four figures at the bottom were taken from [25] and are simulations of the evolution of the ellipses with, the patch with initial data $z(x) = (\cos(x); 3\sin(x))$ displays a combination of a rotating motion with a smaller scale oscillation which leads to loss of convexity. As we can see, both simulations start with a regular and convex geometric figure; as time passes, these simulations lose convexity and form two types of deformed ellipses.

4 The Surface Quasi-Geostrophic Equation

In this chapter, the aim is to establish the local well-posedness for the inviscid surface quasi-geostrophic equation SQG (4.1) in the framework of modified Besov weak–Morrey spaces, which are modeled in Besov spaces and the underlying norm is of weak-Morrey modified space rather than the usual weak- L^p space.

The SQG in non-conservative form is given by

$$\begin{cases} \partial_t \theta + v \cdot \nabla \theta = 0 \\ \theta(x, 0) = \theta_0(x) \end{cases} \quad (4.1)$$

where $\theta = \theta(x, t)$ is a scalar function, $\theta : \mathbb{R}^2 \times [0, \infty) \rightarrow \mathbb{R}$, represents the temperature potential of the fluid, and $v = (v_1, v_2)$ denotes a velocity field such that $\nabla v = 0$. The relationship between v and θ is through the Riesz transforms, \mathcal{R}_1 and \mathcal{R}_2 , using the following expression:

$$v = \mathcal{R}^\perp \theta = (-\mathcal{R}_2 \theta, \mathcal{R}_1 \theta) = (-\partial_2 (-\Delta)^{-\frac{1}{2}} \theta, \partial_1 (-\Delta)^{-\frac{1}{2}} \theta)$$

here the operator Δ is the Laplacian.

The geostrophic theory describes the dynamics of large atmospheric and oceanic currents through the balance between the Coriolis force and pressure gradient within a rotating fluid. In [60] it delves into this theory, explaining how it can be applied to understand large-scale atmospheric and oceanic circulation. However, it may not capture all aspects of fluid motion at smaller scales or in more complex systems. The quasi-geostrophic theory is an extension of the geostrophic theory, which acknowledges that at smaller scales or in situations where factors other than the Earth's rotation may be significant.

The SQG comes from atmospheric science and describes the evolution of the potential temperature on the surface. Therefore, this equation describes the evolution of cold and warm air fronts in a thin layer in the atmosphere. For this reason, the SQG has applications in meteorology and oceanography, playing an important role in weather forecasting and improving understanding of the temperature evolution of geophysical flows and, particularly frontogenesis in atmospheric flows [27, 31].

Constantin, Majda, and Tabak introduced the SQG equation to the mathematical community in [31], conducting numerical and analytical studies. Additionally, the SQG exhibits an analogy with the 3D Euler equations. So far, the mathematical study of the SQG has been divided into two significant cases. The first is the inviscid case (4.1), probably the most straightforward dynamical scalar equation. However, the global regularity problem remains open. In [31], it was established the local well-posedness

and blow-up criterion of (4.1) in Sobolev spaces. The exciting fact about [31], is that the authors also make a numerical study of the problem besides being the first theoretical study. Subsequently, there are various results available in different function spaces. For instance, on the Morrey spaces in [69], on the Triebel-Lizorkin spaces in [26], on the Besov spaces in [67], on the Triebel-Lizorkin-Lorentz spaces in [71], on the Besov–Lorentz spaces in [73], and recently it has been found in generalized spaces by [72].

The second case considers the dissipative term $\kappa(-\Delta)^\alpha \theta$ in the equation (4.1). In this case, it was studied the global well-posedness problem. More precisely, the study on the dissipative SQG unfolds in three directions: the sub-critical case $\alpha > 1/2$, the critical case $\alpha = 1/2$, and the super-critical case $\alpha < 1/2$. For more details of the sub-critical case, the reader should consult [33] and [62]. In [30] it addressed the global regularity issue for the critical case; in particular, it obtained a global existence result of the solution under a smallness condition on the initial data. Since then, global existence results for small initial data have been obtained in various functional settings, e.g., in Sobolev spaces in [34, 57], Besov spaces in [29, 1, 26, 70]. Two papers exist that resolve entirely the global regularity problem without a smallness condition. One is in [52] and the other in [24].

As noted earlier, the well-posedness theory of SQG in the dissipative case has undergone thorough investigation in previous years. Numerous authors have successfully addressed global well-posedness, particularly for critical cases, as documented in references [52, 24, 32, 1]. Nevertheless, limited attention has been given to the super-critical case, with only a handful of papers, such as [37, 51, 64], delving into the discussion of eventual regularity.

Recently, the dissipative case has been examined in various types of spaces, with intermittent regularities discussed in the following papers [53, 55, 68, 21, 66, 20, 15, 18, 35].

In this chapter, the aim is to establish the local well-posedness and blow-up criterion for (4.1) within the framework of modified Besov–weak–Morrey spaces. These spaces are based on Besov spaces, and the associated norm is derived from the weak-Morrey Modified space, as opposed to the conventional weak- L^p space.

4.1 Commutator Estimates in Modified Besov-weak-Morrey Spaces

In this section, we present the commutator estimates in modified Besov-weak-Morrey spaces defined in [42]. In addition, such commutator estimates are linked to the bilinear term $u \cdot \nabla v$, considering $\nabla \cdot u = \nabla \cdot v = 0$. In this work, we verify that for these preliminary results and lemmas, it will suffice that only one of them has null divergence; in this case, $\nabla \cdot u = 0$. Let us define the commutator term

$$R_j(u, v) = \bar{\Delta}_j(u \cdot \nabla v) - S_{j-2}u \cdot \nabla \bar{\Delta}_j v, \quad (4.2)$$

for $u = (u_1, \dots, u_n)$, such that $\nabla \cdot u = 0$ and v is a function. It follows that $R_j(u, v)$ can be decomposed as

$$R_j(u, v) = \sum_{i=1}^4 R_j^i(u, v), \quad (4.3)$$

where

$$\begin{aligned} R_j^1(u, v) &= \sum_{k=1}^n \bar{\Delta}_j T_{\partial_k v} u_k, \\ R_j^2(u, v) &= - \sum_{k=1}^n [T_{u_k} \partial_k, \bar{\Delta}_j] v, \\ R_j^3(u, v) &= \sum_{k=1}^n T_{u_k - S_{j-2} u_k} \partial_k \bar{\Delta}_j v, \\ R_j^4(u, v) &= \sum_{k=1}^n \{ \bar{\Delta}_j R(u_k, \partial_k v) - R(S_{j-2} u_k, \bar{\Delta}_j \partial_k v) \} \end{aligned}$$

with $[T_{u_k} \partial_k, \bar{\Delta}_j] v := T_{u_k} \partial_k \bar{\Delta}_j v - \bar{\Delta}_j T_{u_k} \partial_k v$ and $R(u, v)$ is the rest of the paraproduct of u and v . Let us to check equation (4.3).

By using Bonny's decomposition (2.3), we can write

$$\bar{\Delta}_j(u \cdot \nabla v) = \bar{\Delta}_j \sum_{k=1}^n u_k \partial_k v = \sum_{k=1}^n [\bar{\Delta}_j T_{u_k} \partial_k v + \bar{\Delta}_j T_{\partial_k v} u_k + \bar{\Delta}_j R(u_k, \partial_k v)]$$

and

$$S_{j-2} u \cdot \nabla \bar{\Delta}_j v = \sum_{k=1}^n S_{j-2} u_k \partial_k \bar{\Delta}_j v = \sum_{k=1}^n [T_{S_{j-2} u_k} \partial_k \bar{\Delta}_j v + T_{\partial_k \bar{\Delta}_j v} S_{j-2} u_k + R(S_{j-2} u_k, \partial_k \bar{\Delta}_j v)].$$

Subtracting the last two identities and introducing the term $T_{u_k} \partial_k \bar{\Delta}_j v$, we get

$$\begin{aligned} \bar{\Delta}_j(u \cdot \nabla v) - S_{j-2} u \cdot \nabla \bar{\Delta}_j v &= \sum_{k=1}^n \{ -[T_{u_k} \partial_k, \bar{\Delta}_j] v + T_{u_k - S_{j-2} u_k} \partial_k \bar{\Delta}_j v + \bar{\Delta}_j T_{\partial_k v} u_k \\ &\quad - T_{\partial_k \bar{\Delta}_j v} S_{j-2} u_k + \bar{\Delta}_j R(u_k, \partial_k v) - R(S_{j-2} u_k, \partial_k \bar{\Delta}_j v) \}. \end{aligned}$$

The result follows from the fact that $T_{\partial_k \bar{\Delta}_j v} S_{j-2} u_k = 0$. In fact, by the definition of operator T ,

$$T_{\partial_k \bar{\Delta}_j v} S_{j-2} u_k = \sum_{j' \geq 2} (S_{j'-2} \bar{\Delta}_j v)(\Delta_{j'} S_{j-2} u_k).$$

The operator $S_{j'-2} \bar{\Delta}_j$ vanishes when $j \geq j'$, the last assertion holds true.

We start estimating $R_j^1(u, v)$: using Young's inequality and Hölder type inequality for modified weak-Morrey spaces, we can estimate as

$$\begin{aligned} \|R_j^1(u, v)\|_{W\tilde{\mathcal{M}}_p^l} &\leq \sum_{k=1}^n \sum_{|j-j'|\leq 4} \|\bar{\Delta}_j (S_{j'-2} \partial_k v \bar{\Delta}_{j'} u_k)\|_{W\tilde{\mathcal{M}}_p^l} \\ &\leq C \sum_{k=1}^n \sum_{|j-j'|\leq 4} \|S_{j'-2} \partial_k v \bar{\Delta}_{j'} u_k\|_{W\tilde{\mathcal{M}}_p^l} \\ &\leq C \sum_{k=1}^n \sum_{|j-j'|\leq 4} \|S_{j'-2} \partial_k v\|_{L^\infty} \|\bar{\Delta}_{j'} u_k\|_{W\tilde{\mathcal{M}}_p^l} \end{aligned}$$

By using the definition of $R_j^2(u, v)$ and the orthogonality relations (2.1) and (2.2), we have

$$R_j^2(u, v) = - \sum_{k=1}^n \sum_{|j-j'|\leq 3} [S_{j'-2} u_k \partial_k (\bar{\Delta}_{j'} \bar{\Delta}_j v) - \bar{\Delta}_j (S_{j'-2} u_k \bar{\Delta}_{j'} \partial_k v)]$$

Thus, rewritten the previous equality in terms of their kernels, we get

$$\begin{aligned} R_j^2(u, v) &= - \sum_{k=1}^n \sum_{|j-j'|\leq 3} 2^{jn} \int_{\mathbb{R}^n} \check{\varphi}(2^j(x-y)) [S_{j'-2} u_k(x) - S_{j'-2} u_k(y)] \partial_k \bar{\Delta}_{j'} v(y) dy \\ &= \sum_{k=1}^n \sum_{|j-j'|\leq 3} 2^{j(n+1)} \int_{\mathbb{R}^n} \partial_k \check{\varphi}(2^j(x-y)) [S_{j'-2} u_k(x) - S_{j'-2} u_k(y)] \bar{\Delta}_{j'} v(y) dy, \end{aligned} \quad (4.4)$$

where in the last identity, we have used by parts integration together with the fact that u is free divergence. Now, notice that the fundamental Theorem of calculus allows us to get the identity

$$S_{j'-2} u_k(x) - S_{j'-2} u_k(y) = - \int_0^1 \nabla(S_{j'-2} u_k)(x + \tau(y-x)) \cdot (y-x) d\tau,$$

this implies, via the Cauchy-Schwartz inequality, the estimate

$$|S_{j'-2} u_k(x) - S_{j'-2} u_k(y)| \leq \int_0^1 |\nabla(S_{j'-2} u_k)(x + \tau(y-x))| |y-x| d\tau \leq \|\nabla S_{j'-2} u_k\|_{L^\infty} |x-y|. \quad (4.5)$$

Inserting (4.4) into (4.5), it follows the direct estimate,

$$|R_j^2(u, v)| \leq \sum_{k=1}^n \sum_{|j-j'|\leq 3} 2^{jn} \int_{\mathbb{R}^n} |\partial_k \check{\varphi}(2^j(x-y))| 2^j |x-y| |\bar{\Delta}_{j'} v(y)| dy \|\nabla u_k\|_{L^\infty}.$$

Now, by taking the norm and using Young's inequality for modified weak-Morrey spaces, we arrive to

$$\|R_j^2(u, v)\|_{W\tilde{\mathcal{M}}_p^l} \leq C \|\nabla \check{\varphi}(x) \cdot x\|_{L^1} \|\nabla u\|_{L^\infty} \|v\|_{W\tilde{\mathcal{M}}_p^l}. \quad (4.6)$$

By the definition of $R_j^3(u, v)$, the orthogonality relation (2.1) and the homogeneous Littlewood-Paley decomposition, we get

$$\begin{aligned} R_j^3(u, v) &= \sum_{k=1}^n \sum_{j' \geq 2, |j-j'| \leq 1} S_{j'-2}(u_k - S_{j-2}u_k) \partial_k \bar{\Delta}_{j'} \bar{\Delta}_j v \\ &= \sum_{k=1}^n \sum_{j' \geq 2, |j-j'| \leq 1} S_{j'-2} \left(\sum_{m=j-2}^{\infty} \Delta_m u_k \right) \partial_k \bar{\Delta}_{j'} \bar{\Delta}_j v \\ &= \sum_{k=1}^n \sum_{j' \geq 2, |j-j'| \leq 1} \partial_k \bar{\Delta}_{j'} \bar{\Delta}_j v \sum_{m=j-2}^{j-1} \bar{\Delta}_m S_{j'-2} u_k. \end{aligned}$$

So, by taking the norm and using Hölder's and Young's inequality, as well as Bernstein-type inequalities for modified weak-Morrey spaces, we obtain

$$\begin{aligned} \|R_j^3(u, v)\|_{W\tilde{\mathcal{M}}_p^l} &\leq C \sum_{k=1}^n \sum_{j' \geq 2, |j-j'| \leq 1} \sum_{m=j-2}^{j-1} \|\partial_k \bar{\Delta}_{j'} \bar{\Delta}_j v\|_{W\tilde{\mathcal{M}}_p^l} \|\bar{\Delta}_m S_{j'-2} u_k\|_{L^\infty} \\ &\leq C \sum_{k=1}^n \sum_{j' \geq 2, |j-j'| \leq 1} \sum_{m=j-2}^{j-1} 2^j \|\bar{\Delta}_j v\|_{W\tilde{\mathcal{M}}_p^l} \|\bar{\Delta}_m S_{j'-2} u_k\|_{L^\infty}. \end{aligned}$$

Similarly, the R_j^3 can be estimated as

$$\begin{aligned} \|R_j^3(u, v)\|_{W\tilde{\mathcal{M}}_p^l} &\leq C \sum_{k=1}^n \sum_{j' \geq 2, |j-j'| \leq 1} \|\bar{\Delta}_{j'} \bar{\Delta}_j \partial_k v\|_{L^\infty} \sum_{m=j-2}^{j-1} \|\bar{\Delta}_m S_{j'-2} u_k\|_{W\tilde{\mathcal{M}}_p^l} \\ &\leq C \sum_{k=1}^n \sum_{j' \geq 2, |j-j'| \leq 1} \|\nabla v\|_{L^\infty} \sum_{m=j-2}^{j-1} \|\bar{\Delta}_m S_{j'-2} u_k\|_{W\tilde{\mathcal{M}}_p^l}. \end{aligned} \quad (4.7)$$

Finally, by the definition of $R_j^4(u, v)$, the derivative of the product with the fact that u is free divergence, and adding and subtracting the term

$$\sum_{k=1}^n \bar{\Delta}_j \sum_{l \geq -1} \bar{\Delta}_l S_{j-2} u_k \sum_{|l-l'| \leq 2} \bar{\Delta}_{l'} \partial_k v,$$

we have

$$\begin{aligned} R_j^4(u, v) &= \sum_{k=1}^n \partial_k \bar{\Delta}_j \sum_{l \geq -1} \bar{\Delta}_l (u_k - S_{j-2} u_k) \left(\sum_{|l-l'| \leq 2} \bar{\Delta}_{l'} v \right) \\ &\quad + \sum_{k=1}^n \sum_{l \geq -1} [\bar{\Delta}_j, \bar{\Delta}_l S_{j-2} u_k] \left(\sum_{|l-l'| \leq 2} \bar{\Delta}_{l'} \partial_k v \right) \\ &:= R_j^{4,1}(u, v) + R_j^{4,2}(u, v). \end{aligned}$$

In the $R_j^{4,1}(u, v)$ from the homogeneous Littlewood-Paley decomposition, the orthogonality relation (2.1)

$$\begin{aligned} R_j^{4,1}(u, v) &= \sum_{k=1}^n \partial_k \bar{\Delta}_j \sum_{l \geq -1} \bar{\Delta}_l \left(\sum_{m=j-2}^{\infty} \bar{\Delta}_m u_k \right) \left(\sum_{|l-l'| \leq 2} \bar{\Delta}_{l'} v \right) \\ &= \sum_{k=1}^n \partial_k \bar{\Delta}_j \sum_{l \geq j-3} \sum_{m=j-2}^{\infty} \bar{\Delta}_l \bar{\Delta}_m u_k \sum_{|l-l'| \leq 2} \bar{\Delta}_{l'} v \\ &= \sum_{k=1}^n \partial_k \bar{\Delta}_j \sum_{l \geq j-3} \bar{\Delta}_l (u_k - S_{j-2} u_k) \sum_{|l-l'| \leq 2} \bar{\Delta}_{l'} v. \end{aligned}$$

Now, by taking the norm and using Young's and Hölder's inequality for modified weak-Morrey spaces we arrive to

$$\begin{aligned} \|R_j^{4,1}(u, v)\|_{W\tilde{\mathcal{M}}_p^l} &\leq \sum_{k=1}^n \sum_{l \geq j-3} C \left\| \partial_k \left\{ \bar{\Delta}_l (u_k - S_{j-2} u_k) \sum_{|l-l'| \leq 2} \bar{\Delta}_{l'} v \right\} \right\|_{W\tilde{\mathcal{M}}_p^l} \\ &\leq C \sum_{k=1}^n \sum_{l \geq j-3} \left\| \partial_k \bar{\Delta}_l (u_k - S_{j-2} u_k) \right\|_{L^\infty} \left\| \sum_{|l-l'| \leq 2} \bar{\Delta}_{l'} v \right\|_{W\tilde{\mathcal{M}}_p^l} \\ &\quad + C \sum_{k=1}^n \sum_{l \geq j-3} \left\| \bar{\Delta}_l (u_k - S_{j-2} u_k) \right\|_{W\tilde{\mathcal{M}}_p^l} \left\| \partial_k \sum_{|l-l'| \leq 2} \bar{\Delta}_{l'} v \right\|_{L^\infty} \\ &\leq C \sum_{k=1}^n \sum_{l \geq j-3} (\|\Delta_l \partial_k u_k\|_{L^\infty} + \|S_{j-2} \Delta_l \partial_k u_k\|_{L^\infty}) \left\| \sum_{|l-l'| \leq 2} \bar{\Delta}_{l'} v \right\|_{W\tilde{\mathcal{M}}_p^l} \\ &\quad + C \sum_{k=1}^n \sum_{l \geq j-3} (\|\Delta_l u_k\|_{W\tilde{\mathcal{M}}_p^l} + \|S_{j-2} \Delta_l u_k\|_{W\tilde{\mathcal{M}}_p^l}) \sum_{|l-l'| \leq 2} \left\| \bar{\Delta}_{l'} \partial_k v \right\|_{L^\infty} \\ &\leq C \|\nabla u\|_{L^\infty} \sum_{l \geq j-3} \left\| \sum_{|l-l'| \leq 2} \bar{\Delta}_{l'} v \right\|_{W\tilde{\mathcal{M}}_p^l} + C \|\nabla v\|_{L^\infty} \sum_{k=1}^n \sum_{l \geq j-3} \|\Delta_l u_k\|_{W\tilde{\mathcal{M}}_p^l}. \end{aligned}$$

In $R_j^{4,2}$ from the definition of commutator operator, we have

$$R_j^{4,2}(u, v) = \sum_{k=1}^n \sum_{l \geq -1} \left\{ \bar{\Delta}_j \left(\bar{\Delta}_l S_{j-2} u_k \sum_{|l-l'| \leq 2} \bar{\Delta}_{l'} \partial_k v \right) - \bar{\Delta}_l S_{j-2} u_k \bar{\Delta}_j \sum_{|l-l'| \leq 2} \bar{\Delta}_{l'} \partial_k v \right\}.$$

Notice that,

$$\begin{aligned}
& \text{supp} \left\{ \bar{\Delta}_j \left(\bar{\Delta}_l S_{j-2} u_k \sum_{|l-l'|\leq 2} \bar{\Delta}_{l'} \partial_k v \right) \right\}^\wedge \\
&= \text{supp} \left\{ \varphi_j \left(\bar{\Delta}_l S_{j-2} u_k \sum_{|l-l'|\leq 2} \bar{\Delta}_{l'} \partial_k v \right) \right\}^\wedge \\
&\subset \text{supp} \varphi_j \cap \text{supp} \left(\bar{\Delta}_l S_{j-2} u_k \sum_{|l-l'|\leq 2} \bar{\Delta}_{l'} \partial_k v \right)^\wedge \\
&\subset \left\{ \xi : \frac{3}{4} 2^j \leq |\xi| \leq \frac{8}{3} 2^j \right\} \cap \left\{ \xi : \frac{3}{4} 2^{l+2} \leq |\xi| \leq \frac{8}{3} 2^{l+3} \right\} \\
&= \left\{ \xi : \frac{3}{4} 2^{l+2} \leq |\xi| \leq \frac{8}{3} 2^{l+2} \right\}
\end{aligned}$$

the last equality is because $j = l+2, l+3, \dots$. Furthermore,

$$\begin{aligned}
& \text{supp} \left(\bar{\Delta}_l S_{j-2} u_k \sum_{|l-l'|\leq 2} \bar{\Delta}_{l'} \partial_k v \right)^\wedge \\
&= \text{supp} \left(\varphi_l \psi_{j-2} \hat{u}_k * \sum_{|l-l'|\leq 2} (\bar{\Delta}_{l'} \partial_k v)^\wedge \right) \\
&\subset \text{supp}(\varphi_l \psi_{j-2}) + \text{supp} \sum_{|l-l'|\leq 2} \varphi_{l'} (\partial_k v)^\wedge \\
&\subset \text{supp}(\varphi_l) \cap \text{supp}(\psi_{j-2}) + \text{supp} \sum_{|l-l'|\leq 2} \varphi_{l'} \\
&\subset \left\{ \xi : \frac{3}{4} 2^l \leq |\xi| \leq \frac{8}{3} 2^l \right\} \cap \left\{ \xi : |\xi| \leq \frac{4}{3} 2^{j-2} \right\} + \left\{ \xi : \frac{3}{4} 2^{l-2} \leq |\xi| \leq \frac{8}{3} 2^{l+2} \right\} \\
&\subset \left\{ \xi : \frac{3}{4} 2^l \leq |\xi| \leq \frac{8}{3} 2^l \right\} + \left\{ \xi : \frac{3}{4} 2^{l-2} \leq |\xi| \leq \frac{8}{3} 2^{l+2} \right\} \\
&\subset \left\{ \xi : \frac{3}{4} 2^{l+2} \leq |\xi| \leq \frac{8}{3} 2^{l+3} \right\}.
\end{aligned}$$

On the other hand,

$$\begin{aligned}
& \text{supp} \left\{ \bar{\Delta}_l S_{j-2} u_k \cdot \bar{\Delta}_j \sum_{|l-l'|\leq 2} \bar{\Delta}_{l'} \partial_k v \right\}^\wedge \\
&= \text{supp} \left\{ (\bar{\Delta}_l S_{j-2} u_k)^\wedge * \left(\bar{\Delta}_j \sum_{|l-l'|\leq 2} \bar{\Delta}_{l'} \partial_k v \right)^\wedge \right\} \\
&\subset \text{supp}(\varphi_l \psi_{j-2} \hat{u}_k) + \text{supp} \sum_{|l-l'|\leq 1} \varphi_j \varphi_{l'} (\partial_k v)^\wedge \\
&= \text{supp}(\varphi_l) \cap \text{supp}(\psi_{j-2}) + \text{supp} \sum_{|l-l'|\leq 1} \varphi_j \varphi_{l'} (\partial_k v)^\wedge \\
&\subset \left\{ \xi : \frac{3}{4} 2^l \leq |\xi| \leq \frac{8}{3} 2^l \right\} + \left\{ \xi : \frac{3}{4} 2^{l-1} \leq |\xi| \leq \frac{8}{3} 2^{l+1} \right\} \\
&\subset \left\{ \xi : \frac{3}{4} 2^l \leq |\xi| \leq \frac{8}{3} 2^{l+2} \right\}.
\end{aligned}$$

So,

$$\begin{aligned}
R_j^{4,2}(u, v) &= \sum_{k=1}^n \sum_{j>l+1} [\bar{\Delta}_j, \bar{\Delta}_l S_{j-2} u_k] \left(\sum_{|l-l'|\leq 2} \bar{\Delta}_{l'} \partial_k v \right) \\
&:= B.
\end{aligned}$$

Thus, rewriting the B in terms of their kernels, we get, by using the integration of the parts, together with the fact that u is free divergence

$$\begin{aligned}
B &= 2^{jn} \int \check{\varphi}(2^j(x-y)) \bar{\Delta}_l S_{j-2} u_k(y) \partial_k \sum_{|l-l'|\leq 2} \bar{\Delta}_{l'} v(y) dy \\
&\quad - \bar{\Delta}_l S_{j-2} u_k(\cdot) 2^{jn} \int \check{\varphi}(2^j(x-y)) \cdot \partial_k \sum_{|l-l'|\leq 2} \bar{\Delta}_{l'} v(y) dy \\
&= 2^{jn} \int \{ \check{\varphi}(2^j(x-y)) (\bar{\Delta}_l S_{j-2} u_k(y) - \bar{\Delta}_l S_{j-2} u_k(x)) \} \partial_k \sum_{|l-l'|\leq 2} \bar{\Delta}_{l'} v(y) dy \\
&= -2^{j(n+1)} \int \partial_k \check{\varphi}(2^j(x-y)) \{ \bar{\Delta}_l S_{j-2} u_k(y) - \bar{\Delta}_l S_{j-2} u_k(x) \} \sum_{|l-l'|\leq 2} \bar{\Delta}_{l'} v(y) dy \\
&= -2^{j(n+1)} \int \partial_k \check{\varphi}(2^j(x-y)) \left\{ \int_0^1 \sum_{m=1}^n \bar{\Delta}_l S_{j-2} \partial_m u_k(x + \tau(y-x)) (y_m - x_m) d\tau \right\} \times \\
&\quad \sum_{|l-l'|\leq 2} \bar{\Delta}_{l'} v(y) dy \\
&= -2^{j(n+1)} \int \partial_k \check{\varphi}(2^j(x-y)) \left\{ \sum_{m=1}^n \int_0^1 \bar{\Delta}_l S_{j-2} \partial_m u_k(x + \tau(y-x)) (y_m - x_m) d\tau \right\} \times \\
&\quad \sum_{|l-l'|\leq 2} \bar{\Delta}_{l'} v(y) dy \\
&= - \sum_{m=1}^n \int \partial_k \check{\varphi}(z) z_m \left\{ \int_0^1 \bar{\Delta}_l S_{j-2} \partial_m u_k(x - 2^{-j} z \tau) d\tau \right\} \sum_{|l-l'|\leq 2} \bar{\Delta}_{l'} v(x - 2^{-j} z) dz
\end{aligned}$$

in the last equality, we used the variables change with $z = 2^j(x - y)$.

Now, by taking the norm and using Hölder's inequality for modified weak-Morrey spaces in $R_j^4(u, v)$, we arrive at

$$\begin{aligned}
\|R_j^{4,2}(u, v)\|_{W\tilde{\mathcal{M}}_p^l} &\leq \sum_{k,m=1}^n \sum_{j>l+1} \int \|\partial_k \check{\varphi}(z) z_m\|_{L^\infty} \int_0^1 \|\bar{\Delta}_l S_{j-2} \partial_m u_k(x - 2^{-j}z)\|_{L^\infty} \tau d\tau \times \\
&\quad \left\| \sum_{|l-l'|\leq 2} \bar{\Delta}_{l'} v(x - 2^{-j}z) \right\|_{W\tilde{\mathcal{M}}_p^l} dz \\
&\leq C \sum_{k,m=1}^n \sum_{j>l+1} \int \int_0^1 \|\bar{\Delta}_l S_{j-2} \partial_m u_k\|_{L^\infty} \tau d\tau \left\| \sum_{|l-l'|\leq 2} \bar{\Delta}_{l'} v(x - 2^{-j}z) \right\|_{W\tilde{\mathcal{M}}_p^l} dz \\
&\leq C \sum_{k,m=1}^n \sum_{j>l+1} \|\bar{\Delta}_l S_{j-2} \partial_m u_k\|_{L^\infty} \left\| \sum_{|l-l'|\leq 2} \bar{\Delta}_{l'} v \right\|_{W\tilde{\mathcal{M}}_p^l}.
\end{aligned}$$

Lemma 6. (Commutator estimates) *Let $1 < p < \infty$, $1 \leq l, r \leq \infty$, $p \leq l$ and let $\nabla \cdot u = 0$.*

1. *Assume that $\rho > 0$. Then, there exists a universal constant $C > 0$ such that*

$$\left\| 2^{j\rho} \|R_j(u, v)\|_{W\tilde{\mathcal{M}}_p^l} \right\|_{l^r} \leq C \left(\|\nabla u\|_{L^\infty} \|v\|_{BW\tilde{\mathcal{M}}_{p,r}^{l,\rho}} + \|\nabla v\|_{L^\infty} \|u\|_{BW\tilde{\mathcal{M}}_{p,r}^{l,\rho}} \right) \quad (4.8)$$

where we consider the usual modification for $r = \infty$.

2. *Assume that $s \geq \frac{n}{p} + 1$ and that $r = 1$ in the case $s = \frac{n}{p} + 1$. Then, there exists a universal constant $C > 0$ such that*

$$\left\| 2^{js} \|R_j(u, v)\|_{W\tilde{\mathcal{M}}_p^l} \right\|_{l^r} \leq C \|u\|_{BW\tilde{\mathcal{M}}_{p,r}^{l,s}} \|v\|_{BM\tilde{\mathcal{M}}_{p,r}^{l,s}} \quad (4.9)$$

$$\left\| 2^{j(s-1)} \|R_j(u, v)\|_{W\tilde{\mathcal{M}}_p^l} \right\|_{l^r} \leq C \|u\|_{BW\tilde{\mathcal{M}}_{p,r}^{l,s-1}} \|v\|_{BM\tilde{\mathcal{M}}_{p,r}^{l,s}} \quad (4.10)$$

$$\left\| 2^{j(s-1)} \|R_j(u, v)\|_{W\tilde{\mathcal{M}}_p^l} \right\|_{l^r} \leq \|u\|_{BW\tilde{\mathcal{M}}_{p,r}^{l,s}} \|v\|_{BM\tilde{\mathcal{M}}_{p,r}^{l,s-1}} \quad (4.11)$$

where we consider the usual modification for $r = \infty$.

Lemma 7 (Product estimates). *Let $1 < p \leq l \leq \infty$, $1 \leq r \leq \infty$ and $\rho > 0$. Then,*

$$\|uv\|_{BW\tilde{\mathcal{M}}_{p,r}^{l,\rho}} \leq C (\|u\|_{L^\infty} \|v\|_{BW\tilde{\mathcal{M}}_{p,r}^{l,\rho}} + \|u\|_{BW\tilde{\mathcal{M}}_{p,r}^{l,\rho}} \|v\|_{L^\infty}), \quad (4.12)$$

for all $u, v \in BW\tilde{\mathcal{M}}_{p,r}^{l,\rho} \cap L^\infty$. Moreover, considering $p < \infty$ and assuming either $s > n/p + 1$ with $1 \leq r \leq \infty$ or $s = n/p + 1$ with $r = 1$, we have that

$$\|u \cdot \nabla v\|_{BW\tilde{\mathcal{M}}_{p,r}^{l,s-1}} \leq C \|u\|_{BW\tilde{\mathcal{M}}_{p,r}^{l,s-1}} \|v\|_{BW\tilde{\mathcal{M}}_{p,r}^{l,s}}, \quad (4.13)$$

for all $u \in BW\tilde{\mathcal{M}}_{p,r}^{l,s-1}$ and $v \in BW\tilde{\mathcal{M}}_{p,r}^{l,s}$.

Proof. Proof of inequality (4.12) is given in [42]. We will prove inequality (4.13). From inequality (4.12) and the homogeneous Littlewood-Paley decomposition of u and ∇v , we have

$$\begin{aligned}
\|u \cdot \nabla v\|_{BW\tilde{\mathcal{M}}_{p,r}^{l,s-1}} &\leq C(\|u\|_{L^\infty}\|\nabla v\|_{BW\tilde{\mathcal{M}}_{p,r}^{l,s-1}} + \|u\|_{BW\tilde{\mathcal{M}}_{p,r}^{l,s-1}}\|\nabla v\|_{L^\infty}) \\
&= C\left(\left\|\sum_{j \geq -1} \bar{\Delta}_j u\right\|_{L^\infty} \|\nabla v\|_{BW\tilde{\mathcal{M}}_{p,r}^{l,s-1}} + \|u\|_{BW\tilde{\mathcal{M}}_{p,r}^{l,s-1}} \left\|\sum_{j \geq -1} \bar{\Delta}_j \nabla v\right\|_{L^\infty}\right) \\
&\leq C(\|\nabla v\|_{BW\tilde{\mathcal{M}}_{p,r}^{l,s-1}} \sum_{j \geq -1} \|\bar{\Delta}_j u\|_{L^\infty} + \|u\|_{BW\tilde{\mathcal{M}}_{p,r}^{l,s-1}} \sum_{j \geq -1} \|\bar{\Delta}_j \nabla v\|_{L^\infty}) \\
&\leq C(\|\nabla v\|_{BW\tilde{\mathcal{M}}_{p,r}^{l,s-1}} \sum_{j \geq -1} C2^{j\frac{n}{p}} \|\bar{\Delta}_j u\|_{W\tilde{\mathcal{M}}_p^l} \\
&\quad + \|u\|_{BW\tilde{\mathcal{M}}_{p,r}^{l,s-1}} \sum_{j \geq -1} C2^{j\frac{n}{p}} \|\bar{\Delta}_j \nabla v\|_{W\tilde{\mathcal{M}}_p^l}),
\end{aligned}$$

in the last inequality, we have used inequality (2.7). Now, by using Holder inequality for sequences, it follows that

$$\begin{aligned}
\|u \cdot \nabla v\|_{BW\tilde{\mathcal{M}}_{p,r}^{l,s-1}} &\leq C\left(\|\nabla v\|_{BW\tilde{\mathcal{M}}_{p,r}^{l,s-1}}\|u\|_{BW\tilde{\mathcal{M}}_{p,r}^{l,s-1}} + \|u\|_{BW\tilde{\mathcal{M}}_{p,r}^{l,s-1}}\|\nabla v\|_{BW\tilde{\mathcal{M}}_{p,r}^{l,s-1}}\right) \\
&\leq C\|u\|_{BW\tilde{\mathcal{M}}_{p,r}^{l,s-1}}\|v\|_{BW\tilde{\mathcal{M}}_{p,r}^{l,s}},
\end{aligned}$$

in the cases asserted above. The last estimate follows from the Bernstein inequality (2.6). \square

4.2 On the Well-Posedness of the SQG in the Modified Besov-Morrey Spaces

In this section, we present our research's other fundamental theoretical result, which is the well-posedness of the SQG in modified Besov-weak-Morrey. Theorem 3 guarantees the existence, uniqueness, and continuous dependence of the solution of the SQG equation in this space.

We start with a generic result that will be useful in the rest of this section.

Lemma 8. *Let us consider $1 < p \leq l \leq \infty$ and $u = u(x, t)$ for $(x, t) \in \mathbb{R}^n \times [0, \infty)$. Assume that $u_0 = u(x, 0) \in W\tilde{\mathcal{M}}_p^l$ and*

$$\begin{cases} \partial_t u + v \cdot \nabla u = g(v, u) \\ v = \mathcal{R}^\perp u \end{cases} \quad (4.14)$$

where, $\mathcal{R}^\perp u = (-\mathcal{R}_2 u, \mathcal{R}_1 u)$ and $\nabla \cdot v = 0$. Then there is $C > 0$ such that

$$\begin{aligned}
\|u(t)\|_{BW\tilde{\mathcal{M}}_{p,r}^{l,s}} &\leq C\|u_0\|_{BW\tilde{\mathcal{M}}_{p,r}^{l,s}} \\
&\quad + C \int_0^t \left(\|v(\tau)\|_{BW\tilde{\mathcal{M}}_{p,r}^{l,s}} \|u(\tau)\|_{BW\tilde{\mathcal{M}}_{p,r}^{l,s}} + \|g(v, u)(\tau)\|_{BW\tilde{\mathcal{M}}_{p,r}^{l,s}} \right) d\tau. \quad (4.15)
\end{aligned}$$

Proof. Applying the operator $\bar{\Delta}_j$ in the first equation of (4.14), adding and subtracting the term $S_{j-2}v \cdot \nabla \bar{\Delta}_j u$, we obtain

$$\frac{\partial}{\partial t} \bar{\Delta}_j u + S_{j-2}v \cdot \nabla \bar{\Delta}_j u = -R_j(v, u) + \bar{\Delta}_j g(v, u).$$

Since $\nabla \cdot v = 0$, we immediately conclude that $\nabla \cdot \bar{\Delta}_j v = 0$, leading the system:

$$\begin{cases} \frac{\partial}{\partial t} \bar{\Delta}_j u + S_{j-2}v \cdot \nabla \bar{\Delta}_j u = -R_j(v, u) + \bar{\Delta}_j g(v, u) \\ \nabla \cdot \bar{\Delta}_j v = 0. \end{cases} \quad (4.16)$$

Let us consider the flow $X_j : \mathbb{R}^n \times [0, \infty) \longrightarrow \mathbb{R}^n$ associated with the initial value problem

$$\begin{cases} \frac{d}{dt} X_j(x_0, t) = S_{j-2}v(X_j(x_0, t), t) \\ X_j(x_0, 0) = x_0 \end{cases} \quad (4.17)$$

From chain rule, and considering (4.17) and (4.16), we have

$$\begin{aligned} \frac{d}{dt} \bar{\Delta}_j u(X_j(x_0, t), t) &= \nabla \bar{\Delta}_j u \cdot S_{j-2}v - S_{j-2}v \cdot \nabla \bar{\Delta}_j u - R_j(v, u) + \bar{\Delta}_j g(v, u) \\ &= -R_j(v, u)(X_j(x_0, t), t) + \bar{\Delta}_j g(v, u)(X_j(x_0, t), t). \end{aligned}$$

Integrating from 0 to t and applying the norm $\|\cdot\|_{W\tilde{\mathcal{M}}_p^l}$, we obtain the estimate

$$\begin{aligned} \|\bar{\Delta}_j u(X_j(x_0, t), t)\|_{W\tilde{\mathcal{M}}_p^l} &\leq \|\bar{\Delta}_j u(X_j(x_0, 0), 0)\|_{W\tilde{\mathcal{M}}_p^l} + \int_0^t (\|R_j(v, u)(X_j(x_0, \tau), \tau)\|_{W\tilde{\mathcal{M}}_p^l} \\ &\quad + \|\bar{\Delta}_j g(v, u)(X_j(x_0, \tau), \tau)\|_{W\tilde{\mathcal{M}}_p^l}) d\tau. \end{aligned} \quad (4.18)$$

Since $\nabla \cdot S_{j-2}v = 0$, we know that $X_j(\cdot, t)$ is a volume-preserving diffeomorphism for each $t \geq 0$ with Lipschitz constant $\gamma \geq 1$. From Lemma 4, there exists a positive constant $C_1 = C_1(n, p, l, \gamma)$ and $C_2 = C_2(n, p, l, \gamma)$ such that

$$\begin{aligned} \|\bar{\Delta}_j u(t)\|_{W\tilde{\mathcal{M}}_p^l} &\leq C_1 \|\bar{\Delta}_j u(X_j(x_0, t), t)\|_{W\tilde{\mathcal{M}}_p^l} \leq C_1^2 \|\bar{\Delta}_j u(t)\|_{W\tilde{\mathcal{M}}_p^l} \\ C_2^{-1} \|\bar{\Delta}_j g(v, u)(\tau)\|_{W\tilde{\mathcal{M}}_p^l} &\leq \|\bar{\Delta}_j g(v, u)(X_j(x_0, \tau), \tau)\|_{W\tilde{\mathcal{M}}_p^l} \leq C_2 \|\bar{\Delta}_j g(v, u)(\tau)\|_{W\tilde{\mathcal{M}}_p^l}. \end{aligned}$$

Then, multiplying by C_1 in (4.18) and using the last result, we obtain

$$\begin{aligned} \|\bar{\Delta}_j u(t)\|_{W\tilde{\mathcal{M}}_p^l} &\leq C_1^2 \|\bar{\Delta}_j u_0\|_{W\tilde{\mathcal{M}}_p^l} + C_1 \int_0^t (\|R_j(v, u)(X_j(x_0, \tau), \tau)\|_{W\tilde{\mathcal{M}}_p^l} \\ &\quad + C_2 \|\bar{\Delta}_j g(v, u)(\tau)\|_{W\tilde{\mathcal{M}}_p^l}) d\tau \end{aligned}$$

So, we multiply by 2^{js} on both sides of the inequality, and on the right side way, apply the sequence norm l^r (recall that $\bar{\Delta}_j = 0$ for all $j \leq -2$), from Lemma 6 and again by Lemma 4, we get

$$\begin{aligned}
\|u(t)\|_{BW\tilde{\mathcal{M}}_{p,r}^{l,s}} &\leq C_1^2 \|u_0\|_{BW\tilde{\mathcal{M}}_{p,r}^{l,s}} + C_1 \int_0^t \left(\|2^{js} R_j(v, u)(X_j(x_0, \tau), \tau)\|_{W\tilde{\mathcal{M}}_p^l} \right)_{\ell^r} \\
&\quad + C_2 \|g(v, u)(\tau)\|_{BW\tilde{\mathcal{M}}_{p,r}^{l,s}} d\tau \\
&\leq C \|u_0\|_{BW\tilde{\mathcal{M}}_{p,r}^{l,s}} + C \int_0^t (\|v(X_j(x_0, \tau), \tau)\|_{BW\tilde{\mathcal{M}}_{p,r}^{l,s}} \|u(X_j(x_0, \tau), \tau)\|_{BW\tilde{\mathcal{M}}_{p,r}^{l,s}} \\
&\quad + \|g(v, u)(\tau)\|_{BW\tilde{\mathcal{M}}_{p,r}^{l,s}}) d\tau \\
&\leq C \|u_0\|_{BW\tilde{\mathcal{M}}_{p,r}^{l,s}} + C \int_0^t \left(\|v(\tau)\|_{BW\tilde{\mathcal{M}}_{p,r}^{l,s}} \|u(\tau)\|_{BW\tilde{\mathcal{M}}_{p,r}^{l,s}} + \|g(v, u)(\tau)\|_{BW\tilde{\mathcal{M}}_{p,r}^{l,s}} \right) d\tau
\end{aligned}$$

□

Now, we define the sequence $(\theta^m)_{m \geq 1}$ as the solution of the following iterative scheme

$$\begin{cases} \frac{\partial}{\partial t} \theta^{(m+1)} + v^{(m)} \cdot \nabla \theta^{(m+1)} = 0 \\ v^{(m)} = \mathcal{R}^\perp \theta^{(m)} \\ \theta^{(m+1)}(x, 0) = S_{(m+1)} \theta_0, \end{cases} \quad (4.19)$$

with $\theta^{(1)} = S_1 \theta_0$. The following lemma guarantees that the sequence $(\theta^m)_{m \geq 0}$ is bounded in the Besov-modified-weak Morrey framework.

Lemma 9. *There are $T > 0$ and a constant $C > 0$ such that*

$$\|\theta^{(m)}\|_{L_T^\infty(BW\tilde{\mathcal{M}}_{p,r}^{l,s})} \leq C, \quad \text{for all } m \geq 1.$$

Proof. Notice that, system (4.19) is a particular case of Lemma 8 with $u = \theta^{(m+1)}$, $v = v^{(m)}$ and $g = 0$. Then, it follows that

$$\|\theta^{(m+1)}(t)\|_{BW\tilde{\mathcal{M}}_{p,r}^{l,s}} \leq C_0 \|\theta_0\|_{BW\tilde{\mathcal{M}}_{p,r}^{l,s}} + C \|v^{(m)}\|_{L_T^\infty(BW\tilde{\mathcal{M}}_{p,r}^{l,s})} \int_0^t \|\theta^{(m+1)}(\tau)\|_{BW\tilde{\mathcal{M}}_{p,r}^{l,s}} d\tau.$$

By applying Gronwall's inequality (integral version), we have

$$\|\theta^{(m+1)}(t)\|_{BW\tilde{\mathcal{M}}_{p,r}^{l,s}} \leq C \|\theta_0\|_{BW\tilde{\mathcal{M}}_{p,r}^{l,s}} \exp \left(C \|v^{(m)}\|_{L_T^\infty(BW\tilde{\mathcal{M}}_{p,r}^{l,s})} T \right) \quad (4.20)$$

where $0 < t < T$. Notice that so far (4.20) was obtained from the application of the Lemma 4, which in this case can only be used if X_j^m for all m is the volume-preserving diffeomorphism associated and Lipschitz continuous function with the constant of Lipschitz $\gamma \geq 1$ (see the proof of Lemma 8). To prove the general case, first note that $S_{j-2}v^m$ is a Lipschitz vector field provided that $\nabla v^m \in L_T^\infty(L^\infty(\mathbb{R}^n))$ and taking L' as the Lipschitz constant of $S_{j-2}v^m$, we have that, in general, the function $(X_j^m)^\pm$ is Lipschitz continuous on the second variable, this will be shown with the help of the following affirmation.

Claim 4.2.1. $\|\nabla S_{j-2}v^m\|_{L_T^\infty} \leq C\|\nabla v^m\|_{BW\tilde{\mathcal{M}}_{p,r}^{l,s-1}}$, where $L_T^\infty := L_T^\infty(L^\infty(\mathbb{R}^n))$

In fact, from the homogeneous Littlewood-Paley decomposition, Young's inequality and Lemma 3, equation (2.7), we get

$$\begin{aligned} \|\nabla S_{j-2}v^m\|_{L_T^\infty} &\leq \sum_{j \geq -1} \|S_{j-2}(\bar{\Delta}_j \nabla v^m)\|_{L_T^\infty} \\ &\leq \sum_{j \geq -1} C \|\bar{\Delta}_j \nabla v^m\|_{L_T^\infty} \\ &\leq C \sum_{j \geq -1} 2^{j\frac{n}{p}} \|\bar{\Delta}_j \nabla v^m\|_{W\tilde{\mathcal{M}}_p^l} \end{aligned} \quad (4.21)$$

and by hypothesis, we have the following cases:

1. If $r = 1$ then $s = \frac{n}{p} + 1$, that is, $s - 1 = \frac{n}{p}$. Hence, we have

$$\begin{aligned} C \sum_{j \geq -1} 2^{j\frac{n}{p}} \|\bar{\Delta}_j \nabla v^m\|_{W\tilde{\mathcal{M}}_p^l} &= C \sum_{j \geq -1} 2^{j(s-1)} \|\bar{\Delta}_j \nabla v^m\|_{W\tilde{\mathcal{M}}_p^l} \\ &= C \|\nabla v^m\|_{BW\tilde{\mathcal{M}}_{p,r}^{l,s-1}}. \end{aligned}$$

2. If $r > 1$, then $s \geq \frac{n}{p} + 1$, that is, $\frac{n}{p} - s + 1 \leq 0$. Hence, from Hölder's inequality

$$\begin{aligned} \sum_{j \geq -1} 2^{j\frac{n}{p}} \|\bar{\Delta}_j \nabla v^m\|_{W\tilde{\mathcal{M}}_p^l} &\leq \left| \sum_{j \geq -1} 2^{j(\frac{n}{p}-s+1)} 2^{j(s-1)} \|\bar{\Delta}_j \nabla v^m\|_{W\tilde{\mathcal{M}}_p^l} \right| \\ &\leq \left(\sum_{j \geq -1} |2^{j(\frac{n}{p}-s+1)}|^{\frac{r}{r-1}} \right)^{\frac{r-1}{r}} \left(\sum_{j \geq -1} |2^{j(s-1)} \|\bar{\Delta}_j \nabla v^m\|_{W\tilde{\mathcal{M}}_p^l}|^r \right)^{\frac{1}{r}} \\ &\leq C \|\nabla v^m\|_{BW\tilde{\mathcal{M}}_{p,r}^{l,s-1}}. \end{aligned}$$

Hence, from (2.13), Claim 4.2.1 and Young's inequality, we have

$$\begin{aligned} |(X_j^m)^{\pm 1}(x_0, t) - (X_j^m)^{\pm 1}(y_0, t)| &\leq e \int_0^t L' d\tau |x_0 - y_0| \\ &\leq e \int_0^t \|\nabla S_{j-2}v^m\|_{L_T^\infty(L^\infty(\mathbb{R}^2))} d\tau |x_0 - y_0| \\ &\leq e^{T\|S_{j-2}\nabla v^m\|_{L_T^\infty(BW\tilde{\mathcal{M}}_{p,r}^{l,s-1})}} |x_0 - y_0| \\ &\leq e^{TC\|\nabla v^m\|_{L_T^\infty(BW\tilde{\mathcal{M}}_{p,r}^{l,s-1})}} |x_0 - y_0| \\ &\leq e^{CT\|v^m\|_{L_T^\infty(BW\tilde{\mathcal{M}}_{p,r}^{l,s})}} |x_0 - y_0| \end{aligned}$$

that is, for $0 \leq t \leq T$, we have

$$|(X_j^m)^{\pm 1}(x_0, t) - (X_j^m)^{\pm 1}(y_0, t)| \leq e^{CT\|v^m\|_{L_T^\infty(BW\tilde{\mathcal{M}}_{p,r}^{l,s})}} |x_0 - y_0|. \quad (4.22)$$

Now, we show that for a $T = T_2$ the sequence (θ^m) is bounded in the space $L_{T_2}^\infty(BW\tilde{\mathcal{M}}_{p,r}^{l,s})$.

So, from Young's inequality and choosing a suitable L for our θ_0 , we get

$$\begin{aligned} \|\theta^1(t)\|_{BW\tilde{\mathcal{M}}_{p,r}^{l,s}} &= \|S_1\theta_0\|_{BW\tilde{\mathcal{M}}_{p,r}^{l,s}} \\ &\leq L\|\theta_0\|_{BW\tilde{\mathcal{M}}_{p,r}^{l,s}} \end{aligned} \quad (4.23)$$

Claim 4.2.2. $\|v^m\|_{L_{T_2}^\infty(BW\tilde{\mathcal{M}}_{p,r}^{l,s})} \leq \|\mathcal{R}^\perp\| \|\theta^m\|_{L_{T_2}^\infty(BW\tilde{\mathcal{M}}_{p,r}^{l,s})}$, where $\|\mathcal{R}^\perp\| = \max\{\|\mathcal{R}_1\|, \|\mathcal{R}_2\|\}$

In fact, as $\bar{\Delta}_{-1}f = \mathcal{F}^{-1}(\psi\hat{f})$, $\bar{\Delta}_j = \mathcal{F}^{-1}(\varphi_j\hat{f}) \quad \forall j \geq 0$ and $\mathcal{R}_l\theta = \mathcal{F}^{-1}\left(\frac{i\xi_l}{|\xi|}\hat{\theta}\right)$, then follows that

$$\bar{\Delta}_j\mathcal{R}^\perp\theta^m = \mathcal{R}^\perp\bar{\Delta}_j\theta^m.$$

On the other hand, in [42], it was shown that the Riesz transform is bounded in the framework of modified Morrey spaces $W\tilde{\mathcal{M}}_p^l$ (see Lemma 2.3); with this fact, we show that the sequence of variables (θ^m) limits the sequence of the speed field (v^m) in the framework of modified Besov-weak-Morrey spaces $BW\tilde{\mathcal{M}}_{p,r}^{l,s}$

$$\begin{aligned} \|v^m\|_{BW\tilde{\mathcal{M}}_{p,r}^{l,s}} &= \|\mathcal{R}^\perp\theta^m\|_{BW\tilde{\mathcal{M}}_{p,r}^{l,s}} \\ &= \left\| 2^{js} \|\bar{\Delta}_j\mathcal{R}^\perp\theta^m\|_{W\tilde{\mathcal{M}}_p^l} \right\|_{l^r} \\ &= \left\| 2^{js} \|\mathcal{R}^\perp\bar{\Delta}_j\theta^m\|_{W\tilde{\mathcal{M}}_p^l} \right\|_{l^r} \\ &\leq \left\| \|\mathcal{R}^\perp\| 2^{js} \|\bar{\Delta}_j\theta^m\|_{W\tilde{\mathcal{M}}_p^l} \right\|_{l^r} \\ &= \|\mathcal{R}^\perp\| \|\theta^m\|_{BW\tilde{\mathcal{M}}_{p,r}^{l,s}}. \end{aligned}$$

Let $\tilde{C} > 0$, $T_2 > 0$ and γ such that

$$L\|\theta_0\|_{BW\tilde{\mathcal{M}}_{p,r}^{l,s}} \leq \frac{\tilde{C}}{2\|\mathcal{R}^\perp\|} \quad (4.24)$$

$$\frac{\tilde{C}}{2\|\mathcal{R}^\perp\|} \exp\{L\tilde{C}T_2\} \leq \tilde{C} \quad (4.25)$$

$$\exp\{CT_2\tilde{C}\} \leq \gamma \quad (4.26)$$

Claim 4.2.3. For $T = T_2$ and $m \geq 1$ we have $\|\theta^m\|_{L_{T_2}^\infty(BW\tilde{\mathcal{M}}_{p,r}^{l,s})} \leq \frac{\tilde{C}}{\|\mathcal{R}^\perp\|}$.

In fact, for $m = 1$ de (4.23) and (4.24), we have

$$\begin{aligned} \|\theta^1(t)\|_{BW\tilde{\mathcal{M}}_{p,r}^{l,s}} &\leq L\|\theta_0\|_{BW\tilde{\mathcal{M}}_{p,r}^{l,s}} \\ &\leq \frac{\tilde{C}}{2\|\mathcal{R}^\perp\|} \\ &\leq \frac{\tilde{C}}{\|\mathcal{R}^\perp\|}. \end{aligned}$$

Assuming it holds for m , we now show that it holds for $m+1$. So, from equation (4.22) and (4.26),

$$\begin{aligned}
\left| (X_j^m)^{\pm 1}(x_0, t) - (X_j^m)^{\pm 1}(y_0, t) \right| &\leq e^{CT_2 \|v^m\|_{L_{T_2}^\infty(BW\tilde{\mathcal{M}}_{p,r}^{l,s})}} |x_0 - y_0| \\
&\leq e^{CT_2 \|\mathcal{R}^\perp\| \|\theta^m\|_{L_{T_2}^\infty(BW\tilde{\mathcal{M}}_{p,r}^{l,s})}} |x_0 - y_0| \\
&\leq e^{CT_2 \|\mathcal{R}^\perp\| \frac{\tilde{C}}{\|\mathcal{R}^\perp\|}} |x_0 - y_0| \\
&\leq \gamma |x_0 - y_0|
\end{aligned}$$

for $j \geq -1$ e $t \in [0, T_2]$. Hence (4.20) is true, from the Claim 4.2.2 and (4.25), we have

$$\begin{aligned}
\|\theta^{m+1}(t)\|_{BW\tilde{\mathcal{M}}_{p,r}^{l,s}} &\leq L \|\theta_0\|_{BW\tilde{\mathcal{M}}_{p,r}^{l,s}} \exp \left\{ L \|v^m\|_{L_{T_2}^\infty(BW\tilde{\mathcal{M}}_{p,r}^{l,s})} T_2 \right\} \\
&\leq L \|\theta_0\|_{BW\tilde{\mathcal{M}}_{p,r}^{l,s}} \exp \left\{ L \|\mathcal{R}\| \|\theta^m\|_{L_{T_2}^\infty(BW\tilde{\mathcal{M}}_{p,r}^{l,s})} T_2 \right\} \\
&\leq \frac{\tilde{C}}{2\|\mathcal{R}^\perp\|} \exp \left\{ L \|\mathcal{R}^\perp\| \frac{\tilde{C}}{\|\mathcal{R}^\perp\|} T_2 \right\} \leq \tilde{C}.
\end{aligned}$$

□

Theorem 3. Let $1 < p < \infty$, $1 < l \leq \infty$ and $p \leq l$. Assume either $s > \frac{n}{p} + 1$ with $1 \leq r \leq \infty$ or $s = \frac{n}{p} + 1$ with $r = 1$.

1. (Existence and uniqueness) For $\theta_0 \in BW\tilde{\mathcal{M}}_{p,r}^{l,s}$ there exists an existence-time $T > 0$ such that IVP (4.1) has a unique solution

$$\theta \in L^\infty((0, T); BW\tilde{\mathcal{M}}_{p,r}^{l,s}) \cap C([0, T]; BW\tilde{\mathcal{M}}_{p,r}^{l,s-1}).$$

Moreover, $\theta \in C([0, T]; BW\tilde{\mathcal{M}}_{p,r}^{l,s})$ provided that $r < \infty$.

Proof. On the other hand, from (2.9) and (2.6) of Lemma 3 and Young's inequality, we get

$$\begin{aligned}
\|\bar{\Delta}_j \bar{\Delta}_{m+1} \theta_0\|_{W\tilde{\mathcal{M}}_p^l} &\leq C 2^{-(m+1)} \|D \bar{\Delta}_{m+1} \bar{\Delta}_j \theta_0\|_{W\tilde{\mathcal{M}}_p^l} \\
&\leq C 2^{-(m+1)} 2^j \|\bar{\Delta}_j \bar{\Delta}_{m+1} \theta_0\|_{W\tilde{\mathcal{M}}_p^l} \\
&\leq C 2^{j-(m+1)} \|\bar{\Delta}_j \theta_0\|_{W\tilde{\mathcal{M}}_p^l}
\end{aligned}$$

then,

$$\begin{aligned}
\|\bar{\Delta}_{m+1} \theta_0\|_{BW\tilde{\mathcal{M}}_{p,r}^{l,s-1}} &= \left\| 2^{j(s-1)} \|\bar{\Delta}_j \bar{\Delta}_{m+1} \theta_0\|_{W\tilde{\mathcal{M}}_p^l} \right\|_{l^r} \\
&\leq \left\| 2^{j(s-1)} C 2^{(j-m-1)} \|\bar{\Delta}_j \theta_0\|_{W\tilde{\mathcal{M}}_p^l} \right\|_{l^r} \\
&\leq C 2^{-(m+1)} \left\| 2^{js} \|\bar{\Delta}_j \theta_0\|_{W\tilde{\mathcal{M}}_p^l} \right\|_{l^r} \\
&\leq C 2^{-m} \|\theta_0\|_{BW\tilde{\mathcal{M}}_{p,r}^{l,s}}.
\end{aligned}$$

Claim 4.2.4. *The sequence (θ^m) is Cauchy in the space $L_{T_3}^\infty(BW\tilde{\mathcal{M}}_{p,r}^{l,s})$, for some $T_3 \in (0, T_2]$.*

In fact, for any $m \geq 2$, subtracting (4.19)_m and (4.19)_{m+1}, and adding in both sides of the term $v^m \cdot \nabla \theta^m$, we have

$$\begin{cases} \frac{\partial}{\partial t}(\theta^{m+1} - \theta^m) + v^m \cdot \nabla(\theta^{m+1} - \theta^m) = (v^{m-1} - v^m) \cdot \nabla \theta^m \\ \nabla \cdot (v^m - v^{m-1}) = \mathcal{R}^\perp(\theta^m - \theta^{m-1}) \\ \theta_0^{m+1} - \theta_0^m := (S_{m+1} - S_m)\theta_0 \end{cases} \quad (4.27)$$

Notice that system (4.27) is a particular case of Lemma 8 with $u = \theta^{m+1} - \theta^m$, $v = v^m$ and $g = (v^{m-1} - v^m) \cdot \nabla \theta^m$. For simplicity of notation, we write $z^{m+1} = \theta^{m+1} - \theta^m$ and $w^m = v^m - v^{m-1}$. So, we get from the Lemma 7 (equation (4.13))

$$\begin{aligned} C \|z^{m+1}(t)\|_{BW\mathcal{M}_{p,r}^{l,s-1}} &\leq C_0 \|\bar{\Delta}_{m+1}\theta_0\|_{BW\mathcal{M}_{p,r}^{l,s-1}} + C_3 \int_0^t \|v^m\|_{BW\mathcal{M}_{p,r}^{l,s-1}} \|z^{m+1}\|_{BW\mathcal{M}_{p,r}^{l,s-1}} d\tau \\ &\quad + C_2 \int_0^t \|w^m \cdot \nabla \theta^m\|_{BW\mathcal{M}_{p,r}^{l,s-1}} d\tau \\ &\leq C2^{-m} \|\theta_0\|_{BW\mathcal{M}_{p,r}^{l,s}} + C_3 T \|v^m\|_{L_T^\infty(BW\mathcal{M}_{p,r}^{l,s-1})} \|z^{m+1}\|_{L_T^\infty(BW\mathcal{M}_{p,r}^{l,s-1})} \\ &\quad + C_2 T \|w^m\|_{L_T^\infty(BW\mathcal{M}_{p,r}^{l,s-1})} \|\theta^m\|_{L_T^\infty(BW\mathcal{M}_{p,r}^{l,s})} \\ &\leq C2^{-m} \|\theta_0\|_{BW\mathcal{M}_{p,r}^{l,s}} + C_3 T \|\mathcal{R}\| \|\theta^m\|_{L_T^\infty(BW\mathcal{M}_{p,r}^{l,s-1})} \|z^{m+1}\|_{L_T^\infty(BW\mathcal{M}_{p,r}^{l,s-1})} \\ &\quad + C_2 T \|\mathcal{R}\| \|\theta^m\|_{L_T^\infty(BW\mathcal{M}_{p,r}^{l,s})} \|z^m\|_{L_T^\infty(BW\mathcal{M}_{p,r}^{l,s-1})} \\ &\leq C2^{-m} \|\theta_0\|_{BW\mathcal{M}_{p,r}^{l,s}} + C_3 T \tilde{C} \|z^{m+1}\|_{L_T^\infty(BW\mathcal{M}_{p,r}^{l,s-1})} \\ &\quad + C_2 T \tilde{C} \|z^m\|_{L_T^\infty(BW\mathcal{M}_{p,r}^{l,s-1})}, \end{aligned}$$

then,

$$\begin{aligned} \|z^{m+1}(t)\|_{L_T^\infty(BW\mathcal{M}_{p,r}^{l,s-1})} &\leq C2^{-m} \|\theta_0\|_{BW\mathcal{M}_{p,r}^{l,s}} + C_3 T \tilde{C} \|z^{m+1}\|_{L_T^\infty(BW\mathcal{M}_{p,r}^{l,s-1})} \\ &\quad + C_2 T \tilde{C} \|z^m\|_{L_T^\infty(BW\mathcal{M}_{p,r}^{l,s-1})}. \end{aligned}$$

Consider $0 < T \leq T_2$ such that $C_3 T \tilde{C} \leq \frac{1}{2}$, and we get

$$\frac{1}{2} \|z^{m+1}(t)\|_{L_T^\infty(BW\mathcal{M}_{p,r}^{l,s-1})} \leq C2^{-m} \|\theta_0\|_{BW\mathcal{M}_{p,r}^{l,s}} + C_2 T \tilde{C} \|z^m\|_{L_T^\infty(BW\mathcal{M}_{p,r}^{l,s-1})}.$$

By restringing a little more, if necessary, to $2C_2 T \tilde{C} \leq \frac{1}{2}$, we obtain the estimate

$$\|z^{m+1}\|_{L_{T_3}^\infty(BW\tilde{\mathcal{M}}_{p,r}^{l,s-1})} \leq C2^{-(m-1)} \|\theta_0\|_{BW\tilde{\mathcal{M}}_{p,r}^{l,s}} + \frac{1}{2} \|z^m\|_{L_{T_3}^\infty(BW\tilde{\mathcal{M}}_{p,r}^{l,s-1})}$$

for all $m \geq 2$. By an induction argument, it is easy to get that

$$\|z^{m+1}\|_{L_{T_3}^\infty(BW\mathcal{M}_{p,r}^{l,s-1})} \leq C\|\theta_0\|_{BW\mathcal{M}_{p,r}^{l,s}}(m-1)2^{-(m-1)} + 2^{-(m-1)}\|z^2\|_{L_{T_3}^\infty(BW\mathcal{M}_{p,r}^{l,s-1})},$$

for all $m \geq 2$.

It is a standard argument to show that sequence $(\theta^m)_{m \geq 1}$ is Cauchy. In fact, for $m > n \geq 2$, we can compute

$$\begin{aligned} \|\theta^m - \theta^n\|_{L_{T_3}^\infty(BW\tilde{\mathcal{M}}_{p,r}^{l,s-1})} &\leq \sum_{i=n}^{m-1} \|z^{i+1}\|_{L_{T_3}^\infty(BW\tilde{\mathcal{M}}_{p,r}^{l,s-1})} \\ &\leq \sum_{i=n}^{m-1} \left(C\|\theta_0\|_{BW\mathcal{M}_{p,r}^{l,s}}(i-1)2^{-(i-1)} + 2^{-(i-1)}\|z^2\|_{L_{T_3}^\infty(BW\mathcal{M}_{p,r}^{l,s-1})} \right). \end{aligned}$$

The convergence of the numerical series on the right-hand side implies that the right-hand side is small as desired.

So, there is an $\sigma \in L_{T_3}^\infty(BW\tilde{\mathcal{M}}_{p,r}^{l,s-1})$ such that $\theta^m \rightarrow \sigma$ in $L_{T_3}^\infty(BW\tilde{\mathcal{M}}_{p,r}^{l,s-1})$. Furthermore, from Claim 4.2.3, we have that (θ^m) is bounded in $L_{T_3}^\infty(BW\tilde{\mathcal{M}}_{p,r}^{l,s})$ and from [42, Lemma 3.6] the $BW\tilde{\mathcal{M}}_{p,r}^{l,s}$ has a predual, i. e., there is a vector space whose dual space (set of all continuous linear transformations on this vector space) is $BW\tilde{\mathcal{M}}_{p,r}^{l,s}$, in this case is the modified Besov-block spaces, so by the Banach-Alaoglu Theorem there is a subsequence (θ^{m_k}) and $\theta \in L_{T_3}^\infty(BW\tilde{\mathcal{M}}_{p,r}^{l,s})$ such that $\theta^{m_k} \rightharpoonup^* \theta$ in $L_{T_3}^\infty(BW\tilde{\mathcal{M}}_{p,r}^{l,s})$; but that implies that $\theta^{m_k} \rightharpoonup^* \theta$ in $L_{T_3}^\infty(BW\tilde{\mathcal{M}}_{p,r}^{l,s-1})$, since the parameter s indicates the degree of regularity, then since $L_{T_3}^\infty(BW\tilde{\mathcal{M}}_{p,r}^{l,s}) \subset L_{T_3}^\infty(BW\tilde{\mathcal{M}}_{p,r}^{l,s-1})$. On the other hand, as strong convergence implies weak convergence and from the fact that every subsequence of a convergent sequence converges to the same element, we have that $\theta^m \rightarrow \sigma$ in $L_{T_3}^\infty(BW\tilde{\mathcal{M}}_{p,r}^{l,s-1})$ that $\theta^{m_k} \rightharpoonup^* \sigma$ in $L_{T_3}^\infty(BW\tilde{\mathcal{M}}_{p,r}^{l,s-1})$, then then, by the uniqueness of the weak limit \star , we conclude that $\theta = \sigma$.

Then we prove that θ is a solution of the SQG equation; for each $m \in \mathbb{N}$, of (4.19), we have to

$$\frac{\partial \theta^{m+1}}{\partial t} = -v^m \cdot \nabla \theta^{m+1}$$

integrating from 0 to t

$$\theta^{m+1}(\beta, t) = \theta^{m+1}(\beta, 0) - \int_0^t v^m \cdot \nabla \theta^{m+1} d\tau. \quad (4.28)$$

Since $(\theta^m) \subset C([0, T_3], BW\tilde{\mathcal{M}}_{p,r}^{l,s-1})$ and θ^m converges to θ em $L_{T_3}^\infty(BW\tilde{\mathcal{M}}_{p,r}^{l,s-1})$, we have to $\theta \in C([0, T_3], BW\tilde{\mathcal{M}}_{p,r}^{l,s-1})$. Taking $m \rightarrow \infty$ em (4.28), we have that θ satisfies

$$\theta(t) = \theta_0 - \int_0^t v \cdot \nabla \theta d\tau \quad (4.29)$$

just as wanted.

It remains to show that θ is continuous in time with values in $BW\tilde{\mathcal{M}}_{p,r}^{l,s}$ for $r < \infty$. Considering $\omega_k = S_k\theta$ with $k \in \mathbb{N}$, we have ω_k converge to θ in space $L_{T_3}^\infty(BW\tilde{\mathcal{M}}_{p,r}^{l,s})$ and

$$\begin{aligned} \|\omega_k(t) - \omega_k(s)\|_{BW\tilde{\mathcal{M}}_{p,r}^{l,s}} &= \left\| 2^{js} \left\| \bar{\Delta}_j S_k(\theta(t) - \theta(s)) \right\|_{W\tilde{\mathcal{M}}_p^l} \right\|_{l^r} \\ &= \left\| 2^{js} \left\| S_k \bar{\Delta}_j(\theta(t) - \theta(s)) \right\|_{W\tilde{\mathcal{M}}_p^l} \right\|_{l^r} \\ &\leq C \left(\sum_{j=-1}^{k+1} 2^{jsr} \left\| \bar{\Delta}_j(\theta(t) - \theta(s)) \right\|_{W\tilde{\mathcal{M}}_p^l}^r \right)^{\frac{1}{r}} \\ &\leq C 2^k \left(\sum_{j=-1}^{k+1} 2^{j(s-1)r} \left\| \bar{\Delta}_j(\theta(t) - \theta(s)) \right\|_{W\tilde{\mathcal{M}}_p^l}^r \right)^{\frac{1}{r}} \\ &\leq C 2^k \|\theta(t) - \theta(s)\|_{BW\tilde{\mathcal{M}}_{p,r}^{l,s-1}}. \end{aligned}$$

Since $\theta \in C([0, T_3]; BW\tilde{\mathcal{M}}_{p,r}^{l,s-1})$, we have $\omega_k \in C([0, T_3]; BW\tilde{\mathcal{M}}_{p,r}^{l,s})$ for each k , and consequently, $\theta \in C([0, T_3]; BW\tilde{\mathcal{M}}_{p,r}^{l,s})$. \square

4.3 Numerical Study

In this section, our objective is to numerically study the SQG and obtain computational information, such as global well-posedness, blowing-up, formation of singularities or formation of abrupt gradients in the numerical solution of the SQG. For this study, we began in the first subsection by constructing the 2D fully-discrete nonlocal Lagrangian–Eulerian scheme based on the concept of No-Flow curves to handle the two-dimensional nonlocal operator Riesz transform \mathcal{R} acting on the hyperbolic conservation laws. The construction of the 2D nonlocal fully-discrete Lagrangian–Eulerian scheme for this case is similar to Section 3.4.6 based on the new concept of No-Flow curves, which was first introduced in [12] and has been presented and analyzed successfully for fully discrete schemes in a solid mathematical foundation. The second subsection will focus on approximating and numerically validating the two-dimensional nonlocal operator, the Riesz Transform. In the final subsection, we present numerical simulations considering different types of initial data.

Let us recall that the SQG in conservative form is given by

$$\begin{cases} \partial_t \theta + \nabla \cdot (\theta \mathcal{R}^\perp \theta) = 0 \\ \theta(x, y, 0) = \theta_0(x, y) \end{cases}$$

where $\theta = \theta(x, y, t)$ is a scalar function, $\theta : \mathbb{R}^2 \times [0, \infty) \longrightarrow \mathbb{R}$, which represents the temperature potential of the fluid, $v = (v_1, v_2)$ denotes a velocity field such that $\nabla \cdot v = 0$.

And the relationship between v and θ is through the Riesz transform \mathcal{R}

$$v = \mathcal{R}^\perp \theta = (-\mathcal{R}_2 \theta, \mathcal{R}_1 \theta) = (-\partial_2 (-\Delta)^{-\frac{1}{2}} \theta, \partial_1 (-\Delta)^{-\frac{1}{2}} \theta).$$

4.3.1 A Lagrangian–Eulerian scheme for the SQG

In this subsection, we discuss the new Lagrangian–Eulerian technique with conservation properties for approximating the two-dimensional initial value problem for hyperbolic conservation laws, where the flow is nonlocal. This hyperbolic conservation laws is the SQG,

$$\begin{cases} \partial_t \theta + \partial_x (-\theta \mathcal{R}_2 \theta) + \partial_y (\theta \mathcal{R}_1 \theta) = 0, & (x, y, t) \in \Omega \times (t_0, T] \\ \theta(x, y, 0) = \theta_0(x, y), & (x, y) \in \Omega, \end{cases} \quad (4.30)$$

where, $\Omega \subset \mathbb{R}^2$, $t_0 \geq 0$, $T = t_f > 0$, and $\theta_0 \in L^p(\mathbb{R}^2)$ is a not necessarily regular function.

To develop the 2D fully-discrete nonlocal Lagrangian–Eulerian scheme for solving the nonlocal IVP model (4.30), we first follow an analogous approach to that used for the Lagrangian–Eulerian scheme in the 1D + 1/2 model, as outlined in [6] and [7]. So, we incorporate the concepts described in [6] and [3] to approximate the solution to problem (4.30)

$$\Theta(x_i, y_j, t^n) = \Theta_{i,j}^n \approx \frac{1}{\Delta y} \frac{1}{\Delta x} \int_{y_{j-\frac{1}{2}}}^{y_{j+\frac{1}{2}}} \int_{x_{i-\frac{1}{2}}}^{x_{i+\frac{1}{2}}} \theta(x, y, t^n) dx dy \quad (4.31)$$

$$\bar{\Theta}(x_i, y_j, t^{n+1}) = \bar{\Theta}_{i,j}^{n+1} \approx \frac{1}{\Delta y^{n+1}} \frac{1}{\Delta x^{n+1}} \int_{y_{j-\frac{1}{2}}^{n+1}}^{\bar{y}_{j+\frac{1}{2}}^{n+1}} \int_{\bar{x}_{i-\frac{1}{2}}^{n+1}}^{\bar{x}_{i+\frac{1}{2}}^{n+1}} \theta(x, y, t^{n+1}) dx dy \quad (4.32)$$

with the initial condition $\Theta(x_i^0, y_j^0, t^0) = \Theta_{i,j}^0$ in the cells

$$\left[x_{i-\frac{1}{2}}^0, x_{i+\frac{1}{2}}^0 \right] \times \left[y_{j-\frac{1}{2}}^0, y_{j+\frac{1}{2}}^0 \right] \quad \text{for } i, j \in \mathbb{Z}.$$

It is worth mentioning that the approximation value $\bar{\Theta}(x_i, y_j, t^{n+1})$ is performed over the region $\bar{R}_{i,j}^{n+1}$.

To build the 2D scheme, we need to define the control volume of the Lagrangian–Eulerian scheme, $D_{i,j}^n$, which is a solid in \mathbb{R}^3 formed by the triples (x, y, t) between the region $R_{i,j}^n$ and the region $\bar{R}_{i,j}^{n+1}$ where the region $\bar{R}_{i,j}^{n+1}$ is obtained by the No-Flow curves, $\sigma_{i,j}^n(t)$ with $i, j \in \mathbb{Z}$ and $t^n \leq t \leq t^{n+1}$. Then $\partial D_{i,j}^n = R_{i,j}^n \cup S_{i,j}^n \cup \bar{R}_{i,j}^{n+1}$, where

- $R_{i,j}^n = [x_{1-\frac{1}{2}}^n, x_{1+\frac{1}{2}}^n] \times [y_{1-\frac{1}{2}}^n, y_{1+\frac{1}{2}}^n] \subset \mathbb{R}^2$ is the entry of the non-flow surface region,
 - $\bar{R}_{i,j}^{n+1} = [\bar{x}_{1-\frac{1}{2}}^{n+1}, \bar{x}_{1+\frac{1}{2}}^{n+1}] \times [\bar{y}_{1-\frac{1}{2}}^{n+1}, \bar{y}_{1+\frac{1}{2}}^{n+1}] \subset \mathbb{R}^2$ is the exit of the non-flow surface region,
- and

- $S_{i,j}^n \subset \mathbb{R}^3$, is the lateral surface of the non-flow region.

Remark that in the equation (4.31) the $\theta(x, y, t)$ is the solution of

$$\partial_t \theta + (\partial_x(-\theta \mathcal{R}_2 \theta) + \partial_y(\theta \mathcal{R}_1 \theta)) = 0, \quad \forall (x, y, t) \in \Omega \times \mathbb{R}^+.$$

We assume there is non-flow through the surface $S_{i,j}^n$ (that is, $S_{i,j}^n$ is impervious; that is natural in many applications [12], [9], [14], [13]). As a consequence, the *surface integral* of $S_{i,j}^n$ is zero; that is,

$$\iint_{\bar{R}_{i,j}^{n+1}} \theta(x, y, t^{n+1}) d\bar{R}_{i,j}^{n+1} = \iint_{R_{i,j}^n} \theta(x, y, t^n) dR_{i,j}^n \quad (4.33)$$

referred to as the conservation identity in [6] and [3]. This can be written as

$$\int_{\bar{y}_{j-1/2}^{n+1}}^{\bar{y}_{j+1/2}^{n+1}} \int_{\bar{x}_{j-1/2}^{n+1}}^{\bar{x}_{j+1/2}^{n+1}} \theta(x, y, t^{n+1}) dx dy = \int_{y_{j-1/2}^n}^{y_{j+1/2}^n} \int_{x_{j-1/2}^n}^{x_{j+1/2}^n} \theta(x, y, t^n) dx dy \quad (4.34)$$

At first, we do not know exactly what the no-flow surface $S_{i,j}^n$ looks like; we only know that the edge of the ingress coincides with $\partial R_{i,j}^n$ in the t^n plane, and the outlet end of surface $S_{i,j}^n$, which intersects the t^{n+1} plane. Let us suppose that the surface $S_{i,j}^n$ is given by a family of No-Flow curves, $\gamma(t)$ with $t^n \leq t \leq t^{n+1}$, then we will take a $\gamma_{i\pm 1/2,j}^n(t)$, $\gamma_{i,j\pm 1/2}^n(t)$ representative curve at the midpoint of each side of the edge $\partial R_{i,j}^n$ and it will be defined with the help of the scalar functions, $\sigma_{i\pm 1/2,j}^n(t)$ and $\sigma_{i,j\pm 1/2}^n(t)$ with $t^n \leq t \leq t^{n+1}$, such that for $t = t^n$ we have $\sigma_{i\pm 1/2,j}^n(t^n) = x_{i\pm 1/2}$, $\sigma_{i,j\pm 1/2}^n(t^n) = y_{j\pm 1/2}$ and these four functions in time t^{n+1} intersect the plane t^{n+1} , see Figura 2. Then to build $\bar{R}_{i,j}^{n+1}$, we define the four parametric curves,

$$\gamma_{i\pm 1/2,j}^n(t) = [\sigma_{i\pm 1/2,j}^n(t), y_j, t]^T, \quad \gamma_{i,j\pm 1/2}^n(t) = [x_i, \sigma_{i,j\pm 1/2}^n(t), t]^T \quad \text{with } t^n \leq t \leq t^{n+1}. \quad (4.35)$$

So, we have to $\gamma_{i\pm 1/2,j}^n(t), \gamma_{i,j\pm 1/2}^n(t) \in S_{i,j}^n$ for $t^n < t < t^{n+1}$.

By [6], the construction of No-Flow side curves is not unique.

Notice that, for $t^n < t < t^{n+1}$, we have that $\gamma_{i\pm 1/2,j}^n(t)$ is in plane- y_j , $\gamma_{i,j\pm 1/2}^n(t)$ is in plane- x_i , furthermore

$$\frac{d}{dt} \gamma_{i\pm 1/2,j}^n(t) = \left[\frac{d}{dt} \sigma_{i\pm 1/2,j}^n(t), 0, 1 \right]^T \quad \text{and} \quad \frac{d}{dt} \gamma_{i,j\pm 1/2}^n(t) = \left[0, \frac{d}{dt} \sigma_{i,j\pm 1/2}^n(t), 1 \right]^T$$

Similar to a conservation law with partially nonlocal velocity, we obtain the following initial value problems. It's clear that the No-Flow curve depends directly on the approach

of the operator.

$$\begin{cases} \frac{d}{dt}\sigma_{i\pm 1/2,j}^n(t) &= \frac{-\theta(\sigma_{i\pm 1/2,j}^n(t), y_j, t)\mathcal{R}_2\theta(\sigma_{i\pm 1/2,j}^n(t), y_j, t)}{\theta(\sigma_{i\pm 1/2,j}^n(t), y_j, t)} \\ \sigma_{i\pm 1/2,j}^n(t^n) &= x_{i\pm 1/2}^n \end{cases} \quad (4.36)$$

and

$$\begin{cases} \frac{d}{dt}\sigma_{i,j\pm 1/2}^n(t) &= \frac{\theta(x_i, \sigma_{i,j\pm 1/2}^n(t), t)\mathcal{R}_1\theta(x_i, \sigma_{i,j\pm 1/2}^n(t), t)}{\theta(x_i, \sigma_{i,j\pm 1/2}^n(t), t)} \\ \sigma_{i,j\pm 1/2}^n(t^n) &= y_{j\pm 1/2}^n. \end{cases} \quad (4.37)$$

approximating the $\sigma_{i\pm 1/2,j}^n(t)$ and $\sigma_{i,j\pm 1/2}^n(t)$ curves by Taylor's series, we obtain

$$\begin{aligned} \sigma_{i\pm 1/2,j}^n(t) &= \sigma_{i\pm 1/2,j}^n(t^n) + \frac{d}{dt}\sigma_{i\pm 1/2,j}^n(t^n)(t - t^n) \\ \sigma_{i,j\pm 1/2}^n(t) &= \sigma_{i,j\pm 1/2}^n(t^n) + \frac{d}{dt}\sigma_{i,j\pm 1/2}^n(t^n)(t - t^n). \end{aligned}$$

Thus, from (3.102), we get an approximation for $\sigma_{i\pm 1/2,j}^n(t)$

$$\sigma_{i\pm 1/2,j}^n(t) = x_{i\pm 1/2}^n + (t - t^n)f_{i\pm 1/2,j}^n \quad \text{for } t^n \leq t \leq t^{n+1} \quad (4.38)$$

where, $f_{i\pm 1/2,j}^n = -\mathcal{R}_2\theta(\sigma_{i\pm 1/2,j}^n(t), y_j^n, t)$.

Similarly, from (4.37), we get an approximation for $\sigma_{i,j\pm 1/2}^n(t)$

$$\sigma_{i,j\pm 1/2}^n(t) = y_{j\pm 1/2}^n + (t - t^n)g_{i,j\pm 1/2}^n \quad \text{for } t^n \leq t \leq t^{n+1} \quad (4.39)$$

where, $g_{i,j\pm 1/2}^n = \mathcal{R}_1\theta(x_i^n, \sigma_{i,j\pm 1/2}^n(t), t)$.

So, a significant finding emerges: the No-Flow curves $f_{i\pm 1/2,j}^n$ and $g_{i,j\pm 1/2}^n$ approximate the velocity nonlocal $\mathcal{R}_2\theta(\sigma_{i\pm 1/2,j}^n(t), y_j^n, t)$ and $\mathcal{R}_1\theta(x_i^n, \sigma_{i,j\pm 1/2}^n(t), t)$, respectively, for this conservation law.

Furthermore, the approximation to the control volume $D_{i,j}^n$ is given by

$$D_{i,j}^n = \{(x, y, t) \mid \sigma_{i-1/2,j}^n(t) < x < \sigma_{i+1/2,j}^n(t), \sigma_{i,j-1/2}^n(t) < y < \sigma_{i,j+1/2}^n(t), t^n < t < t^{n+1}\}. \quad (4.40)$$

The conservative Lagrangian-Eulerian scheme for this case is given for the steps next.

1. *The Lagrangian evolution* is given by

$$\bar{\Theta}_{i,j}^{n+1} = \frac{A(R_{i,j}^n)}{A(\bar{R}_{i,j}^{n+1})}\Theta_{i,j}^n \quad \text{with} \quad A(R_{i,j}^n) = \Delta x \times \Delta y \quad \text{and} \quad A(\bar{R}_{i,j}^{n+1}) = \bar{\Delta}x^{n+1} \times \bar{\Delta}y^{n+1} \quad (4.41)$$

where

$$\bar{\Delta}x^{n+1} = \Delta x + (f_{i+1/2,j}^n - f_{i-1/2,j}^n)\Delta t \quad \text{and} \quad \bar{\Delta}y^{n+1} = \Delta y + (g_{i,j+1/2}^n - g_{i,j-1/2}^n)\Delta t$$

2. The Eulerian remap is given by

$$\Theta_{i,j}^{n+1} = \frac{1}{A(\bar{R}_{i,j}^{n+1})} (K_1 + K_2 + K_3) \quad (4.42)$$

where K_1 , K_2 and K_3 are defined as the $1D + 1/2$ model along with the CFL restriction.

4.3.2 Approximation of the Riesz transform

Let be θ a scalar function, $\theta : \mathbb{R}^2 \times [0, \infty) \rightarrow \mathbb{R}$. We know that the Riesz transform is defined as the integral singular operator,

$$\mathcal{R}_j(\theta)(x, t) = \frac{1}{2\pi} \text{p.v.} \int_{\mathbb{R}^2} \frac{(x_j - y_j)}{|x - y|^3} \theta(y, t) dy. \quad (4.43)$$

where $x = (x_1, x_2)$ and $y = (y_1, y_2)$ belong to \mathbb{R}^2 , $t > 0$ and $j = 1, 2$.

For $h > 0$, let be

$$\tau = \{x^{(m,n)} : x^{(m,n)} = (x_1^m, x_2^n), \text{ where } x_1^m = x_1^0 + mh \text{ and } x_2^n = x_2^0 + nh\}_{m,n=0}^N$$

a uniform grid on the plane of the $(N + 1)^2$ cells that determine the closed region $C_\tau = [x_1^0, x_1^N] \times [x_2^0, x_2^N]$. Given a fixed $x \in \mathbb{R}^2$ and assuming that the grid must be such that the function $\theta(x, t)$ can be approximated by zero outside C_τ . Then, for each interior point $x^{(k,l)} \in \tau$ with $k, l = 1, \dots, N - 1$, then we can approximate the Riesz transform on the plane,

$$\begin{aligned} \mathcal{R}_1(\theta)(x^{(k,l)}, t) &\approx \frac{1}{2\pi} \lim_{\epsilon \rightarrow 0^+} \sum_{n=0}^{N-1} \sum_{m=0}^{N-1} \int_{\|x^{(k,l)} - y\|_{\max} > \epsilon} \frac{x_1^k - y_1}{\|x^{(k,l)} - y\|_{\max}^3} \theta(y, t) dy \\ &= \frac{1}{2\pi} \left[\sum_{n=0}^{l-2} \sum_{m=0}^{N-1} + \sum_{n=l+1}^{N-1} \sum_{m=0}^{N-1} + \sum_{n=l-1}^l \sum_{m=0}^{k-2} + \sum_{n=l-1}^l \sum_{m=k+1}^{N-1} \right] \times \\ &\quad \int_{x_2^n}^{x_2^{n+1}} \int_{x_1^m}^{x_1^{m+1}} \frac{x_1^k - y_1}{\|x^{(k,l)} - y\|_{\max}^3} \theta(y, t) dy_1 dy_2 \\ &\quad + \frac{1}{2\pi} \lim_{\epsilon \rightarrow 0^+} \left\{ \int_{x_2^{l-1}}^{x_2^l - \epsilon} \int_{x_1^{k-1}}^{x_1^{k+1}} + \int_{x_2^l + \epsilon}^{x_2^{l+1}} \int_{x_1^{k-1}}^{x_1^{k+1}} + \int_{x_2^l - \epsilon}^{x_2^l + \epsilon} \int_{x_1^{k-1}}^{x_1^k - \epsilon} + \int_{x_2^l - \epsilon}^{x_2^l + \epsilon} \int_{x_1^k + \epsilon}^{x_1^{k+1}} \right\} \times \\ &\quad \frac{x_1^k - y_1}{\|x^{(k,l)} - y\|_{\max}^3} \theta(y, t) dy_1 dy_2. \end{aligned}$$

As the values of $\theta(x^{(k,l)}, t)$ are known in each cell $[x_1^m, x_1^{m+1}] \times [x_2^n, x_2^{n+1}]$, then we can approximate the $\theta(y, t) := \theta_t(y)$ by the zero-degree Taylor polynomial

$$\begin{aligned} \theta_t(y) &= \theta_t(x_1^m, x_2^n) + \partial_1 \theta_t(\xi_1, \xi_2)(y_1 - \xi_1) + \partial_2 \theta_t(\xi_1, \xi_2)(y_2 - \xi_2) \\ &\approx \theta_t(x_1^m, x_2^n) \end{aligned}$$

where $\xi_1 \in [x_1^m, y_1]$ and $\xi_2 \in [x_2^n, y_2]$.

On the other hand, note that

$$\|x^{(k,l)} - y\|_{\max} = \max \left\{ |x_1^k - y_1|, |x_2^l - y_2| : x_1^m \leq y_1 \leq x_1^{m+1} \text{ and } x_2^n \leq y_2 \leq x_2^{n+1} \right\}.$$

Then, we have the following approximations

$$\begin{aligned} & \int_{x_2^n}^{x_2^{n+1}} \int_{x_1^m}^{x_1^{m+1}} \frac{x_1^k - y_1}{\|x^{(k,l)} - y\|_{\max}^3} \theta(y, t) dy_1 dy_2 \\ & \approx \|x^{(k,l)} - y\|_{\max_{y \in Q_0}}^{-3} \int_{x_2^n}^{x_2^{n+1}} \int_{x_1^m}^{x_1^{m+1}} (x_1^k - y_1) \theta_t(x_1^m, x_2^n) dy_1 dy_2 \\ & = \|x^{(k,l)} - y\|_{\max_{y \in Q_0}}^{-3} \theta_t(x_1^m, x_2^n) \int_{x_2^n}^{x_2^{n+1}} \int_{x_1^m}^{x_1^{m+1}} (x_1^k - y_1) dy_1 dy_2 \\ & = \|x^{(k,l)} - y\|_{\max_{y \in Q_0}}^{-3} \theta_t(x_1^m, x_2^n) \frac{1}{2} [(x_1^k - x_1^m)^2 - (x_1^k - x_1^{m+1})^2] (x_2^{n+1} - x_2^n) \\ & = \frac{h}{2} \|x^{(k,l)} - y\|_{\max_{y \in Q_0}}^{-3} \theta_t(x_1^m, x_2^n) [(x_1^k - x_1^m)^2 - (x_1^k - x_1^{m+1})^2] \end{aligned}$$

where $Q_0 = [x_1^m, x_1^{m+1}] \times [x_2^n, x_2^{n+1}]$.

$$\begin{aligned} & \lim_{\epsilon \rightarrow 0^+} \int_{x_2^{l-1}}^{x_2^l - \epsilon} \int_{x_1^{k-1}}^{x_1^{k+1}} \frac{x_1^k - y_1}{\|x^{(k,l)} - y\|_{\max}^3} \theta(y, t) dy_1 dy_2 \\ & \approx \|x^{(k,l)} - y\|_{\max_{y \in Q_1}}^{-3} \lim_{\epsilon \rightarrow 0^+} \int_{x_2^{l-1}}^{x_2^l - \epsilon} \int_{x_1^{k-1}}^{x_1^{k+1}} (x_1^k - y_1) \theta_t(x_1^{k-1}, x_2^{l-1}) dy_1 dy_2 \\ & = 0 \end{aligned}$$

where $Q_1 = [x_1^{k-1}, x_1^{k+1}] \times [x_2^{l-1}, x_2^l - \epsilon]$.

$$\begin{aligned} & \lim_{\epsilon \rightarrow 0^+} \int_{x_2^l + \epsilon}^{x_2^{l+1}} \int_{x_1^{k-1}}^{x_1^{k+1}} \frac{x_1^k - y_1}{\|x^{(k,l)} - y\|_{\max}^3} \theta(y, t) dy_1 dy_2 \\ & \approx \|x^{(k,l)} - y\|_{\max_{y \in Q_2}}^{-3} \lim_{\epsilon \rightarrow 0^+} \int_{x_2^l + \epsilon}^{x_2^{l+1}} \int_{x_1^{k-1}}^{x_1^{k+1}} (x_1^k - y_1) \theta_t(x_1^{k-1}, x_2^l + \epsilon) dy_1 dy_2 \\ & = 0 \end{aligned}$$

where $Q_2 = [x_1^{k-1}, x_1^{k+1}] \times [x_2^l, x_2^{l+1}]$.

$$\begin{aligned} & \lim_{\epsilon \rightarrow 0^+} \int_{x_2^l - \epsilon}^{x_2^l + \epsilon} \int_{x_1^{k-1}}^{x_1^k - \epsilon} \frac{x_1^k - y_1}{\|x^{(k,l)} - y\|_{\max}^3} \theta(y, t) dy_1 dy_2 \\ & \approx \|x^{(k,l)} - y\|_{\max_{y \in Q_3}}^{-3} \lim_{\epsilon \rightarrow 0^+} \int_{x_2^l - \epsilon}^{x_2^l + \epsilon} \int_{x_1^{k-1}}^{x_1^k - \epsilon} (x_1^k - y_1) \theta_t(x_1^{k-1}, x_2^l - \epsilon) dy_1 dy_2 \\ & = 0 \end{aligned}$$

where $Q_3 = [x_1^{k-1}, x_1^k] \times [x_2^l, x_2^l]$.

$$\begin{aligned}
& \lim_{\epsilon \rightarrow 0^+} \int_{x_2^l - \epsilon}^{x_2^l + \epsilon} \int_{x_1^k + \epsilon}^{x_1^{k+1}} \frac{x_1^k - y_1}{\|x^{(k,l)} - y\|_{\max}^3} \theta(y, t) dy_1 dy_2 \\
& \approx \|x^{(k,l)} - y\|_{\max_{y \in Q_4}}^{-3} \lim_{\epsilon \rightarrow 0^+} \int_{x_2^l - \epsilon}^{x_2^l + \epsilon} \int_{x_1^k + \epsilon}^{x_1^{k+1}} (x_1^k - y_1) \theta_t(x_1^k + \epsilon, x_2^l - \epsilon) dy_1 dy_2 \\
& = 0
\end{aligned}$$

where $Q_4 = [x_1^k, x_1^{k+1}] \times [x_2^l, x_2^l]$.

Therefore,

$$\begin{aligned}
\mathcal{R}_1(\theta)(x^{(k,l)}, t) & \approx \frac{1}{2\pi} \left[\sum_{n=0}^{l-2} \sum_{m=0}^{N-1} + \sum_{n=l+1}^{N-1} \sum_{m=0}^{N-1} + \sum_{n=l-1}^l \sum_{m=0}^{k-2} + \sum_{n=l-1}^l \sum_{m=k+1}^{N-1} \right] \frac{h}{2} \|x^{(k,l)} - y\|_{\max_{y \in Q_0}}^{-3} \times \\
& \quad \theta_t(x_1^m, x_2^n) [(x_1^k - x_1^m)^2 - (x_1^k - x_1^{m+1})^2]
\end{aligned} \tag{4.44}$$

Similarly, we can get

$$\begin{aligned}
\mathcal{R}_2(\theta)(x^{(k,l)}, t) & \approx \frac{1}{2\pi} \lim_{\epsilon \rightarrow 0^+} \sum_{n=0}^{N-1} \sum_{m=0}^{N-1} \int_{\|x^{(k,l)} - y\|_{\max} > \epsilon} \frac{x_2^l - y_2}{\|x^{(k,l)} - y\|_{\max}^3} \theta(y, t) dy \\
& = \frac{1}{2\pi} \left[\sum_{n=0}^{l-2} \sum_{m=0}^{N-1} + \sum_{n=l+1}^{N-1} \sum_{m=0}^{N-1} + \sum_{n=l-1}^l \sum_{m=0}^{k-2} + \sum_{n=l-1}^l \sum_{m=k+1}^{N-1} \right] \times \\
& \quad \int_{x_2^n}^{x_2^{n+1}} \int_{x_1^m}^{x_1^{m+1}} \frac{x_2^l - y_2}{\|x^{(k,l)} - y\|_{\max}^3} \theta(y, t) dy_1 dy_2 \\
& \quad + \frac{1}{2\pi} \lim_{\epsilon \rightarrow 0^+} \left\{ \int_{x_2^{l-1}}^{x_2^l - \epsilon} \int_{x_1^{k-1}}^{x_1^{k+1}} + \int_{x_2^l + \epsilon}^{x_2^{l+1}} \int_{x_1^{k-1}}^{x_1^{k+1}} + \int_{x_2^l - \epsilon}^{x_2^l + \epsilon} \int_{x_1^{k-1}}^{x_1^k - \epsilon} + \int_{x_2^l - \epsilon}^{x_2^l + \epsilon} \int_{x_1^k + \epsilon}^{x_1^{k+1}} \right\} \times \\
& \quad \frac{x_2^l - y_2}{\|x^{(k,l)} - y\|_{\max}^3} \theta(y, t) dy_1 dy_2.
\end{aligned}$$

Each parcel can be approximated by

$$\begin{aligned}
& \int_{x_2^n}^{x_2^{n+1}} \int_{x_1^m}^{x_1^{m+1}} \frac{x_2^l - y_2}{\|x^{(k,l)} - y\|_{\max}^3} \theta(y, t) dy_1 dy_2 \\
& \approx \|x^{(k,l)} - y\|_{\max_{y \in P_0}}^{-3} \int_{x_2^n}^{x_2^{n+1}} \int_{x_1^m}^{x_1^{m+1}} (x_2^l - y_2) \theta_t(x_1^m, x_2^n) dy_1 dy_2 \\
& = \frac{h}{2} \|x^{(k,l)} - y\|_{\max_{y \in P_0}}^{-3} \theta_t(x_1^m, x_2^n) [(x_2^l - x_2^n)^2 - (x_2^l - x_2^{n+1})^2]
\end{aligned}$$

where $P_0 = [x_1^m, x_1^{m+1}] \times [x_2^n, x_2^{n+1}]$.

$$\begin{aligned}
& \lim_{\epsilon \rightarrow 0^+} \int_{x_2^{l-1}}^{x_2^l - \epsilon} \int_{x_1^{k-1}}^{x_1^{k+1}} \frac{x_2^l - y_2}{\|x^{(k,l)} - y\|_{\max}^3} \theta(y, t) dy_1 dy_2 \\
& \approx \|x^{(k,l)} - y\|_{\max_{y \in P_1}}^{-3} \lim_{\epsilon \rightarrow 0^+} \int_{x_2^{l-1}}^{x_2^l - \epsilon} \int_{x_1^{k-1}}^{x_1^{k+1}} (x_2^l - y_2) \theta_t(x_1^{k-1}, x_2^{l-1}) dy_1 dy_2 \\
& = \|x^{(k,l)} - y\|_{\max_{y \in P_1}}^{-3} \theta_t(x_1^{k-1}, x_2^{l-1}) \lim_{\epsilon \rightarrow 0^+} \left\{ -\frac{1}{2} (\epsilon^2 - h^2) (2h) \right\} \\
& = h^3 \|x^{(k,l)} - y\|_{\max_{y \in P_1}}^{-3} \theta_t(x_1^{k-1}, x_2^{l-1})
\end{aligned}$$

where $P_1 = [x_1^{k-1}, x_1^{k+1}] \times [x_2^{l-1}, x_2^l - \epsilon]$.

$$\begin{aligned}
& \lim_{\epsilon \rightarrow 0^+} \int_{x_2^l + \epsilon}^{x_2^{l+1}} \int_{x_1^{k-1}}^{x_1^{k+1}} \frac{x_2^l - y_2}{\|x^{(k,l)} - y\|_{\max}^3} \theta(y, t) dy_1 dy_2 \\
& \approx \|x^{(k,l)} - y\|_{\max_{y \in P_2}}^{-3} \lim_{\epsilon \rightarrow 0^+} \int_{x_2^l + \epsilon}^{x_2^{l+1}} \int_{x_1^{k-1}}^{x_1^{k+1}} (x_2^l - y_2) \theta_t(x_1^{k-1}, x_2^l + \epsilon) dy_1 dy_2 \\
& = \|x^{(k,l)} - y\|_{\max_{y \in P_2}}^{-3} \theta_t(x_1^{k-1}, x_2^l) \lim_{\epsilon \rightarrow 0^+} \left\{ -\frac{1}{2} ((-h)^2 - \epsilon^2) (2h) \right\} \\
& = -h^3 \|x^{(k,l)} - y\|_{\max_{y \in P_2}}^{-3} \theta_t(x_1^{k-1}, x_2^l)
\end{aligned}$$

where $P_2 = [x_1^{k-1}, x_1^{k+1}] \times [x_2^l + \epsilon, x_2^{l+1}]$.

$$\begin{aligned}
& \lim_{\epsilon \rightarrow 0^+} \int_{x_2^l - \epsilon}^{x_2^l + \epsilon} \int_{x_1^{k-1}}^{x_1^{k+1} - \epsilon} \frac{x_2^l - y_2}{\|x^{(k,l)} - y\|_{\max}^3} \theta(y, t) dy_1 dy_2 \\
& \approx \|x^{(k,l)} - y\|_{\max_{y \in P_3}}^{-3} \lim_{\epsilon \rightarrow 0^+} \int_{x_2^l - \epsilon}^{x_2^l + \epsilon} \int_{x_1^{k-1}}^{x_1^{k+1} - \epsilon} (x_2^l - y_2) \theta_t(x_1^{k-1}, x_2^l - \epsilon) dy_1 dy_2 \\
& = \|x^{(k,l)} - y\|_{\max_{y \in P_3}}^{-3} \theta_t(x_1^{k-1}, x_2^l) \lim_{\epsilon \rightarrow 0^+} \left\{ -\frac{1}{2} ((-\epsilon)^2 - \epsilon^2) (h - \epsilon) \right\} \\
& = 0
\end{aligned}$$

where $P_3 = [x_1^{k-1}, x_1^k] \times [x_2^l - \epsilon, x_2^l + \epsilon]$.

$$\begin{aligned}
& \lim_{\epsilon \rightarrow 0^+} \int_{x_2^l - \epsilon}^{x_2^l + \epsilon} \int_{x_1^k + \epsilon}^{x_1^{k+1}} \frac{x_2^l - y_2}{\|x^{(k,l)} - y\|_{\max}^3} \theta(y, t) dy_1 dy_2 \\
& \approx \|x^{(k,l)} - y\|_{\max_{y \in P_4}}^{-3} \lim_{\epsilon \rightarrow 0^+} \int_{x_2^l - \epsilon}^{x_2^l + \epsilon} \int_{x_1^k + \epsilon}^{x_1^{k+1}} (x_2^l - y_2) \theta_t(x_1^k + \epsilon, x_2^l - \epsilon) dy_1 dy_2 \\
& = 0
\end{aligned}$$

where $P_4 = [x_1^k, x_1^{k+1}] \times [x_2^l, x_2^l]$.

Therefore,

$$\begin{aligned} \mathcal{R}_2(\theta)(x^{(k,l)}, t) \approx & \frac{1}{2\pi} \left[\sum_{n=0}^{l-2} \sum_{m=0}^{N-1} + \sum_{n=l+1}^{N-1} \sum_{m=0}^{N-1} + \sum_{n=l-1}^l \sum_{m=0}^{k-2} + \sum_{n=l-1}^l \sum_{m=k+1}^{N-1} \right] \frac{h}{2} \|x^{(k,l)} - y\|_{\max_{y \in P_0}}^{-3} \times \\ & \theta_t(x_1^m, x_2^n) [(x_2^l - x_2^n)^2 - (x_2^l - x_2^{n+1})^2] \\ & + \frac{h^3}{2\pi} \left\{ \|x^{(k,l)} - y\|_{\max_{y \in P_1}}^{-3} \theta_t(x_1^{k-1}, x_2^{l-1}) - \|x^{(k,l)} - y\|_{\max_{y \in P_2}}^{-3} \theta_t(x_1^{k-1}, x_2^l) \right\}. \end{aligned} \quad (4.45)$$

To test our numerical approximation of the Riesz transform, we study \mathcal{R}_1 (4.44) and \mathcal{R}_2 (4.45), separately to the 2D Gaussian function u and validate our approximation using the following identity

$$\mathcal{R}_i \mathcal{R}_j (\Delta u) = -\frac{\partial^2 u}{\partial x_i \partial x_j}. \quad (4.46)$$

It is worth noting that the machine simulation time for the Figure 20 was approximately 18 days. This simulation is a fundamental part of validating the numerical approximation of the Riesz Transform that we are proposing.

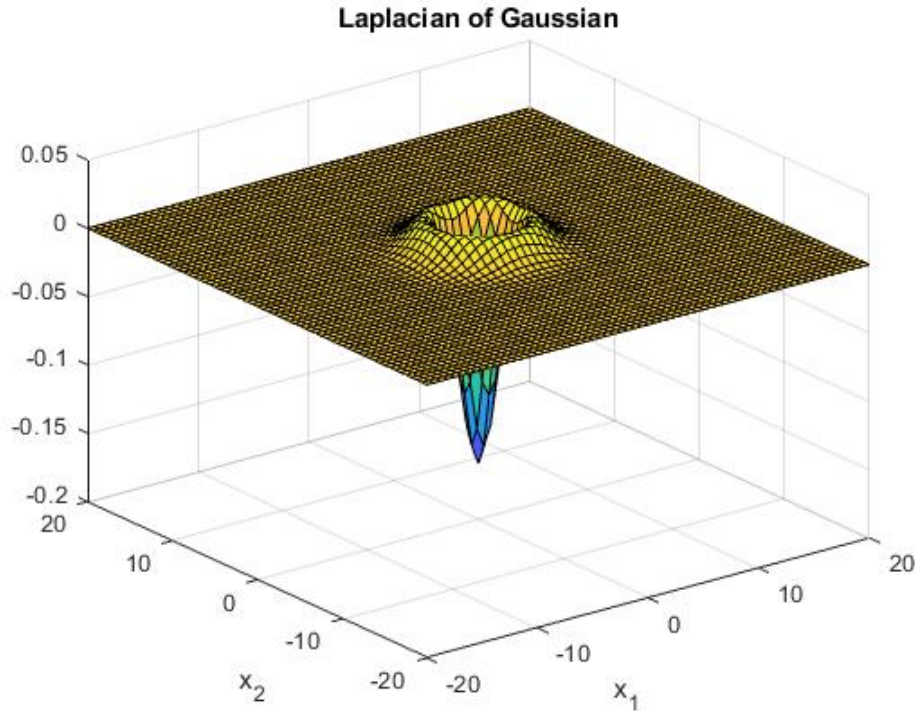


Figure 17 – The laplacian of Gaussian 2D Δu , where $u(x_1, x_2) = \frac{1}{\pi} e^{-\frac{x_1^2 + x_2^2}{8}}$.

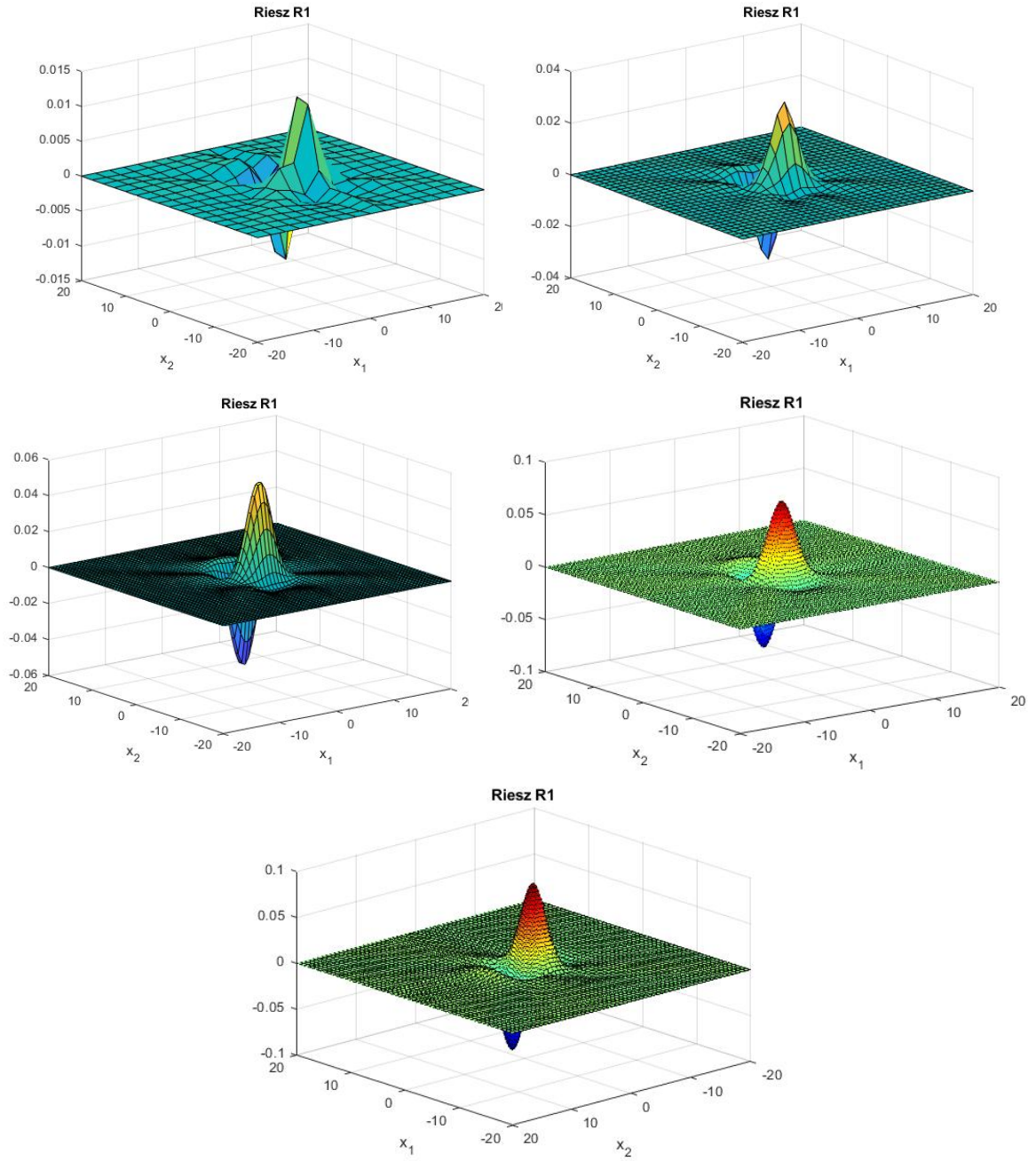


Figure 18 – Numerical approximation of the Riesz transform \mathcal{R}_1 for Laplacian of Gaussian, considering a sequence of meshes $m = 16, 32, 64, 128, 256$.

m	Error
16	1.0027
32	0.9680
64	0.7765
128	0.4593
256	0.1855

Table 1 – Error table for the numerical approximation of the Riesz transform to equation (4.46).

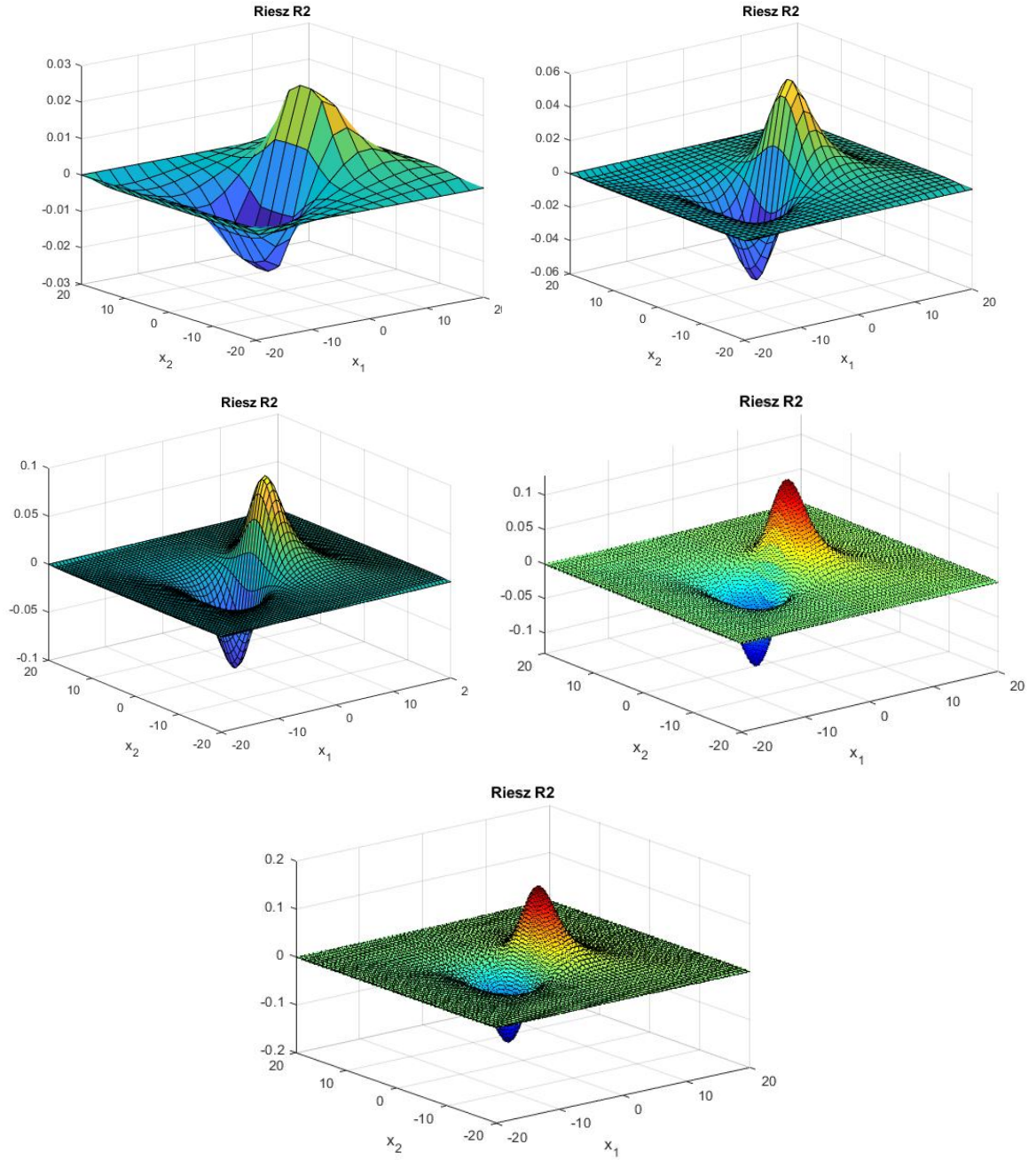


Figure 19 – Numerical approximation of the Riesz transform \mathcal{R}_2 for Laplacian of Gaussian, considering a sequence of meshes $m = 16, 32, 64, 128, 256$.

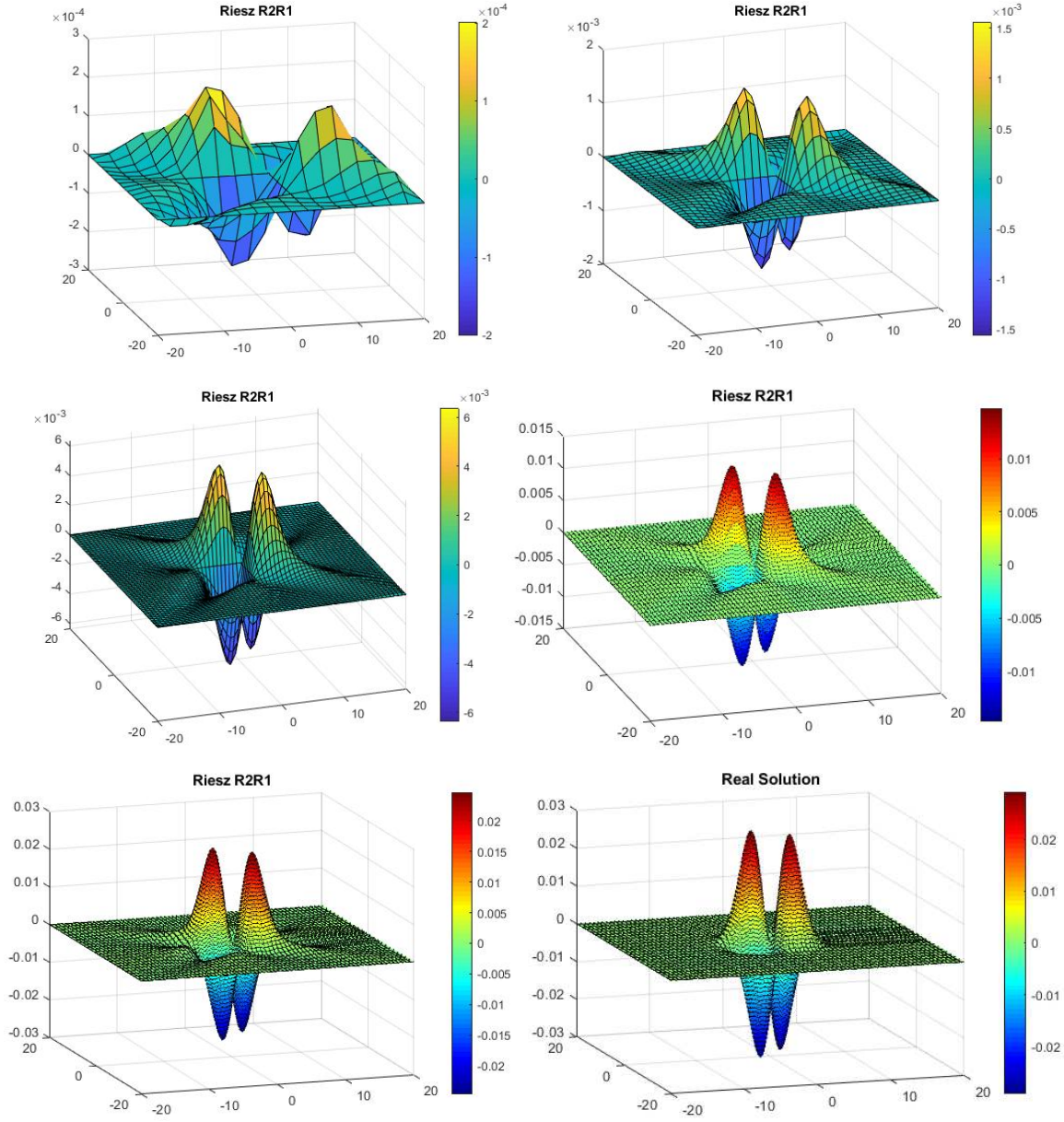


Figure 20 – Numerical approximation simulation of the Riesz transform for a sequence of meshes $m = 16, 32, 64, 128, 256$. In the last picture we plot $-\frac{\partial^2 u}{\partial x_i \partial x_j}$. However, in the other pictures, we have a numerical approximation of the Riesz transform $\mathcal{R}_i \mathcal{R}_j(\Delta u)$, where $u(x_1, x_2) = \frac{1}{\pi} e^{-\frac{x_1^2 + x_2^2}{8}}$.

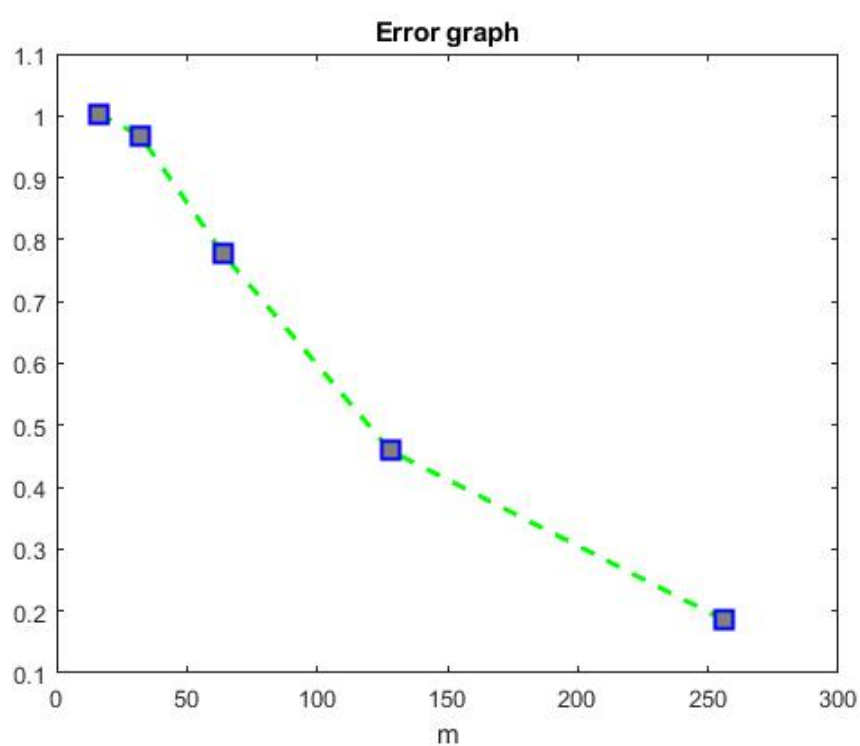


Figure 21 – Plot of the numerical error for the approximation of the Riesz transform to equation (4.46).

4.3.3 Numerical Simulations for the SQG

In this section, we study numerically through simulations the issue of global well-posedness, finite time blow-up, the formation of singularities or the formation of abrupt gradients in solutions for the SQG considering measuring initial data, belonging to the Schwartz spaces $\mathcal{S}(\mathbb{R}^2)$.

We first focus on describing the “big picture” of the analysis of numerical results by showing coherency between the theoretical arguments and numerical approximation. The key idea is to investigate the characteristics of the measurable initial datum, which might lead to a blow-up, global discussion, or formation of singularities in the numerical solution of SQG. The blow-up can be viewed as a singular point with mass-preserving accumulation.

Then our attention to a numerical experimental study of the nonlinear transport equation characterized with a nonlocal flux function, the Riesz transform (1.1). As mentioned before, we will use the Lagrangian-Eulerian method for solving this nonlinear transport equation (1.1). This scheme were able to compute qualitatively correct approximations by showing strong evidence of blow-up of concentration type with mass-preserving of the measure initial datum and measure initial datum measure weak-Morrey type with respect to the underlying nonlinear transport equation with doubly nonlocal flux; also this scheme were able to compute qualitatively correct approximations by showing strong evidence of attenuation of regularization type with mass-preserving of the measure initial datum and measure initial datum measure weak-Morrey type with respect to the underlying nonlinear transport equation with doubly nonlocal flux.

In order to perform the numerical study of the SQG equation nonlinear at hand to get additional insights on the nonlinear interplay among nonlocal equations, critical functional spaces, and singular measures, we also proposed a robust and consistent way to treat the model (1.1) in a finite computational domain $\Omega = [a, b] \times [c, d]$. Our prior rigorous results allow us to identify the most simple and mathematically correct treatment of boundary conditions, namely, enlarge the domain far enough that these spurious reflections cannot interfere with the numerical simulations. We rewrite model (1.1) in the computational domain $\Omega = [a, b] \times [c, d]$,

$$\begin{cases} \partial_t \theta + \nabla \cdot (-\theta \mathcal{R}_2 \theta, \theta \mathcal{R}_1 \theta) = 0, & (x, y, t) \in \Omega \times (0, T], \\ \theta(x, y, 0) = f(x, y), & (x, y) \in \Omega, \end{cases} \quad (4.47)$$

where \mathcal{R}_j with $j = 1, 2$ is the Riesz transform, which is given by (4.43). Furthermore, $f(x, y)$ can be the Gaussian, $f(x, y) = \frac{e^{-\frac{(x^2+y^2)}{8}}}{\pi}$, or other initial data as long as it is measurable.

As already pointed out in our results, the term blow-up of concentration type means solutions assuming singular measures, e.g., giving mass to points (singular points with mass concentration but preserving the initial total mass). Indeed, our analysis enables us to shed light on the effects of the initial data $f(x, y)$ as singular measures. Thus, possible natural questions are: What is the maximum mass of Dirac measure (or any other singular measure) so that we have the existence of a global-in-time flow in our framework? Do solutions evolve as a singular measure? Or do they regularise (a diffusion mechanism and mass-preserving) for $t > 0$?

To better understand the qualitative behavior numerically of the SQG equation, we will present the simulations in two subsections: Section 4.3.3 will look at simulations with measurement data as initial data.

Simulations for measured data

In this subsection, we will show evidence of regularization of the attenuation type for the solution θ of the SQG equation considering measured data, one of them being the Gaussian. The machine simulation time was approximately 20 days.

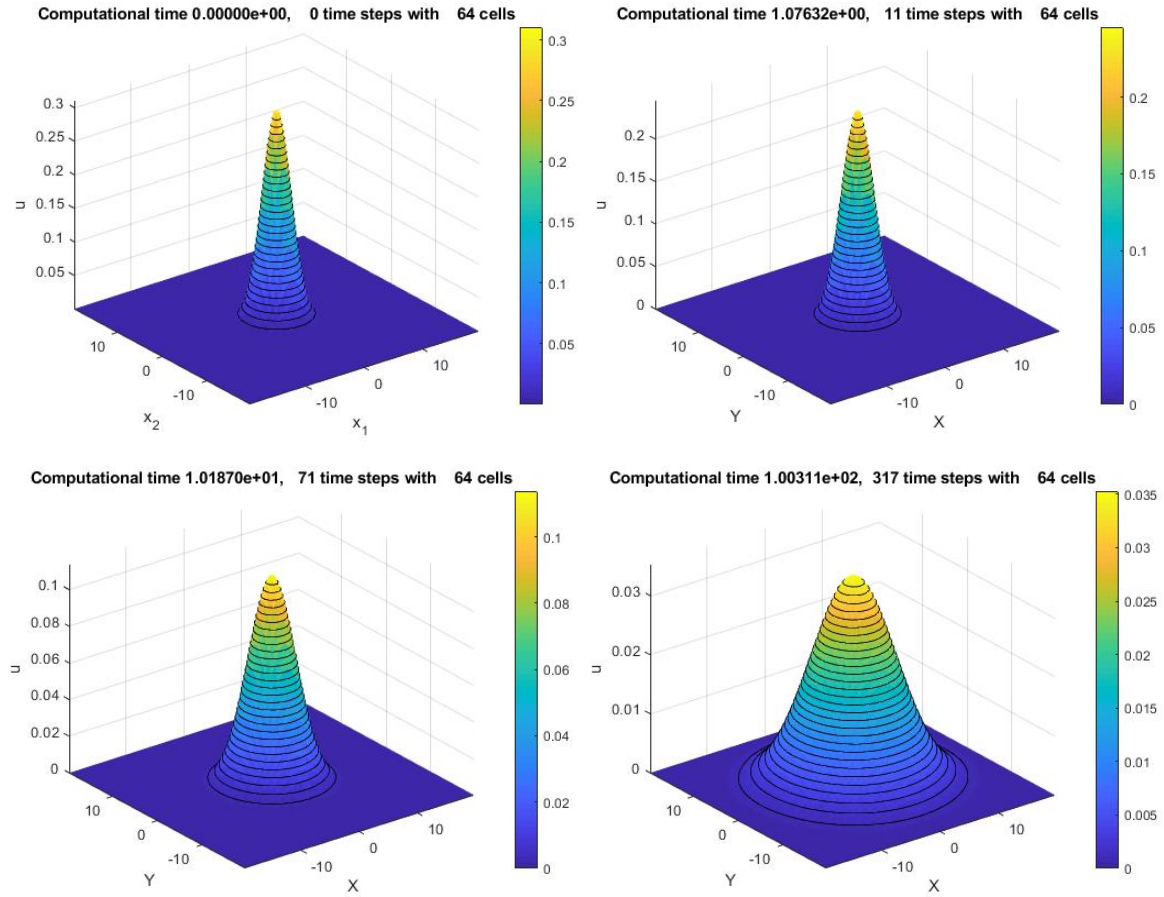


Figure 22 – Numerical simulations for $\partial_t \theta + \nabla \cdot (-\theta \mathcal{R}_2 \theta, \theta \mathcal{R}_1 \theta) = 0$ with a Gaussian initial data, $\alpha = 0.5$ and mesh $m = 64$ for a sequence of times $T = 0, 1, 10, 100$. On the top, you can observe a decrease in height of the approximate solution as time evolves, while on the bottom the approximate solution is shown diffusion and reduction in height as time evolves. Evidence of attenuation of regularization type.

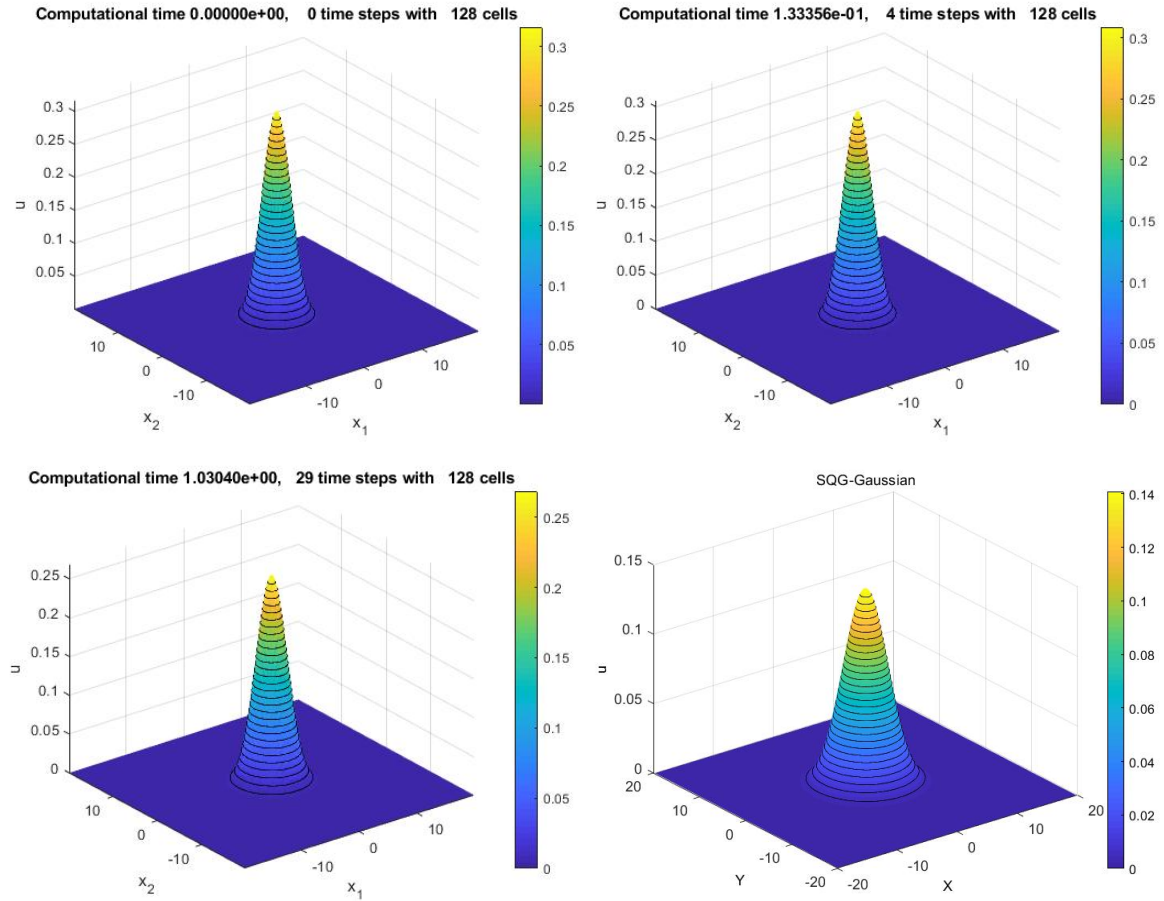


Figure 23 – Numerical simulations for $\partial_t \theta + \nabla \cdot (-\theta \mathcal{R}_2 \theta, \theta \mathcal{R}_1 \theta) = 0$ with a Gaussian initial data, $\alpha = 0.5$ and mesh $m = 128$ for a sequence of times $T = 0, 0.1, 1, 10$. At the top, you can observe a decrease in height of the approximate solution as time evolves, while at the bottom, the approximate solution exhibits diffusion and a reduction in height over time. This provides evidence of an attenuation of a regularization type.

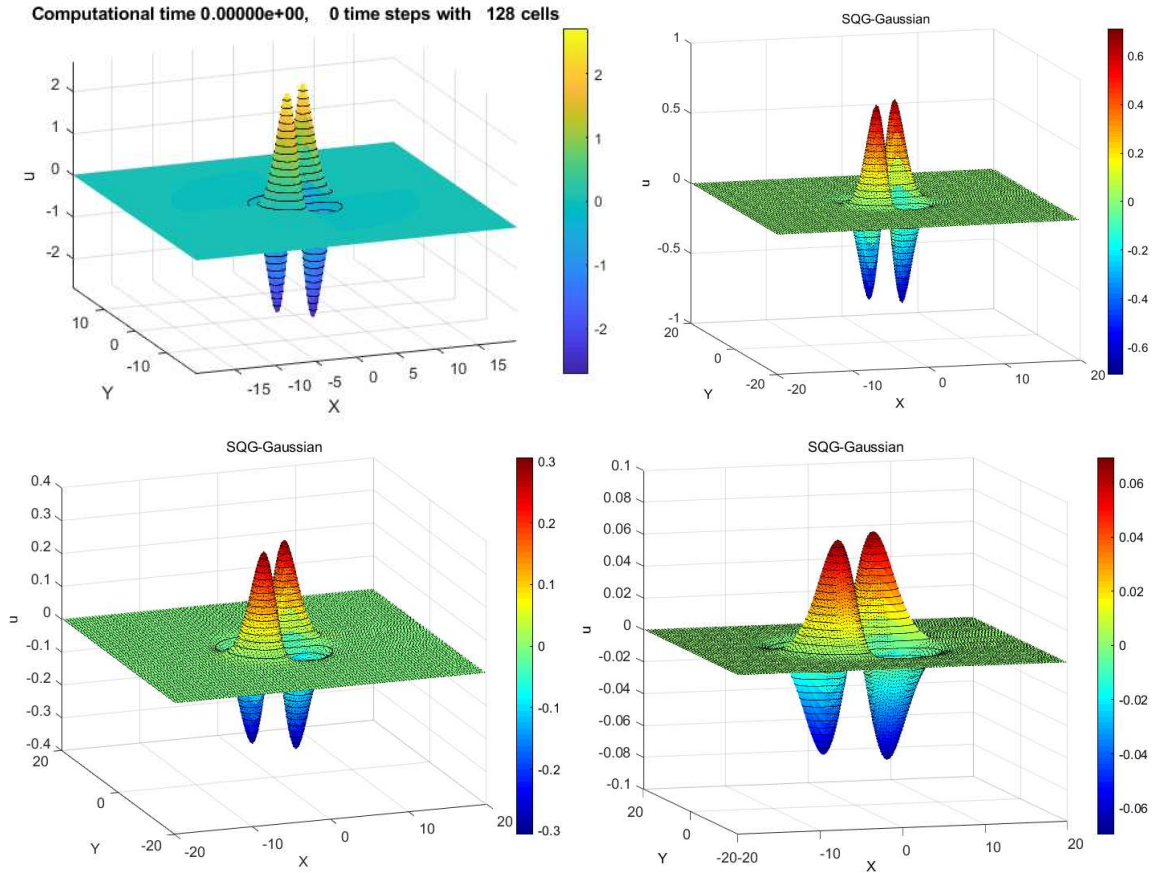


Figure 24 – Numerical simulations for $\partial_t \theta + \nabla \cdot (-\theta \mathcal{R}_2 \theta, \theta \mathcal{R}_1 \theta) = 0$ with the initial data $f(x, y) = \frac{3xy}{2\pi} \exp\{-(x^2 + y^2)/5\}$, $\alpha = 0.5$ and mesh $m = 128$ for a sequence of times $T = 0.0001, 0.1, 1, 10$. At the top, you can observe a decrease in height of the approximate solution as time evolves, while at the bottom, the approximate solution exhibits diffusion and a reduction in height over time. This provides evidence of an attenuation of a regularization type.

5 Conclusions and Perspectives

This thesis aims to conduct an analytical-numerical study of two nonlinear transport equations with nonlocal or doubly nonlocal flux. One of them is the well-known SQG equation, and the other is a model we are proposing for studying this type of transport equation, which we call a conservation law with partially nonlocal velocity. The nonlocal flux and the nonlinear transport equation model the evolution of relevant flow problems in pure and applied sciences. They appear in connection with dynamics models in continuous fluid mechanics and dynamics of fluids in porous media; for instance, vortex sheet evolution, the incompressible porous medium equation, interface models between incompressible fluids, magnetostrophic flow equation, patch problems in meteorology, to name a few of the significant interest on the subject matter of nonlocal models. The starting point is to motivate the problem and to establish several bases and existence of “regular” solutions for all time leading to important questions such as well-posedness, blow-up, asymptotic behavior, self-similarity, among other. For concreteness, in the mathematical part, we study the issue of well-posedness for these two nonlinear transport equations with nonlocal or doubly nonlocal flux with initial data belonging to in the framework of Besov spaces. In order to obtain this part, new mathematical results were developed and demonstrated. On the numerical part, the numerical solutions were obtained by using the novel Lagrangian-Eulerian method, for this we develop and validate the numerical approximations of nonlocal operators concerning those two transport equation; this numerical solutions were discussed and compared with the mathematical results achieved. Indeed, the underlying two transport equation problem analyzes in the framework of Besov spaces allows us to consider measure initial data and measured data of weak-Morrey type. Therefore, in the numerical approximations of the two aforementioned transport equations, under distinct initial conditions, evidence of either blow-up or attenuation of solutions was observed. This qualitative behavior depends on the sign of the flux and the conditions imposed on the initial data.

There is much to learn from the current work of well-posedness and evidence of blow-up or attenuation of solutions for SQG equation, a conservation law with partially nonlocal velocity model and a conservation law with partially nonlocal velocity with rotation with initial data in the framework of Besov spaces, from both viewpoints: theoretical and numerical. For instance, the $BW\tilde{\mathcal{M}}_{p,r}^{l,s}$ -space has been considered to study important issues as a local-in-time well-posedness and blow-up criterion for the incompressible Euler equations, covering critical and supercritical cases of the regularity. The Euler equations can be seen as a particular case of the Navier-Stokes equations when viscosity is neglected. On the other hand, less work appears in the literature concerning numerical convergence

analysis for approximation methods to model nonlinear transport equations with nonlocal flux and related equations. The functional space for numerical analysis convergence proofs linked to the numerical schemes we consider in this thesis is of particular interest in this subject matter.

In this chapter, we recapitulate the primary outcomes of the whole thesis and give a glimpse of possible future extensions of the present work.

5.1 Concluding Remarks

Concerning a conservation law with partially nonlocal velocity,

$$\begin{cases} \partial_t \theta \pm \nabla \cdot (\theta \Lambda_1^{\alpha-1} \mathcal{H}_1 \theta, \theta \Lambda_2^{\alpha-1} \mathcal{H}_2 \theta) = 0 \\ \theta(x, y, 0) = \theta_0 \end{cases}$$

we were able to prove theoretical and numerical results such as:

- In the mathematical part, we studied the issues of well-posedness with initial data belonging to the Besov space $B_{1,\infty}^\lambda$ with $\lambda > 5$. The well-posedness for the solution was established through analytical study, and the novelty lies in the definition of two nonlocal partial operators, namely the partial Hilbert transform and the partial Riesz potential. This fact prompted us to establish the Bernstein inequality for these partial nonlocal operators, with one of the new tools employed being the partial Fourier Transform. Furthermore, another novelty is that two commuting operators depend on the two nonlocal partial operators already mentioned. The estimates for these commutator operators were derived by means of Bernstein's inequality, which was established in this work.
- In the numerical part, we have successfully implemented the fully discrete 2D Lagrangian-Eulerian numerical scheme, and the novelty lies in its application to the doubly nonlocal case. In this approach, we consider the velocity field to be a composition of two nonlocal operators, the partial Hilbert transform and the partial Riesz potential. These two nonlocal operators have previously been approximated numerically. This marks the first instance of such an application in this context. For this numerical study, we are considering two cases. In the first case, we analyze *a conservation law with partially nonlocal velocity and positive flux* $\partial_t \theta + \nabla \cdot (\theta \Lambda_1^{\alpha-1} \mathcal{H}_1 \theta, \theta \Lambda_2^{\alpha-1} \mathcal{H}_2 \theta) = 0$ and obtain evidence of attenuation of regularization-type. In the second case, we analyze *a conservation law with partially nonlocal velocity and negative flux* $\partial_t \theta - \nabla \cdot (\theta \Lambda_1^{\alpha-1} \mathcal{H}_1 \theta, \theta \Lambda_2^{\alpha-1} \mathcal{H}_2 \theta) = 0$ and obtain evidence of blow-up of concentration-type; for both cases we consider measure initial data and measure initial data weak Morrey type. The observations of the numerical solution

of the transport equation (1.3) indicate both global well-posedness and finite time blow-up of solutions. These results maintain the same qualitative behavior as the one-dimensional case of the nonlinear transport equation (1.3) with doubly nonlocal velocity. Furthermore, we study a conservation law with partially nonlocal velocity with rotation $\partial_t \theta + \nabla \cdot (-\theta \Lambda_2^{\alpha-1} \mathcal{H}_2 \theta, \theta \Lambda_1^{\alpha-1} \mathcal{H}_1 \theta) = 0$ we have obtained similar results of SQG equation as rotating counterclockwise and losing regularity or formation of abrupt gradients.

Hence, the proof of well-posedness and numerical evidence of blow-up or attenuation from a conservation law with partially nonlocal velocity forces us to review some results obtained for a nonlinear one-dimensional transport equation with nonlocal velocity $u_t - (u \mathcal{H} u)_x = \nu u_{xx}, \nu > 0$ in the pseudomeasure space \mathcal{PM} (see [2]), as the global well-posedness and finite time blow-up of solutions for this one-dimensional nonlocal transport equation.

On the other hand, concerning the nonlinear transport equations with nonlocal flux, the SQG,

$$\begin{cases} \partial_t \theta + \nabla \cdot (\theta \mathcal{R}^\perp \theta) = 0 \\ \theta(x, 0) = \theta_0(x) \end{cases}$$

we were able to prove theoretical and numerical results such as:

- In the mathematical part, we studied the issues of well-posedness with initial data belonging to the modified Besov-weak-Morrey spaces $BW\tilde{\mathcal{M}}_{p,r}^{l,s}$. The well-posedness of a solution was established through an analytical study using some of the tools described in [42].
- In the numerical part, we successfully fully implemented the fully discrete 2D Lagrangian-Eulerian numerical scheme, and its novelty lies in its application to the nonlocal case. In this approach, by its very definition, the velocity is a non-local operator, the Riesz transform. This nonlocal operator has previously been approximated numerically and validated with a well-known identity. This marks the first instance of such an application in this context. For this numerical study we are considering measure initial data and obtaining evidence of attenuation of regularization-type. The observations of the numerical solution of the SQG equation give us some indications of the global well-posedness of solutions. These results maintain the same qualitative behavior as the nonlinear transport equation (1.3) with doubly nonlocal velocity.

5.2 Outlook for Future Work

Tracking the advancements in the state-of-the-art regarding the surface quasi-geostrophic equation framework, we want to continue studying analytically and theoretically to more understand this transport equation. Furthermore, We aim to persist in the analytical and numerical exploration of a conservation law with partially nonlocal velocity, as it represents a novel approach to studying nonlocal transport equations by defining partial nonlocal operators in the velocity field. This approach has yielded mathematical insights, including Bernstein's inequality and estimates for the commutator operators associated with the partial nonlocal operators. Therefore, we anticipate developing the following research topics:

Analytical:

- As a conservation law with partially nonlocal velocity and negative flux offers numerical evidence of blow-up of concentration type (similar to the 1D case), we have more than one motive to prove the blow-up of solution this model in classical Besov spaces. Additionally, would like to demonstrate the blow-up of solutions for the in the modified Besov-weak-Morrey spaces.
- As a conservation law with partially nonlocal velocity and positive flux offers numerical evidence of attenuation of regularization type (similar to the 1D case), we have one motivation to prove the global well-posedness of solution for this model in classical Besov spaces. Additionally, would like to demonstrate the blow-up of solutions for the in the modified Besov-weak-Morrey spaces.
- As a first study, we proved the well-posedness of a conservation law with partially nonlocal velocity in classical Besov spaces. Now, we would like to demonstrate the well-posedness for this model in the modified Besov-weak-Morrey spaces.
- We would like to demonstrate the well-posedness of the SQG this time by obtaining the velocity field through a composition of the Riesz transform with the Riesz potential.
- As the numerical simulations of a conservation law with partially nonlocal velocity with rotation exhibit similarities with the findings in the study of the geometric properties of the SQG in [25]. So, we would like to investigate the geometric features of the level curves of a conservation law with partially nonlocal velocity with rotation, including loss of convexity and formation of sinks or sources or saddles.

Numerical:

- Only a few numerical simulations have been presented for the SQG. Therefore, we would like to conduct additional numerical simulations, incorporating diverse types of initial data. Furthermore, we plan to enhance our study by refining the mesh.
- We observed that the numerical simulations for a conservation law with partially nonlocal velocity with rotation closely resemble those obtained for the SQG in [31, 46] and [25]. This new model could be considered a prototype for SQG. Consequently, we aim to conduct additional numerical simulations to explore further and validate this resemblance.
- We would like to prove of the convergence of the Lagrangian-Eulerian method of a conservation law with partially nonlocal velocity and the SQG.

Theoretical-Numerical

- We would like to study the interplay between computation and analysis, which leads to further theoretical insights based in numerical observations of the SQG and a conservation law with partially nonlocal velocity with rotation.
For example, we would like to investigate global well-posedness, finite-time blowing-up, the formation of singularities, and the emergence of abrupt gradients in solutions for both the SQG and a conservation law with partially nonlocal velocity with rotation.

Bibliography

- [1] Hammadi Abidi and Taoufik Hmidi. On the global well-posedness of the critical quasi-geostrophic equation. *SIAM journal on mathematical analysis*, 40(1):167–185, 2008.
- [2] E Abreu, LCF Ferreira, J Galeano, and J Pérez. On a 1d model with nonlocal interactions and mass concentrations: an analytical-numerical approach. *Nonlinearity*, 35(4):1734, 2022.
- [3] Eduardo Abreu, Elena Bachini, John Pérez, and Mario Putti. A geometrically intrinsic lagrangian-eulerian scheme for 2d shallow water equations with variable topography and discontinuous data. *Applied Mathematics and Computation*, 443:127776, 2023.
- [4] Eduardo Abreu, Mathilde Colombeau, and Eugeny Panov. Weak asymptotic methods for scalar equations and systems. *Journal of mathematical analysis and applications*, 444(2):1203–1232, 2016.
- [5] Eduardo Abreu, Mathilde Colombeau, and Evgeny Yu Panov. Approximation of entropy solutions to degenerate nonlinear parabolic equations. *Zeitschrift für angewandte Mathematik und Physik*, 68(6):1–17, 2017.
- [6] Eduardo Abreu, Ciro Diaz, Juan Galvis, and John Pérez. On the conservation properties in multiple scale coupling and simulation for darcy flow with hyperbolic-transport in complex flows. *Multiscale Modeling & Simulation*, 18(4):1375–1408, 2020.
- [7] Eduardo Abreu, Jean François, Wanderson Lambert, and John Pérez. A class of positive semi-discrete lagrangian–eulerian schemes for multidimensional systems of hyperbolic conservation laws. *Journal of Scientific Computing*, 90(1):1–79, 2022.
- [8] Eduardo Abreu, Jean Francois, Wanderson Lambert, and John Pérez. A semi-discrete lagrangian–eulerian scheme for hyperbolic-transport models. *Journal of Computational and Applied Mathematics*, 406:114011, 2022.
- [9] Eduardo Abreu, Wanderson Lambert, John Perez, and A Santo. A new finite volume approach for transport models and related applications with balancing source terms. *Mathematics and Computers in Simulation*, 137:2–28, 2017.
- [10] Eduardo Abreu, Wanderson Lambert, John Pérez, and Arthur Santo. A weak asymptotic solution analysis for a lagrangian–eulerian scheme for scalar hyperbolic

- conservation laws. *Hyperbolic Problems: Theory, Numerics, Applications*, pages 223–230, 2018.
- [11] Eduardo Abreu, Vitor Matos, John Pérez, and Panters Rodriguez-Bermudez. A class of lagrangian–eulerian shock-capturing schemes for first-order hyperbolic problems with forcing terms. *Journal of Scientific Computing*, 86(1):1–47, 2021.
- [12] Eduardo Abreu and John Pérez. A fast, robust, and simple lagrangian–eulerian solver for balance laws and applications. *Computers & Mathematics with Applications*, 77(9):2310–2336, 2019.
- [13] Eduardo Abreu, John Perez, and Arthur Santo. Lagrangian-eulerian approximation methods for balance laws and hyperbolic conservation laws. *Revista UIS Ingenierías*, 17(1):191–200, 2018.
- [14] Eduardo Abreu, John Pérez, and Arthur Santo. A conservative lagrangian-eulerian finite volume approximation method for balance law problems. *Proceeding Series of the Brazilian Society of Computational and Applied Mathematics*, 6(1), 2018.
- [15] Mustapha Amara and Jamel Benameur. Global solution of anisotropic quasi-geostrophic equations in sobolev space. *Journal of Mathematical Analysis and Applications*, 516(1):126512, 2022.
- [16] Boris Andreianov and Darko Mitrović. Entropy conditions for scalar conservation laws with discontinuous flux revisited. 32(6):1307–1335, 2015.
- [17] José Aquino, AS Francisco, Felipe Pereira, T Jordem Pereira, and HP Amaral Souto. A lagrangian strategy for the numerical simulation of radionuclide transport problems. *Progress in Nuclear Energy*, 52(3):282–291, 2010.
- [18] Achraf Azanzal, Chakir Allalou, and Said Melliani. Well-posedness and blow-up of solutions for the 2d dissipative quasi-geostrophic equation in critical fourier-besov-morrey spaces. *Journal of Elliptic and Parabolic Equations*, 8(1):23–48, 2022.
- [19] Hajer Bahouri, Jean-Yves Chemin, and Raphaël Danchin. *Fourier analysis and nonlinear partial differential equations*, volume 343. Springer, 2011.
- [20] Jamel Benameur and Saber Ben Abdallah. Asymptotic behavior of critical dissipative quasi-geostrophic equation in fourier space. *Journal of Mathematical Analysis and Applications*, 497(1):124873, 2021.
- [21] Moez Benhamed. Global well-posedness and blow-up criterion for the periodic quasi-geostrophic equations in lei-lin-gevrey spaces. *Mathematical Methods in the Applied Sciences*, 40(18):7488–7509, 2017.

- [22] Jean-Michel Bony. Calcul symbolique et propagation des singularités pour les équations aux dérivées partielles non linéaires. 14(2):209–246, 1981.
- [23] Raimund Bürger, Kenneth H Karlsen, and John D Towers. An engquist–osher-type scheme for conservation laws with discontinuous flux adapted to flux connections. *SIAM Journal on numerical analysis*, 47(3):1684–1712, 2009.
- [24] Luis A Caffarelli and Alexis Vasseur. Drift diffusion equations with fractional diffusion and the quasi-geostrophic equation. *Annals of Mathematics*, pages 1903–1930, 2010.
- [25] Angel Castro, Diego Córdoba, Javier Gómez-Serrano, and Alberto Martín Zamora. Remarks on geometric properties of sqg sharp fronts and α -patches. *arXiv preprint arXiv:1401.5376*, 2014.
- [26] Dongho Chae. The quasi-geostrophic equation in the triebel–lizorkin spaces. *Nonlinearity*, 16(2):479, 2003.
- [27] Dongho Chae, Antonio Córdoba, Diego Córdoba, and Marco A Fontelos. Finite time singularities in a 1d model of the quasi-geostrophic equation. *Advances in Mathematics*, 194(1):203–223, 2005.
- [28] Dongho Chae and Jihoon Lee. Global well-posedness in the super-critical dissipative quasi-geostrophic equations. *Communications in mathematical physics*, 233(2):297–311, 2003.
- [29] Qionglei Chen, Changxing Miao, and Zhifei Zhang. A new bernstein’s inequality and the 2d dissipative quasi-geostrophic equation. *Communications in mathematical physics*, 271(3):821–838, 2007.
- [30] Peter Constantin, Diego Cordoba, and Jiahong Wu. On the critical dissipative quasi-geostrophic equation. *Indiana University mathematics journal*, pages 97–107, 2001.
- [31] Peter Constantin, Andrew J Majda, and Esteban Tabak. Formation of strong fronts in the 2-d quasigeostrophic thermal active scalar. *Nonlinearity*, 7(6):1495, 1994.
- [32] Peter Constantin and Vlad Vicol. Nonlinear maximum principles for dissipative linear nonlocal operators and applications. *Geometric And Functional Analysis*, 22(5):1289–1321, 2012.
- [33] Peter Constantin and Jiahong Wu. Behavior of solutions of 2d quasi-geostrophic equations. *SIAM journal on mathematical analysis*, 30(5):937–948, 1999.
- [34] Antonio Córdoba and Diego Córdoba. A maximum principle applied to quasi-geostrophic equations. *Communications in mathematical physics*, 249(3):511–528, 2004.

- [35] Diego Córdoba and Luis Martínez-Zoroa. Non existence and strong ill-posedness in ck and sobolev spaces for sqg. *Advances in Mathematics*, 407:108570, 2022.
- [36] D da Silva. *Soluções de Riemann para um escoamento bifásico com fonte de Dirac em um meio poroso*. PhD thesis, Master Thesis, Fluminense Federal University, 2016.
- [37] Michael Dabkowski. Eventual regularity of the solutions to the supercritical dissipative quasi-geostrophic equation. *Geometric and Functional Analysis*, 1(21):1–13, 2011.
- [38] Juan Gabriel Galeano Delgado. *Well-posedness and blow-up of global solutions for a nonlinear transport equation with nonlocal flux and measure data: theory and numerics Boa colocação e blow-up de soluções globais para uma equação de transporte não linear com fluxo não local e*. PhD thesis, [sn], 2016.
- [39] Stefan Diehl. A conservation law with point source and discontinuous flux function modelling continuous sedimentation. *SIAM Journal on Applied Mathematics*, 56(2):388–419, 1996.
- [40] Jim Douglas, Felipe Pereira, and Li-Ming Yeh. A locally conservative eulerian–lagrangian numerical method and its application to nonlinear transport in porous media. *Computational Geosciences*, 4(1):1–40, 2000.
- [41] Jim Douglas, Felipe Pereira, and Li Ming Yeh. A locally conservative eulerian–lagrangian method for flow in a porous medium of a mixture of two components having different densities. In *Numerical Treatment of Multiphase Flows in Porous Media*, pages 138–155. Springer, 2000.
- [42] Lucas CF Ferreira and Jhean E Pérez-López. On the well-posedness of the incompressible euler equations in a larger space of besov–morrey type. *Dynamics of Partial Differential Equations*, 19(1):23–49, 2022.
- [43] Gerald B Folland. *Real analysis: modern techniques and their applications*, volume 40. John Wiley & Sons, 1999.
- [44] Laurent Gosse. *Computing qualitatively correct approximations of balance laws*, volume 2. Springer, 2013.
- [45] Loukas Grafakos. *Classical fourier analysis*, volume 2. Springer, 2008.
- [46] Isaac M Held, Raymond T Pierrehumbert, Stephen T Garner, and Kyle L Swanson. Surface quasi-geostrophic dynamics. *Journal of Fluid Mechanics*, 282:1–20, 1995.
- [47] Magdalena Huacasi Machaca. Estudio y aplicación de un método lagrangiano-euleriano para leyes de conservación hiperbólicas con flujo doblemente no local. 2021.

- [48] Shi Jin and Xin Wen. Two interface-type numerical methods for computing hyperbolic systems with geometrical source terms having concentrations. *SIAM Journal on Scientific Computing*, 26(6):2079–2101, 2005.
- [49] Kenneth H Karlsen and John D Towers. Convergence of the lax-friedrichs scheme and stability for conservation laws with a discontinuous space-time dependent flux. *Chinese Annals of Mathematics*, 25(03):287–318, 2004.
- [50] Kenneth Hvistendahl Karlsen and John D Towers. Convergence of a godunov scheme for conservation laws with a discontinuous flux lacking the crossing condition. *Journal of Hyperbolic Differential Equations*, 14(04):671–701, 2017.
- [51] Alexander Kiselev. Nonlocal maximum principles for active scalars. *Advances in Mathematics*, 227(5):1806–1826, 2011.
- [52] Alexander Kiselev, Fedor Nazarov, and Alexander Volberg. Global well-posedness for the critical 2d dissipative quasi-geostrophic equation. *Inventiones mathematicae*, 167(3):445–453, 2007.
- [53] Omar Lazar. Global existence for the critical dissipative surface quasi-geostrophic equation. *Communications in Mathematical Physics*, 322(1):73–93, 2013.
- [54] Pierre Gilles Lemarié-Rieusset. Recent developments in the navier-stokes problem. 2002.
- [55] Pengtao Li and Qixiang Yang. Well-posedness of quasi-geostrophic equations with data in besov-q spaces. *Nonlinear Analysis: Theory, Methods & Applications*, 94:243–258, 2014.
- [56] Claudio Masolo. Understanding ontological levels. In F. Lin and U. Sattler, editors, *Proceedings of the Twelfth International Conference on the Principles of Knowledge Representation and Reasoning (KR 2010)*, pages 258–268. AAAI Press, 2010.
- [57] Hideyuki Miura. Dissipative quasi-geostrophic equation for large initial data in the critical sobolev space. *Communications in mathematical physics*, 267(1):141–157, 2006.
- [58] S Mochon. An analysis of the traffic on highways with changing surface conditions. *Mathematical Modelling*, 9(1):1–11, 1987.
- [59] Daniel N Ostrov. Solutions of hamilton–jacobi equations and scalar conservation laws with discontinuous space–time dependence. *Journal of Differential Equations*, 182(1):51–77, 2002.
- [60] Joseph Pedlosky. *Geophysical fluid dynamics*, volume 343. New York and Berlin, Springer-Verlag, 1982.

- [61] J Pérez. *Lagrangian-Eulerian approximation methods for balance laws and hyperbolic conservation laws university of campinas*. PhD thesis, Ph. D. Thesis, University of Campinas (Unicamp)-Institute of Mathematics, Statistics and Scientific Computin, 2015.
- [62] Serge G Resnick. *Dynamical problems in non-linear advective partial differential equations*. PhD thesis, 1996.
- [63] Yoshihiro Sawano et al. *Theory of Besov spaces*, volume 56. Springer, 2018.
- [64] Luis Silvestre. Eventual regularization for the slightly supercritical quasi-geostrophic equation. *Annales de l'Institut Henri Poincaré C*, 27(2):693–704, 2010.
- [65] Elias M Stein. *Singular integrals and differentiability properties of functions*, volume 2. Princeton university press, 1970.
- [66] Jinyi Sun and Shangbin Cui. Sharp well-posedness and ill-posedness of the three-dimensional primitive equations of geophysics in fourier–besov spaces. *Nonlinear Analysis: Real World Applications*, 48:445–465, 2019.
- [67] Hengheng Wang and Houyu Jia. Local well-posedness for the 2d non-dissipative quasi-geostrophic equation in besov spaces. *Nonlinear Analysis: Theory, Methods & Applications*, 70(11):3791–3798, 2009.
- [68] YANG Wanrong and JIU Quansen. Global regularity for modified critical dissipative quasi-geostrophic equations. *Acta Mathematica Scientia*, 34(6):1741–1748, 2014.
- [69] Jiahong Wu. Quasi-geostrophic-type equations with initial data in morrey spaces. *Nonlinearity*, 10(6):1409, 1997.
- [70] Jiahong Wu. Existence and uniqueness results for the 2-d dissipative quasi-geostrophic equation. *Nonlinear Analysis: Theory, Methods & Applications*, 67(11):3013–3036, 2007.
- [71] Zhaoyin Xiang and Wei Yan. On the well-posedness of the quasi-geostrophic equation in the triebel-lizorkin-lorentz spaces. *Journal of Evolution Equations*, 11(2):241–263, 2011.
- [72] Huan Yu, Xiaoxin Zheng, and Quansen Jiu. Remarks on well-posedness of the generalized surface quasi-geostrophic equation. *Archive for Rational Mechanics and Analysis*, 232(1):265–301, 2019.
- [73] Qian Zhang and Yehua Zhang. Local well-posedness for the quasi-geostrophic equations in besov–lorentz spaces. *Rendiconti del Circolo Matematico di Palermo Series 2*, 69(1):53–70, 2020.

-
- [74] Xuhuan Zhou, Weiliang Xiao, and Jiecheng Chen. Fractional porous medium and mean field equations in besov spaces. *Electron. J. Differential Equations*, 2014(199):1–14, 2014.